Contribution of Na_v Channels to the Development and Function of the Retina

by

Benjamin J Smith

Submitted in partial fulfilment of the requirements
for the degree of Doctor of Philosophy

at

Dalhousie University
Halifax, Nova Scotia
August 2017

TABLE OF CONTENTS

LIST OF TABLES

LIST OF FIGURES

ABSTRACT

Voltage gated (Na_v) channel isoforms are precisely located in the nervous system and expressed sequentially during development. Because Na_v channels control the rising phase of action potentials isoform differences may play a fundamental role in neural encoding of information. However perinatal mortality, developmental compensation, and a lack of isoform specific small molecule blockers has limited the investigation into specific roles filled by Na_v channels. Using the macroscopic light response of the whole retina I first investigated into the contribution of TTX-sensitive Na_v channels as a function of light adaptation and in response to daily rhythms in ambient light. Further work using a $Na_v1.6$ knockout mouse revealed a surprising role of $Na_v1.6$ in retrograde signaling in the optic nerve following eye opening. This retroaxonal feedback mechanism operating while the retina is still developing after eye opening controls photoreceptor light sensitivity via TrkB receptors and appears to require $Na_v1.6$ in the optic nerve.

Finally two projects focused specifically on the role of individual Na_v channel isoforms in retinal signaling. First using a newly developed subtype specific blocker A803467 I investigated the function of $Na_v1.8$ in the retina finding, in particular, a selective reduction in the oscillatory potentials (OPs) as well as a reduction in the light responses of sustained ON retinal ganglion cells. Secondly I developed a method using membrane permeablized antibodies to common Na_v channel isoforms to identify unique contributions of each to retinal processing. In combination with small molecule blockers and a knockout mouse to $Na_v1.6$ this method identified $Na_v1.6$ as a key component of light responses in ON cone bipolar cells, as well as supporting the majority of spiking activity in retinal ganglion cells. Interestingly $Na_v1.1$ appears to be predominately involved in sustaining spiking in response to longer duration stimuli rather than contributing to the amplitude of the spiking response. Together these results define new roles for Na_v channel isoforms in the retina and optic nerve and contribute both to our understanding of how the retina uses the unique properties of Na_v channel isoforms to adapt to visual input.

LIST OF ABBREVIATIONS USED

4,9ahTTX	4,9-anhydro-tetrodotoxin
AIS	Axonal initial segment
AMPA	α-amino-3-hydroxy-5-methyl-4-isoxazolepropionic acid
BDNF	Brain-derived neurotrophic factor
Ca_v	Voltage-gated calcium channel
CBCs	Cone bipolar cells
CNQX	6-cyano-7-nitroquinoxaline-2,3-dione
CR_i	Cone-rod photoreceptor range
CSN	Central nervous system
CPPG	α-cyclopropyl-4-phosphonophenylyglycine
DB	Depolarizing bipolar cell
DS	Directionally selective
DRG	Dorsal root ganglion
ERG	Electroretinogram
GABA	Gamma-aminobutyric Acid
$GABA_aR$	$GABA_a$ receptor
$GABA_cR$	$GABA_c$ receptor
Gly	Glycine
HB9+	Cells positive for the motor neuron transcription factors HB9
HEK	Human Embryonic Kidney
IPL	Inner plexiform layer
ISI	Inter-stimulus interval
IT	Implicit time
KO	Knockout
L-AP4	L-(+)-2-Amino-4-phosphonobutyric acid
log cd m s^{-2}	Logatithm of candela per square meter
MEA	Multielectrode array
mGluR6	Metabotropic glutamate receptor 6

Mp	Membrane-permeable
mV	Millivolt
nA	Nano-ampere
Na_v	Voltage-gated sodium channel
NMDA	N-methyl D-aspartate
OPs	Oscillatory potentials
P14	Post-natal day ….
pH	Hydrogen potential
PDA	Cis-2,3-piperidine dicarboxylic acid
PNS	Peripheral nervous system
p/nSTR	Positive / negative scotopic negative response
PSTH	Post-stimulus time histogram
RBCs	Rod bipolar cells
RC_i	Rod-cone photoreceptor range
RGC	Retinal ganglion cell
RG_i	Retinal ganglion cell range
R_i	Rod photoreceptor range
SBAC	Starburst amacrine cell
$Scn8a^{dmu}$	$Na_v1.6$, voltage-gated sodium channel mutant: degenerating muscle mouse
STI	Sustained transient index
Thy1-ChR2	Channelrhdopsin2 under thymus cell antigen 1 promotor
TrkB	Tropomyosin receptor kinase B
TrpM1	Transient receptor potential cation channel subfamily M member 1
TTX	Tetrodotoxin
VGAT	Vesicular GABA transporter
VGLUT3+	Vesicular glutamate transporter type 3 positive
VIP	Vasoactive intestinal polypeptide
WFA	Wide field amacrine
μ g/ μ L/μm	Microgram / microliter / micrometer

ACKNOWLEDGEMENTS

Many thanks to my supervisors Drs. Francois Tremblay and Patrice Cote. I wrote a paper for Patrice's Advanced Cell Bio class at a point where I was just trying to get out of school as quickly as possible. While writing the paper, I was lucky that Francois took the time to teach me about ERGs, connexins and congenital stationary night blindness. Between them, Francois and Patrice showed me the difference between the science in textbooks and the joy of real science, discussing new results and strategies to investigate them. While I've learned a lot from both Francois and Patrice, the most important thing I'll take away is their shared enthusiasm for new ideas. I'm grateful for their patience and the fact that during my thesis science never has lost its fun.

Thanks to Dr. Steve Barnes and Dr. Bill Baldridge, my committee members. In hindsight, I wish I had not avoided official committee meetings at all costs. Nonetheless, I spent a lot of enlightening evenings talking science with Steve in the retina lab and working with Bill on calcium imaging in retinal ganglion cells for my honours project taught me a lot amount about designing experiments and scientific writing.

Thanks to Dr. Peter Lukasiewicz, for serving as my external examiner and, additionally, for influencing the direction of many of the projects I undertook. Without his work on serial inhibition of rod bipolar cells and Na_v channels in ON-cone bipolar cells, many of my results would have been much harder to interpret.

Thanks to Craig Stamp for teaching me to think like a scientist. Also for all the egg sandwiches and coffee. Thanks to Dave Quinn for teaching me that things done are won and the value of metrics.

Thanks to Dr. Melanie Kelly, Dr. Bal Chauhan, Dr. Xu Wang, Dr. Joanna Borowska-Fielding, Dr. Margaret Luke, Dr. Anna Szczesniak, Dr. Alex Straiker, Dr. Bryan Daniels,

Elizabeth Cairns, Janette Nason, and Jill King for working on shared projects during my time in the Retina Lab, you were all great to collaborate with. I'd also like to thank the summer students I worked with but in particular, Ben Clarke and Sally Dickinson; it was great working with such dedicated partners and both the results and their skills at presenting and explaining them was beyond what I could have hoped for. In addition to the people I worked with directly on collaborative projects, the Retina Lab as a whole was a great place to work.

Finally, I would like to thank my parents for their generosity and support through graduate school. I was going a bit loony at times and having family around to rein me in kept me sane, also mostly free of scurvy. I'd also like to thank Nate for great conversations about pairwise correlations and Ising models and Kate for listening to science rants, measuring photoreceptors, and asking great questions. I'd also like to thank Dr. Andrea Makkay, for being an invaluable resource to talk to about grad school and science for the first half of my thesis. Thanks to Emilie Hyland for playing crib, also listening to science rants, and exploring for rocks with me.

CHAPTER 1: INTRODUCTION

1.1 Preamble

Understanding the retina can be divided into three fundamental problems: first, how are cells in different classes wired together to form neural circuits; second, what are the developmental mechanisms controlling the formation of neural circuitry; and third, what are the molecular components within a given population of cells that control the transformation of information within a neuron from input to output. Significant recent progress has been made on the first and second of these problems with the technological advances of connectomics (e.g. Helmstadtler et al., 2013; Briggman et al., 2011; Wei et al., 2011; Yonehara et al., 2011), optogenetics (e.g. Lee et al., 2014; Krishnaswarmy et al., 2015; Park et al., 2015), and the generation of fluorescently identified members of many subtypes of retinal cells (e.g. Huberman et al., 2009; Farrow et al., 2013; Kim et al., 2008; Trenholm et al., 2011; Rivlin-Etzion et al., 2011). Many of the developmental rules governing the synaptic connections between cell classes has have also been elucidated (Sun et al., 2013; Duan et al., 2014; Briggman et al., 2011; Wei et al., 2011; Yonehara et al., 2011). However, generating a parts list or molecular toolbox (see Ishida, 2004) allowing the production of biophysically accurate models of individual retinal cell types has not advanced as quickly. Although fluorescently identified subtypes of nearly every class of retinal cell have been produced (Siegert et al., 2009) the primary focus has been on the developmental and mature circuit interactions rather than the differing intrinsic properties of these cells (although see e.g. Hu et al., 2013; Detwiler and Margolis 2007) and more importantly the contribution of specific protein isoforms to the intrinsic properties of a given cell type.

1.2 Purpose of the study

In the work presented here, I focused on voltage-gated sodium (Na_v) channels as a key to answer three primary questions. First Côté et al., (2005) reported an unusual visual phenotype in juvenile mice lacking $Na_v1.6$ consisting of a profound reduction in photoreceptor function. I was interested in discovering the origin of this reduction in photoreceptor function because in adult mice Na_v channels, predominately involved in

binary information transfer, have no known contribution to the graded potentials of photoreceptors. Second I was interested in the neural circuitry underlying the high frequency oscillations in the macroscopic ERG signal, the composite retinal response to a brief light flash. Third I was interested in whether Na_v channel subtypes contribute to intrinsic differences in how neurons communicate, specifically using the light responses of retinal ganglion cells as a model.

CHAPTER 2: LITERATURE REVIEW

2.1 Basic Neural Retinal Circuitry in relation to Na_v channel isoforms distribution

Anatomically the neural retina is divided into three nuclear layers connected by two synaptic layers, the outer and inner plexiform layers. The distal outer nuclear layer contains the photoreceptor cell bodies, the inner nuclear layer contains bipolar and amacrine cells, while the most proximal ganglion cell layer contains retinal ganglion cells and displaced amacrine cells. Functionally, the retina can be divided into parallel vertical excitatory pathways and horizontally ramifying inhibitory circuit elements. The vertical pathways can be divided into rod circuit, highly sensitive due to its convergent nature, and the parallel cone-driven pathways, less light sensitive but able to sort the visual signal by colour and spatiotemporal frequency. The rod pathway, active in low light conditions, consists of a highly convergent rod to rod bipolar cell circuit which, instead to connecting to the ganglion cells directly, is instead piggybacking onto the cone-driven pathways primarily via the AII amacrine cells on the cone bipolar cells. In contrast to the single photoreceptor and bipolar cell in the rod pathway, the cone pathways are diverse, starting from 2-3 types of spectrally selective photoreceptors that diverge into approximately 12 types (9 anatomically defined, vs. 12 physiologically defined) of cone bipolar cells (Helmstadtler et al., 2013; Wassel et al., 2009; Breuninger et al., 2011; Ichinose et al., 2014), feeding forward to at least 12 types of retinal ganglion cells (Field and Chinchilnisky 2007; Masland et al., 2012; Sanes and Masland 2015 but see Baden et al., 2016). Within the horizonal ramifying inhibitory interneurons, one can find 1-3 types of horizontal cells depending on species and approximately 30 types of amacrine cells including a subset of interplexiform cells with dendrites ramifying in both inner and outer plexiform layers (reviewed in Sanes and Masland 2015).

Each of the retinal cell types listed above, as well as the Müller cells – the major glial cell of the retina – have been reported to express Na_v channels in at least one species (e.g. Kawai et al., 2001; Liu et al., 2016; Puthessary et al., 2013; Bloomfield 1992; Fohlmeister et al., 1990). The next sections will focus on the basic connections and roles of cell types in the neural retina as well as the relevance of Na_v channels to their function.

2.1.1 Photoreceptors

Photoreceptors convert light in the visible spectrum into a graded change in glutamate output, with increased light levels suppressing glutamate release. Photoreceptors can be divided into sensitive but noisy and slow-responsive rods (able to respond to single photons), and less sensitive cones showing shorter integration times and requiring higher light levels. The latter can be divided into types based on the wavelength sensitivity of the opsin they express. In general, mammals have two types of cones sensitive to either short or long wavelengths although some species, such as members of the Cercopithecidae family (old-world primates have a 3rd cone type evolved from the long wavelength one). There have been a few reports of photoreceptors spiking in response to depolarization following light offset (Maricq & Korenbrot, 1988; Barnes & Deschenes, 1992; Fain & Quandt, 1980; Kawai et al., 2001; Piccolino and Gerschenfeld 1980), particularly after blocking potassium channels.

Spikes may provide a temporally precise light off signal and may encode supersaturating light stimuli, potentially contributing to negative after images (Xu et al., 2005). In most cases, these regenerative potentials have been shown to be based on voltage-gated calcium (Ca_v) channels and photoreceptors generally don't have Na_v currents (Non-mammals: Barnes and Hille 1989; Mammals: Cia et al., 2004; Mojumder et al., 2007); however, in work using human retinas the group of Ei-ichi Miyachi (Kawai et al., 2001; Kawai et al., 2005; Ohkuma et al., 2007) indicated that TTX-sensitive Na_v channels drive spiking in rods and some cones. However, this series of papers has serious caveats. For example, Copenhagen (2001) notes that retinal pigment epithelial cells rapidly undergo transdifferentiation and begin to express Na_v currents in culture, and that many of the photoreceptors were harvested from detached retinas, so possibly the photoreceptors recorded from represent an abnormal adaptation of the photoreceptor either to detachment from the pigment epithelium or to surgery and subsequent culture. In addition, in the 15 years since the initial report, no further demonstration of photoreceptor Na_v channels or spiking by another group has been reported.

2.1.2 Horizontal cells

Horizontal cells feedback onto photoreceptors, playing important roles in the creation of receptive fields and color opponency. This process is incompletely understood despite substantial evidence for multiple mechanisms modulating Ca_v channels in photoreceptor axon terminals. Plausible components for the horizontal cell feedback mechanism include a combination of autaptic GABA release, pH modulation, and/or ephaptic feedback via hemi-channels (reviewed in Thoreson and Mangel 2012; Kemmler et al., 2014; Liu et al., 2013; Vroman et al., 2014; Wang et al., 2014). Horizontal cells also provide feedforward GABAergic inhibition to bipolar cell dendrites (Herrmann et al., 2011; Yang and Wu 1991). Lateral inhibition appears to be the primary function of horizontal cells, with a gap-junction coupled network of horizontal cells sampling from an extensive array of photoreceptors to subtract ambient light levels from local light responses. This lateral inhibition is thought to generate, in combination with inner retinal inhibition (Shields and Lukasiewicz 2003), the center-surround organization of the receptive fields. Gain control in response to changing ambient illumination and colour opponency also appears to be products of horizontal cell lateral inhibition (reviewed in Thoreson and Mangel 2012). Lateral inhibition in the inner retina commonly utilizes Na_v channels to facilitate rapid signaling (e.g. Chavez et al., 2010; Cook and McReynolds, 1998; Shields and Lukasiewicz, 2003), suggesting the possibility that circuits within the outer retina might employ Na_v channels in a similar fashion.

There is some evidence for Na_v channels in horizontal cells. Horizontal cells from mice demonstrated small Na_v currents (Schubert et al., 2006) and more prominent currents blocked by TTX (Liu et al., 2016; Fig. 1). Isolated horizontal cells from rabbit (Lohrke and Hofmann, 1994) and cat (Ueda et al., 1992) both show Na_v channels in at least a subset of horizontal cells. Mouse and rat horizontal cells show $Na_v1.2$ and $Na_v1.6$ by immunohistochemistry in both cell bodies and processes, with additional expression of $Na_v1.1$ in rabbits (Mojumder et al., 2007). Cat and monkey horizontal cells also show immunostaining with a non-specific Na_v channel antibody (Miguel-Hidalgo et al., 1994). In lower vertebrates, Martin et al. (1996) report a TTX-sensitive Na_v channel in turtles and isolated horizontal cells from teleosts have a large sodium current (Shingai and Christensen, 1983), but both are not thought to spike under normal conditions (Lasater, 1986; Shingai and Christensen, 1986). Instead, Na_v currents increase the depolarizing

overshoot following offset of light stimuli (Lasater, 1986; Davis and Linn, 2003a). An additional level of complexity was added to this story by Davis and Linn (2003a) who showed that NMDA receptor activation produces a long-term down regulation of Na_v and Ca_v currents, likely via calcium-induced calcium release (Linn and Davis, 2003b). In mammalian retina, this method of Na_v channel modulation is unlikely to operate given the evidence against NMDA glutamate receptor expression (Mouse: Hack et al., 2001; Schubert et al., 2006; Stroh et al., 2013, Rabbits: Blanco and de la Villa, 1999; Hack et al. 2001).

Overall these results, based largely on morphological analysis and with limited physiological evidence for the expression of Na_v channels, combined with no evidence for horizontal cell spiking, suggest that in mammalian horizontal cells Na_v currents operate by amplifying analog currents rather than by playing a role in spike generation. One caveat is that in cone bipolar cells a majority of cells did not spike in response to light flashes (Saszik and DeVries, 2012) but did spike consistently in response to a flickering light pattern designed to briefly hyperpolarize the cell relieving Na_v channel inactivation, raising the possibility that horizontal cell spikes may only be revealed by an as yet untested flickering stimulus. Future work may thus reveal specific stimuli or ambient light conditions that allow Na_v channel-driven spiking in response to light in horizontal cells.

2.1.3 Bipolar cells

The segregation of signals resulting from the onset of a light stimulus (ON cells) vs. the offset of a light stimulus (OFF cells) first occurs in the dendrites of the cone bipolar cells, the second-order retinal neurons. Expression of mGluR6, a metabotropic glutamate receptor (Masu et al., 1995) coupled to transient receptor potential cation channel subfamily M member 1 (TrpM1) channels (Morgans et al., 2009; Koike et al., 2010) in ON cells and ionotropic α-amino-3-hydroxy-5-methyl-4-isoxazolepropionic acid (AMPA) or kainate-sensitive glutamate receptors in OFF cells (DeVries 2000; Li and DeVries 2006; Borghuis et al., 2014; Puthessary et al. 2014) differentiates the ON

and OFF pathways. An array of approximately 12 cone bipolar cell types (CBCs), of both the ON and OFF variety, pool responses from a smaller number of cones (Helmstadtler et al., 2013; Wassel et al., 2009; Breuninger et al., 2011; Ichinose et al., 2014). On the other hand, the primary rod pathway includes a single type of ON-bipolar cell (RBC), which collects responses from many rods, thereby increasing the sensitivity of the low light pathway (Dunn et al., 2006). Together, these various bipolar cell types ensure that signals from various sources remain properly segregated.

It is now established that light responses within a type (ON vs. OFF) of cone bipolar cell exist on a spectrum from tonic (sustained for the duration of the stimulus) to phasic (a transient response near the onset of the stimulus). In the ON pathway, sustained and transient subtypes have different responses to the mGluR antagonist (RS)- α-cyclopropyl-4-phosphonophenylyglycine ((RS)-CPPG; Awatramani and Slaughter 2000) and agonist L-(+)-2-Amino-4-phosphonobutyric acid (L-AP4; Ichinose et al., 2014). However, a molecular mechanism underlying this difference has not been described. In the OFF pathway, it was initially suggested that differences in sustained vs. transient cells may be due to expression of AMPA receptors in transient cells and kainate receptors in sustained cells, primarily based on results from ground squirrel retina (DeVries 2000; Li and DeVries 2006). In the mouse retina, Borghuis et al. (2014) showed that kainate receptors drive both sustained and transient bipolar cell responses, similar to results from the primate retina (Puthessery et al., 2014). However, Ichinose and Hellmer (2016) found that while all OFF CBCs have at least a small kainate receptor component, these cells also have a significant AMPA contribution (~50%). Multiple other contributing factors have been suggested to support the cone bipolar cell tonicity. For instance, modifiers of glutamate receptor dynamics (Cao et al., 2012), differences in axonal calcium dynamics (Baden et al., 2013), and amacrine cell input (Eggers and Lukasiewicz 2011; Nirenberg and Meister 1997; Dong and Hare 2003) have all been suggested as contributing to tonicity.

Classically, both RBCs and CBCs were considered to carry analog signals only; however, in the last 15 years, evidence from a range of experimental techniques and in a number of model species (fish, amphibians, rodents and primates) has demonstrated the

presence of Na_v channels and in some cases, temporally-precise spiking in a subset of CBCs. Na_v channels were first found in rat (Pan and Hu 2000) and fish (Zenisek et al. 2001) bipolar cells, around the same time that it was demonstrated that fish bipolar cells could generate calcium spikes (e.g. Burrone and Lagnado, 1997). These results implied for the first time that at least some CBC subtypes use a combination of graded and binary signaling. Further work (Ma and Pan 2005) in isolated bipolar cells identified TTX-sensitive spikes in a subset of CBCs. Later work in rats (Cui and Pan 2008) identified two types of Na_v-containing bipolar cells that spiked following current injection ramifying in the middle of the inner plexiform layer.

First, they reported that rat ON-type CBCs with axons ramifying in inner plexiform strata 3 (their type 3a and 3b cells) can be split into two groups on the basis of Na_v channels expression and depolarization-induced spiking. These cells appeared to be identical morphologically to type 5 CBCs in rat (Euler & Wässle, 1995) and mice (Ghosh et al., 2004; Ivanova & Müller, 2006). Second, OFF CBCs with axons terminating in sublamina 2 proximal to the OFF cholinergic band also expressed Na_v channels (CB2, equivalent to type 3 CBCs in rats: Euler & Wässle, 1995 and mice: Ghosh et al., 2004; Pignatelli & Strettoi, 2004; Ivanova & Müller, 2006). Unlike CB3a cells, which consistently spiked, CB2 cells rarely spiked. Further work in ground squirrel (Sazsik and Devries, 2012) and primates (Puthessery et al., 2014) generally confirmed and extended these initial findings.

Until recently, there was no direct *in vitro* evidence for Na_v channels or TTX-sensitive spikes on mouse CBCs. In fact, Trenholm et al. (2012) and Ichinose et al. (2014) did not record spiking activity in mouse ON CBCs, in contrast to AII amacrine cells (Trenholm et al., 2012). This may be accounted for by the fact that in both cases, recording pipettes did not contain creatine phosphate, which prevents rapid rundown of spikes during whole cell recording (Baden et al., 2011). Supporting a role for Na_v channels in mouse CBCs, Baden et al. (2013) recorded fast calcium transients similar to spikes found in fish cells; however, it was not reported whether these spikes were Na_v-channel dependent. Other evidence for the presence of Na_v channels in ON CBCs includes the fact that the ERG b-wave, which is derived from the light evoked activity produced by these cells, is reduced following treatment with TTX even when the cone to

ON CBC circuit is essentially isolated by ionotropic glutamate receptor blockers (Rats: Bui & Fortune, 2004, 2006; Mojumder et al., 2007; 2008; mice: Miura et al., 2009; Smith and Côté, 2012; Smith et al., 2013).

2.1.4 Amacrine cells

As a population, amacrine cells provide inhibition in the inner plexiform layer, typically receiving input from bipolar cells and providing reciprocal feedback (e.g. Chavez et al., 2006; Grimes et al., 2010; Molnar and Werblin 2007a,b) or feedforward lateral inhibition to bipolar cell terminals (e.g. Lukasiewicz & Werblin, 1990; Eggers and Lukasiewicz, 2006, 2010; Eggers et al. 2007), as well as nested or serial inhibition to other amacrine cells (e.g. Eggers et al., 2007; Eggers and Lukasiewicz, 2010; Hsueh et al., 2008), or direct inhibition of RGCs (e.g Wei et al., 2011; Briggman et al., 2011; Yonehara et al., 2011**)**. Other specialized amacrine cells, generally types with large dendritic arbors, are important in global release of neuromodulators (reviewed in Brecha 2004).

Amacrine cells are commonly categorized based on the spread of their dendritic arbors (reviewed in Werblin 2011) into narrow, medium and wide field cells. Narrow-field amacrine cells (lateral dendritic spread <100 μm) much like bipolar cells, are able to use graded signals because the restricted extent of their dendritic arbor prevents signal degradation. Functionally, narrow-field amacrine cells tend to stratify in many strata of the IPL and use glycine as a primary neurotransmitter (Werblin, 2011). Input to these cells tends to be derived either from the ON or OFF pathway but not both. This, in combination with stratification that crosses the ON-OFF boundary in the IPL, suggests that narrow-field cells support crossover inhibition from the ON to OFF pathway and vice-versa (e.g. Munch et al., 2009; Molnar et al., 2009; reviewed in Werblin 2011). This speculation is borne out in the AII amacrine cell subtype that receives input from both rod bipolar cells and electrically-coupled ON cone bipolar cells and inhibits both OFF cone bipolar cells and OFF RGCs (e.g. Munch et al., 2009; Manookin et al., 2008; Murphy and Rieke, 2006; Manookin et al., 2010).

Medium-field amacrine cells (~200 μm lateral dendritic spread) tend to be GABAergic (Chen et al., 2010) and multistratified (reviewed in Werblin 2011). Functionally, there is evidence that GABAergic lateral inhibition both augments horizontal cell derived center-surround inhibition generated by horizontal cells in the outer retina (Ichinose and Lukasiewicz 2005; Zaghloul et al. 2007; Russell & Werblin, 2010) as well as nested, or serial inhibitory circuitry between amacrine cells to form disinhibitory circuits (e.g. Eggers et al., 2007; Eggers and Lukasiewicz, 2010; Murphy-Baum and Taylor 2015).

Wide-field amacrine cells with extensive dendritic arbors, in some cases nearly spanning the whole retina, generally require action potentials to prevent signal degradation. They tend to ramify in a single strata of the inner plexiform layer, primarily use GABA as a neurotransmitter and have dendritic arbours > 1000 μm in width. At least 11 subtypes of wide-field amacrine cell have been described morphologically (Lin and Masland, 2006), however, because the wide-field amacrine cells are typically sparse to prevent overlap of their extensive dendritic fields, this survey may have missed some subtypes (Masland et al., 2012). In addition to massive dendritic arbors, they are often electrically coupled (Völgyi et al., 2001), resulting in very wide spread modulation of visual function (e.g. Werblin 2011).

The ability to generate action potentials has long been considered to link form and function in amacrine cells. In general, wide-field amacrine cells are much more likely to generate action potentials, driving neurotransmitter release over large patches of retina. For instance, Bloomfield (1992) demonstrated a correlation between spiking amacrine cells and their dendritic field size: amacrine cells with a dendritic field size > 436 μm exhibit spike activity. However, although the trend for wide-field amacrine cells to spike was conserved, in other studies some medium and narrow field amacrine cells also spiked. In tiger salamander for instance, Heflin and Cook (2007) found that more narrow-field than wide-field cells fired single action potentials while wide-field cells were more likely to show sustained spiking. Although small- and medium-field amacrines can produce trains of action potentials in some cases (Heflin and Cook 2007), there is accumulating evidence that they may use Na_v channels in unconventional, i.e

non-spiking, ways, particularly AII and vesicular glutamate transporter type 3 positive (VGLUT3+) cells, two atypical amacrine cells that act as intermediates in the excitatory pathway. In addition to producing single spikes, Na_v channels have also been implicated in boosting the graded responses of amacrine cells in a range of species (Fish: Wantanabe et al. 2000, rabbit: Bloomfield 1996; rat: Koizumi et al., 2001). Some cells (most notably AIIs; see below and Miller et al., 2006) produce spikelets, which have strong similarities to dendritic spiking in RGCs, (Trenholm et al., 2014, Sivyer and Williams 2013; Oesch et al., 2005; Velte and Masland 1999).

Given the number of amacrine cell types a distinct morphology has been historically required to explore the intrinsic properties and network interactions of amacrine cells. The better understood amacrine cell subtypes, for example the AII, starburst, polyaxonal, and A17 cells, all have such distinctive morphologies. However, in the past 15 years fluorescent protein expression driven by cell-type specific promoters has made similar explorations possible in cell types with less distinctive morphologies, e.g. dopaminergic, VGLUT3+, and VIP positive amacrine cells (Park et al., 2015; Akrouh and Kerschensteiner 2015). Of the amacrine cell types with relatively well-described intrinsic and network properties, five (AII, starburst, polyaxonal, VGLUT3+, and dopaminergic amacrine cells) contain Na_v channels, while there is evidence for spatially restricted processing facilitated by the low density of dendritic Na_v channels in A17 cells (Grimes et al., 2010) and little evidence either way in the three types of VIP expressing amacrine cells (Park et al., 2015; Akrouh and Kerschensteiner 2015). Because of the increase in subtype-specific expression of fluorescent proteins reviewing in any detail the known circuitry and synaptic partners of all well-studied amacrine cell types would be quite expansive. More specific details about the AII, Starburst, Dopaminergic, Polyaxonal and VGLUT3+ amacrine cells can be found in Appendix 1.

2.1.5 Retinal Ganglion Cells

RGCs integrate synaptic inputs from bipolar and amacrine cells and, in combination with their intrinsic properties, these inputs generate a time varying pattern of

spikes that propagate to higher visual centers. In general, RGCs are either feature detectors tuned to respond to specific aspects of visual scenes (reviewed in Field and Chinchilnisky, 2007; Masland et al., 2012; Sanes and Masland, 2015; but see Baden et al., 2016), or simply encode the brightness of a single section of the visual field (e.g. midget ganglion cells, Dacey et al., 1993; Zhang et al., 2012). Visual features range in complexity from ambient light levels (intrinsically photosensitive RGCs, Berson et al., 2002) to directional motion (reviewed in Vaney, 2012), separating the visual field into between 12 and 30 parallel channels (Roska and Werblin, 2001; Baden et al., 2016). Integration of synaptic input and translation to a pattern of spikes occurs at the axon initial segment (AIS), a thin unmyelinated region of axon stretching between the axon hillock and the initial myelinated section of the optic nerve (reviewed in Rasband 2010; Kole and Stuart 2012). The AIS is relatively stereotypical within polarized neurons, containing $Na_v1.1$, 1.2, and 1.6 channels (Boiko et al., 2003; Van Wart et al., 2007; Duflocq et al., 2008; Hu et al., 2009), targeted to the AIS with Ankyrin G (Zhou et al., 1998) at high density (e.g. Hu et al. 2009, Lorincz and Nusser 2010).

Like amacrine cells, expression of fluorescent reporters in specific types of retinal ganglion cells in combination with connectomics, population-wide recording with multielectrode arrays and genetically encoded calcium indicators, has yielded a rapidly expanding body of knowledge on all aspects of RGC form and function. An excellent recent review elaborating the function and connectivity of classically studied cells (e.g. α ON, OFF sustained and OFF transient cells) as well as elaborating more recently defined subtypes (e.g. suppressed by contrast a.k.a uniformity detector cells) can be found in Sanes and Masland (2015). Because all RGCs must use Na_v channel-dependent action potentials to communicate via the optic nerve and because there is little consistent evidence that Na_v channel distribution varies between RGC types, I will focus here on the role of Na_v channels in RGCs in general. A more circuit-based approach to Na_v channel function in the input to RGCs (in particular the local edge detector or W3B subtype) is contained in appendix 2.

The distribution of Na_v channels in ganglion cell AIS (Wollner and Catteral 1986; Van Wart et al., 2007; Schaller and Caldwell, 2000, Van Wart and Matthews 2006; Boiko

et al., 2001; 2003) and their contribution to spiking has been extensively studied and is well understood in comparison to the roles of Na_v channels in the more distal retina (Fohlmeister and Miller 1997; Fohlmeister et al., 1990; Carras et al., 1992; Sheasby and Miller 1999; Hidaka and Ishida, 1998; Stys et al., 1993), particularly in the context of RGC responses to extracellular stimulation by prosthetics (Fried et al., 2009; Tsai et al., 2011; Eickenscheidt and Zeck 2014). However, in addition to the role of integration at the AIS there is recent evidence, particularly in directionally selective (DS) RGCs, that Na_v channels in may play additional roles in active dendritic signaling (Fohlmeister and Miller, 1997; Velte and Masland, 1999; Tayor et al, 2000; Sivyer and Williams 2013; Trenholm et al., 2014; Trenholm et al., 2013; Oesch et al., 2005; Hidaka et al., 2004).

In the relatively well-studied ON- (Sivyer and Williams 2013) and ON-OFF DS cells (Oesch et al., 2005 Trenholm et al., 2014; Trenholm et al., 2013) Na_v channels support active dendritic conductance. In ON-OFF DS cells dendritic spikelets enhance directional selectivity by initiating somatic spikes (Oesch et al., 2005). Interestingly, in the HB9+ subtype of ON-OFF DS cells, Na_v dendritic channels play an obligatory role in fine scale synchrony by allowing backpropagation of somatic action potentials to pass through electrical synapses to neighbouring cells. The combination of backpropagating dendritic spikelets and temporally coincident synaptic input triggers somatic action potentials in neighbouring cells with high synchrony (Trenholm et al., 2014). ON DS cells also show dendritic spikes, which act in conjunction with starburst amacrine cells (SBAC) inhibition to reduce spikes in response to null direction movement (Sivyer and Williams 2013).

A number of papers have suggested that intrinsic properties of RGCs play a minor role at most in controlling kinetics of the light response. Baylor and Fettiplace (1979) show that regardless of a cells light response, a current step elicits a sustained spiking response. Similar results were obtained from a range of studies on salamander (Diamond and Copenhagen 1995; Sheasby and Fohlmeister 1999), ferret (Wang et al., 1997) and goldfish (Vaquero et al., 2001) with current injections driving primarily sustained responses in most RGCs. Amongst cat RGCs, only theta cells showed transient responses to current injection, surprisingly, however, these cells have sustained light responses

(O'Brien et al., 2002). Recordings from rat using similar methods (Wong et al., 2012) showed sustained responses to current injection in every cell type tested.

Nevertheless, there is some evidence that intrinsic properties of RGCs may determine whether they generate transient or sustained responses. In goldfish Tabata and Kano (2002) showed that whole-cell recording can make spiking responses to current injection markedly more sustained compared to using a perforated patch. This explains differences with previous results in goldfish (Vaquero et al., 2001) and potentially the general predominance of sustained responses to current injection. In mouse retina, Qu and Myhr (2008) found both transient and sustained responses to sustained depolarization, albeit from immature (P20-24) RGCs. Similarly, optogenetic stimulation of mouse RGCs drives sustained and transient responses from synaptically isolated cells (Thyagarajan et al., 2010, see Fig. 6; Pan et al., 2014).

Does the heterogenous expression of Na_v channel isoforms govern intrinsic excitability of RGCs? In general, there is widespread evidence for variances in intrinsic excitability of RGCs, as I detail below. However, whether tonicity is a function of intrinsic excitability and whether Na_v channels are responsible for differences in excitability remains an open question. In fact, in the retina, evidence for Na_v channel contributions to RGC intrinsic excitability are rare. First, the genetic elimination of $Na_v1.6$ causes reduced maximum sustained (~30%) and instantaneous firing rates in RGCs; however, RGCs retain the ability for sustained firing albeit at reduced rates (Van Wart and Matthews 2005). In addition, when channelrhodopsin-2 is targeted to the axon initial segment with the Ankyrin-G binding motif and disrupts the spatial organization of Na_v channels, channelrhodopsin-2 responses shift from predominately sustained to predominately transient (Zhang et al., 2015).

To begin addressing this question, it is important to know how different RGC subtypes differ in excitability. In mouse, both sustained and transient OFF- but not ON-alpha ganglion cells show maintained activity during synaptic block (Detwiler and Margolis 2007) and there is a pronounced difference in spike rate (transient cells: ~20 Hz; sustained cells ~40 Hz), suggesting that a difference in intrinsic properties may contribute to the light responses of these cells. Although direct proof for this hypothesis hasn't yet been obtained, persistent Na_v current was suggested to play a role in the

differences between alpha cell types (Detwiler and Margolis, 2007) and different Na_v channel isoforms have different capabilities to support persistent current (e.g. Rush et al., 2005; Chen et al., 2008). In rabbits, directionally-selective cells differ from brisk-transient and local-edge detectors in the size of an axonal low threshold region that seems similar to the AIS (Fried et al., 2009). The size of this region is inversely proportional to the threshold for electrical stimulation (Fried et al., 2009).

On the other hand in rabbit (but not in mice) ON-cells have a lower threshold than OFF-cells (Jensen and Rizzo 2006 vs. Jensen and Rizzo 2009). Additionally no difference can be observed in spiking patterns in response to stimulation between ON- and OFF- parasol RGCs in primates (Sekirnjak et al., 2008) and spike waveforms from the 5 most prominent cell types in primate retinas (ON- and OFF-parasol, ON- and OFF-midget, and small bistratified cells) show obvious differences in spike waveform, but not in response probability as a function of stimulus amplitude (Jepson et al., 2013). Clearly differences in RGC excitability and underlying causes are an interesting open question in retinal physiology.

2.2 The Voltage-gated sodium channels

Voltage-gated sodium channels (Na_v channels) are a family of proteins known primarily for generating the rising phase of action potentials, the basis of binary communication in the nervous system. This thesis uses Na_v channels as a tool to interrogate retinal function rather than studying the biophysics of the Na_v channel isoforms in depth. Here I focus on the physiological differences between Na_v channel isoforms expressed in heterologous expression systems as well as, in the case of $Na_v1.6$, the effects of a 'null' mutation, ie. a naturally occurring mutation resulting in complete loss of function*, of isoforms on spiking responses in neurons. Briefly, Na_v channels are a family of proteins composed of a pore forming α subunit, sufficient for functional expression in heterologous expression systems (e.g. Smith et al., 1998), and a modulatory β subunit. Na_v channel α-subunits open upon depolarization from negative membrane

* The work presented here uses naturally occurring $Na_v1.6$ mutant mice (*Scn8a*^{dmu}, DeRepentigny et al., 2001; Côté et al., 2005). However, since the literature on $Na_v1.6$ and other Na_v channels makes use of models harbouring a variety of both artificial and natural genetic lesions, for simplicity the word 'knockout' is used to generally designate both types of null mutations.

potentials and inactivate within a few milliseconds, creating a large but transient depolarizing current that contributes to the initiation of action potentials. In addition to the transient Na_v current underlying the rising phase of action potentials, some Na_v channel isoforms support a steady-state, non-inactivating, or persistent current (French et al., 1990; Cepeda et al., 1995; Smith et al., 1998; Rush et al., 2005; Osorio et al., 2010) that plays a role in initiating action potentials near threshold (Crill, 1996) and may support repetitive firing (e.g. Royeck et al., 2008). Persistent Na_v current is known to play a role in amplifying EPSCs (Deisz et al., 1991; Stuart and Sakmann, 1995; Schwindt and Crill 1995; Carter et al., 2012; Gonzalez-Burgos and Barrioneuvo 2001) and IPSCs (Stuart, 1999; Hardie and Pearce 2006) in CNS neurons.

As well as transient and persistent Na_v currents, some Na_v channels open transiently during recovery from inactivation (resurgent currents: Raman and Bean, 1997; Raman et al., 1997; Lewis and Raman 2014) in response to repolarizing steps to more negative potentials. Resurgent currents reactivate in response to mild repolarizations following depolarization to positive potentials. Resurgent currents may be important in determining neural firing patterns (ISI, regularity) in Purkinje cells (Raman and Bean, 1997) and may be useful for allowing high frequency spiking (Raman & Bean, 2001; Aman & Raman, 2007, 2010) by circumventing fast inactivation. In addition, resurgent currents may be important for sustained firing by reducing the effect of cumulative inactivation (Kaliq et al., 2003; reviewed in Lewis and Raman 2014). Using global and tissue-specific knockout mice in combination with immunohistochemistry, electrophysiology and computational modeling has lead to increased understanding of the functional role of individual α-subunit isoforms in a range of neurons, particularly $Na_v1.1$ and 1.6 in Purkinje cells and hippocampal GABAergic interneurons.

There are ten different Na_v channel α subunits and while there appear to be relatively small functional differences between subtypes studied in isolation (Chen et al., 2008; Rush et al., 2005; Smith et al., 1998; Smith et al., 1998; Also see Table 1), both temporal expression patterns and selective expression of isoforms on multiple scales ranging from tissues to intracellular distribution within neurons (e.g. Van Wart and Matthews 2006a,b; Boiko et al,. 2001, 2003) suggest that isoforms are functionally

unique. Mammalian retinas express at least 6 Na_v channel α subunit isoforms (Na_v1.1, 1.2, 1.3, 1.6, 1.8, and 1.9) (Mojumder, et al., 2007; O'Brien, et al., 2008; Fjell et al., 1997) with what appears to be specific and restricted expression. Such restricted expression occurs both in terms of cell types expressing specific Na_v channel isoforms, and in temporal patterns of Na_v channel isoform expression during development (e.g. shifts from Na_v1.2 to 1.6 in RGC axon initial segment (Boiko et al., 2001; 2003). Examples of retinal cell type-specific expression include AII amacrine cells (Kaneko et al., 2007; Wu et al., 2011) and primate DB3a and DB4 cone bipolar cells (Puthussery et al., 2013), which express Na_v 1.1, while Na_v1.8 is expressed in starburst amacrine cells and a subset of RGCs (O'Brien et al., 2008). Again, the precise expression patterns of individual Na_v channel subtypes suggest the possibility that Na_v channel expression is a factor in differentiating parallel pathways through the retina.

When individual α subunits are expressed in *Xenopus* oocytes small differences in isoform function and modulation can be appreciated (See Table 1). Most of the heterologous expression studies have focused on Na_v1.1, 1.2, and 1.6, key Na_v channel isoforms in CNS neurons (Westenbroek et al., 1989; Trimmer and Rhodes, 2004). Na_v channels have three possible states; resting (closed), activated (open), and inactivated (closed and temporarily unable to open in response to maintained depolarization), and typical electrophysiological experiments on the characteristics of individual isoforms are designed to discover differences in the transitions between these states.

To represent the relationship between membrane voltage and current flow, a cell is held at a hyperpolarized holding potential (typically -100 mV) and depolarizing voltage steps open a certain percentage of the Na_v channel population allowing a given amount of current to flow. Pre-pulses of depolarizing voltage steps inactivate a given percentage of the Na_v channel population and reduce the amount of current in response to a test pulse, creating an inactivation curve that measures the fast inactivation properties of the Na_v channel isoform. Inactivation of Na_v channels has a fast and a slow component, while the mechanism of fast inactivation is generally thought to be due to a tethered particle (e.g. Armstrong and Bezanilla 1977; Vassilev et al., 1988), slow inactivation is less well understood. To explore the Na_v channel kinetics, the heterologous expression studies

performed to date have focused on activation and fast and slow inactivation as well as the analysis of transient, persistent and resurgent sodium currents.

When expressed in oocytes, $Na_v1.1$ and $Na_v1.2$ share many electrophysiological properties (Smith and Goldin, 1998) especially when co-expressed with β subunits. $Na_v1.1$ and $Na_v1.2$ have similar activation curves but fast inactivation occurs at more positive potentials for $Na_v1.1$, an effect more pronounced with β subunit co-expression. $Na_v1.1$ also recovers from inactivation faster than $Na_v1.2$. When expressed in the tsA201 human embryonic kidney (HEK) cell variant, Chen et al., (2008) report that the kinetics and voltage dependence of activation and fast inactivation of $Na_v1.1$ and $Na_v1.2$ cells are basically identical. Differences between $Na_v1.6$ vs. $Na_v1.1$ and $Na_v1.2$ seem to depend both on the model system used and co-expression of β subunits.

In most cases (e.g Smith et al., 1998; Patel et al., 2015; Chen et al., 2008), peak transient sodium currents were similar between $Na_v1.1$, $Na_v1.2$, and $Na_v1.6$; however in dorsal root ganglion (DRG) cells, direct comparison of $Na_v1.2$ and 1.6 shows that $Na_v1.6$ generates a larger peak sodium current (Rush et al., 2005). When $Na_v1.2$ and $Na_v1.6$ are compared across groups in early experiments expressing single Na_v channel isoforms (Burbidge et al., 2002; Dietrich et al., 1998), $Na_v1.6$ activated and tended to inactivate at more hyperpolarized potentials. When compared directly in *Xenopus* oocytes, $Na_v1.6$ activated at more depolarized potentials and inactivated at more hyperpolarized potentials relative to $Na_v1.1$ and $Na_v1.2$ but these differences are reduced in the presence of β subunits (Smith et al., 1998). In a more recent oocyte study, $Na_v1.2$ activation and fast inactivation curves occur at more positive potentials than $Na_v1.6$ (Lee and Goldin, 2008) but again the expression of β subunits reduces these differences.

In contrast to studies in oocytes, in the tsA201 HEK cells the voltage dependence of activation and fast inactivation are essentially identical between $Na_v1.2$ and $Na_v1.6$ (Chen et al., 2008). When $Na_v1.1$ and $Na_v1.6$ are compared in HEK cells, they have similar voltage dependence of activation and similar peak current amplitudes; however the voltage dependence of fast inactivation is slightly hyperpolarized for $Na_v1.6$ and $Na_v1.6$ recovers from fast inactivation more quickly (Patel et al., 2015). In cultured DRG neurons, the voltage dependence of activation and fast inactivation is hyperpolarized for

$Na_v1.6$ relative to $Na_v1.2$ (Rush et al., 2005). Slow inactivation occurs faster for $Na_v1.6$ than for $Na_v1.2$ in both oocytes and cultured dorsal root ganglion cells (Lee and Goldin 2008; Rush et al., 2005) and slow inactivation of $Na_v1.6$ occurs at relatively depolarized voltages relative to $Na_v1.2$ making it potentially more resistant to slow inactivation at physiologically relevant membrane potentials (Chen et al., 2008).

All of the common CNS Na_v channel isoforms can support some level of persistent sodium current ($Na_v1.6$; Smith et al., 1998; Rush et al., 2005; Chen et al., 2008; but see Burbidge et al., 2002; $Na_v1.2$: Rush et al., 2005 but see Chen et al., 2008; $Na_v1.1$: Smith et al., 1998), however, while $Na_v1.6$ has a prominent persistent current that increases with depolarization (Smith et al., 1998; Burbidge et al., 2002) the persistent current derived from $Na_v1.1$ channels decreases with voltage (Smith et al., 1998). The persistent current supported by $Na_v1.2$ is quite small in all three studies, varying from roughly half that of $Na_v1.6$ (Rush et al., 2005) to ~$1/10^{th}$ (Chen et al., 2008; Smith et al., 1998).

Like with persistent current, all three CNS Na_v channel isoforms are able to support some level of resurgent current in at least one study although there are caveats in many cases ($Na_v1.6$: Smith et al., 1998; Rush et al., 2005; but see Burbidge et al., 2002 and Chen et al., 2008; $Na_v1.2$: Rush et al., 2005 but see Chen et al., 2008; $Na_v1.1$: Smith et al., 1998; Patel et al., 2015). All three isoforms produced a current resembling resurgent current in *Xenopus* oocytes (Smith et al., 1998) however this may just be a consequence of persistent current and not a true resurgent current. Both $Na_v1.2$ and 1.6 produced resurgent current but resurgent current derived from $Na_v1.6$ was larger and more $Na_v1.6$ transfected cells showed resurgent currents (Rush et al., 2005). However, there is no resurgent current in $Na_v1.6$ expressing tsA201 cells even with coexpression of a β subunit (Chen et al., 2008). Both $Na_v1.1$ and $Na_v1.6$ produce persistent current in HEK293 cells in the presence of a β subunit with peak resurgent currents produced by $Na_v1.6$ being roughly twice as large as Nav1.1 currents.

Even given the differences in recording protocols and between heterologous expression systems there are some consistent differences between commonly expressed CNS Na_v channel isoforms. In terms of the voltage dependence of activation and

inactivation $Na_v1.1$ and $Na_v1.2$ are more similar to each other than to $Na_v1.6$ (e.g. Smith et al., 1998) but these differences are reduced in the presence of β subunits and vary between expression systems. $Na_v1.6$ consistently produces larger persistent and/or resurgent currents relative either to $Na_v1.2$ (Rush et al., 2005; Chen et al., 2008) , $Na_v1.1$ (Patel et al., 2015), or either (Smith et al., 1998). $Na_v1.6$ is better able to sustain repetitive firing (Rush et al., 2005) than $Na_v1.2$, possibly due to resistance to slow inactivation (Chen et al., 2008). However, $Na_v1.6$ undergoes more use dependent reduction relative to $Na_v1.1$, consistent with the hypothesis that $Na_v1.1$ plays a role in maintained fast firing (Patel et al., 2015).

In addition to commonly expressed TTX-sensitive Na_v channel isoforms there is evidence for the retinal expression of TTX-resistant Na_v channel isoforms ($Na_v1.8$; $Na_v1.9$) typically expressed in the peripheral nervous system (O'Brien et al., 2008; Smith et al., 2016). In heterologous expression systems $Na_v1.8$ and $Na_v1.9$ have very distinct physiological properties the most prominent being very slow inactivation kinetics, a persistent sodium current, and a substantially more depolarized voltage dependence of activation (Vijayaragavan et al., 2001, Akopian 1996). This means that $Na_v1.8$ is relatively resistant to inactivation when the neuron is depolarized. In combination with β subunits $Na_v1.8$ inactivates more quickly than $Na_v1.7$ (Vijayaragavan et al., 2001). In response to low (<25 Hz) repetitive stimulation the current conducted by $Na_v1.8$ channels is reduced substantially, in contrast to $Na_v1.7$, which exhibits only ~10% reduction in current at stimulation frequencies below 25 Hz. However, in response to repetitive stimulation at 100 Hz $Na_v1.8$ can support ~15% larger currents than $Na_v1.7$.

In opposition to relatively small physiological differences between Na_v isoforms, there is substantial anatomical evidence for isoform specificity. In general: $Na_v1.1$, 1.2, 1.3, and 1.6 are expressed in CNS neurons, $Na_v1.4$ in skeletal muscle; $Na_v1.5$ in heart; $Na_v1.7$, $Na_v1.8$, and 1.9 in PNS neurons (Catterall, 2000; Goldin et al., 2000; Goldin, 2001; Trimmer and Rhodes, 2004). Within retinal cell types, Na_v 1.1 is expressed in AII amacrine cells (Kaneko et al., 2007; Wu et al., 2011) and primate DB3a and DB4 cone bipolar cells (Puthussery et al., 2013) and $Na_v1.8$ is present in starburst amacrine cells and a subset of retinal ganglion cells (O'Brien et al., 2008). Within RGCs, there is

remarkable intracellular specificity of expression (e.g. $Na_v1.1$, 1.2 and 1.6 are expressed in the AIS while nodes of Ranvier express predominately $Na_v1.6$ (Schaller and Caldwell, 2000, Van Wart and Matthews 2006; Van Wart et al., 2007; Boiko et al,. 2001; 2003).

Similar examples of intracellular expression of Na_v channels have been explored, principally in pyramidal cells. For example, Lorincz and Nusser (2010) show that only $Na_v1.6$ is expressed in pyramidal cell dendrites and shows a pronounced gradient with decreasing concentration moving away from the soma, while Hu et al. (2009) suggest that polarized expression of $Na_v1.2$ (proximal) and 1.6 (distal) in the axon initial segment are necessary for initiating axonal action potentials ($Na_v1.6$) and action potential backpropagation to the soma ($Na_v1.2$). In RGCs, $Na_v1.6$ (Van Wart and Matthews 2006a,b; Boiko et al,. 2001; 2003) is linked to developmental increase in intrinsic excitability (e.g. Van Wart and Matthews 2006a), again arguing that subtype expression may control diverse aspects of neuronal function.

2.3 Physiological characteristics differentiating Na_v channels isoforms known to be expressed in the retina.

Mammalian retinas express at least 6 voltage gated sodium channel α subunit isoforms ($Na_v1.1$, 1.2, 1.3, 1.6, 1.8, and 1.9; Mujunber et al., 2007; O'Brien et al., 2008, fjell et al., 1997). As mentioned above, several studies have identified the very precise location of specific Na_v channel isoforms both to subtypes of cells and to intracellular regions. This suggests that expression of Na_v channel isoforms is linked to the intrinsic properties governing the cells translation of visual information. However, only a few studies have explored how the precise expression of Na_v channels affects retinal function and these studies have wholly focused on the function of $Na_v1.6$ (e.g. Van Wart and Matthews 2006; Côté et al., 2005). In this section, I will use the known properties of Na_v channel isoforms in other cell types to infer how they might augment retinal signalling.

2.3.1 $Na_v1.6$

Of the Na_v channel isoforms expressed in the retina, the majority of knockout studies have focused on $Na_v1.6$. $Na_v1.6$ is primarily located in the axon initial segment

and at nodes of Ranvier in myelinated axons (Schaller and Caldwell, 2000; Boiko et al., 2001; Boiko et al., 2003; Van Wart and Matthews, 2006; Van Wart et al., 2007; Lorincz and Nusser, 2008, 2010) as well as in dendrites (Krzemien et al., 2000; Lorincz and Nusser, 2010). While there are some notable exceptions, typically neurons lacking $Na_v1.6$ tend to show minor reductions in transient current, but substantial reductions in persistent, and resurgent sodium currents, correlated with deficits in maximal firing rate and repetitive firing, elevation of spike threshold and reduced spike gain and pacemaking. It has been suggested that the well-documented reductions in persistent and resurgent currents in many neuron types in the absence of $Na_v1.6$ directly cause changes in spiking output, in particular reductions in repetitive spiking and gain (Levin et al. 2006; Mercer et al. 2007; Raman et al. 1997).

As specific examples of $Na_v1.6$ function, peak transient sodium current was reduced in cerebellar Purkinje cells in global knockout mice by ~30-50% (Raman et al., 1997; Aman and Raman, 2007). However, in cell type specific knockouts targeting Purkinje cells (Levin et al., 2006) there was no significant change in peak transient current. There was also no change in transient currents in cerebellar granule cells (Osorio et al., 2010), trigeminal mesencephalic neurons (Enomoto et al., 2007), or hippocampal pyramidal cells (Royeck et al., 2008). The voltage dependence of activation is shifted to more positive potentials in hippocampal pyramidal cells (Royeck et al., 2008); however, shifts in the voltage dependence of activation are not observed following genetic deletion of $Na_v1.6$ in globus pallidus neurons (Mercer et al., 2007), cerebellar neurons (Raman et al., 1997) and mesencephalic trigeminal neurons (Enomoto et al., 2007). There is no shift in the voltage dependence of fast inactivation in hippocampal pyramidal cells (Royeck et al., 2008). In cell types without changes in voltage dependence of activation, inactivation is also normal; however, Raman et al., (1997) found that in the absence of $Na_v1.6$, Purkinje cells inactivate at more hyperpolarized potentials. On average, the absence of $Na_v1.6$ has only minor effects on transient sodium currents in neurons.

In contrast to the minor effects on transient sodium current, removing $Na_v1.6$ causes significant reductions in both persistent and resurgent currents across a broad range of neuronal subtypes. Reductions in resurgent current average around 70% in most cell types (Levin et al., 2006; Royeck et al., 2008; Mercer et al., 2007; Do and Bean,

2003; Enomoto et al., 2007; Cummins et al., 2005) with the only exception being cerebellar granule cells (Osorio et al., 2010). Adding to the evidence that $Na_v1.6$ is an important facilitator of resurgent sodium current, $Na_v1.8^{-/-}$ DRG cells transfected with $Na_v1.6$ produce resurgent currents while the DRG cells from $Na_v1.6$ KO mice lack resurgent current (Cummins et al., 2005). The persistent sodium current is also significantly reduced by ~ 40% in many (Osorio et al., 2010; Royeck et al., 2008; Do and Bean 2003; Enomoto et al., 2007; Maurice et al., 2001), but not all neuronal subtypes (e.g. Mercer et al., 2007).

The reductions in persistent and resurgent current in $Na_v1.6$ knockout mice can have significant implications on the function of the affected neurons. Purkinje cells have been a key model neuron for studying the contribution of $Na_v1.6$ to sodium currents and in turn spiking. Deficits in repetitive firing correlated with very reduced resurgent current have been reported in $Na_v1.6$ knockout by Raman et al., (1997), Aman and Raman (2007), and Grieco and Raman (2004). In one key study, Khaliq et al., (2003) combined modeling and electrophysiology to study the functional effects of loss of resurgent current on maintained firing in Purkinje cells. The absence of $Na_v1.6$ in Purkinje cells caused irregular and relatively slow spontaneous activity (~30% of control rate), reduced maximal (~50% of controls) and repetitive firing (~14% of controls) in response to depolarizing current, and spiking became noticeably more transient at higher current steps (their Fig. 2). This study suggested that resurgent current supported by $Na_v1.6$ is indispensable in supporting high frequency spiking.

Like in Purkinje cells, RGCs show reduced maximal firing rates (~30%) in $Na_v1.6$ knockout mice in response to depolarizing current (Van Wart and Matthews, 2006) as well as a reduced but not eliminated ability to maintain spiking in response to depolarizing current steps. In a detailed study of globus pallidus cells, which exhibit sustained high frequency spiking, Mercer et al., (2007) showed that, while essentially all sodium currents are normal in $Na_v1.6$ knockout mice, significant reductions in resurgent current cause ~50% reduction in maintained spiking, irregularity in spiking, increased spiking threshold, and an earlier failure to maintain spiking in response to increasing injected current ramps. Interestingly, however, the maximal spike rate was only reduced by ~25%. Lack of $Na_v1.6$ also causes significant changes in spiking in pyramidal cells

(Royeck et al., 2008), reducing evoked spiking by ~50%, delaying the time to first spike and reducing gain. In mesencephalic trigeminal neurons, the absence of $Na_v1.6$ causes profound changes in spiking response to depolarizing current (Enomoto et al., 2007). While normal mice have responses to 1 second current steps that are ~35% transient vs. sustained, $Na_v1.6$ knockout mice have ~30% of cells which respond with a single spike and ~55% have transient responses. This dramatic shift towards transient responses is also apparent in the number of spikes elicited by depolarizing current with maximal spike number for knockout mice of ~15% of controls. In contrast, in cerebellar granule cells where only persistent current is reduced in the absence of $Na_v1.6$, peak, spike rate and maintained firing are normal; however, firing did become more irregular (Osorio et al., 2010). In subthalamic nucleus cells, despite significant reductions in transient, resurgent and persistent currents, both spontaneous spiking and sustained spiking in response to depolarizing current is unchanged (Do and Bean 2004).

2.3.2 $Na_v1.1$

While a majority of knockout studies have focused on $Na_v1.6$ a few recent studies have looked at effects of knocking out $Na_v1.1$, a common retinal Na_v channel isoform. At P15 in $Na_v1.1$ KO mice, peak, persistent and resurgent Na_v currents were reduced between 58-69% in Purkinje neurons (Kalume et al., 2007) and peak transient current was reduced by a similar amount in GABAergic interneurons (Yu et al., 2006), without significant changes in the voltage dependence of activation or inactivation or action potential threshold. These findings fit with results from Raman and Bean (1997) and Khaliq et al. (2003) showing that in Purkinje cells, which express only $Na_v1.1$ and $Na_v1.6$, elimination of $Na_v1.6$ reduces peak transient Na_v current by ~30%.

There are notable changes in firing frequency and responses to prolonged current injection in all neuron types that have been recorded from in the absence of $Na_v1.1$. In Purkinje cells, spontaneous activity was slightly reduced (~20%) and firing in response to injected current was also reduced (~30%). Parvambumin positive interneurons from heterozygous mice with a knock-in loss of function mutation in $Na_v1.1$ showed more transient responses to a depolarizing pulse (Ogiwara et al., 2007). GABAergic interneurons also have more transient spike trains and reduced maximal firing (Yu et al.,

2006). Interestingly, there was no change in pyramidal cell function (Yu et al., 2006) but this may be due to low levels of $Na_v1.1$ expression in normal pyramidal cells (Ogiwara et al., 2007).

2.3.3 $Na_v1.2$

$Na_v1.2$ is the predominate Na_v channel in rat CNS in terms of protein expression (excluding the retina and optic nerve) (Gordon et al., 1987) and possibly because of this, $Na_v1.2$ mice suffer perinatal lethality at earlier ages than $Na_v1.1$ or 1.6 KO mice (Planells-Cases et al., 2000). Early mortality of $Na_v1.2$ knockout mice mostly precludes experiments similar to those done on $Na_v1.1$ and $Na_v1.6$ knockouts. However, in cultured hippocampal neurons isolated from newborn mice, peak sodium current is reduced by ~60% with a small depolarizing shift in the voltage dependence of activation and no significant changes in voltage dependence of inactivation. In retinal ganglion cells, there is a transition from early expression of $Na_v1.2$ to $Na_v1.6$ in the axon initial segment and nodes of Ranvier of the myelinated optic nerve (Boiko et al., 2001, Boiko et al. 2003), coincident with a shift to higher frequency firing that defines the mature neuron. Although there is a substantial reduction in peak sodium current after $Na_v1.2$ is eliminated, this may not be representative of the contribution of $Na_v1.2$ to mature neurons.

2.3.4 $Na_v1.8$

$Na_v1.8$ Knockout mice have no slow TTX-resistant currents in DRG cells (Akopian et al., 1999) and action potential electrogenesis in these cells is changed dramatically (Reganathan et al., 2001) despite the compensatory upregulation of TTX-sensitive Na_v channels (Akopian et al., 1999). Action potential generation is substantially reduced in a majority of $Na_v1.8$-deficient cells, although action potential thereshold is not significantly changed (Reganathan et al., 2001). Sustained depolarizing current can induce repetitive firing in the absence of $Na_v1.8$ but the pattern of spiking is changed, both in that spike trains either contain bursts rather than steady spiking, or the spike trains are more transient (Reganathan et al., 2001). Behaviourally these changes in

DRG spiking manifest themselves as slowed responses to noxious mechanical stimuli and to a lesser extent heat (Akopian et al., 1999).

2.3.5 Compensatory mechanisms

Caveats must be applied to the information that we do have about Na_v channel isoform function. Global $Na_v1.6$ mutants die at postnatal day 20-25 (P20-25), raising the possibility that our understanding is restricted to immature systems. For example, in cerebellar granule cells mature expression of $Na_v1.6$ is not reached until P35-40 (Osorio et al., 2010). In addition, mutants may not give an accurate view of the true function Na_v isoforms in normal animals because of the occurrence of adaptation and compensation throughout development. For example, it has been shown that the absence of $Na_v1.6$ can be compensated for by upregulation of $Na_v1.2$ in the optic nerve (van Wart et al, 2006, Vega et al., 2008) and by upregulation of calcium and potassium channels (Swensen et al., 2005). Nonlinear loss of sodium current in GABAergic hippocampal interneurons from $Na_v1.1$ KO mice also suggests compensation in KO mice (Yu et al., 2006) which has been confirmed by immunohistochemical visualization of $Na_v1.3$ upregulation.

2.4 Electroretinogram

Non-invasive *in vivo* electrophysiology provides one of very few links between our detailed knowledge of retinal circuitry in animal models and human retinal function. However, in contrast to the broad array of techniques available to interrogate retinal cell function directly *in vitro*, extra care must be taken in the interpretation of *in vivo* electrophysiology. For this reason, it is desirable to develop precise ways of blocking or modulating small sections of neural circuitry, for example by blocking Na_v channel isoforms expressed only in a subset of cells.

The electroretinogram (ERG) is a composite signal generated by the retina in response to light stimuli. Choice of stimulus and recording methods determine what retinal cell types can be observed, since contributions from some cell types can only be observed indirectly via changes in more strongly represented cells. A general rule of thumb is that radially extensive cells (e.g. bipolar cells) and their modulatory inhibitory

cells can readily be observed, while laterally extensive cells (e.g. RGCs) that don't modulate radial cells are difficult or impossible to observe except in cases where choice of stimulus strongly favors their responses over those of radial cells. In the dark-adapted retina, the convergence of many photoreceptors onto a single bipolar cell, several bipolar cells onto a single AII amacrine cell, and so on (See Dunn et al., 2006) means that, by starting from a very dim stimulus the relatively small RGC driven responses, ie. the positive and negative scotopic threshold response (p/nSTR), can be observed before they are essentially lost in the larger positive b-wave, which is generated by the light responses of the rod, and later the cone driven, ON (or depolarizing) bipolar cells. At higher light levels, the hyperpolarization of predominately rod photoreceptors generates the electronegative a-wave. The intensity-response curve is the standard way of representing the change in ERG amplitude and time to peak as stimulus intensity increases.

Fitting the intensity response curve to increasing stimulus strengths with two saturating hyperbolic functions, termed Naka-Rushton curves in the ERG literature (Naka and Rushton 1966a,b; Fulton and Rushton, 1978; Hood and Birch, 1992; Robson and Frishman, 1995;Abd-El-Barr et al., 2009; Herrmann et al., 2011; Smith et al., 2015), corresponding to the saturating intensity response functions of the rod- and cone-driven pathways can isolate three parameters to aid in the comprehension of the effects of experimental manipulation on the ERG. These parameters are: the maximum amplitude of the b-wave at saturation (variously V_{max}, R_{max}, B_{max}), the stimulus strength needed to reach the half maximal amplitude (variously S, $I_{0.5}$, R), and dimensionless slope variables (Hill coefficients, n). An additional method to aid comprehension involves averaging over stimulus paradigms known to affect specific photosensitive cell populations, namely the retinal ganglion cells at the lowest intensities (–3.6 to –6 log cd m s^{-2}, designated as the 'RG_i' range in this thesis); the primarily rod–driven responses at lower flash intensities (–1.5 to –3.6 log cd m s^{-2}, 'R_i'); the rod-cone mixed responses corresponding to intermediate flash intensities (–0.6 to –1.5 log cd m s^{-2}, 'Rc_i'), and finally the increasing cone–driven responses superimposed on the saturated rod driven portion of the b-wave corresponding to the highest flash intensity range (1.0 to –0.6 log cd m s^{-2}, 'Cr_i') (e.g. Tanimoto *et al*. 2009; 2012; Smith et al., 2012; 2013). The function of the dark-

adapted cone circuitry can be tested in dark-adapted conditions by presenting paired flashes, the first of the two flashed being bright enough to saturate the rods, followed by the cone-stimulating flash separated by a time interval too brief for the rods to regenerate functional rhodopsins (Pepperberg et al., 1997).

In addition to the dark-adapted ERG, similar recordings presented over increasing background luminances provides a way to study shifts in retinal circuitry driven both by the increasing saturation of the rods and network light adaptation (e.g. Herrmann et al., 2011). Once the background becomes bright enough to saturate the rods, the ERG represents the cone pathway alone. However, switching between dark and rod saturating backgrounds quickly demonstrates that the cone pathway light adapts over a period of approximately 20 minutes with the amplitude of the b-wave growing by approximately 50% (e.g. Jackson et al., 2012). This light adaptation is modulated by dopamine and is susceptible to both short term daily rhythms and longer term circadian regulation (Jackson et al., 2012). Other stimulus protocols exist, many designed to isolate the contributions of the RGCs (e.g pattern and multifocal ERGs: Miura et al., 2009; Porciatti 2007; Porciatti 2015).

At this point we have considerable, yet not comprehensive, knowledge of the cell populations underlying the low frequency components of the ERG. In dark-adapted conditions, the a-wave is generated predominately by the rod photoreceptors, although a small reduction in amplitude is evident following ionotropic glutamate receptor block with CNQX or PDA (Smith et al., 2014a; Robson et al., 2003; Jamison et al., 2001; Dang et al., 2011). Whether this postreceptoral a-wave contribution is due to suppression of a neuromodulator like dopamine, horizontal cell feedback, or neurons in the OFF pathway, is unknown. In mouse, however, we do know that RGCs are not responsible (Smith et al., 2014a). In the light-adapted ERG, despite the small amplitude of the a-wave, a similar post-receptoral component can be observed (Smith et al., 2013; Bush and Sieving 1994; Fried burg et al., 2004).

The dark-adapted b-wave was initially thought to be derived from the Müller cells (Miller and Dowling 1970), possibly because of potassium siphoning, or spatial buffering by the Müller cells in response to light responses in the ON bipolar cells. Basically, as

the ON bipolar cells, amacrine cells and RGCs respond to light, the extracellular potassium concentration increases and drives electrical currents in the Müller cells. Current source density analysis largely supported this hypothesis (e.g. Karwoski et al., 1985; Karwoski and Xu, 1999; Newman 1985). Evidence for an ON-bipolar cell contribution to the b-wave came from using pharmacologic blockers of mGluR6 (2-amino-4-phosphonobutyric acid (Slaughter and Miller, 1981; Gurevich and Slaughter, 1993) and from analyzing genetic mutations (Masu et al. 1995; Chang et al., 2006) that prevent ON bipolar cell light responses. This prompted a model in which the light responses of ON-bipolar cells drove small currents, not necessarily recordable from the cornea, which were amplified by the Muller cells. At this point however, the Muller cells have been essentially eliminated as a significant contributor to the b-wave. Blocking potassium channels in the Muller cells using barium did not change the b-wave (Lei and Perlman, 1999; Frishman et al., 1992; Frishman and Steinberg 1989), nor did a genetic knockout of an inward rectifying potassium channel localized to Muller cells (Kofuji et al., 2000). Furthermore, I observed that the intravitreal injection of aminoadipic acid, a glial toxin, does not reduce the b-wave in mice (B. Smith, unpublished results).

Ongoing research suggests that the b-wave is influenced by the inhibitory circuitry synapsing with ON bipolar cells, either the horizontal cells or amacrine cells. In mice lacking the vesicular GABA transporter (VGAT) in horizontal cells (Cx57-VGAT), the b-wave is essentially normal suggesting that amacrine cells (Smith et al., unpublished results) but not horizontal cells, are the dominant inhibitory modulators of the b-wave. In mice, genetic knockout or pharmacologic block of $GABA_cRs$, localized predominately to ON-bipolar cell axon terminals (Eggers and Lukasiewicz, 2006; Eggers et al., 2007; Dong and Werblin 1998) causes a significant decrease in the rod-driven b-wave (e.g. Herrmann et al., 2011; Smith et al., 2013; Smith et al., 2015; Kapousta-Bruneau, 2000).

In mice, the reduction in b-wave amplitude following $GABA_c$ receptor antagonists or genetic knockout is mimicked by blocking Na_v channels. This suggests that the Na_v channel dependent lateral inhibitory circuit releasing GABA onto rod bipolar cell axon $GABA_cRs$ (Chávez *et al.*, 2006; Chavez *et al.*, 2010; Moore-Dotson *et al*, 2015; Castilho *et al*, 2015) is responsible. In Smith et al., (2015), we showed that both this inhibitory pathway and a $GABA_aR$-dependent serial inhibitory pathway are under the

control of dopamine via D1 receptors, and play a role in modulating the rod pathway during light adaptation. In the cone-driven pathway, similar reductions following treatment with $GABA_cR$ antagonists is observed (Smith et al., 2013) indicating that GABAergic modulation plays a similar role in both pathways, however due to the diversity of ON cone bipolar cell subtypes *in vitro* investigation of circuitry modulating the cone-driven pathways is not refined enough to indicate what amacrine cell types or types might be involved. The effect on the b-wave of an additional amacrine cell forming a reciprocally inhibitory circuit (e.g. Chavez et al., 2006) with the rod-bipolar cell axon terminal has also been investigated. There is evidence that, in rabbits, the loss of A17 cells increases the decay of the b-wave (Dong and Hare 2003) suggesting that A17 cells play a role in shortening, or sharpening temporal responses of rod bipolar cells. In mice however, there appears to be little effect on the temporal aspects of the b-wave (Smith et al., 2015) although a small increase in the amplitude of the b-wave can be observed.

In addition to the well-characterized low frequency components of the ERG, a group of high frequency (50-150 Hz) oscillations occur on the rising limb of the ERG b-wave that are referred to collectively as the oscillatory potentials (OPs) in both ligh-t and dark-adapted retinas. It is believed that these oscillations arise from light-evoked inner-retinal activity; however, the precise cellular generators are unknown (reviewed in Wachtmeister (1998). In fact, even the number of generators of the OPs is contested, (Multiple generators: Wachtmeister & Dowling, 1978; Lachapelle et al., 1983; Dong et al., 2004; single source Bui et al., 2002; Derr et al., 2002). New analysis methods utilizing the wavelet transform also suggest different frequency oscillators that are only partially overlapping in time (e.g Forte et al., 2008). Studying the rod and cone pathway contributions to the OPs in isolation in mice, Lei et al., (2006) showed that these two components differ slightly in frequency suggesting that, depending on stimulus intensity and background, the OPs may contain summed components generated in both rod and cone pathways. A secondary goal of this thesis was to use the restricted expression of certain Na_v channel isoforms, e.g. $Na_v1.8$, to identify the neurons in the inner retina that generate the OPs.

2.5 Retroaxonal modification of retinal function

During development, synaptic modification by activity-induced long-term potentiation and long-term depression is fundamental to the process of neural circuit formation. While this process is recognized to play a role in the early formation of retinal synaptic connections, it has classically been proposed to play a minor role following eye opening (Wiesel and Hubel, 1963a,b; Sherman and Stone, 1973; Reuter, 1976; Hendrickson and Boothe, 1976; Baro, Lehmkuhle and Kratz, 1990). However, the role of visual input on refining retinal circuitry following eye opening has recently been investigated more closely e.g. Tian and Copenhagen (2001,2003), Di Marco et al., 2009; Giovannelli et al., 2008; Chan and Chiao, 2008; Akimov and Renteria 2014). Intrinsic excitability of RGCs is increased rapidly following eye opening (Qu, 2008; Boiko et al., 2003; Wang et al., 1997; Deplano et al., 2004; Giovannelli et al., 2008) due to upregulation of $Na_v1.6$, as mentioned above. In mice, a period of functional photoreceptors maturation following eye opening (~P10-P12) has been observed with the a-wave increasing abruptly between P14 and P18 (approximately 2 fold) with little change after P25 (Vistamehr and Tian, 2004; Gibson et al., 2013). Visual activity during development modulates photoreceptor function since dark-rearing mice until p30 reduces a-wave amplitude by roughly 30% (Vistamehr and Tian, 2004).

Retroaxonal modulation (Harris 2008) of RGC function during development has been extensively studied in the *Xenopus* retinotectal circuit (Du et al., 2009; Du and Poo 2004). BDNF applied to the optic tectum can modulate bipolar cell inputs to RGCs within tens of minutes, an effect which is sensitive to suppression of axonal transport by colchicine and transection. Exogenous BDNF applied to the tectum modulates RGC dendritic structure (Lom et al., 2002) and in mammals SC lesion, kainic acid, or BDNF function blocking antibodies trigger RGC cell death in neonatal rats (Spalding et al., 2004,2005). Antero- and retrograde transport of BDNF in the optic nerve is a well documented phenomenon (e.g. Quigley et al., 2000 Ma et al., 1998; reviewed in Zweifel et al., 2005).

Na_v channel dependent activity is known to contribute to surface expression of TrkB and BDNF (Du et al., 2000), release of BDNF (Santi et al., 2006, Balkowiec and Katz 2000,2002; Gartner and Staiger 2002), and trafficking of BDNF in cultured neurons (Kohara et al., 2001). Moreover, intravitreal injection of TTX reduces both anterograde

and retrograde transport of BDNF in the optic nerve (Chytrova and Johnson 2004) in the developing chick retina. TrkB global knockouts (Rohrer et al., 1999,2001,2003,2004) and retina specific conditional knockout mice (Grishanin et al., 2008) have reduced photoreceptor light sensitivity at P16. BDNF expression in the retina is enhanced by constant light rearing (Pollock et al., 2001) and reduced by constant dark rearing (Landi et al., 2007; Pollock et al., 2001) or monocular deprivation (Mandolesi et al., 2005; Seki et al., 2003). BDNF trafficking along retinal ganglion cell axons (Chytrova and Johnson, 2004) and release of BDNF is modulated by Nav channel-dependent neural activity Chytrova and Johnson, 2004; Kohara et al., 2001; Kojima et al., 2001).

2.6 Work presented

In this thesis, I start by identifying the overall contribution of Na_v channels to the mouse and rat ERGs (Smith et al., 2013, CHAPTER 3). Serendipitously, this group of experiments indicated that the contribution of ON-cone bipolar cell Na_v channels to the light-adapted ERG depends on the time of day. Further work showed that during light adaptation, D1 dopamine receptors have a stronger effect on cone ON-bipolar cell Na_v channels than at night, suggesting a daily rhythm in the gain of light-adapted cone pathways (Smith 2015a, CHAPTER 4).

Once these preliminary studies were completed, I began to answer the primary questions guiding this thesis. With regards to the mechanism underlying reductions in photoreceptor function in mice lacking $Na_v1.6$ (Cote et al., 2005; Smith et al., 2012), I found that blocking Na_v channels in the optic nerve but not in the retina at P16 by retrobulbar injection of TTX in control mice recreated almost exactly the ERG phenotype of the mice lacking the $Na_v1.6$. In both mice with Na_v channels blocked in the optic nerve specifically and in $Na_v1.6$ null mice, a TrkB receptor agonist caused nearly complete recovery of photoreceptor function (CHAPTER 5). This loss of function was restored by a TrkB agonist, suggesting that reduced BDNF levels in the retina due to deficient activity-dependent retroaxonal transport is the cause of reduced photoreceptor function in P16 $Na_v1.6$ knockout mice.

Next, I targeted the function of $Na_v1.8$ using a newly developed subtype specific blocker A803467. Because $Na_v1.8$ is expressed only within the SBACs, and a subset of RGCs, when I found that A803467 selectively suppressed the amplitude of the OPs, in combination with a side project that showed little contribution of the RGCs to the OPs in mice (Smith et al., 2014b), this led to the identification of one cell type (SBACs) that are necessary to generate the OPs (Smith et al., 2017, CHAPTER 6). By identifying for the first time an amacrine cell subtype underlying the OPs, as well as a direct contribution of Na_v 1.8 to the light responses of a subset of ON sustained RGCs, this project represents progress on two of the three questions guiding this thesis work.

Finally, I developed a method for the subtype-specific block of Na_v channel isoforms using membrane-permeable antibodies (CHAPTER 7). The membrane-permeable antibody method was validated against pharmacological broad spectrum and where possible from isoform-specific blockers as well as the $Na_v1.6$ KO mouse, using the ERG. The contribution of individual Na_v channel isoforms to RGC light responses was assessed using the MEA, and, to control for network contributions from Na_v channels I stimulated of RGCs directly using channelrhodopsin. Of particular interest, this work found that $Na_v1.6$ is the Na_v channel isoform contributing to cone ON-bipolar cell light responses, as well as driving the majority of RGC responses to both network light input and direct optogenetic stimulation. Interestingly, while the shape of the RGC response was not changed in the absence of $Na_v1.6$, blocking $Na_v1.1$, which had a relatively small effect on the peak spike frequency, caused the light response of sustained cells to become more transient. This showed for the first time that, while the input of RGCs is subject to multifaceted modulation, in some cases they also require postsynaptic properties to appropriately encode input.

CHAPTER 3: VOLTAGE-GATED SODIUM CHANNELS CONTRIBUTE TO THE B-WAVE OF THE RODENT ELECTRORETINOGRAM BY MEDIATING INPUT TO ROD BIPOLAR CELL GABA(C) RECEPTORS

Publication Information

Smith, B. J., Tremblay, F., & Côté, P. D. (2013). Voltage-gated sodium channels contribute to the b-wave of the rodent electroretinogram by mediating input to rod bipolar cell GABA(c) receptors. *Experimental Eye Research*, *116*, 279–290.

Copyright permission: Appendix 2

3.1 Abstract

Voltage-gated sodium (Na_v) channels are known to augment cone bipolar cell light responses, increasing the electroretinogram (ERG) b-wave in response to stimulus strengths above the cone threshold. However previous *in vivo* studies on a number of animal models have not found a role for Na_v channels in augmenting the b-wave in scotopic conditions below the cone threshold. We recorded ERGs from mice and rats using a series of TTX concentrations and tested retinal output to ensure complete Na_v channel block. We found that TTX concentrations sufficient to completely suppress retinal output caused large (~40%) decrease in the scotopic electroretinogram (ERG) response to high stimulus strengths (1.0 log cd s/m^2). In addition the b-wave was reduced by ~20% even at stimulus strengths that should predominately excite the rod pathway (-2.2 log cd s/m^2). Modulating stimulus strength and background luminance showed that Na_v channel contribution to the b-wave is strongest in mesopic conditions with low strength stimuli. Blocking $GABA_c$ receptors indicted that Na_v channels predominately contribute to the b-wave by supporting $GABA_c$ input to rod bipolar cells in addition to directly amplifying the light response of cone ON bipolar cells. We also determined that saturating levels of TTX reduced the rat b-wave below cone threshold. Na_v channels increase the ERG b-wave in both rod and cone bipolar cell-dominated circuits. In circuits involving rod bipolar cells the effect is mediated indirectly via GABAergic inhibitory cells, while Na_v channels directly located on cone bipolar cells amplify light responses in the cone pathways.

3.2 Introduction

Voltage-gated sodium (Na_v) channels are found in most of the cell types in the retina. *In vitro* electrophysiological studies have recorded Na_v currents in retinal ganglion cells (Lipton and Tauck. 1987, Skaliora et al. 1993, Tsai et al. 2011, Weick and Demb. 2011), in some amacrine cell subtypes including AII, (Tian et al. 2010, Wu et al. 2011), A17 (Hartveit. 1999), dopaminergic (Feigenspan et al. 1998, Gustincich et al. 1997), and starburst (Cohen. 2001), and more recently in cone bipolar cells (Ichinose et al. 2005, Ichinose and Lukasiewicz. 2007, Ma et al. 2005, Pan and Hu. 2000, Saszik and DeVries. 2012, Zenisek et al. 2001).

Na_v channels in ON cone bipolar cells have recently been demonstrated to contribute to the amplitude of the positive component of the ERG generated predominately by the ON bipolar cells (Robson and Frishman. 1998, Robson et al. 2004, Xu and Karwoski. 1994) referred to as the b-wave (Mojumder et al. 2007, 2008). This result has been repeated in a number of species including rat (Bui and Fortune. 2006, Bui and Fortune. 2004, Li et al. 2005, Mojumder et al. 2007, 2008), mouse (Miura et al. 2009), and frog (Popova and Kupenova. 2010), and in most cases Na_v channels on cone ON bipolar cells increase the dark-adapted ERG b-wave at stimulus strengths sufficiently high to stimulate cones (but see Bui and Fortune. 2004). Interestingly in spite of *in vitro* electrophysiological, *in situ* hybridization, and immunohistochemical results showing Na_v to be present in a majority of the cell types in the retina (Côté et al. 2005, Fjell et al. 1997, Mojumder et al. 2007, Kaneko and Watanabe. 2007, O'Brien et al. 2008) including amacrine cells that synapse with rod bipolar cells (RBCs) (Chávez et al. 2006, 2010) previous results have not shown that Na_v channels contribute to the rod-generated portion of the ERG.

Na_v channels, probably in retinal ganglion cells, have been shown to contribute to ERGs in response to weak stimulus strengths (Bui and Fortune. 2006, Mojumder et al. 2007, 2008, Popova and Kupenova. 2010) however in most studies blocking Na_v channels has little effect on the scotopic ERG b-wave at stimulus strengths above the scotopic threshold response but below the range of sensitivity of the dark-adapted cone

bipolar cells (Bui and Fortune. 2004, Li et al. 2005, Mojumder et al. 2007, 2008, Popova and Kupenova. 2010, Viswanathan et al. 2004) consistent with a lack of evidence of Na_v channels in rod bipolar cells (RBC) (Pan and Hu. 2000). In rabbits however after a short dark adaptation TTX increases the b-wave, an effect attributed to third order inhibitory neurons (Dong and Hare. 2003) an effect similar to the findings of Awatramani et al., (2001) in salamander. A recent *in vivo* study in rats found that TTX strongly reduced the amplitude of the b-wave in the range where rods should be contributing the b-wave when the retina was partially light adapted by a dim background (Mojumder et al. 2008). This effect was suggested to act via the secondary rod pathway which passes rod signals to the ON cone pathway via gap junctions between rods and cones (Abd-El-Barr et al. 2009), or via an Na_v channel-dependent interneuron that contributes to the b-wave only under mesopic conditions (Mojumder et al. 2008).

Recently it has been shown that lateral inhibition in the inner retina is mediated primarily by $GABA_c$ receptors on RBCs (mouse: Eggers and Lukasiewicz. 2006) and is strongly dependent on Na_v channels (rat: Chávez et al. 2006, 2010). Similarily lateral inhibition of bipolar cells is Na_v channel-dependent in many species (Cook and McReynolds. 1998, Shields and Lukasiewicz. 2003, Vigh. 2011, Volgyi et al. 2002). In addition, $GABA_c$ receptors on RBCs have recently been shown to mediate chloride currents hyperpolarizing the cell membrane and increasing the drive for cations to enter the cell during a light response (Herrmann et al. 2011). Blocking $GABA_c$ receptors substantially reduces the amplitude of the scotopic b-wave (Dong and Hare. 2002, Herrmann et al. 2011, Kapousta Bruneau. 2000, Mojumder et al. 2008, Möller and Eysteinsson. 2003) suggesting that Na_v channels on amacrine cells in the inner retina could, in theory, increase the scotopic b-wave generated by rods. However inhibitory cells in both the inner and outer retina release GABA onto RBCs and the relative contribution of amacrine vs. horizontal cells to the b-wave is unknown.

Here we investigated the contribution of Na_v channels to the rodent ERG b-wave and found that in both mice and rats Na_v channels contribute strongly to the scotopic b-wave at stimulus strengths too low to excite cone bipolar cells. At saturating concentrations the scotopic b-wave was reduced by approximately 40%, indicating that Na_v channels substantially amplify both rod and cone pathways. We also found an

increased contribution of Na_v channels in response to dim but not bright stimulus strengths in mesopic conditions. The effects of TTX on RBCs were found to act predominately on $GABA_c$-mediated input. Isolating the photoreceptor-to bipolar cell circuit by blocking ionotropic glutamate receptors showed a direct contribution of Na_v channels to ON bipolar cells isolated to stimulus strengths that stimulate cones in addition to rods. The combined indirect contribution of Na_v channels on $GABA_c$-mediated input and direct contribution of Na_v channels on cone bipolar cells explain the majority of Na_v contributions to the ERG b-wave across diverse lighting conditions.

3.3 Material and methods

3.3.1 Ethics approval

All animal procedures were completed in accordance to animal care guidelines established by the Canadian Council on Animal Care and in accordance with the ARVO statement for the Use of Animals in Ophthalmic and Vision Research. Mice and rats were housed under a 12-hour light/dark cycle with free access to food and water.

3.3.2 Electroretinography

C57Bl-6 mice between 8 and 16 weeks of age (Charles River Laboratories, St. Constant, QC, Canada) were dark-adapted for at least 8 hours before being anesthetized under dim red light by intraperitoneal injection of Avertin (2,2,2 Tribromoethanol, Sigma Aldrich, St-Louis, MO) dissolved in amylene hydrate (tertiary amyl alcohol, 275 mg/kg, Sigma Aldrich). The pupils were dilated with the mydriatic agent cyclopenolate HCl 0.5% (Alcon, Fort-Worth, TX) and a 0.5% proparacaine hydrocloride (Alcon) was applied as a topical analgesic to reduce eye movement and irritation. Body temperature was maintained at 37°C with a heated pad and monitored rectally. Mice were sacrificed by anesthetic overdose followed by cervical dislocation. ERGs from adult Long-Evans rats (Charles River) were obtained with a procedure identical to that used in mice with the exception that anesthesia was induced using ketamine (90 mg/kg), xylazine (5 mg/kg) and acepromazine (2.5 mg/kg). The active electrode was a Dawson-Trick-Litzkow-plus microconductive fiber (Diagnosys, Littleton, MA) placed on the corneal surface and

hydrated with 2.5% hydroxypropyl methylcellulose solution to maintain conductivity. Platinum subdermal electrodes (Grass Instruments, Quincy, Mass) were placed in the base of the nose (reference) and in the tail (ground).

Signal from the corneal electrodes was amplified 10,000 fold using a differential amplifier with a bandwidth of 0.3-300 Hz (P511, Grass instruments) and acquired at 1 kHz by an A/D board (PCI 6281, National Instruments, Austin, TX, USA) and displayed and stored for processing using LabVIEW 9.0 dedicated software (National Instruments). Flash stimuli were generated by a Ganzfeld stimulator (LKC Technologies, Gaithersburg, MD, USA) that produced a maximum illumination of 10.1 log cd s/m^2 at the corneal surface. Stimulus strengths were attenuated by up to 7.0 log units by manual interposition of neutral density filters (Kodak Wratten, Rochester, NY, USA). The interval between stimuli varied from 5 s at the lowest strengths to 30s at the highest ones, repeated flashes did not attenuate the ERG even at high stimulus strength indicating that inter stimulus light adaptation did not occur; 2–10 responses were averaged depending on stimulus strength.

According to the Seeliger group (2001, Tanimoto et al. 2009, Tanimoto et al. 2012), the range of the scotopic b-wave can be subdivided into four sections in mice according to the elicited cellular responses. We refer to those stimulus ranges as follows: cone-rod mixed response with substantial cone contribution (Cr_i) corresponding to the highest stimulus strength range (1.0 to -0.6 log cd s/m^2), rod-cone mixed responses with less cone contribution (Rc_i) corresponding to intermediate stimulus strengths (-0.6 to -1.5 log cd s/m^2), rod-driven responses (R_i) at lower stimulus strengths (-1.5 to -3.6 log cd s/m^2), and finally predominantly retinal ganglion cell-elicited responses (Rg_i) at the lowest strengths (-3.6 to -6 log cd s/m^2). Background luminances ranged from darkness (scotopic) to 1.5 log cd/m^2 (photopic) with the intermediate range (mesopic) divided into low (m_L -0.5 to 0.6 log cd/m^2 backgrounds) and high (m_H 0.5 to 0.6 log cd/m^2) backgrounds (see Fig 2O).

3.3.3 Intravitreal injection

Following application of a topical anesthetic to the cornea of anesthetized mice 0.5 µl of 10 mM cobalt chloride ($CoCl_2$, Sigma Aldrich), 3, 5, or 20 µM tetrodotoxin (TTX, Abcam Biochemicals, Toronto, Ontario), 200 µM 6-Cyano-7-nitroquinoxaline-2,3-dion (CNQX, TOCRIS Bioscience, Bristol, UK), or 150 µM 1,2,5,6-Tetrahydropyridin-4-yl) methylphosphinic acid (TPMPA, TOCRIS Bioscience), dissolved in phosphate buffered saline pH 7.4 was injected into the vitreous via a 30-gauge needle mounted on a Hamilton syringe under dim red light. The injection site was located approximately 0.5 mm behind the ora serrate. Following injection the mice and rats were further dark-adapted for approximately 30 minutes to allow for diffusion of the drug before recording. Drug concentration at the retina was calculated using an estimated vitreal volume of 50 µL for rat (Hughes. 1979) and 5 µL for mouse (Jeon et al. 1998, Kaplan et al. 2010). It should be noted that these diverge slightly from previous estimates of rat vitreal volume (Bui and Fortune. 2004, Mojumder et al. 2007) and substantially from previous estimates of mouse vitreal volume (Miura et al. 2009, Robson et al. 2004, Saszik et al. 2002, Shirato et al. 2008). For example, Miura et al. (2009) use an estimated vitreal volume of 20 µL, and therefore estimated drug concentrations at the retina in that report should be multiplied by 4 for comparison with our study.

3.3.4 VEP protocol

Under general anesthesia and after the overlying skin had been injected with lidocaine and incised, a craniotomy (approximately 3×3 mm) was centered 2mm lateral to the sagittal suture behind the coronal suture. The craniotomy site was over the visual cortex contralateral to the stimulated eye. A platinum subdermal electrode was gently lowered to the pial surface of the cortex with the help of a micromanipulator, 2 mm anterior and 1 mm lateral to lambda. The reference electrode was inserted in the nose. VEP recordings were obtained in response to 1.0 cd s/m^2 flash stimulus in dark conditions after 20 minutes of dark adaptation. Responses to 50 flash stimuli were averaged after 10 000 fold amplification with a bandwidth of 1–300 Hz. The response amplitude was measured from trough to peak.

3.3.5 Data Analysis

Analysis of ERG waveforms was completed using a custom ERG analysis toolbox written for Matlab (Mathworks, Natick, MA). Waveforms were low pass filtered at 50 Hz to remove high frequency oscillatory potentials (Lei et al. 2006). The a-wave amplitude was measured from the baseline to the maximum negative trough and the b-wave was measured from the a-wave trough to the maximum positive peak. In addition to the reported b-wave measurements we recorded, a-wave amplitudes and implicit times (IT) were examined to ensure that effects on b-wave amplitude and IT were not due to effects on the photoreceptors. All drug treatments except CNQX and CNQX+TTX either had no effect on the a-wave or caused it to increase slightly. Consistent with Dang et al. (2011), both CNQX and CNQX+TTX decreased the a-wave amplitude but there was no difference between these two drug treatments. Comparison of a- and b-wave amplitudes was carried out using Microsoft Excel (Redmond, WA). Isocline data representation graphics were generated with OriginLab (Northampton, MA).

3.4 Results

3.4.1 TTX concentration for Nav saturation

We examined the effect of TTX on the b-wave of the mouse ERG in response to a bright stimulus (1.0 log cd s/m^2) at concentrations similar to those previously used in rats (3 μM predicted at retina) (Mojumder et al. 2008) (n=13). We found that the b-wave was significantly reduced (p<0.01, Fig. 1A) in all conditions of light adaptation and notably did not find a more potent effect in mesopic conditions. Our results differed from previously reported results in the rat; therefore we tested the efficacy of various concentrations of TTX to abolish the retinal output by recording the cortical visual evoked potential (VEP). This was done while blocking input and output from the contralateral retina with high (10mM) cobalt chloride and an opaque patch (n=4). At a predicted vitreal concentration of 3 μM TTX, Na_v channels are still able generate retinal output to the cortex since the VEP was only reduced by approximately 50% (Fig. 1B). When 20 μM TTX was applied, no reliable cortical activity could be detected. Since the IC_{50} of TTX sensitive Na_v channels *in vitro* is in the low nanomolar range and 0.1 μM is sufficient to block RGC spiking in mouse whole mount retina (Margolis and Detwiler.

2007), this suggests that intravitreal injection of TTX in mouse results in substantial reduction of actual relative to predicted TTX concentration potentially due to drug loss via the injection hole or due to drug retention in the vitreous.

We then applied predicted intravitreal concentrations of 6 (Bui and Fortune. 2004), and 20 μM TTX (Miura et al. 2009), which corresponds to the average and maximum previously published predicted intravitreal TTX concentrations in rodents (Fig. 1A) and found no difference in the effect of 6 (n=9) or 20 (n=10) μM TTX on the scotopic or mesopic b-wave amplitude (p<0.01 for both). However, in photopic conditions 20 μM TTX caused a significantly larger b-wave reduction compared to 6μM. In all conditions the effect of 6 and 20 μM TTX was significantly increased relative to the effect obtained with 3 μM TTX.

3.4.2 TTX reduces the mouse b-wave across a wide range of background luminance and stimulus strengths.

Finding that a 6-20 μM predicted TTX concentration at the retina significantly reduced the scotopic ERG and completely blocked cortical light responses, we next examined the effects of TTX in this concentration range (≥6μM, n=14) on the mouse ERG across a range of stimulus strengths for 7 background luminances ranging from complete darkness to photopic conditions (1.5 log cd Tanimoto et al. 2012). Results from 5 background conditions are presented for brevity in Fig. 2 (D-H: amplitude; I-M implicit time). In dark-adapted retina, TTX reduced the ERG b-wave to 59.7±2.8 and 62.9±2.7% of control in the Cr_i and Rc_i ranges (Fig 2O, see also Materials and Methods for stimulus strength and background luminance definitions), respectively, while the reduction is less important in the R_i (67.9±6.4%) and Rg_i (56.1±9.1%) range of stimuli (Table 1). This shows that TTX reduces the amplitude of the b-wave even at stimulus strengths too low to excite cones. TTX increased the b-wave implicit time significantly through the high scotopic range of stimulus strengths but not at the brightest or dimmest stimuli.

We then looked at the effect of TTX on the ERG when both the stimulus strength and the background luminance were varied (Fig. 2E-H) and these results are summarized in Fig. 2N as contour plots. TTX significantly reduced the b-wave in all backgrounds and

nearly all stimulus strengths (area outside of the hatched area in Fig. 2N). We found that the strongest effects of TTX on the b-wave occurred at backgrounds from -0.5 to 0.6 log cd/m^2 with stimulus strengths between -0.2 to -1.5 log cd s/m^2 (mRc$_i$) and that in general TTX had a significantly stronger effect in this range in comparison to other backgrounds and stimuli (see Table 1 for statistical comparisons between background and stimulus regimes). At maximum stimulus strength there was no significant difference in the effect of TTX as the background luminance increased. When backgrounds were increased significant b-wave implicit time (IT) changes were only observed with the dimmest stimulus strengths in mesopic conditions (Fig. 2J and K).

3.4.3 TTX reduces Gaba$_c$-mediated amplification of the scotopic b-wave.

Contrary to previous results (Bui and Fortune. 2004, Mojumder et al. 2007, 2008) we documented a significant effect of TTX on the scotopic b-wave at all stimulus strengths, so we looked for a mechanism explaining our results. In the *in vitro* retinal slice preparations in rats, GABA$_c$ input to RBCs is attenuated by TTX (Chávez et al. 2006, 2010) and in both *in vitro* and *in vivo* preparations, blocking GABA$_c$ receptors decreases the amplitude of the scotopic b-wave (Herrmann et al. 2011, Kapousta Bruneau. 2000). Therefore we tested the Na$_v$ channel dependency of GABA$_c$ input to the RBCs *in vivo* (Fig. 2A, D and N).

In dark-adapted conditions, TPMPA (n=13) significantly reduced the amplitude of the b-wave at the Cr$_i$ (73.3±2.9%), Rc$_i$ (72.6± 2.8%), R$_i$ (73.4± 6.2%), and Rg$_i$ (52.0±7.1%) stimulus ranges. The effect of TPMPA on the b-wave was similar to TTX in Rg$_i$ and R$_i$ range but diverges in the Rc$_i$ range. Cone ON bipolar cells begin to contribute to the ERG around -1.5 log cd s/m^2 (Jaissle et al. 2001), i.e. the low end of the Rc$_i$ range, which is approximately where the effects of TPMPA and TTX on the b-wave amplitude began to diverge and became significantly different (p<0.005 for -1.2 log cd s/m^2 and higher stimulus strengths). In scotopic conditions, there was no increase in the b-wave IT, in opposition to the effect seen with TTX. When we looked at the effect of TPMPA when both stimulus strength and background luminance varied we found that the effect was similar to that seen for TTX with a significantly increased effect seen in the m$_L$Rc$_i$ range relative to other backgrounds and stimulus strengths (Fig. 2E, F and N**,** Table 1). At

maximum stimulus strength there was no significant difference in the effect of TPMPA as the background luminance increased. Similar to TTX when backgrounds were increased significant b-wave implicit time (IT) changes were only observed with the dimmest stimulus strengths in mesopic conditions (Fig. 2 J,K).

Both TTX and TPMPA reduced the amplitude of the scotopic b-wave. To test whether they acted on the same retinal circuitry contributing to b-wave we injected both drugs (*n*=9, Figs. 2A, D and N). The effect of TPMPA+TTX in scotopic conditions was consistent at all stimulus strengths in the R_i and Cr_i ranges reducing the amplitude of the b-wave to an average of 62.2±0.2% of control, and in the R_i range where it was reduced to an average of 63.2±4.1% of control. There is no significant difference between the effects of TTX+TPMPA and of TTX alone on the scotopic b-wave at any stimulus strength. Similarly to TTX alone but not TPMPA alone, the mixture of TTX and TPMPA significantly increased the scotopic b-wave IT over the Rg_i and R_i ranges (Fig. 2I) suggesting that Na_v channels but not $GABA_c$ receptors decrease the b-wave time to peak in response to dim stimuli. These results indicate that the $GABA_c$-mediated increase in b-wave amplitude is predominately Na_v channel-dependent.

In response to increasing levels of light adaptation TPMPA+TTX acted similarly to both TPMPA and TTX alone, causing a significantly larger reduction of b-wave amplitude in the m_LRc_i range (Figs 2B,E, and F and 3C and Table 1). At all background luminances the effects of a mixture of TPMPA and TTX on the b-wave amplitude and IT was similar to the effect of TTX alone (Fig. 2N) demonstrating that $GABA_c$ input to ON bipolar cells is heavily dependent on Na_v channels.

3.4.4 The effect of TTX on rod bipolar cell contribution to the b-wave is dependent on iontropic glutamate receptors.

We have shown that Na_v channels contribute to the scotopic ERG b-wave predominately via a $GABA_c$-mediated pathway and an additional component, which was insensitive to TPMPA and restricted to the Rc_i and Cr_i ranges. We blocked input to OFF

bipolar cells, horizontal cells (Schubert et al. 2006) and most inner retinal neurons (Bui and Fortune. 2004, Mojumder et al. 2007, 2008, Yang et al. 2011) with CNQX (200 μM) to determine the effect of Na_v channels on ON bipolar cells in the absence of input from most amacrine and horizontal cells (excluding cells coupled by gap junctions to ON bipolar cells). We first injected CNQX and compared the results to control eyes (*n*=6) to determine the effects of CNQX on the mouse ERG. In an additional set of experiments we injected CNQX+TTX and compared to CNQX-injected in the fellow eye as a control (*n*=13) to provide a paired test of the difference between CNQX and CNQX+TTX in the same animal. The amplitude and implicit times of a- and b-waves in CNQX-injected eyes were not significantly different between the two sets of experiments (Fig. 3A, C and I).

CNQX substantially reduced the scotopic b-wave to 59.4±2.9% of controls in the Cr_i range, 59.4 ±3.1 in Rc_i, 40.6±3.1% in R_i, and 21.7±4.2% in the Rg_i range (Fig. 3A and C, Table 1). When the rod to RBC circuit is isolated using CNQX and stimulated with low strength stimuli (Rg_i and R_i) there is no significant difference between eyes injected with TTX+CNQX and fellow eyes injected only with CNQX (Fig. 3B, C and G). As stimulus strength increases, and the cone circuitry begins to contribute (Rc_i), the effects of CNQX and CNQX+TTX start to diverge significantly (CNQX+TTX reduced to 74.3±3.3% of CNQX in Cr_i). The divergence of CNQX+TTX vs. CNQX alone occurred at the low end of the Rc_i range, corresponding to the stimulus strength where TPMPA and either TPMPA+TTX or TTX alone diverge. CNQX increased the b-wave IT at stimulus strengths above Rc_i and CNQX+TTX increased it further but this only reached significance (p<0.05) at Cr_i (Fig. 3F).

We examined the effects of TTX in the isolated photoreceptor-to-bipolar cell circuit across a range of adapting backgrounds and stimulus strengths (Fig. 3). The effect of CNQX on the b-wave amplitude was reduced as the background luminance increased (b-wave reduced to 55% vs. reduction to 90% normalized to control group p<.001 for 1.0 log cd s/m^2). In contrast to TTX, TPMPA, and TPMPA+TTX, CNQX did not cause a substantially increased effect on the b-wave in mesopic vs. scotopic conditions with low strength stimuli indicating that the strong effect of TTX in response to scotopic stimulus strengths in mesopic backgrounds is not due to Na_v channels directly on bipolar cells.

CNQX+TTX significantly reduced the b-wave compared to CNQX at stimulus strengths in the Cr_i range in mesopic and photopic conditions. CNQX significantly increased the b-wave IT from -0.2 to -0.8 log cd s/m^2 (p<0.05) and -0.8 log cd s/m^2 (p<0.05) for mesopic backgrounds but there was no change in photopic backgrounds. TTX+CNQX did not significantly increase the b-wave IT compared to CNQX as the background luminance increased.

3.4.5 Na_v channels amplify the rod-generated b-wave in both mouse and rat retinas.

The original research on Na_v channel-dependent $GABA_c$-mediated inhibition of RBCs was performed in rat retinal slice preparations (Chávez et al. 2010) and previous *in vivo* research was also preformed in rat (Mojumder et al. 2008). To determine whether the effects we saw with 6-20 μM TTX were specific to mice we tested the effects of different concentrations of TTX on the rat ERG (Fig. 4). We first injected 3 μM TTX (n=8) similar to Mojumder et al., (2008) and replicated their analysis method by measuring the b-wave amplitude at 65 and 110 ms post stimulus with the difference that we measured the b-wave amplitude from the trough of the a-wave rather than the baseline. The b-wave amplitude was only significantly reduced in response to stimulus strengths greater or equal to -0.6 log cd s/m^2 at 65 ms post stimulus (b-wave reduced by 19±1.1% at stimulus strengths >-0.6 log cd s/m^2). There was a slight trend towards an increase in b-wave amplitude at 110 ms following 3 μM TTX for stimulus strengths below -1.8 log cd s/m^2 and a trend towards a decrease above this stimulus strength but this only reached significance for stimulus strengths between -3.0 to -4.2 log cd s/m^2. When we used a mesopic (-0.5 log cd/m^2) background the b-wave was significantly reduced for stimulus strengths -0.8 log cd s/m^2 and higher to 62.9±1.3% of control. The effect of 3 μ M TTX was larger in mesopic conditions relative to scotopic conditions (63.7% vs. 81.1% of control p<0.005 1.0 log cd s/m^2). A-wave amplitude and IT were similar to controls in mesopic conditions.

We then blinded the control eye with high concentration $CoCl_2$ (10 mM, no b-wave and a substantially reduced a-wave were seen in injected eye, not shown) and an opaque patch and recorded the VEP generated by the eye with 3 μM TTX after a 15-

minute dark adaptation period following the -0.5 log cd/m^2 background (n=7). We were still able to record a VEP (~15 μ V). In some rats, we then injected an additional aliquot of TTX to reach an estimated concentration of 6 μ M and re-recorded the VEP after a further dark adaptation of 20 minutes (n=4). We found that 6 μ M predicted vitreal concentration of TTX reduced the VEP to noise levels indicating a complete block of Na_v channels in retinal ganglion cells. We also injected some eyes with 6 μ M TTX directly (n=3) as a control for time, surgical trauma from the VEP, and possible effects of mesopic light adaptation and found that the results were not significantly different from those with VEP intervention so we pooled the results from both conditions. No significant effect on the a-wave amplitude or implicit time in scotopic conditions was found with 6 μ M TTX (not shown). At 65 ms the b-wave was significantly reduced for stimulus strengths above -2.4 log cd s/m^2 (p<0.05) with an average reduction to 57.5±1.1% of control in scotopic conditions but there was no significant reduction in response to any stimulus strength at 110 ms. In mesopic conditions at 65 ms the b-wave was significantly reduced above -1.4 log cd s/m^2 (p<0.005) to 37.2±3.2 % reduction. At 80 ms the b-wave was also significantly decreased for stimulus strengths above -1.4 log cd s/m^2 (p<0.05). In both scotopic and mesopic conditions 6 μM TTX reduced the b-wave more than 3 μM by about 20%.

When the b-wave amplitude following TTX at 65 ms was normalized to control responses (Fig. 4H) the b-wave was more reduced in a mesopic adapting background (-0.5 log cd/m^2) compared to scotopic at 3 μM TTX (average reduction to 81.2±1.1% of normal at stimulus strengths >-1.2 log cd s/m^2 in scotopic vs. 33.6± 3.5% at stimulus strengths above -1.4 log cd s/m^2 in mesopic) and at 6 μM TTX (average reduction to 58.5±1.2% at stimulus strengths > -1.2 log cd s/m^2 vs. 37.2±3.2% of normal at stimulus strengths above -1.4 log cd s/m^2 in mesopic).

3.5 Discussion

In this study we examined the effects of blocking Na_v channels on the rodent ERG. We report that when TTX concentrations are sufficient to fully suppress retinal

output in mice and rats, the b-wave is reduced over most of the dynamic range of the dark-adapted ERG even in conditions where rod- rather than cone-bipolar cells are active.

3.5.1 Na_v channels boost bipolar cell signaling through both rod- and cone-dominated pathways.

Using low predicted concentrations of TTX in mice, we found that the scotopic b-wave was reduced at stimulus strengths that should excite predominately the RBC pathway (not shown). Furthermore, at brighter stimulus strengths the reduction after TTX was so large that it was unlikely that the total effect was on the cone pathways only. This raised two possibilities: either RBCs express Na_v channels, contrary to previous research (Pan and Hu. 2000), or TTX alters synaptic input to RBCs. When iGluRs are blocked with CNQX (Fig. 3) the effects of TTX are restricted to stimulus strengths above -1.2 log cd s/m^2, which is approximately when cone ON bipolar cells start to contribute to the scotopic b-wave (Tanimoto et al. 2012). Additionally, the size of the Na_v channel-dependent component is attenuated to 15% in the presence of CNQX, compared to a reduction of 40% in non pre-treated retina at 1.0 log cd s/m^2. This suggests that the contribution of Na_v channels to the portion of the b-wave generated by RBCs is due to Na_v channels on inhibitory cells pre-synaptic to the RBCs. Our results following TTX injection in photopic conditions are similar to previous results (Miura et al. 2009) although in their hands TTX caused the photopic b-wave to reach 40% of normal, a slightly larger effect than we found. This discrepancy may be explained by the fact that they used higher stimulus strengths, and also injected TTX in light-adapted rather than dark-adapted mice.

3.5.2 The rod bipolar cell component of the ERG is dependent on ionotropic glutamate receptor-expressing cells that increase rod bipolar cell light responses via $GABA_c$ receptors.

Finding that even non-saturating concentrations of TTX reduced the b-wave in conditions where the RBCs should be the primary contributors, we examined the contribution of iGluR expressing cells (horizontal cells, OFF bipolar cells, amacrine cells and ganglion cells) to the b-wave with the blocker CNQX. CNQX reduced the amplitude

of the scotopic ERG to approximately 45% of normal but the reduction of the photopic ERG was minor at 90% of normal. This suggests a strong dependence of the RBC-generated b-wave on cells with iGluR input. We have not seen any significant contribution of retinal ganglion cells to the scotopic b-wave at stimulus strengths above -3.6 log cd s/m^2 (BJS, unpublished data)**,** and the contribution of the OFF bipolar cells has also been shown to be quite small in mice (Shirato et al. 2008)**.** This suggests that the amplitude of the RBC-generated component of the mixed rod-cone b-wave is increased by synaptic input from amacrine or horizontal cells. Further, it has recently been demonstrated that $GABA_c$ receptors on mouse RBCs mediate a tonic chloride current increasing amplitude and operational range of the scotopic b-wave (Herrmann et al. 2011, Varela et al. 2005). This work, along with previous results in the rat retina *in vitro* (Kapousta Bruneau. 2000) and *in vivo* (Mojumder et al. 2008, Möller and Eysteinsson. 2003), shows conclusively that inhibiting $GABA_c$ receptors reduces the b-wave in scotopic and mesopic conditions. Our results with the $GABA_c$ receptor blocker TPMPA in mouse are similar to these previous studies.

3.5.3 $GABA_c$-mediated amplification of rod bipolar cell signaling is Na_v channel-dependent.

Na_v channel-dependent $GABA_c$-mediated input to RBCs via lateral inhibition in the inner retina (Chávez et al. 2006, 2010) suggests that Na_v channels could contribute to the $GABA_c$-mediated increase in the ERG b-wave. Injection of TTX caused effects on the ERG that were grossly similar to TPMPA, i.e. b-wave reduction especially in response to low strength stimuli in mesopic backgrounds (Figs 2 and 3) and an increase in number of OPs (Fig. 2 A, visible in example waveforms but not quantified). This observation supports our conclusion that the TTX-mediated reduction of the b-wave elicited by stimulus strengths lower than -0.6 log cd s/m^2 (Rc_i range and lower) was caused by blocking Na_v channels on inhibitory cells presynaptic to $GABA_c$ receptors on RBCs. A cocktail of TTX and TPMPA did not significantly change the effect on the b-wave amplitude compared to TTX alone indicating that both drugs acted on an identical pathway. Chavez et al., (2006, 2010) show $GABA_c$ feedback by A17 cells is minor and predominately mediated by spillover from the primary A17 synapses with $GABA_a$

receptors. These findings are consistent with our results showing that there was not a substantial difference in the effects of TTX and TPMPA+TTX on the b-wave. It is notable that at stimulus strengths where the effects of TPMPA+TTX varied most from TTX alone both TTX and TTX+TPMPA but not TPMPA alone increased the implicit time, suggesting that TTX may act on a $GABA_c$ receptor independent pathway to reduce the b-wave slightly in addition to increasing its latency. This is consistent with the small alterations to the b-wave we saw when injecting other inhibitory neurotransmitter antagonists (BJS, unpublished data).

Although we could not conclusively differentiate between Na_v channel-dependent $GABA_c$ feedback acting at the inner vs. the outer retina there are several reasons to suggest an inner rather than outer retinal source: 1) In isolated RBCs $GABA_c$ acts predominately in the axon terminal and causes hyperpolarization while $GABA_a$ acts predominately at the dendrites and causes depolarization (Vaquero and Villa. 1999, Varela et al. 2005) and axotomized RBCs lose the effect of GABA receptor block on dynamic range (Euler and Wässle. 1998) although Herrmann et al. (2011), report dendritic $GABA_c$ currents in slice preparations, and 2) mouse horizontal cells have relatively small transient Na_v currents (Feigenspan and Weiler. 2004, Schubert et al. 2006) and the dark resting potential of mammalian horizontal cells is approximately -35 mV (Massey and Miller. 1987), which should cause voltage-dependent inactivation of Na_v channels. In addition the hyperpolarizing light responses of horizontal cells should inactivate Na_v channels while depolarizing light reponses in ON amacrine cells should be amplified by Na_v channels (Chávez et al. 2010) suggesting that $GABA_c$ input increasing the b-wave acts predominately at RBC axon terminals rather than dendrites.

3.5.4 Effect of TTX in the absence of iGluR-dependent light responses in multiple cell types.

The effects of TPMPA in comparison either to TPMPA+TTX or TTX alone diverge at stimulus strengths above -1.2 log cd s/m^2 (Figs 2 and 3) suggesting that in addition to a Na_v channel-dependent $GABA_c$-mediated component, Na_v channels can contribute to the ERG b-wave by a second mechanism at higher stimulus strengths. We hypothesized that this could be attributed to Na_v channels on cone ON bipolar cells as

seen in previous work in rat (Bui and Fortune. 2004, Mojumder et al. 2007, 2008), mouse (Miura et al. 2009) and frog (Popova and Kupenova. 2010). To study this contribution in the absence of input to almost all inhibitory cells we used CNQX to block iGluRs. As mentioned above CNQX reduced the effect of TTX in scotopic conditions and isolated it to stimulus strengths above - 1.2 log cd s/m^2. As the background luminance increased, the reduction in CNQX+TTX injected eyes normalized to CNQX injected fellow eyes was increased. This indicated that in the absence of inhibitory signaling Na_v channels contribute slightly more strongly to the b-wave in photopic relative to scotopic conditions. In the study by Miura et al. (2009), the effects of TTX were reduced when TTX was injected in the presence of 2,3, *cis*-piperidine dicarboxylic acid (PDA), a ionotropic glutamate receptor antagonist, whereas in photopic conditions in our study mice and in Mojumder et al., (2007, 2008) TTX in the presence of CNQX maintains its full effect in rat eyes. The discrepancy may come from injecting in light-adapted conditions rather than dark or in using PDA vs CNQX, since PDA may act as a partial NMDA receptor agonist (Leach et al. 1986).

We suggest that TTX reduces the b-wave in scotopic and mesopic conditions by acting on two individual retinal circuits; reducing $GABA_c$ input to RBCs as well as blocking Na_v channels on ON cone bipolar cells. We first found the Na_v-independent $GABA_c$-mediated contributions to the scotopic b-wave by subtracting the effects of TTX from the effect of the TPMPA+TTX mixture and normalizing to the control eyes (Fig. 5, Line A) this shows that the Na_v-independent $GABA_c$ input to the RBCs only contributes slightly to the scotopic b-wave. We found the size of Na_v-dependent $GABA_c$ feed back by subtracting the values for line A from the normalized size of the b-wave after TPMPA (Line B) to obtain Line C. We found the contribution of Na_v channels on bipolar cells to the scotopic b-wave by subtracting the size of the b-wave after CNQX and TTX from the effects of CNQX and normalizing to the b-wave amplitude of the CNQX control eyes (Line E). We added the values of line E to the normalized effect of TTX to show the contribution of Na_v channels to the b-wave when the direct contribution of Na_v channels on bipolar cells is removed (Line D). Lines D and C match closely suggesting that the effect of TTX on the scotopic b-wave is almost completely composed of a presynaptic

effect reducing $GABA_c$ input to RBCs in combination with Na_v channels on cone ON bipolar cells.

3.5.5 The mechanisms explaining the effects of TTX on the b-wave are mostly preserved between mice and rats.

Scotopic conditions

Our results following TTX delivery to the dark-adapted rat and mouse retina differ from previous studies in rodents, studies that used different TTX concentration (Bui and Fortune. 2004, Mojumder et al. 2007), rabbit (Dong and Hare. 2000), and frog (Popova and Kupenova. 2010) although the results are similar to those in monkey after a short dark-adaptation (Hare and Ton. 2002). In the scotopic mouse ERG, we found that Na_v channels contributed to the b-wave across the entire dynamic range. In most previous studies (Bui and Fortune. 2004, Mojumder et al. 2007, 2008, Popova and Kupenova. 2010) the effect of TTX in scotopic conditions was restricted to weak stimuli that generate threshold responses and high strength stimuli that generate a mixed rod-cone response. Considering that previous results in rats showed predominately an effect on the cone pathway (Mojumder et al. 2007, 2008) we considered the possibility that TTX concentrations used in those studies may have been too low to saturate inhibitory cell spiking but sufficiently high to suppress a cone bipolar cell response (Mojumder et al. 2007).

In agreement with Mojumder (2008) we also found that in rats 3 μ M TTX reduced the scotopic b-wave at stimulus strengths above -1.8 log cd s/m^2 but we also determined that this concentration of TTX was not sufficient to block retinal ganglion cell output. This result demonstrates that although nanomolar concentrations of TTX are able to block Na_v channels on cone bipolar cells (Pan and Hu. 2000) and on amacrine cells mediating lateral inhibition on RBC terminals (Chávez et al. 2010), predicted intravitreal concentrations of TTX may be inaccurate, since 0.5 µM TTX can fully block RGC spiking in wholemount preparations (Margolis and Detwiler. 2007).

In the mouse, using the same 3µM TTX concentration, we found the effect of TTX on the b-wave to extend even into stimulus strengths sufficiently low to

predominately excite RBCs (not shown). At 6 μ M TTX, a concentration high enough to silence the ganglion cell output, the rat scotopic b-wave was more reduced for all stimulus strengths used. This shows that both rat and mouse have a similar response to saturating concentrations of TTX, and this applies to the full range of stimuli. This conclusion is reasonable considering that the *in vitro* results suggest that $GABA_c$-mediated feedback onto RBCs is Na_v channel-dependent in rat slices (Chávez et al. 2010). Bui and Fortune (2004) on the other hand found that a predicted intravitreal concentration of 6 μ M TTX had no effect in scotopic conditions in rats, contradicting our hypothesis that the discrepancies between our results and those of Mojumder et al., (2008) may be due to insufficient levels of TTX. However Bui and Fortune (2004) also do not see an effect of TTX at high stimulus strengths, which should generate mixed rod cone responses but do see an effect on the cone pathway in rod saturating conditions. These results conflict with those of Mojumder et al. (2008) and our results, even with lower concentrations of TTX (3 μ M) suggesting the possibility that the retinal concentration of TTX in Bui and Fortune (2004) may be lower than predicted.

However it is difficult to explain how TTX could have an effect on the cone bipolar cell pathway in light-adapted but not dark-adapted conditions, especially considering the results of Mojumder et al., (2008) and Ichinose and Lukasiewicz (Ichinose and Lukasiewicz. 2007) both which suggest that cone bipolar cell Na_v channels are suppressed in light-adapted relative to dark-adapted conditions. In our experiments using the VEP as a positive control for the effect of TTX on retinal ganglion cell output we found that concentrations high enough to suppress the VEP reduced the b-wave in scotopic conditions even at stimuli where the rod pathway should predominately contribute to the ERG.

Mesopic conditions

Our results in mesopic conditions in both mice and rats were different than those of Mojumder et al. (2008) in rats. We found that 3μM TTX reduced the b-wave to 80.1±0.73% of control in scotopic backgrounds and 62.9±1.32% in mesopic (averaged over -0.6 to 1.0 log cd s/m^2 stimulus strengths). This confirms that in rats TTX has a

slightly larger effect in mesopic conditions, something we confirmed for 6 μ M TTX (b-wave reduced to 58.2±1.4% vs. 36.6±0.4 of control for scotopic and mesopic conditions respectively averaged over same stimulus strengths as above. Mojumder et al. (2008), however, report a substantially bigger effect of TTX in mesopic relative to scotopic conditions than we did (3-5 times larger reduction of b-wave amplitude in dimmest mesopic background relative to dark-adapted ERG at maximum stimulus strength in their Figs. 4, 9b, and 14b). One question that is raised is the following: if the effect seen by Mojumder et al. (2008) should be due to an incomplete effect of TTX, why is it so large in mesopic relative to scotopic conditions and compared to our findings in mice and rats?

The differences between our results and those of Mojumder et al. (2008) may be attributable in part to the fact that Brown Norway rats show a substantially increased a-wave and slow negative component following TTX injection in mesopic conditions. We used Sprague-Dawley rather than Brown Norway rats, which did not exhibit the large negative responses in mesopic conditions following TTX injection as in Mojumder et al. (2008). Another potential cause for the discrepancy is the quantification methodology used by Mojumder et al. (2008) in which the b-wave was measured from baseline rather than from the trough of the a-wave. Mojumder et al. (2008) show that TTX substantially increases the amplitude of a negative component. Should the a-wave increase following TTX application (which was seen in the Brown Norway rat model), the effect on the amplitude of the b-wave would appear to increase even if the actual amplitude of the b-wave is the same when measured from the a-wave trough. In support of this hypothesis Mojumder et al. (2008) show that the amplitude of the negative components of the ERG are reduced after NMDA, a neurotoxin to suppress inner retinal contributors to the ERG, which could explain why the effect of TTX on the b-wave is reduced when NMDA is added. Mojumder et al. (2008) suggest that Na_v channel-dependent inner retinal circuitry may contribute to the b-wave in mesopic, but not photopic or scotopic, adapting conditions. We believe this to be unlikely because, if true, NMDA alone should have reduced the mesopic b-wave, which was not the observed in their study. We therefore suggest that a combination of the large NMDA-sensitive negative response and the measure of the b-wave amplitude from the baseline rather than the trough of the a-wave

resulted in the finding by Mojumder et al. (2008) of an increased effect of TTX in mesopic background conditions.

It is difficult at this time to speculate on the contribution of the individual isoforms to the rod bipolar cell-generated b-wave. Four TTX-sensitive channel isoforms, Nav1.1, Nav1.2, Nav1.3, and Nav1.6, are known to be present in the inner retina (Côté et al. 2005, Fjell et al. 1997, Mojumder et al. 2007, Kaneko and Watanabe. 2007, O'Brien et al. 2008) and while they are all known to be expressed in retinal ganglion cells, their expression pattern in amacrine and other cell types is more equivocal. Moreover, the use of 'whole-body' knockout animals is problematic in this regard because of their short lifespan (Côté et al. 2005, Yu et al. 2006) and aberrant photoreceptor maturation (Côté et al., 2005, Smith and Côté. 2012). However, we expect that with the development of isoform-specific blockers (for example Rosker et al. 2007) and cell type-specific conditional knockout animals, that it will be possible to elucidate this question.

3.6 CONCLUSIONS

This study investigated the contribution of Na_v channels to the rodent electroretinogram using varied concentrations of TTX and measuring cortical responses to ensure completely blocked Na_v channels. We provide a mechanism showing that TTX acts mainly on two contributors to the ERG in a range of lighting conditions and stimulus strengths, $GABA_c$-mediated feedback onto RBCs and directly on Na_v channels in cone bipolar cells.

Table 3.1. Statistical comparison between normalized b-wave amplitudes after drug application.

	sRg_i	sR_i	sRc_i	sCr_i	m_LRc_i	m_LCr_i	m_HRc_i	m_HCr_i	pC_i
TTX	56.1 (9.1)	67.9 (6.4)	62.9 (2.7)	59.7 (2.8)	38.1 (3.3)	54.3 (2.3)	50.1 (4.0)	61.2 (2.0)	67.1 (3.1)
TPMPA	52.0 (7.1)	73.4 (6.2)	72.6 (2.8)	73.3 (2.9)	43.1 (3.0)	66.1 (2.6)	75.6 (6.0)	77.1 (3.8)	84.4 (3.7)
TPMPA +TTX	54.5 (7.0)	63.2 (4.1)	62.2 (2.8)	62.2 (2.7)	38.9 (6.1)	51.1 (4.7)	45.3 (10.1)	50.1 (4.6)	61.1 (4.4)
CNQX	21.7 (4.2)	40.6 (3.1)	59.4 (3.1)	59.4 (2.9)					
CNQX +TTX	123.8 (17.8)	117.5 (10.8)	75.0 (2.7)	74.3 (3.3)	67.4 (6.7)	61.0 (2.0)	72.6 (17.3	64.6 (4.9)	78.5 (10.4)

ANOVA Post Hoc

	sRg_i	sR_i	sRc_i	sCr_i	m_LRc_i	m_LCr_i	m_HRc_i	m_HCr_i
sR_i		X						
sRc_i			X					
sCr_i				X				
m_LRc_i		•	•	•	X			
m_LCr_i					•	X		
m_HRc_i							X	
m_HCr_i					•			X
pC_i					•		•	

	sRg_i	sR_i	sRc_i	sCr_i	m_LRc_i	m_LCr_i	m_HRc_i	m_HCr_i
sR_i	•	X						
sRc_i			X					
sCr_i				X				
m_LRc_i		•	•	•	X			
m_LCr_i					•	X		
m_HRc_i	•				•		X	
m_HCr_i	•				•			X
pC_i	•				•	•		

	sRg_i	sR_i	sRc_i	sCr_i	m_LRc_i	m_LCr_i	m_HRc_i	m_HCr_i
sR_i		X						
sRc_i			X					
sCr_i				X				
m_LRc_i		•	•	•	X			
m_LCr_i						X		
m_HRc_i							X	
m_HCr_i								X
pC_i					•			

	sRg_i	sR_i	sRc_i	sCr_i
sR_i	•	X		
sRc_i	•	•	X	
sCr_i	•	•		X

	sRg_i	sR_i	sRc_i	sCr_i	m_LRc_i	m_LCr_i	m_HRc_i	m_HCr_i
sR_i		X						
sRc_i	•	•	X					
sCr_i	•	•		X				
m_LRc_i	•	•			X			
m_LCr_i	•	•				X		
m_HRc_i	•						X	
m_HCr_i	•	•						X
pC_i	•							

Data points within each response zone of the ERG (see Fig. 2H) were averaged and subjected to a post hoc analysis (ANOVA, Bonferroni correction). Standard errors are in parentheses and dots indicate significance (p<0.05), shaded area highlights mesopic backgrounds.

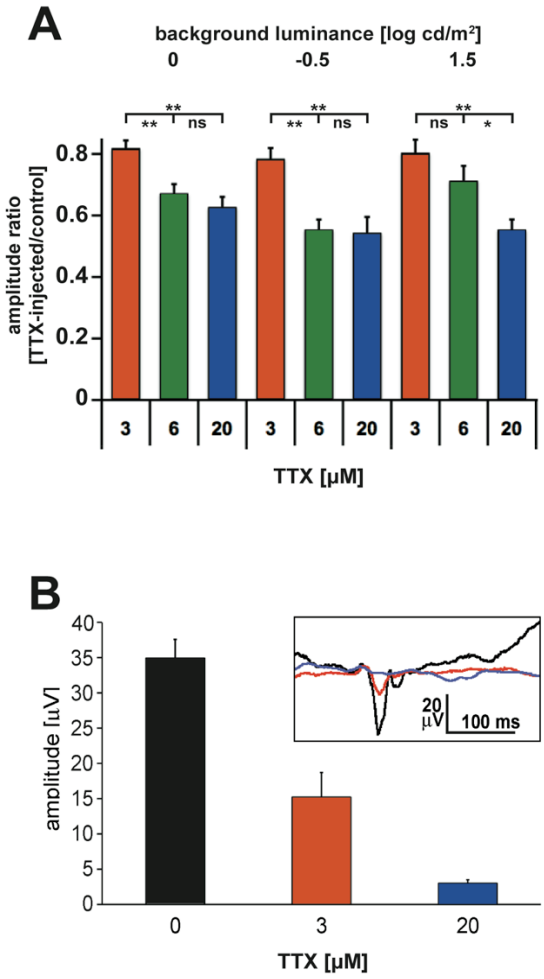

Figure 3.1: Comparison of the effects of varying concentrations (3, 6, and 20 μ M) of TTX on the amplitude of the b-wave in response to a high-strength stimulus. A) Normalized b-wave responses to high strength stimuli (1.0 log cd s/m^2) over scotopic, mesopic (-0.5 log cd/m^2), and photopic (1.5 log cd/m^2) backgrounds. TTX-treated eyes were compared to un-injected control eyes using paired Student's *t*-test. All TTX concentrations reduced the b-wave significantly compared to un-injected controls. The result of an ANOVA post-hoc analysis is indicated by significance levels *=$p\leq$ 0.01. B) Amplitude of cortical visual evoked potentials at 0, 3, and 20 μ M TTX. Inset depicts example traces. Error bars are standard error.

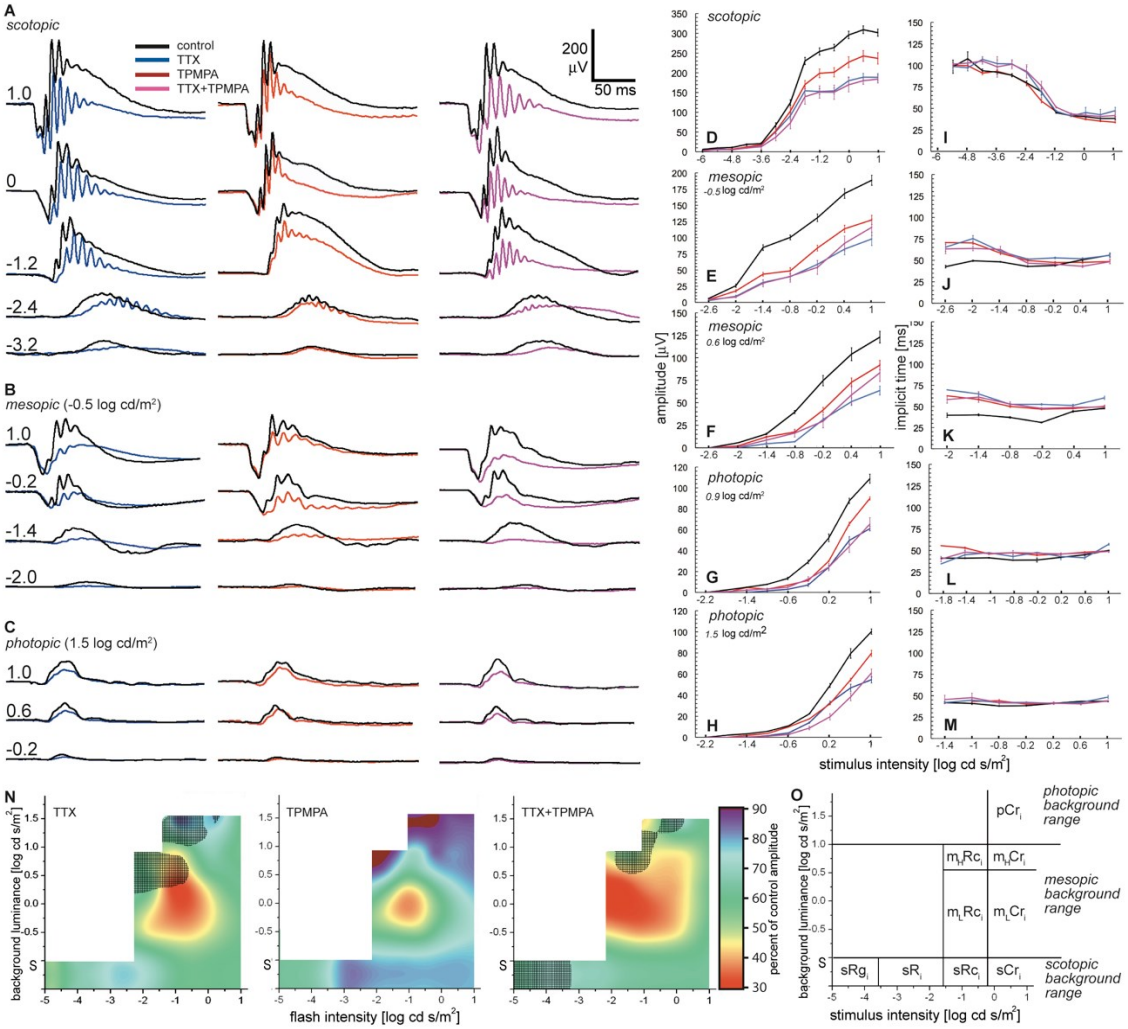

Figure 3.2: Na_v channels contribute predominately to $GABA_c$-mediated input to rod bipolar cells. A-C) Example waveforms from ERG recordings of TTX, TPMPA, or TTX+TPMPA-injected retinas in the scotopic (A), mesopic (B) and photopic (C) ranges. B-wave amplitude (D-H) and implicit time (I-M) responses to increasing stimulus strengths presented over increasing background luminances (from D, I: dark-adapted to H, M: 1.5 log cd/m^2) for eyes injected with TTX, TPMPA, or a combination of both. Control is the average of the paired un-injected control eyes from all drug treatments. Error bars are standard error. N) Contour representation of b-wave amplitudes as a function of both stimulus strength and background luminance for TTX, TPMPA, and TPMPA+TTX-treated eyes normalized to paired un-injected control eyes. Contour representation is derived from 7 backgrounds from -0.5 to 1.5 log cd/m^2. Hatched areas represent data points that are non-significant versus control (p>0.05). O) Schematic representation of the areas corresponding to the stimulus strength ranges and backgrounds used (see Materials and Methods).

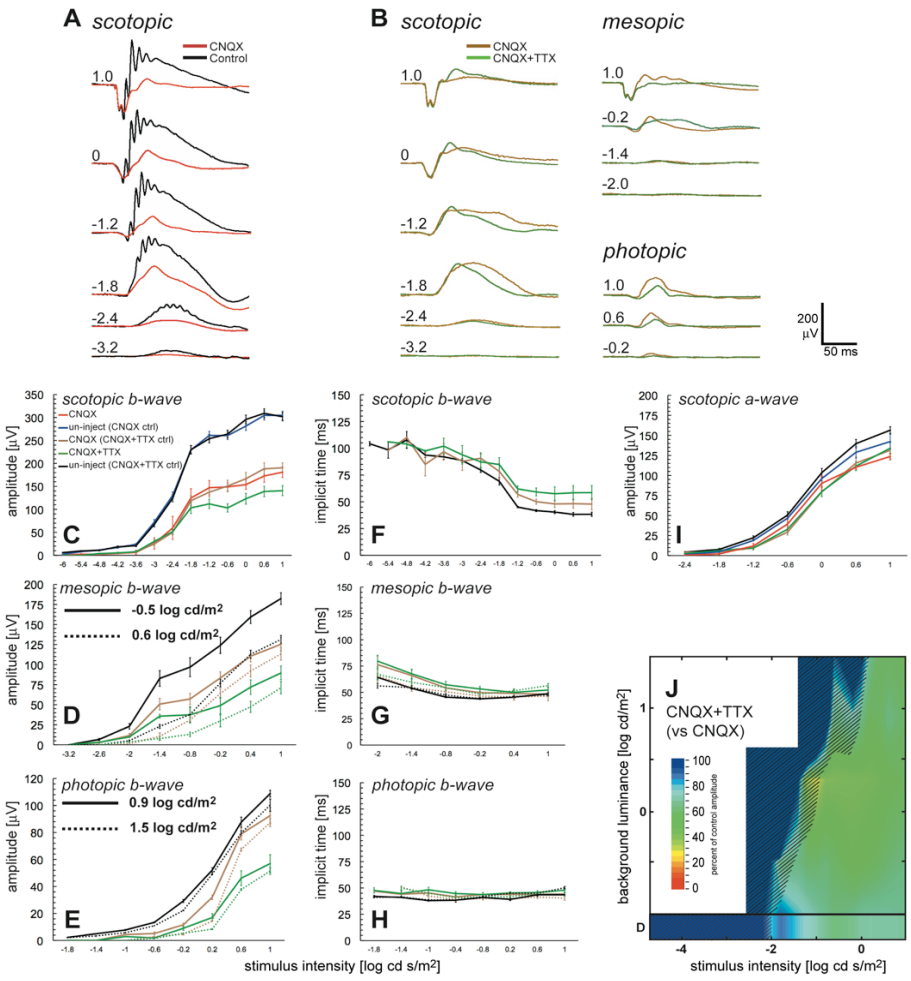

Figure 3.3: Na_V channels on ON bipolar cells contribute to b-wave amplitude when stimulus strength is sufficient to stimulate cone pathways. A, B) Example waveforms from ERG recordings of A) dark-adapted CNQX-injected retinas (compared to uninjected control) and B) CNQX+TTX-injected retinas (compared to CNQX-injected) either dark-adapted or recorded under mesopic or photopic backgrounds**.** C, D, E) amplitude and F, G, H) implicit time b-wave responses to increasing stimulus strengths presented over increasing background luminances (C, F: dark-adapted, D, G: -0.5 and 0.6 log cd/m^2, and E, H: 0.9 and 1.5 log cd/m^2) for un-injected eyes (controls) or injected with CNQX or CNQX+TTX. Control is the average of the paired control eyes from all drug treatments. I) scotopic a-wave amplitude. Error bars are standard error. J) Contour representation of b-wave amplitudes as a function of both stimulus strength and background luminance for CNQX+TTX treated eyes normalized to paired CNQX treated eyes. Contour representation is derived from 7 backgrounds from -0.5 to 1.5 log cd/m^2. Hatched areas represent data points that are non-significant versus control (p>0.05).

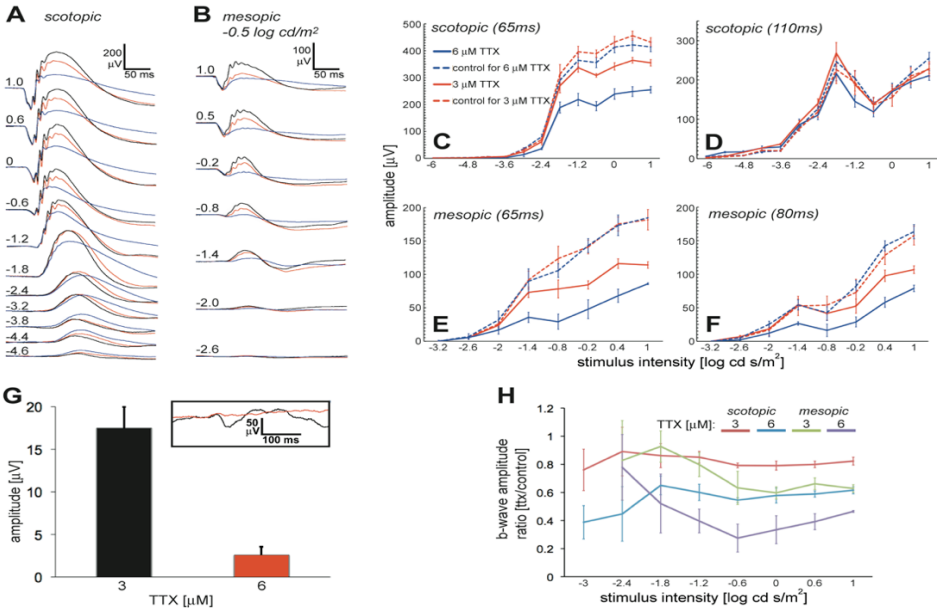

Figure 3.4: In rats, low concentration (3 µM) TTX acts predominately at higher stimulus strengths while higher (6 µM) TTX reduces b-wave amplitude at both high and lower stimulus strengths. A-B) Example ERG recording traces of TTX-injected retinas in the A) scotopic and B) mesopic ranges. C-F) B-wave amplitude responses to increasing stimulus strengths presented over C, D) dark-adapted and E, F) mesopic (-0.5 log cd/m^2) backgrounds measured at C) 65 and D) 110 ms (scotopic) and E) 65 and F) 80 ms (mesopic). G) Controlling for saturating concentrations of TTX using cortical visual evoked potentials at 3 and 6 µM TTX, contralateral eye blinded by high concentration cobalt and CNQX. H) B-wave responses normalized to un-injected control eyes. Error bars are standard error.

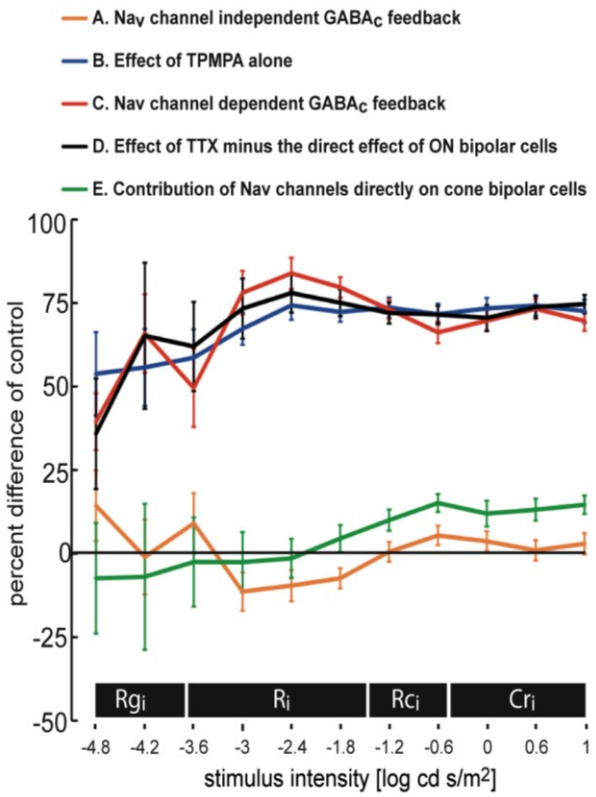

Figure 3.5: Contribution of individual Na_v channel-dependent components contributing to the amplitude of the b-wave. The individual components are defined as A) Na_v channel independent $GABA_c$-mediated effects on B-wave amplitude [(TTX/control)-((TTX+TPMPA)/control)], B) Total $GABA_c$-mediated effects on B-wave amplitude [TPMPA/control], C) Na_v channel-dependent $GABA_c$ feedback [TPMPA-((TTX/control)-((TTX+TPMPA)/control))], D) Indirect effect of TTX of the b-wave amplitude in the absence of direct effects due to Na_v channels in cone bipolar cells [(TTX/control)-(((CNQX)-(TTX+CNQX))/control)], E) contribution of Na_v channels directly on bipolar cells [((CNQX)-(TTX+CNQX))/control]. Error bars are standard error. The black bars indicate stimulus strength ranges used (see Materials and Methods).

CHAPTER 4: D1 DOPAMINE RECEPTORS MODULATE CONE ON BIPOLAR CELL Na_v CHANNELS TO CONTROL DAILY RHYTHMS IN PHOTOPIC VISION

Publication information

Smith, B. J., Côté, P. D., & Tremblay, F. (2015). D1 dopamine receptors modulate cone ON bipolar cell Nav channels to control daily rhythms in photopic vision. *Chronobiology International*, *32*(1), 48–58. http://doi.org/10.3109/07420528.2014.951054

4.1 Abstract

In amphibians, voltage-gated sodium (Nav) channels in cone ON bipolar cells (ON-CBC) amplify cone signals in the dark and in mesopic background light. During light adaptation however dopamine, acting through D1 receptors (D1R), suppresses Nav channels and therefore act as a gain control mechanism. Curiously in rodents Nav channel contributions to the ON-CBC generated light-adapted electroretinogram (ERG) b-wave appear exist even in fully light-adapted conditions. We sought to determine how rodent ON-CBC Nav channels are regulated by dopamine via D1R during light adaptation and during the circadian cycle. We first tested the sensitivity of Nav channels in mouse ON-CBCs to modulation by dopamine via D1Rs . Although light-adaptation had little effect on Nav channel contributions to the b-wave, these channels were found to be modulated by D1Rs. We pharmacologically isolated the cone to ON-CBC circuit in fully light-adapted retinas to confirm these results. Retinal dopamine release following light adaptation has been previously shown to be increased in mice during circadian night. We first show that circadian fluctuations in ON-CBC function are suppressed in dark-adapted retinas, indicating that circadian fluctuations are a function of light adaptation. Secondly, we show that at night the mouse retina behaves similarly to those of frogs and salamanders with a gain control mechanism utilizing D1R modulation of Nav channels to suppress ON-CBC light responses in light-adapted conditions during circadian night. Taken together, these results suggest that circadian control of ON-CBC function contains an initial phase after approximately 18-30 hrs of dark adaptation, leading to substantial changes in b-wave amplitude after a relatively short time in free run dependent on D1R modulation of Nav channels.

4.2 Introduction

In mammalian chronobiology, the retina is perhaps best known for its role in the transmission of light information to the master circadian pacemaker located within the suprachiasmatic nucleus (SCN) of the hypothalamus, via its melanopsin-containing intrinsically photosensitive retinal ganglion cells (ipRGC) (Berson, 2003). The retina does, however, contain its own intrinsic circadian clock (Tosini & Menaker, 1996) which is known to autonomously control a variety of physiological events. In particular, circadian rhythms were found to influence light adapted retinal sensitivity (Tassi & Pins, 1997; Barnard et al., 2006; Storch et al., 2007; Cameron et al., 2008a; Jackson et al., 2012) as analyzed by the electroretinogram (ERG), a common method for assessing retinal function and sensitivity and a non-invasive method to assess ON bipolar cell light responses (Frishman, 2006). It was determined that the ERG component that is primarily affected by the retinal clock is the b-wave, a waveform driven by the cone ON bipolar cells (ON-CBC) (Manglapus et al., 1998; Barnard et al., 2006; Storch et al., 2007). While ON-CBCs do not express the clock gene *Per1* and show very low levels of *Per2* and *Cry2*, and therefore do not appear to have the necessary molecular machinery to support circadian rhythmicity (Liu et al., 2012), adjacent dopaminergic amacrine cells that regulate ON-CBC function do possess the necessary components (Witkovsky et al., 2003; Gustincich et al., 2004; Ruan et al., 2006; Dorenbos et al., 2007; Ruan et al., 2008; Liu et al., 2012). Indeed, retinal dopamine synthesis and release is well known to be stimulated by light and in some species by circadian rhythm with dopamine levels being increased during circadian daytime (Iuvone et al., 1978; Nir et al., 2000; Doyle et al., 2002a; Doyle et al., 2002b; Li et al., 2013).

Due to circadian effects on light responses of ON-CBCs, the b-wave of both the dark and light adapted ERGs are influenced by the circadian rhythm (Storch et al., 2007). During light adaptation in midday, the amplitude of the cone isolated b-wave increases (Peachey et al., 1993; Bui & Fortune, 2006), at midnight light adaptation still occurs but the maximum amplitude reached is reduced relative to midday (Barnard et al., 2006; Storch et al., 2007; Cameron et al., 2008a; Jackson et al., 2012). It is unclear however how ON-CBCs may modulate their activity in response to dopamine during the circadian cycle, especially in mammals. A recent report by Jackson et al., (2012) suggests that in

constant darkness after 42 to 54 hours (DD2), D4 dopamine receptors (D4R) appear responsible for the b-wave circadian rhythm. However D4Rs do not maintain circadian rhythm at DD1 (18-30 hours in dark) since a substantial b-wave decrease is observed at midnight relative to midday in D4R retina-specific knockout mice. This opens the door to modulation by other dopamine receptors at DD1. We were interested in discovering the mechanism leading to the strong suppression of the CBC light response in DD1. ON-CBCs in many animal species express voltage gated sodium (Nav) channels (Pan & Hu, 2000; Zenisek et al., 2001; Ichinose et al., 2005; Ma et al., 2005; Ichinose & Lukasiewicz, 2007; Saszik & DeVries, 2012). While Nav channels are best known for their role in the initiation and propagation of the action potential in excitable cells (Catterall, 2012), the Nav channels present on ON-CBCs may play a role in increasing the gain in dark-adapted conditions. In salamander, the bipolar cell Nav channels are strongly suppressed by D1Rs in daytime photopic conditions to prevent saturation (Ichinose & Lukasiewicz, 2007) making the photopic responses insensitive to action of Nav blocker such as tetrodotoxin (TTX). In frog, D1R block increases the photopic b-wave (Popova & Kupenova, 2011). Interestingly, recent results indicate that in mammals ON-CBC Nav channels may be functional in photopic conditions as indicated by the ERG b-wave. In response to TTX , the photopic b-wave can still be reduced in rats (Bui & Fortune, 2004; Bui & Fortune, 2006) and mice (Miura et al., 2009; Smith & Côté, 2012; Smith et al., 2013). Furthermore, the photopic b-wave is reduced rather than increased in D1 dopamine receptor (D1R) knockout mice, (Jackson et al., 2012; Zhang et al., 2012; Lavoie et al., 2014) and after D1R block in rabbits (Huppé-Gourgues et al., 2005), indicating that dopamine acting though D1Rs are unlikely to suppress Nav channels during light adaptation in mice and rats, unlike it is proposed for amphibians.

Here we use the ERG b-wave of C57Bl/6 mice as an index to measure the influence of dopaminergic input on Nav-sensitive ON-CBCs during light adaptation in daylight and at night. While melatonin is necessary for maintenance of long term (3-10 days in darkness) circadian rhythm of dopamine metabolites in mice (Doyle et al., 2002a; Pozdeyev et al., 2008; Sengupta et al., 2011), many studies on circadian rhythmicity in ON-CBC light responses in mice (Barnard et al., 2006; Storch et al., 2007; Cameron et al., 2008a; Jackson et al., 2012) are based on use of melatonin deficient C57Bl/6 mice

(Roseboom et al., 1998), which have rhythmic expression of tyrosine hydroxylase and the primary dopamine metabolite 3,4-dihydroxyphenylacetic acid (DOPAC), during DD1 (18-30 hours in complete darkness; Dkhissi-Benyahya et al., 2013). This rhythmic expression of TH and DOPAC is absent in C57Bl/6 OPN4-/- mice (Dkhissi-Benyahya et al., 2013). Our results suggest that in mice a retinal circuit involving D1R mediated inhibition of Nav channels, a circuit that is used to prevent saturation of ON-CBC light responses in amphibians, is inactive during daytime and is repurposed to suppress ON-CBC light responses at night.

4.3 Material and Methods

4.3.1 Ethics approval

All animal procedures were done in accordance to animal care guidelines established by the Canadian Council on Animal Care and in compliance with the ARVO statement for the Use of Animals in Ophthalmic and Vision Research. Circadian rhythm experimentation protocols conform to the standards of the Journal (Portaluppi et al., 2010). Animals had *ad libitum* access to food and water.

4.3.2 Electroretinography

C57BL/6 mice between 8 and 24 weeks of age (Charles River Laboratories, St. Constant, QC, Canada) were anesthetized by intraperitoneal injection of Avertin (2,2,2 Tribromoethanol, Sigma Aldrich, St-Louis, MO) dissolved in amylene hydrate (tertiary amyl alcohol, 275 mg/kg, Sigma Aldrich). The pupils were dilated with the mydriatic agent cyclopenolate HCl 0.5% (Alcon, Fort-Worth, TX) and a 0.5% proparacaine hydrocloride (Alcon) was applied as a topical anesthetic. Body temperature was maintained at 37°C with a heated pad and monitored rectally. Mice were sacrificed by anesthetic overdose followed by cervical dislocation. The active electrode was a Dawson-Trick-Litzkow-plus microconductive fiber (Diagnosys, Littleton, MA) placed on the corneal surface and hydrated with 2.5% hydroxypropyl methylcellulose solution to maintain conductivity. Platinum subdermal electrodes (Grass Instruments, Quincy, Mass) were placed in the base of the nose (reference) and in the tail (ground).

Signal from the corneal electrodes was amplified 10,000 fold using a differential amplifier with a bandwidth of 0.3-300 Hz (P511, Grass instruments). Signal was acquired at 1 kHz by an A/D board (PCI 6281, National Instruments, Austin, TX, USA) and displayed and stored for processing using LabVIEW 9.0 dedicated software (National Instruments). Flash stimuli were generated by a Ganzfeld stimulator (LKC Technologies, Gaithersburg, MD, USA) that produced a maximum integrated luminance of 10.1 log cd s/m^2 at the corneal surface. Stimulus strengths were attenuated by up to 7.0 log units by manual interposition of neutral density filters (Kodak Wratten, Rochester, NY, USA). The interval between stimuli varied between 30 s for paired flash experiments to 1 s for light adapted stimuli, 5-20 responses were averaged depending on stimulus strength. Paired flash stimuli to isolate dark-adapted cone responses used a 500 ms inter-flash interval**,** slightly less than Mojumder et al., (2008) in rats but which caused no changes in ERG response in photopic conditions compared to a 1 s inter-flash interval.

4.3.3 Light adaptation and circadian rhythm protocols

Circadian midday CT6 was defined as recordings occurring between 12:00 and 16:00, after 18 hours of dark adaptation. Circadian midnight (CT18) was defined as recordings taking place between 0:00 and 2:00 after 30 hours of dark adaptation. The paired-flash paradigm (PF) was applied at the end of the dark adaptation period and therefore refers to dark-adapted cone activity. Because of software issues, only one flash intensity (1.0 log cd m s^{-2}) was used. Intensity series (LA; spanning 2 log units) were performed after 25 minutes of light adaptation in most cases, and after 5-6 hours in case of data presented in figure 2. A background luminance of 1.5 log cd m^{-2} was used as rod-desensitizing background (Jackson et al., 2012).

4.3.4 Intravitreal injection

Following application of a topical anesthetic to the cornea of anesthetized mice, 1 µl of 20 µM tetrodotoxin (Smith et al., 2013)(TTX, Abcam Biochemicals, Toronto, Ontario), 200 µM 6-Cyano-7-nitroquinoxaline-2,3-dion (CNQX, Tocris Bioscience, Bristol, UK), 1mM SKF-38393 (Tocris), and 200 µM SKF-83566 (Tocris), dissolved in

phosphate buffered saline pH 7.4 was injected into the vitreous via a 30-gauge needle mounted on a Hamilton syringe under dim red light (dark adapted mice for circadian rhythm and paired flash recordings) or room lighting (light adapted mice). A summary of action site in the retina and effects on retinal circuitry can be found in Table 1. The injection site was located approximately 0.5 mm behind the ora serrate. Following injection we waited approximately 20 minutes to allow for diffusion of the drug before recording. Drug concentration at the retina was calculated using an estimated vitreal volume of 5 μL for mouse (Jeon et al., 1998; Kaplan et al., 2010).

4.3.5 Data analysis

Analysis of ERG waveforms was completed using a custom ERG analysis toolbox written for Matlab (Mathworks, Natick, MA). Waveforms were low pass filtered at 50 Hz (Butterworth 8th order filter) to reduce the contribution of the large amplitude oscillatory potentials that could interfere with the measurement of the slow b-wave potential (Lei et al., 2006). The resulting b-wave was measured from the a-wave trough to the maximum positive peak. Compilation of b-wave amplitudes was carried out using Microsoft Excel (Redmond, WA) with statistical analysis using STATA 12 software (College Station, TX). For the paired-flash paradigm, paired t-test strategy was used, while data from light-adapted intensity series were analyzed through repeated-measured ANOVA.

4.4 Results

4.4.1 In photopic conditions, endogenous dopamine is unable to fully suppress amplification of ON-CBC light responses by Nav channels.

We began by determining if the D1R contribution to the photopic mouse ERG response recorded in daytime is similar to what has been previously obtained in salamander (Ichinose & Lukasiewicz, 2007). We used the D1R agonist SKF38393 in combination with TTX to test how D1R activation modulates ON-CBC function in midday after light adaptation (LA) following 18 hours of free run (CT6)(Fig 1). We found that the D1R agonist SKF38393 is able to decrease the b-wave amplitude at all

stimulus strengths above -0.2 log cd m s^{-2} in condition of light adaptation, reaching a maximum 31.5±3.5% reduction at 1.0 log cd m s^{-2} (Fig 1B). As previously shown by us (Smith & Côté, 2012; Smith et al., 2013) and others (Bui & Fortune, 2004; Bui & Fortune 2006; Miura et al., 2009), the action of TTX alone significantly reduced the photopic b-wave for stimulus strengths above -0.6 log cd m s^{-2} reaching a maximum reduction of 40.7±3.6% at 1.0 log cd m s^{-2} (Fig 1 B,C; $p \leq 0.001$; ANOVA) while the combination of TTX with the D1R agonist SKF38393 reduced the photopic b-wave slightly more for flash intensities above 0.2 log cd m s^{-2} reaching a maximum reduction of 50.6±4.9% at 1.0 log cd m s^{-2} (Fig 1B,C; $p \leq 0.001$; ANOVA); however, no difference could be detected between TTX alone and TTX combined with D1R agonist SKF38393, thus suggesting that D1Rs exercise the majority of their action during daytime light adaptation through control of Nav channels. In dark-adapted conditions (using the paired-flash (PF) paradigm; see methods), TTX significantly reduced the ERG b-wave amplitude to a maximum of 43.1±1.7%, while its combination with the D1R agonist SKF38393 did not add any significant effect (maximum reduction of 44.1±4.0%; Fig 1C). Interestingly, we found that the effect of TTX alone and in combination with the D1R agonist SKF38393 were similar in dark-adapted and light-adapted retinas (Fig 1C). This suggests that, in the mouse model, light adaptation suppresses ON-CBC Nav channels to the same extent they do in dark-adapted conditions, a conclusion quite different from the one described in salamander (Ichinose & Lukasiewicz, 2007).

These results show that Nav channels can be suppressed by an exogenous D1R agonist but that in midday light adaptation causes almost no suppression of Nav channels in mice. We confirmed this by injecting the D1R antagonist SKF83566 (Fig 1, blue traces). If light adaptation caused dopamine release to suppress Nav channels via D1R, then blocking D1R should increase the photopic b-wave. Like others using D1R knockout mice (Jackson et al., 2012; Zhang et al., 2012; Lavoie al. 2013; Lavoie et al., 2014), and pharmacologic D1R block in rabbits (Huppé-Gourgues et al., 2005), rather than an increase we instead found that D1R antagonist SKF83566 reduced the photopic b-wave for all flash intensities above -0.6 log cd m s^{-2} reaching a 23.6±4.6% reduction at 1.0 log cd m s^{-2} (Fig 1, blue traces).

4.4.2 Nav channel light adaptation amplification is independent of other synaptic input on ON-CBCs.

In order to better circumscribe the influence of dopamine on light adaptation of the ON-CBCs, the cone to ON-CBC circuit was isolated by blocking ionotropic glutamate receptors thus avoiding indirect network effects of dopamine. We injected CNQX and TTX in light-adapted eyes at midday (Fig 2, CT6) after 5-6 hours of light adaptation, similar to the experiments of Ichinose & Lukasiewicz (2007) in salamander. CNQX, slightly but not significantly reduced the ERG b-wave amplitude (Fig 2B, p=0.078, 9.3±2.5% reduction at 1.0 log cd m s^{-2}). The addition of TTX on the eyes pre-treated with CNQX significantly reduced the photopic b-wave amplitude at all flash energies above -0.6 log cd m s^{-2} reaching a maximum 41.2%±6.9% reduction at 1.0 log cd m s^{-2} (Fig 2, green traces). These results show that unlike the salamander (Ichinose & Lukasiewicz, 2007), ON-CBC responses in mice are amplified by Nav channels in absence of other network influence.

To ensure that the D1R agonist SKF38393 was acting on Nav channels directly on ON-CBCs, we added CNQX + SKF38393 in light-adapted eyes. The photopic b-wave was significantly reduced at flash intensities above 0.2 log cd m s^{-2} reaching maximum reduction at 1.0 log cd m s^{-2} of 46.5±1.9% (Fig 2, orange traces). The reduction in the amplitude of the photopic b-wave due to CNQX + SKF38393 were similar to the effects of CNQX + TTX, suggesting that D1R activation primarily reduces the b-wave amplitude by suppressing Nav channels. To verify for additive effects of TTX and SKF38393 we injected CNQX + TTX + SKF38393 in light-adapted eyes. The photopic b-wave was significantly reduced for all flash intensities above -1.0 log cd m s^{-2} reaching a maximum reduction at 1.0 log cd m s^{-2} of 47.9±2.9% (Fig 2, red traces). From these results, we conclude that the TTX-sensitive portion of the photopic b-wave is primarily due to Nav channels directly on ON-CBC, and the activity of these channels can be suppressed by D1R. In the mouse, contrary to what was described in salamander, Nav channels in mice remain functional under normal light-adapted conditions in midday.

4.4.3 Nav channels have little amplifying effect on light adapted ON-CBC in circadian night (CT18).

Up to this point, our results point to different mechanisms of gain control in the light-adapted cone pathway in mammals, in comparison to data from amphibians. In the next series of experiments we investigated the idea that the daylight dopamine control of Nav channels on the ON-CBCs has been repurposed to suppress ON-CBC light responses at night. We have measured dark- and light-adapted ERGs after 30 hours (CT18; subjective midnight) of free run under continuous darkness. We first confirmed previous work (Cameron et al., 2008a; Cameron et al., 2008b) showing that in C57Bl/6 mice, light-adapted ERGs have reduced amplitude at CT18 relative to CT6 for all flash intensities above -0.6 log cd m s^{-2} reaching a maximum about 30% reduction (Fig 3, gray traces). We injected TTX in light-adapted eyes to block Nav channels at CT18 and found that when TTX was injected at CT18, the effect of TTX was considerably reduced compared to similar recordings at CT6. (Fig 3D, red traces), the maximum reduction obtained at CT18 being 12.9±7.4% at 1.0 log cd m s^{-2} (p=0.05). We found that CNQX injected eyes had similar amplitude at CT6 (86.45±2.5 μV) and CT18 (99.9±6.9 μV)(Fig 3, gold traces), amplitude matching those obtained in control conditions at CT6. TTX added to CNQX-treated eyes had the same effect as TTX added by itself and no difference was noted between CT6 and CT18 with either of the two drugs (Fig 4C, green traces, 53.1±6.6 μV) and CT18 (60.3±5.1 μV).

We also looked at the effect of circadian rhythm on dark-adapted ON-CBC using both PF recordings and mixed rod cone responses elicited by bright stimuli well above cone threshold (1.0 log cd m s^{-2}). We did not see a significant variation in the PF ERGs between CT6 and 18 (Fig 4, gray traces; 114.9±4.6 μV midday vs. 108.5±6.7 μV midnight, 1.0 log cd m s^{-2}, p=0.43) or using the dark-adapted bright flash ERG(not shown, CT6 309.7± 8.9 μV vs. CT18 310±11.6 μV, p=0.84 at 1.0 log cd m s-2;see also (Cameron et al., 2008a; Jackson et al., 2012)). This would suggest that a circadian effect on the ON-CBCs is primarily a function of light adaptation rather than a direct effect on cone circuitry in both light and dark-adapted conditions.

Since we have previously shown that the D1R agonist SKF38393 is able to suppress the Nav channel component of the photopic ERG during the day (Fig 1) we considered the possibility that D1Rs suppress Nav channels at night, similar the mechanism previously described for salamanders during the day (Ichinose & Lukasiewicz, 2007). When we added the D1R antagonist SKF83566 to block D1Rs at CT18 the light-adapted b-wave was significantly increased relative to control for all flash intensities above -0.6 log cd m s^{-2} (Fig 4, blue with horizontal stripes) reaching a maximum 137.5±7.2% increase relative to control at 1.0 log cd m s^{-2}. In the presence of SKF83566 the photopic b-wave amplitude is similar to control eyes at CT6 or eyes injected with CNQX at CT18 (SKF83566, 93.0±2.5 μV; CNQX, 99.9±6.9 μV; CT6 control 96.4±5.2 μV).

Interestingly, we observed that at CT18, D1R antagonist SKF83566 increased photopic b-wave amplitude to the size of control eyes at CT6 (Fig 4, gray with horizontal stripes, 96.4 ±5.2 μV at 1.0 log cd m s^{-2}) rather than the amplitude of SKF83566 at CT6 (Fig 4, blue, 70.9±3.4 μV). To help resolve this we looked at the effect of the D1R antagonist SKF83566 on the dark-adapted cone b-wave. During the day SKF83566 reduced the amplitude of the cone isolated b-wave (Fig 4, blue vertical stripes, 21.4±3.9% reduction at 1.0 log cd m s^{-2} p=0.03) while at night the D1R antagonist SKF83566 had no significant effect on cone-isolated b-wave (0.01±2% reduction at 1.0 log cd m s^{-2}, p= 0.89), supporting the assumption that the dopamine control of Nav channels on ON-CBCs at CT18 is involved with gain control following light-adaptation rather than light sensitivity in the cone ON pathway *per se*.

In summary, our results showed that, unlike in the salamander, light adaptation of the ON-CBCs in mice is not controlled during daytime by D1R receptor modulation of Nav channels. Rather, dopamine release during light adaptation at midnight generates daily rhythms in amplitude of ON-CBCs light responses through D1R modulation of Nav channels.

4.5 Discussion

We found that during circadian day dopamine, acting through D1R, is able to strongly inhibit Nav channels in mouse ON-CBCs similar to previous results obtained in salamander (Ichinose & Lukasiewicz, 2007). Surprisingly, in mice we found that light adaptation during midday is unable to cause sufficient dopamine release to strongly suppress Nav channels as seen in salamander. At night however dopamine released during light adaptation is able to strongly suppress Nav channels via D1R leading to the robust daily rhythm that reduces ON-CBC function at midnight relative to midday as previously shown by others (Barnard et al., 2006; Storch et al., 2007; Cameron et al., 2008a; Jackson et al., 2012). These results demonstrate the mechanism of daily rhythms in the cone ON pathway and show that similar neural circuits can be adapted for novel functions between species (frogs and salamanders vs. mice).

4.5.1 ON-CBC light responses are amplified by intrinsic Nav channels even after light adaptation in mice.

During circadian day, blocking Nav channels in mice substantially reduced ON-CBC light responses consistent with previous results in both mice and rats (Bui & Fortune, 2004; Bui & Fortune, 2006; Mojumder et al., 2007; Mojumder et al., 2008; Miura et al., 2009; Smith & Côté, 2012; Smith et al., 2013). Consistent with the results of Ichinose & Lukasiewicz (2007) we found that a D1 agonist was able to suppress ON-CBC function to the same extent as TTX even in conditions of iGluR block. One potential difficulty is that even though we injected CNQX + TTX, CNQX + SKF38393, and CNQX + TTX + SKF38393 in fully light-adapted eyes, similar to Ichinose & Lukasiewicz (2007), both CNQX and TTX could reduce dopamine release from dopaminergic amacrine cells. During the day, however, the amplitude of the photopic b-wave after CNQX injection was slightly reduced and TTX added furter reduction in the photopic b-wave amplitude.

It is worth noting that the presence of CNQX alone slightly reduced rather than increased the amplitude of the b-wave as observed in salamander. If CNQX was suppressing light adaptation-dependent dopamine release, then control eyes should have b-wave amplitudes similar to TTX injected eyes, and CNQX or D1R antagonist

SKF83566 should increase the b-wave amplitude, as seen at night in the mouse and during the day in salamander.

It is interesting to consider why mice avoid suppressing ON-CBC cell Nav currents during light adaptation in contrast to salamander. In ground squirrel Nav channels generate action potentials which are strongest during a flicker stimulus that should light adapt the retinas (Saszik & DeVries, 2012) and increase dopamine release (Dong & McReynolds, 1992). Suppressing light adaptation-dependent dopamine release onto ON-CBC D1Rs may maintain their ability to encode stimuli with high temporal fidelity even in fully light-adapted conditions in day.

4.5.2 Nav channels on ON-CBC are suppressed at night by dopamine released during light adaptation.

We determined, using a combination of paired flash stimulus to isolate dark-adapted cone ERGs as well as by examining the mixed rod cone ERG elicited by a bright flash, that during circadian night (CT18) the reduction of ON-CBC light responses is a function of light adaptation. As shown by Cameron et al., (2008) there is little variation in the mixed rod-cone ERG between CT6 and CT18, although they did saw a circadian rhythm with peaks at CT1 and CT13, and reductions at CT6 and CT18. Similarly Jackson et al., (2012) did not find a significant difference in the dark-adapted b-wave amplitude between CT6 and CT18 even at high stimulus strength.

We found that the circadian rhythm in the cone ON pathway on DD1 is due mainly to increased suppression of ON-CBC Nav channels by D1R as a consequence of light adaptation-dependent dopamine release. We also noted that there are opposing effects of D1R activation on ON-CBC light responses that seem to alternate between night and day. At night in dark-adapted eyes, D1R activation no longer suppresses the cone driven b-wave and at night, light adaptation suppresses intrinsic ON-CBC Nav channels. Some previous evidence supports this mechanism of gain control during circadian night. For instance light adaptation during circadian day causes dopamine release only from axons stratifying in sublamina 1 of the inner plexiform layer adjacent to OFF cone bipolar cell terminals, but not perikarya in rat dopaminergic amacrine cells and

does not significantly increase overall retinal dopamine levels (Vugler et al., 2007). In addition dopamine release driven by 90 minutes of light adaptation is significantly higher at CT18 than CT6 in mice. (Cameron et al., 2009). In figure 5, we propose a model of Nav channel contributions to ON-CBC light responses in relation to dopamine levels. During midday (CT6), dopamine release has relatively little effect on ON-CBC Nav channels in both dark- and light-adapted conditions, and blocking D1Rs decreases the cone driven b-wave in both light and dark adapted conditions (inset graph) likely due to effects on inhibitory circuitry (Herrmann et al., 2011)**.** At midnight (CT18) dopamine release during light adaptation is increased and reduces the amplification of ON-CBC light responses by Nav channels in light adapted relative to dark adapted conditions.

Our results, when added to the results of Jackson et al., (2012), suggest that there are two mechanisms of circadian rhythm in C57BL/6 mice in the absence of melatonin. Jackson et al., (2012) conclude that D4 receptors are necessary and sufficient to couple the intrinsic retinal circadian rhythm to the function of ON-CBC. However they also show circadian rhythmicity in ON-CBC in D4 knockout mice in DD1 with similar amplitude to control mice. This strong modulation of b-wave amplitude disappears in DD2, at which point control mice also show reduced effects of circadian rhythmicity on the amplitude of the photopic b-wave. Our results show that the robust circadian rhythm seen after 6-18 hours in dark (DD1) is controlled predominantly by D1R and Nav channels. These results, together, suggest that coupling of circadian oscillators in dopaminergic amacrine cells to ON-CBC function is more complex than previously thought and contains at least two phases: one leading to substantial changes in b-wave amplitude effects after relatively short time in free run which quickly loses rhythm and an additional persistent oscillator mediated by D4 receptors.

4.6 CONCLUSIONS

In conclusion, our results suggest that circadian rhythm modulation of cone pathway function in mice involves an early mechanism based on D1Rs and Nav channels that acts in the short-term (DD1, 6-18 hours). However, it appears that longer-term modulation is taken over by a mechanism based on D4Rs affecting persistent circadian rhythms after 42 hours (DD2) (Jackson et al., 2012). The strong similarity between the

circuit we describe and a previously described circuit suppressing ON-CBC function during light adaptation in amphibians (Ichinose & Lukasiewicz, 2007) suggests that this circuit may have been repurposed in mice. We speculate that a neural circuit under the control of the retinal circadian clock is able to reduce dopamine release onto ON-CBC D1R during light adaptation in midday.

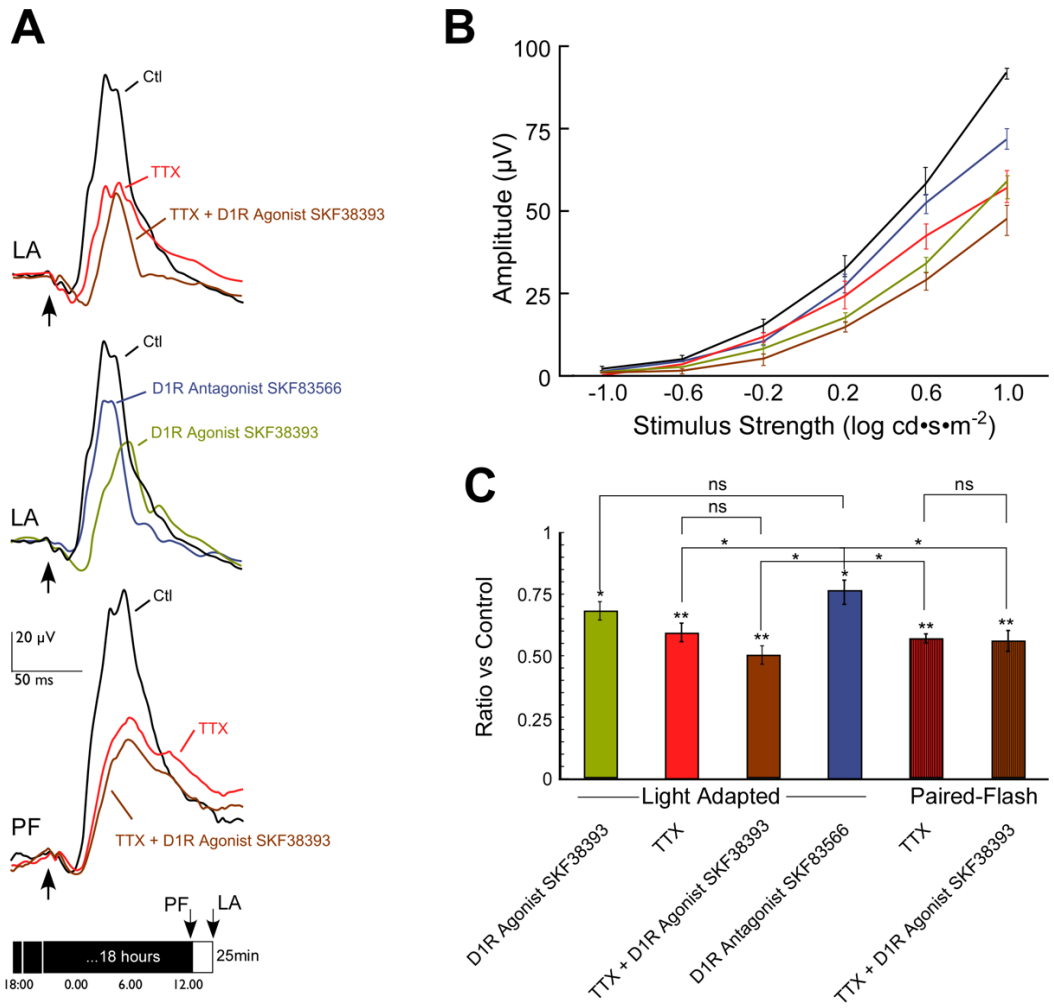

Figure 4.1: D1 receptors modulate cone ON bipolar cell Na_V channels but are not strongly activated by dopamine release during light adaptation. A) Example waveforms at 1.0 log cd s m^{-2} stimulus strength from light-adapted ERG recordings in control conditions (Black), after D1R Antagonist SKF83566 (blue), TTX (red), D1R Agonist SKF38393 (light green), or TTX + SKF38393 (brown) injected retinas. The two top set of traces are from light-adapted (LA) conditions, while the bottom set is from Dark-adapted cones (paired-flash, PF). Calibration as indicated, arrow is flash onset and the cartoon illustrates the protocol followed for obtaining those traces. B) Photopic b-wave amplitude responses to increasing stimulus strengths for SKF83566, TTX, SKF38393, or TTX + SKF38393 injected retinas. Control is the average of the paired un-injected control eyes from all drug treatments. C) b-wave amplitude normalized to paired control eyes from SKF38393, TTX, TTX + SKF38393 and SKF83566 -injected retinas in light adapted conditions, and TTX and TTX + SKF38393 injected eyes from paired flash experiments. ANOVA (*post hoc* Bonferroni correction), ***: $p \leq 0.001$; *: $p \leq 0.05$; *ns*: not significant.

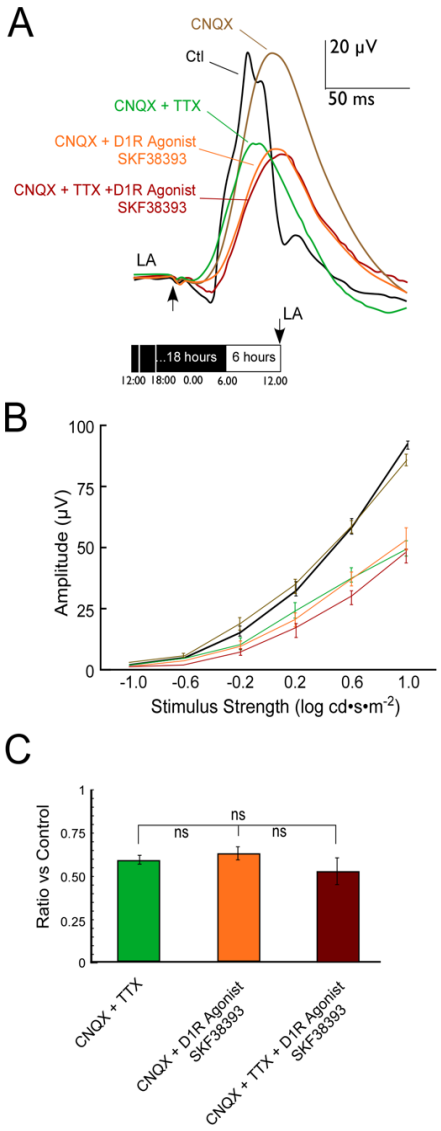

Figure 4.2: D1 receptors suppress the photopic b-wave primarily by acting on Na_v channels directly in ON cone bipolar cells rather than through inhibitory pathways. A) Example waveforms at 1.0 log cd s m^{-2} stimulus strength from light-adapted ERG recordings in control condition (black), and for CNQX (light brown), CNQX+TTX (green), CNQX + SKF38393 (orange), or CNQX + TTX + SKF38393 (dark red) injected retinas, in fully light adapted conditions. Calibration as indicated, arrow is flash onset and the cartoon illustrates the protocol followed for obtaining those traces. B) Photopic b-wave amplitude responses to increasing stimulus strengths for control, CNQX, CNQX + TTX, CNQX + SKF38393, and CNQX + TTX + SKF38393 injected retinas. Control is the average of the paired un-injected control eyes from all drug treatments C) B-wave amplitude normalized to mean amplitude from CNQX injected eyes for CNQX + TTX, CNQX + SKF38393, or CNQX + TTX + SKF38393 treated retinas. ANOVA (*post hoc* Bonferroni correction), ***: $p \leq 0.001$; *ns*: not significant.

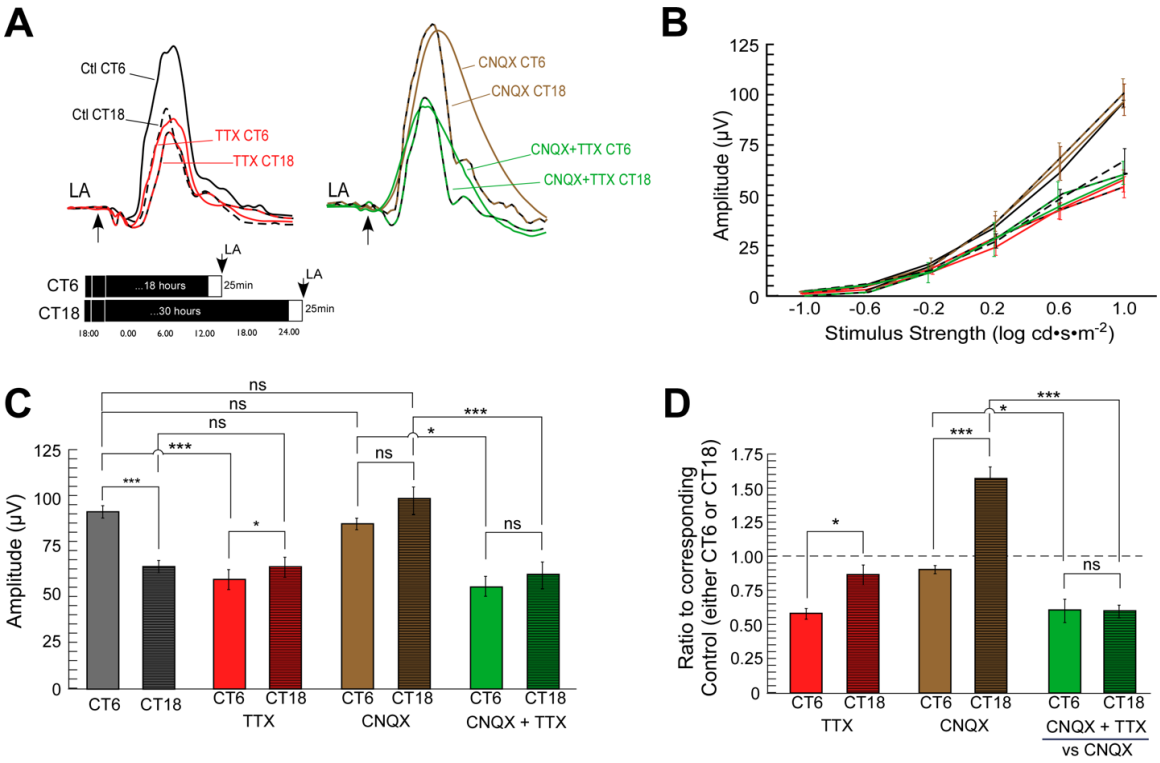

Figure 4.3: Circadian modulation of the ON cone bipolar cell circuit in mice in conditions of light adaptation A) Example waveforms at 1.0 log cd s m^{-2} stimulus strength from light-adapted ERG recordings from control eyes at CT6 (black) and CT18 (black dotted), compared to recordings obtained after TTX injections at CT6 (red) and CT18 (red dotted). Those recordings could be contrasted to those obtained in conditions where the ON-CBCs are isolated from network interactions, after CNQX (light brown) and combination of TTX and CNQX (green) at CT6 and CT18 (continuous vs dotted lines). Calibration as indicated, arrow is flash onset and the cartoon illustrates the two protocols followed. B) Photopic b-wave amplitude responses to increasing stimulus strengths for the same conditions illustrated in A. C) b-wave amplitude measured at CT6 (solid color) and CT18 (horizontal hatched) in control conditions (gray), and after TTX (red) CNQX (light brown) and CNQX plus TTX (green) injections. D) Ratio of b-wave amplitude after TTX (red) and CNQX (light brown) injections, to control b-wave amplitude and ratio of CNQX plus TTX to CNQX initial conditions (green), at CT6 (solid color) and CT18 (horizontal hatched). ANOVA (*post hoc* Bonferroni correction), ***: $p \leq 0.001$; *: $p \leq 0.05$; *ns*: not significant.

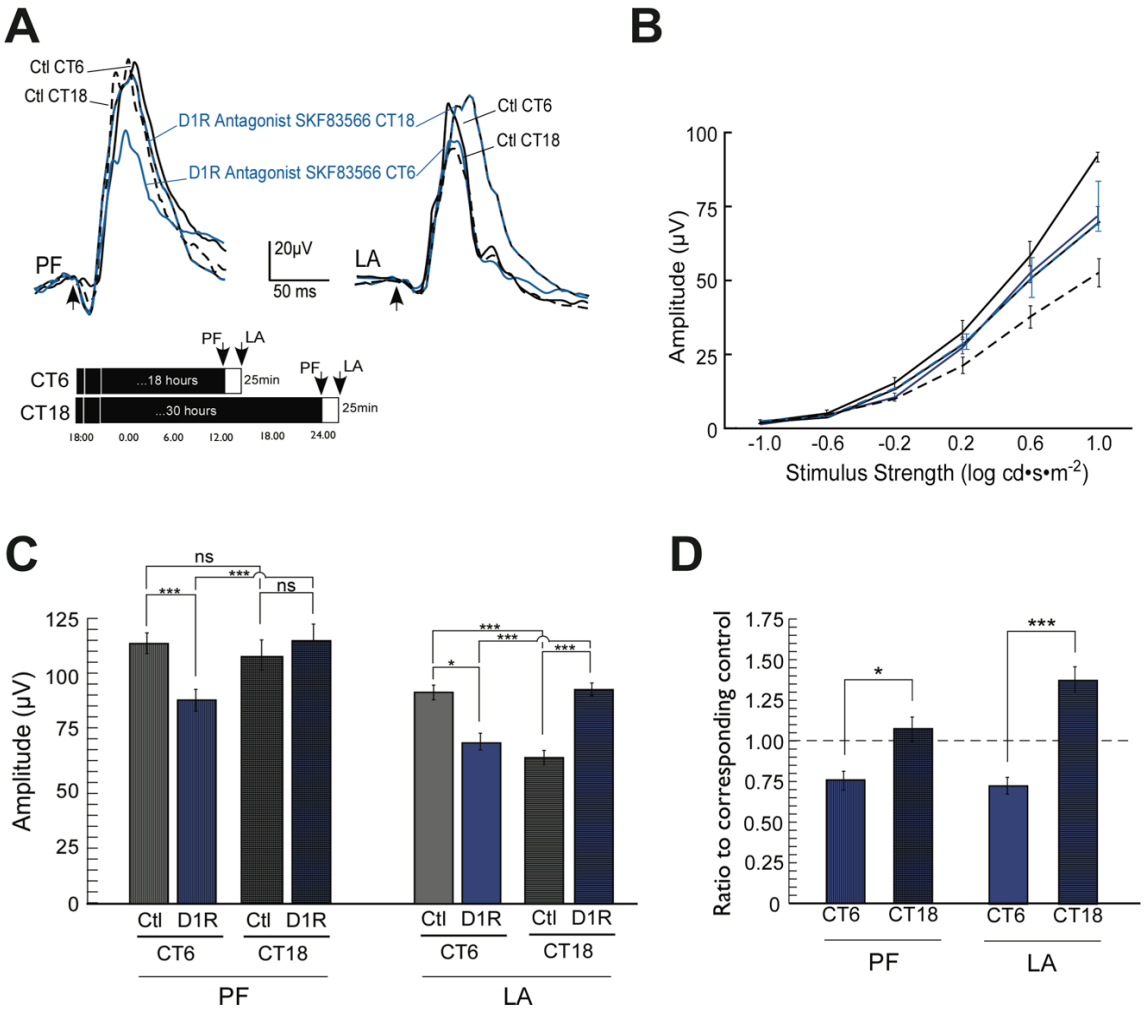

Figure 4.4: Daily rhythms in cone ON bipolar cell responses are generated primarily by D1 receptor modulation of intrinsic Na_v channels.
A) Example waveforms at 1.0 log cd s m^{-2} stimulus strength from dark- (PF) and light-adapted (LA) ERG recordings at CT6 (solid lines) and CT18 (dotted lines), in control conditions (black) and after D1R Antagonist SKF83566 (Blue). Calibration as indicated, arrow indicates flash onset and the cartoons represents the timing of the protocol used. B) Photopic b-wave amplitude responses to increasing stimulus strengths for the control conditions and after SKF83566 injection at CT6 and CT18 (color code as in A). C) b-wave amplitude comparison from 1.0 log cd s m^{-2} stimulus strength for dark- (paired flash, PF; vertical hatched) and light-adapted (LA; solid color) b-wave recordings at CT6 (no hatch) and CT18 horizontal hatch), in control conditions (gray) and after injection of D1R Antagonist SKF83566. D) Same data as in C but presented as ratio to respective b-wave control amplitude. ANOVA (*post hoc* Bonferroni correction), ***, $p \leq 0.001$; **, $p \leq 0.01$; *, $p \leq 0.05$; *ns*, not significant.

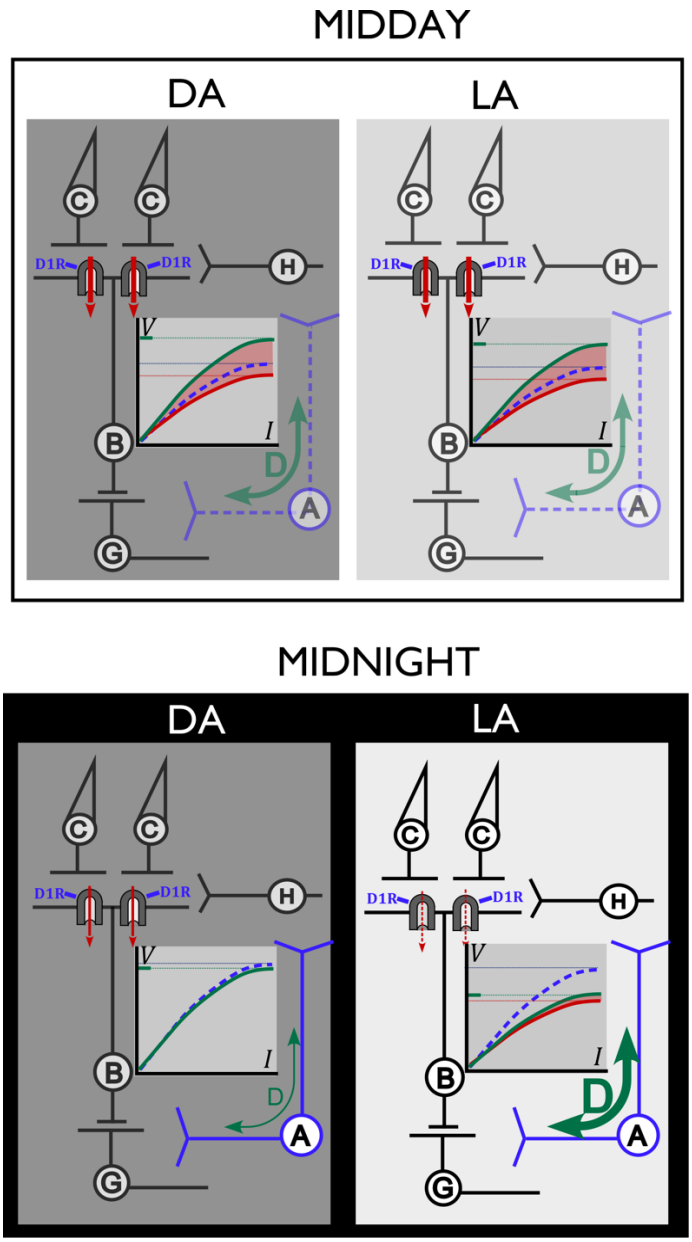

Figure 4.5: Schematic representation of retinal network to illustrate the proposed role of ON-CBC Nav channels during circadian midday and midnight. See discussion for details. C: cones; B: ON-CBC; H: horizontal cells; A: amacrine cells; G: ganglion cells; D and corresponding orange arrow: level of available dopamine; Red arrows: Activity of Nav channels; Inset graph: Amplitude of b-wave in function of strength of light stimulus for control condition (green) and after D1R antagonist SKF 83566 application (blue), the red area under the curve corresponding to the proposed influence of the Nav channel activity.

CHAPTER 5: Na_V CHANNEL DEPENDENT RETROAXONAL MODULATION OF PHOTORECEPTOR FUNCTION DURING DEVELOPMENT

Publication information:

Smith, B. J., Tremblay, F. and Côté, P. D. Na_v channel-dependent retroaxonal modulation of photoreceptor function during development. To be submitted to the journal *Developmen*t.

5.1 Abstract

Juvenile (postnatal day 16) mice lacking $Na_v1.6$ channels (*Scn8a*^{dmu}) have reduced photoreceptor function, which is unexpected given that Na_v channels do not contribute appreciably to photoreceptor function in adults. We demonstrate that acute block of Na_v channels in juvenile (P16) wild-type mice with TTX had no effect on photoreceptor function; however long-term (8-12 hour) TTX block, as well as prolonged dark adaptation from P8, caused significant reduction in photoreceptor function at P16. Injecting TTX into the retrobulbar space at P16 to specifically block Na_v channels in the optic nerve caused a reduction in photoreceptor function comparable to that seen in P16 *Scn8a* null-mutant mice. In both P16 *Scn8a*^{dmu} and retrobulbar TTX-injected mice, photoreceptor function was restored following intravitreal injection of the TrkB receptor agonist 7,8 dihydroxyflavone, suggesting that Na_v-dependent retrograde transport of BDNF can acutely modulate photoreceptor function at P16. We found that in *Scn8a*^{dmu} mice, photoreceptor function recovers by P22-25 despite more precarious general health of the animal; retrobulbar injection of TTX still reduced the photoreceptor response at this age but to a lesser extent, suggesting that Na_v-dependent modulation of photoreceptor function is largely transient, peaking just after eye opening. Together, these results suggest that the general photosensitivity of the retina is modulated following eye opening by retrograde feedback through activity-dependent axonal retinal ganglion cell signaling, which targets TrkB receptors.

5.2 Introduction

During development, neural networks must adapt to appropriately encode environmental input. Synaptic modification by activity-induced long-term potentiation and long-term depression is a fundamental process of forming mature neural circuits (Feldman and Knudsen, 1998; Katz and Shatz, 1996; Zhang and Poo, 2001). Long-range spread of retrograde signals from postsynaptic neurons leading to changes in excitability of presynaptic cells has been demonstrated in both in cultured cells (Ganguly et al., 2001; Li et al., 2004) and the developing retinotectal circuit (Du and Poo, 2004; Du et al., 2009). *In-vivo* long-range rapid retrograde feedback from the output synapses of the retinal ganglion cells (RGC) in the optic tectum modifies their input synapses from the bipolar cells (Du and Poo, 2004; Du et al., 2009). This feedback requires axonal transport in the optic nerve and both retinal and tectal neurotrophin receptor TrkB expression (Du et al., 2009).

The rod driven pathways of the retina are convergent, that is at each level presynaptic input is pooled to maximize sensitivity (e.g. Dunn et al., 2006). Given that BDNF is a diffusible factor in the retina (e.g. Ikeda et al., 1999) the strongest retrograde effects would be exerted early in the retinal network. Therefore we considered whether retrograde gain control can spread past the bipolar cell axon terminal to more effectively modulate the gain of the retina as a whole during development. Although a retrograde feedback mechanism transmitted via the optic nerve and controlling photoreceptor gain contravenes much of what we know about visual circuit development there is some evidence supporting the possible existence of such a circuit.

Using the electroretinogram (ERG) a-wave to measure photoreceptor function *in vivo* in mice (Robson and Frishman, 1998; Hetling and Pepperberg, 1999; Smith et al., 2014), a period of functional maturation following eye opening (~P10-P12) has been observed with the a-wave increasing abruptly between P14 and P18 (approximately 2 fold) with little change after P25 (Vistamehr and Tian, 2004; Gibson et al., 2012). Visual activity during development modulates photoreceptor function as dark-rearing mice until p30 reduces a-wave amplitude by roughly 30% (Vistamehr and Tian, 2004). The

mechanism regulating network plasticity in the juvenile retina remains elusive; however, it is notable that the intrinsic excitability of RGCs increases rapidly following eye opening (Wang et al., 1997; Boiko et al., 2003; Deplano et al., 2004; Qu and Myhr, 2008;Giovannelli et al., 2008). Development of retinal ganglion cell excitability is regulated predominately by expression of voltage-gated sodium channels (Na_v) (Wang et al., 1997; Boiko et al., 2003) with replacement of $Na_v1.2$ with $Na_v1.6$ isoforms at axon initial segments and nodes of Ranvier (between P7 and P24 in the mouse).

In mice lacking $Na_v1.6$ (*Scn8a*^{dmu} and Scn8a^{med}), there is a strong reduction in photoreceptor function (Coté, 2005; Smith and Côté, 2012) temporally coincident with upregulation of $Na_v1.6$ in RGCs and optic nerve (Wang et al., 1997; Boiko et al., 2003). In these animals, photoreceptor dysfunction is not associated with structural abnormality of the photoreceptors, nor with decrease in photoreceptor number. Photoreceptors are generally believed to be devoid of Na_v channels (Mojumder et al., 2007) with $Na_v1.6$ being predominately located in the inner retina (Coté, 2005; Mojumder et al., 2007); therefore, the influence of these channels is likely to be indirect. Furthermore, acute application of TTX in dark-adapted conditions has very little effect on photoreceptor function as measured by the a-wave (Mojumder et al., 2008; Smith and Côté, 2012) suggesting that the effect is either developmental or that the Na_v channels influencing the photoreceptors are not located in the retina proper..

It is possible that the increase in RGC activity following upregulation of $Na_v1.6$ modulate the photoreceptor function via release of neurotrophins. Previous work demonstrates that neurotrophin receptor TrkB global knockouts (Rohrer et al., 1999; Rohrer, 2001; Rohrer and Ogilvie, 2003; Rohrer et al., 2004) and retina-specific conditional knockout mice (Grishanin et al., 2008) have reduced photoreceptor light sensitivity at P16. BDNF expression in the retina is enhanced by constant light rearing (Pollock et al., 2001) and reduced by constant dark rearing (Pollock et al., 2001; Landi et al., 2007) or monocular deprivation (Seki et al., 2003; Mandolesi et al., 2005). Furthermore, BDNF trafficking along chick retinal ganglion cell axons (Chytrova and Johnson, 2004) and release of BDNF appears modulated by Na_v channel-dependent neural activity (Kohara, 2001; Chytrova and Johnson, 2004).

These facts argue that Na_v-dependent retroaxonal feedback in the optic nerve may modulate the photoreceptor function during a transient period following eye opening. Here we first demonstrate that both light evoked spiking and the *in vitro* ERG recorded in isolation from the retinogeniculate circuit are similar between *Scn8a*^{dmu} and control mice at P16 in contrast to the pronounced reduction in photoreceptor function seen *in vivo*. Because light evoked spiking in RGCs and photoreceptor function were similar *in vitro* between *Scn8a*^{dmu} and control mice we used retrobulbar injection of TTX to interrupt spiking in the optic nerve directly. Retrobulbar TTX reduced photoreceptor function to a similar extent as genetic loss of $Na_v1.6$ function. We were able to restore photoreceptor function with intravitreal injection of a TrkB agonist suggesting that Na_v channels in the optic nerve are key to a retrograde feedback mechanism modulating photoreceptor function via BDNF acting at TrkB. Similar to TrkB knockout mice, who have a reduction in a-wave amplitude at P16 but not in adults we found that in *Scn8a*^{dmu} mice photoreceptor function is essentially restored by P22-25, and that retrobulbar TTX has a reduced effect on the a-wave at this stage.

5.3 Material and methods

5.3.1 Mice

All animal procedures were approved by the Dalhousie University Committee on Laboratory Animals, and completed in accordance to animal care guidelines established by the Canadian Council on Animal Care and the ARVO statement for the Use of Animals in Ophthalmic and Vision Research. Mice were housed under a 12-hour light / dark cycle with free access to food and water.

Scn8a^{dmu} mice, which harbor a function-blocking mutation in the *Scn8a* gene, have been described previously (De Repentigny et al., 2001; Coté, 2005). The mutation was found to consist of a single nucleotide deletion in the sequence coding for the first interdomain loop of $Na_v1.6$ and, as a result, homozygotes are devoid of functional $Na_v1.6$. The resulting frameshift in the open reading frame results in the presence of a stop codon a short distance downstream of the mutation. Control mice were genotyped wild-type littermates.

5.3.2 Electroretinogram

ERGs and intravitreal injections were done as previously described (Smith *et al*., 2012, 2013, 2015). In brief homozygous *Scn8a*^{dmu} at P16, P18 and P22-25 and wild-type littermates of the same age were dark adapted for at least 12 hours before being anesthetized under dim red light by intraperitoneal injection of Avertin (2,2,2 Tribromoethanol, Sigma Aldrich, St-Louis, MO) dissolved in amylene hydrate (tertiary amyl alcohol, 275mg/kg, Sigma Aldrich). The pupils were dilated with the mydriatic agent cyclopenolate HCl 0.5% (Alcon, Fort-Worth, TX) and a 0.5% proparacaine hydrocloride (Alcon) was applied as a topical analgesic to reduce eye movement and irritation. Body temperature was maintained at 37ºC with a heated pad and monitored rectally. Flash stimuli were generated by a Ganzfeld stimulator (LKC Technologies, Gaithersburg, MD) that produced a maximum illumination of 10.1 log cd s m^{-2} at the corneal surface. Flash strengths were attenuated by up to 7.0 log units by manual interposition of neutral density filters (Kodak Wratten, Rochester, NY). The stimulus interval between flashes varied from 5 s at the lowest stimulus strengths to 30 s at the highest. Mice were sacrificed by anesthetic overdose followed by cervical dislocation and tails were collected to confirm genotype using a previously described protocol (Coté, 2005). Long-term dark adaptation from P8 took place with cage bedding and food changed under dim red light. In some cases, following intravitreal injection of TTX, P16 and P22-25 mice were allowed to recover from anesthesia on a heated pad in the dark for 8-12 hours before recording a second time.

5.3.3 Retrobulbar injection

Twenty micromolar tetrodotoxin (TTX, Abcam Biochemicals, Toronto, ON, Canada) and 200 μM 7,8-Dihydroxyflavone (7,8 DHF, TOCRIS Bioscience, Bristol, UK) were injected in volume of 1 μl within the vitreous body with a 30 gauge needle attached to a 5μl Hamilton syringe. Two microliters of 20 μM TTX was injected into the retrobulbar space (e.g. see Chou et al., 2013). In some cases, intravitreal injection of 1 μl of 7,8 DHF preceded or followed the TTX retrobulbar injections.

5.3.4 Multi-electrode array recording

The retina was dissected free from the eyecup and pigmentary epithelium and positioned with brushes, photoreceptor side down, on a piece of filter membrane (Millipore, Billerica, MA). The membrane was transferred to the cylindrical chamber of a MEA electrode (8 x 8 grid of 30μm electrodes, with 200um spacing: 60MEA200/30iR-ITO, Multi Channel System MCS GmbH, Reutlingen, Germany). This preparation was stabilized by the weight of a harp slice grid (SHD-26H/10, Warner Instruments LLC, Hamden, CT, USA). Ames solution bubbled with carbogen (pH □7.4, 35– 36 °C) was continuously superfused (2 mL/min) over the preparation. A full-field flash was presented to the retina (LED 530 nm, 1 s duration) every 10 s. Data were digitized and sampled at 50 kHz, recorded with MC_Rack software (Multi Channel Systems) and spikes high-pass filtered at 200 Hz. The signal were amplified and low pass filtered between 1 Hz and 50 Hz to isolate local field potentials. Baseline recordings were obtained after a 30-min to 2-hour period once the number of cells recorded and responses appeared stable. Spikes recorded on each electrode were sorted into individual cells offline (Offline Sorter, Plexon, Dallas, TX, USA) and then analyzed with Neuroexplorer software (Nex Technologies, Littleton, MA, USA). For each cell, Post-Stimulus Time Histograms (PSTHs) were computed over 60 consecutive sweeps over 1900 ms.

5.3.5 Data Analysis

Analysis of ERG waveforms was completed using a custom ERG analysis toolbox written for Matlab (Mathworks, Natick, MA, USA). The amplitude of the a-wave was measured as the difference between the baseline and the response at 18 ms post-stimulus and b-wave amplitude was measured from a-wave trough b-wave peak following the trough. Comparison of a- and b-wave parameters was performed using repeated-measured ANOVA (Microsoft Excel,Redmond, WA, USA) on whole intensity series, while differences were numerically reported as average of responses in pre-determined stimulus ranges as used previously (Smith et al., 2017), corresponding to

cone–rod mixed response with substantial cone contribution (Cri: 1.0 to 0.6 log cd s m 2) and rod–cone mixed responses with less cone contribution (Rci: 0.6 to 1.5 log cd s m 2).

5.4 RESULTS

5.4.1 Prolonged reduction in neural activity but not acute block of Na_v channels can reduce photoreceptor function in juvenile mice.

Dark-rearing suppresses a- and b-wave amplitudes in ERGs recorded *in vivo* while ERGs recorded *in vitro* from isolated retinas show no reduction a- or b-waves in rod-driven ERGs after dark-rearing (Dunn et al., 2013). We therefore recorded ERGs in P16 mice following prolonged dark adaptation from P8 to P16-17 (similar to (Hooks and Chen, 2006), fig 1 blue), and a short time after intravitreal injection of TTX (20-40 minutes; fig 1 red) periods. We did not find that the reduction in the a-wave following these treatments reached the levels of P12 mice or P16 *Scn8a*^{dmu} mice (as seen in Coté, 2005) but they were comparable to the amplitude of P14 control mice.

However, similar to dark-rearing experiments lasting until P30 (Vistamehr and Tian, 2004), we found long-term dark adaptation caused significant reductions in a-wave amplitude with significant reductions compared to P16 controls at stimulus strengths above -1.8 log cd s/m^2 (Cr_i: 56.9±2.2; Rc_i: 63.9±6.9% of age matched controls, fig 1,B,D). Implicit time was also significantly delayed in long-term, dark-adapted eyes compared to P16 controls for all stimulus strengths tested (Cr_i: 9.8±0.6; Rc_i: 19.7±2.4 ms delay relative to age matched controls: fig 1C). Injecting TTX intravitreally caused a non-significant increase the amplitude and IT of the a-wave at short time periods (20-40 minutes) post injection compared to paired control eyes (fig 1B-D).

We found that prolonged dark-adaptation significantly reduced photoreceptor light sensitivity in juvenile mice. The lack of an acute effect of TTX on photoreceptor function as measured by the a-wave, both in juvenile and adult mice (Smith et al., 2013), suggests that the reduced photoreceptor function is not due to conventional synaptic circuitry.

5.4.2 In vitro visual function is relatively normal in Scn8a^{dmu} mice

We recorded light evoked RGC spiking responses (fig 2A) and local field potentials (fig 2B,C; LFPs a.k.a microERGs; Fujii et al., 2015) from dark adapted retinas in control (P16 n=3 retinas; black) and *Scn8a*^{dmu} mice (P16 n=3 retinas; red). We were surprised to find that while *in vivo* ERGs are greatly reduced in *Scn8a*^{dmu} mice (Cote et al., 2005; Smith and Cote, 2012) the amplitude of the first negative component of the local field potential measured at 11 ms, when the light response is generated predominately by photoreceptors (e.g. Fujii et al., 2015) was relatively preserved. While we found significant reductions for the dimmer two stimulus strengths tested (~50% reductions) these reductions were considerably smaller than seen *in vivo***.** With the maximum stimulus strength, close to saturation level, no significant differences could be observed between the P16 control and the *Scn8a*^{dmu} mice (fig 2D). Similar results were obtained for maximal spike rate in RGCs (fig 2B,C; control n=152; *Scn8a*^{dmu} n=172 cells), which were relatively preserved, especially at the higher stimulus strengths (significant reductions at 1.81 lux: ~15% reduction; -0.81 lux: ~80% reduction). Observing this contrast between *in vivo* and *in vitro* evaluations of retinal function, we hypothesized that isolation from the postsynaptic projections of the RGCs in both control and *Scn8a*^{dmu} mice was responsible for the relatively small effect observed *in vitro*.

Previously, it has been demonstrated that loss of TrkB receptor function can suppress photoreceptor function transiently in juvenile mice (See Rohrer et al., 1999; Rohrer, 2001; Grishanin et al., 2008). One hypothesis put forward was that the reduced photoreceptor function in *Scn8a*^{dmu} mice might be due to a paracrine effect mediated by BDNF (Coté, 2005). BDNF expression in the retina is enhanced by constant light rearing (Pollock et al., 2001) and reduced by constant dark rearing (Pollock et al., 2001; Landi et al., 2007) or monocular deprivation (Mandolesi et al., 2005). TTX injection lowers levels of retinal BDNF mRNA (Chytrova and Johnson, 2004). In order to test whether Na_v channels in RGCs might contribute to the photoreceptor function, we injected retrobulbar TTX, alone or in combination with 7,8 DHF, a TrkB agonist.

5.4.3 Na_v channels in the optic nerve are necessary for retroaxonal modulation of photoreceptor function via TrkB receptors.

We found that applying TTX directly to the optic nerve via retrobulbar injection strongly suppressed photoreceptor function at P16 (fig 3 green). We found significant reductions in a-wave amplitude for all stimulus strengths above -1.8 log cd s/m^2 (Cr_i: 43.7±3.9; Rc_i: 44.3±6.9% of control eyes) but there was no significant change in the a-wave IT (fig 3B-D). When 7,8 DHF was intravitreally injected in a subset of the eyes previously treated with retrobulbar TTX (fig 3 red), we observed a substantial recovery of photoreceptor function (Cr_i: 85.1±2.8; Rc_i: 99.6±2.8% of control eyes; fig 3B,D).

We also reversed the order of experiments i.e. we first injected 7,8 DHF intravitreally followed by retrobulbar TTX. Doing this allowed us to see the effects of 7,8 DHF in isolation as well as controlling for potential surgical trauma due to the retrobulbar injection of TTX. Intravitreal 7,8 DHF (fig 2 blue) mildly but significantly reduced the a-wave amplitude for stimulus strengths above -1.2 log cd s/m^2 (Cr_i: 84.9±2.4; Rc_i: 77.7±6.2% of control eyes; fig 2B,D) but did not significantly change the a-wave IT (fig 3C). Injecting retrobulbar TTX after 7,8 DHF (Fig 3 orange) had little effect on photoreceptor function (Cr_i: 110.4±4.3; Rc_i: 124.9±5=6.2% of matched 7,8 DHF injected eyes) although the a-wave IT was slightly delayed in at stimulus strengths above -0.6 log cd s/m^2 (Cr_i: 3.1±0.6 ms delay relative to control eyes Fig 3C).

Since 7,8 DHF can rescue photoreceptor function when retrobulbar TTX is used to suppress optic nerve activity, we tested whether 7,8 DHF could rescue photoreceptor function in P16 *Scn8a*^{dmu} mice (fig 3; purple, compare to dmuP16(brown)). We found a substantial recovery of photoreceptor function in eyes injected with 7,8 DHF for stimulus strengths above -1.2 log cd s/m^2 (Cr_i: 219.1±23.9% of paired *Scn8a*^{dmu} eyes; fig 3B,D). There were no significant changes in a-wave IT following 7,8 DHF injection in *Scn8a*^{dmu} eyes (fig 3C).

5.4.4 Optic nerve Na_v channel function has a transient effect on photoreceptor sensitivity.

We recorded ERGs from *Scn8a*^{dmu} mice and control littermates at two additional developmental stages, P18 and P22-25. As demonstrated previously (fig 3) and consistent with Coté et al. (2005), P16 *Scn8a*^{dmu} mice we found with a significant reduction in dark adapted a-wave amplitude at stimulus strengths above -1.8 log cd s/m^2 (Cr_i: 22.1±0.5; Rc_i: 22.2±8.1% of controls; fig 3 brown, B,C). At P18, the a-wave amplitude in *Scn8a*^{dmu} mice had increased (fig 4A, P18 brown) but was still significantly reduced relative to P18 controls for all stimulus strengths above 1.8 log cd s/m^2 (Cr_i: 54.9±5.0; Rc_i: 29.0±1.9% of controls; fig 4B) while the a-wave IT was not significantly changed in P18 *Scn8a*^{dmu} mice relative to control (fig 4C), in contrast to P16 mice (Coté et al., 2005), where a significant increase was noted. Both these results point towards a normalization of the photoreceptor function in *Scn8a*^{dmu} mice at P18 relative to P16.

At P20-25 a-wave amplitude in *Scn8a*^{dmu} mice was not significantly different than that of age-matched controls for all stimulus strengths tested suggesting that at this age photoreceptor function belatedly matured in *Scn8a*^{dmu} mice (Cr_i: 94.6±2.6; Rc_i: 96.5±6.8% of controls (fig 3A,F). We did find a significant increase in a-wave implicit time (IT) for stimulus strengths above -1.2 log cd s/m^2 (1.6±0.3 ms delay in Cr_i relative to controls). This could be due to a slightly decreased a-wave slope or due to a delay in b-wave initiation so we measured a-wave amplitude at a fixed time of 9 ms post flash. At 9 ms, there was no significant change in a-wave amplitude at any stimulus strength (Cr_i: 86.1±4.5; Rc_i: 125.5±17.0 % of controls; fig 3D).

Two explanations could be provided to explain the maturation delay of the photoreceptor function in *Scn8a*^{dmu} mice. First, that compensation by other ion channel types might restore RGC function in the absence of $Na_v1.6$ ((Swensen and Bean, 2005; Van Wart et al., 2007)). Another explanation could be that the modulation of photoreceptor function by BDNF via TrkB receptors might be restricted to juvenile mice (~P16-P20 or possibly earlier, e.g. see (Rohrer et al., 1999; Grishanin et al., 2008)). To differentiate between these possibilities, we injected retrobulbar TTX at P25 (fig 4 green), at which point *Scn8a*^{dmu} mice have essentially normal photoreceptor function. Retrobulbar TTX caused a significant reduction in photoreceptor function for stimulus strengths above -1.8 log cd s/m^2 (Cr_i: 75.8±3.3; Rc_i: 57.5±6.6% of control eyes). The a-wave IT was slightly delayed but this delay only reached significance sporadically (-0.6

and -1.8 log cd s/m^2). The difference between the effects of retrobulbar TTX at P16 (~45% of control) vs. the effects at P22 (~75% of control) suggests that there exists a period around P16 where neural activity in RGCs can strongly affect photoreceptor function via TrkB receptors.

5.5 DISCUSSION

We studied how Na_v-dependent activity in the optic nerve modulates photoreceptor function in the period following eye opening while the mouse retina is still maturing. Our results suggest that there is a period from approximately P12 to P25 where Na_v-channel dependent activity, primarily in the optic nerve and reliant on $Na_v1.6$ isoform, can modulate photoreceptor activity via TrkB. This feedback loop reversing the normal direction of information transmission between the retina and the brain appears to be important in controlling the global light sensitivity of the retina during an especially sensitive period of neural development.

5.5.1 Na_v-dependent retroaxonal signaling enhances photoreceptor function during a transient period following eye opening.

A few isolated reports suggest that there may be a link between inner retinal activity and photoreceptor function during development. Strongly reduced photoreceptor function was reported at P16 in the Na_v null (*Scn8a*^{dmu}) mice (Coté, 2005), and dark-rearing mice can lead to reduced photoreceptor function at P30 (Vistamehr and Tian, 2004). We found that long-term dark adaptation (dark-rearing from P8 to P16) caused a substantial reduction in photoreceptor function at P16, similar to that seen in P16 *Scn8a*^{dmu} mice. To test whether Na_v channels might directly modulate photoreceptor function during development, we injected TTX and recorded ERGs immediately. Like previous results in adult mice and rats (Mojumder et al., 2008; Smith et al., 2013) and consistent with immunohistochemistry in adult mice and rats that do not show Na_v channels on photoreceptors (Mojumder et al., 2007), we found that at P16 acute intravitreal injection of TTX slightly increased the amplitude of the a-wave rather than

decreasing it. This argues against both transient expression of Na_v channels in photoreceptors and/or direct Na_v-dependent synaptic modulation of photoreceptors during development in *Scn8a*^{dmu} mice.

The results in Coté et al., (2005) were unresolved as to whether the visual defect in *Scn8a*^{dmu} mice was due to a developmental delay or whether $Na_v1.6$ could directly modulate photoreceptor function in early development. We report here that visual function in *Scn8a*^{dmu} mice recovers fully by P20-25; however this could be due to compensation both by Na_v and other ion channels, which is known to occur in Na_v-channel KO mice (e.g. see Swensen and Bean, 2005). The fact that photoreceptor function is suppressed after prolonged but not acute intravitreal injection and rapidly following retrobulbar injection of TTX argues for a direct modulatory effect of feedback via the optic nerve on photoreceptor function. This feedback circuit requires Na_v channels, probably $Na_v1.6$, in the optic nerve to function. We found that the a-wave reduction following retrobulbar TTX was substantially reduced by P25, additional evidence that this modulation is transient and occurs shortly following eye opening in mice.

5.5.2 Na_v-dependent retroaxonal modulation of photoreceptor function via TrkB receptors.

$Na_v1.6$ is expressed predominately in RGC axon initial segment and nodes of Ranvier in the optic nerve and is substantially upregulated betweenP10 and P16 (Boiko et al., 2003, Coté et al, 2005). In combination with our results with retrobulbar TTX, it appears that lack of $Na_v1.6$ in RGCs is the likely cause of photoreceptor dysfunction in *Scn8a*^{dmu} mice. Coté et al (2005) suggested that one potential mechanism linking RGC activity to photoreceptor function is activity-dependent production and trafficking of neurotrophins. This hypothesis gains support from findings in global TrkB knockout mice, which show substantial loss of photoreceptor function early in development (Rohrer et al., 1999; Grishanin et al., 2008).

BDNF mRNA in rat visual cortex increases sharply following eye opening and is suppressed by dark rearing (Schoups et al., 1995; Pollock et al., 2001)). Likewise, retina

BDNF protein and mRNA levels are reduced by dark rearing (Pollock et al., 2001) and increased by constant light rearing (Pollock et al., 2001). In the mouse retina, BDNF protein level is reduced in dark-reared eyes at P30 (Landi et al., 2007) and exogenous BDNF can reverse dark-rearing induced changes in retinal GABAergic circuitry (Lee et al., 2006). Aa well, antero- and retrograde transport of BDNF in the optic nerve is a well-documented phenomenon (Ma et al., 1998; Quigley et al., 2000; reviewed in Zweifel et al., 2005).

Retroaxonal modulation (Harris, 2008) of RGC function during development has been extensively studied in the *Xenopus* retinotectal circuit (Du:2009iz; Du and Poo, 2004). BDNF applied to the optic tectum can modulate bipolar cell inputs to RGCs within tens of minutes, and the effect is sensitive to the suppression of axonal transport by colchicine and transection. Na_v channel-dependent activity is known to contribute to surface expression of TrkB and BDNF (Du and Yang, 2000), the release of BDNF (Santi et al., 2006; Balkowiec and Katz, 2002; Balkowiec et al., 2000; Gärtner and Staiger, 2002), and trafficking of BDNF in cultured neurons (Kohara, 2001). Intravitreal injection of TTX reduces both anterograde and retrograde transport of BDNF in the optic nerve (Chytrova and Johnson, 2004) in developing chick retina.

When we added the TrkB agonist 7,8-DHF, we were able to rapidly recover photoreceptor function in mice with retrobulbar injection of TTX but 7,8-DHF alone did not significantly increase the amplitude of the a-wave. These results argue that the effect of 7,8-DHF in eyes injected with retrobulbar TTX effectively consists in a recovery of photoreceptor function by TrkB activation in the absence of Na_v-channel-dependent activity in the optic nerve rather than a general increase in photoreceptor function in the presence of a TrkB agonist. We also found that pretreatment with 7,8-DHF prevented subsequent retrobulbar TTX application from affecting photoreceptor function. In addition we found partial recovery of photoreceptor function in P16 *Scn8a*^{dmu} mice following treatment with 7,8-DHF, suggesting that the reduced photoreceptor function in *Scn8a*^{dmu} mice was largely due to reduced production of BDNF in RGCs.

Scn8a^{dmu} mice and mice injected with TTX in the retrobulbar space showed much less effect at P20-25 relative to P16. Grishanin et al., (2008) showed similar results in

that retina-specific *TrkB* knockout mice displayed significantly reduced photoreceptor function and smaller b-waves at P16 but not in adult mice. The a- and b-wave ratios in these mutants and controls were similar suggesting that the b-wave reduction was due to decreased photoreceptor function (Grishanin et al., 2008). In combination, these results are consistent with the hypothesis that the mammalian retino-geniculate/colliculus circuits modulate photoreceptor function via retroaxonal signaling following eye opening. TrkB receptors not being expressed in rod photoreceptors (Rohrer et al., 1999), additional work will be necessary to determine exactly how Na_v-dependent activity in the optic nerve modulates photoreceptor function.

Oddly, while applying TTX to the optic nerve caused a rapid decline in photoreceptor activity, applying TTX intravitreally at P16 had little acute affect and in fact caused a slight increase in a-wave amplitude. Clearly, since blocking RGC activity intravitreally with TTX should interrupt the forward propagation of information from the retina as well as retrobulbar TTX, why then doesn't acute treatment with TTX reduce photoreceptor function at P16? Either Na_v channels are necessary for retrograde movement of BDNF in the optic nerve, or when TTX is applied intravitreally some compensatory increase in retinal BNDF can make up for the lost retroaxonal feedback. The retina can produce BDNF in both RGCs and amacrine cells (Cellerino and Kohler, 1997) and in early development of the chick retina, blockade of spontaneous retinal activity by TTX causes retinal BDNF build up concomitant with reduced levels of BDNF in the optic nerve (Chytrova and Johnson, 2004). It is then more likely that acute treatment with TTX does not reduce photoreceptor function because of compensation by increased retinal release of BDNF. However, because TTX has multiple sites of activity in the developing retina including both inhibitory amacrine cells and RGCs it is difficult, in the absence of studies on activity-dependent axonal trafficking of BDNF in mammalian retina, to determine why acute treatment with intravitreal TTX does not suppress photoreceptor activity but blocking activity in the optic nerve alone does.

In combination with previous work showing a transient reduction in photoreceptor function in TrkB, global- and retina-specific knockout mice (Compare Rohrer et al., 1999 and Grishanin et al., 2008), the fact that the pronounced reduction in photoreceptor function caused by retrobulbar TTX injection can be reversed by intravitreal injection of

a TrkB agonist, all suggest that retroaxonal feedback in the optic nerve can transiently modulate photoreceptor function during development via TrkB receptors. These results show that retinal modulation by retroaxonal signaling extends beyond RGCs to the photoreceptor input to modify the light sensitivity of the entire retina. In support to this conclusion, it is interesting to note that patients presenting with congenital optic nerve hypoplasia have been reported to have impaired retinal photoreceptor sensitivity (Cibis and Fitzgerald, 1994; McCulloch et al., 2007; Chaplin et al., 2009).

5.6 CONCLUSION

In conclusion, we demonstrated that during development the excitability of the retina can be transiently modulated by Na_v channel-dependent feedback from the optic nerve. This feedback reaches the first neurons in the retina, rapidly and profoundly suppressing the light sensitivity of the entire retina when interrupted. We hypothesize that this pathway represents a mechanism for suppressing input from a poorly functioning retina and thus accelerates the reorganization of the visual tract to support vision via the contralateral correctly functioning eye.

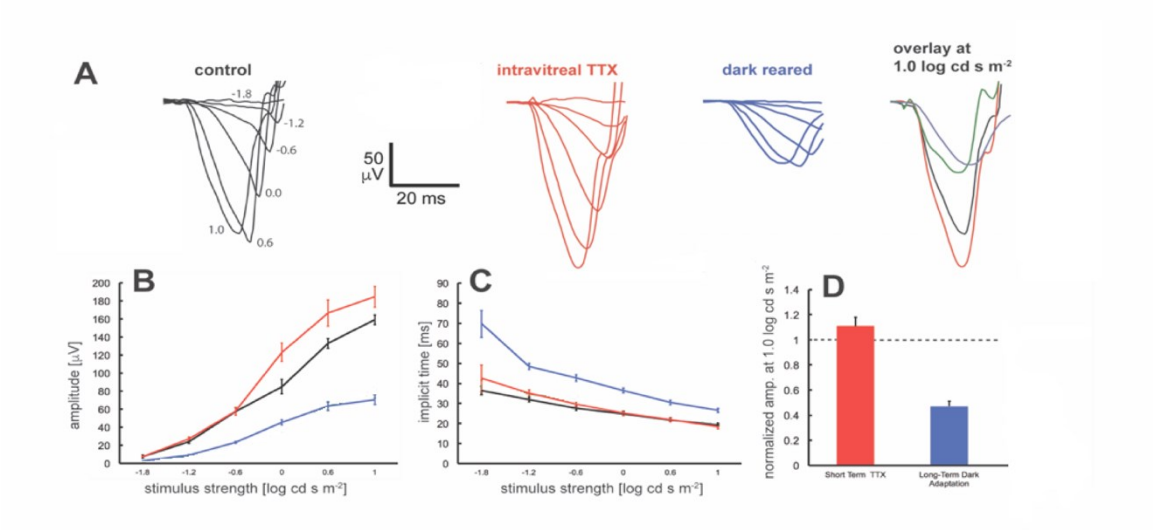

Figure 5.1: Chronic but not acute suppression of retinal activity reduces photoreceptor function.
A) Example waveforms from dark-adapted ERG recordings of P16 control mice (black), acute intravitreal injection of TTX (red), and prolonged (since P8) dark adaptation (blue). B) averaged a-wave amplitude at P16 from experimental conditions in (A) C) A-wave implicit time D) normalized a-wave amplitude at the brightest stimulus strength used (1.0 log cd s/m^2).

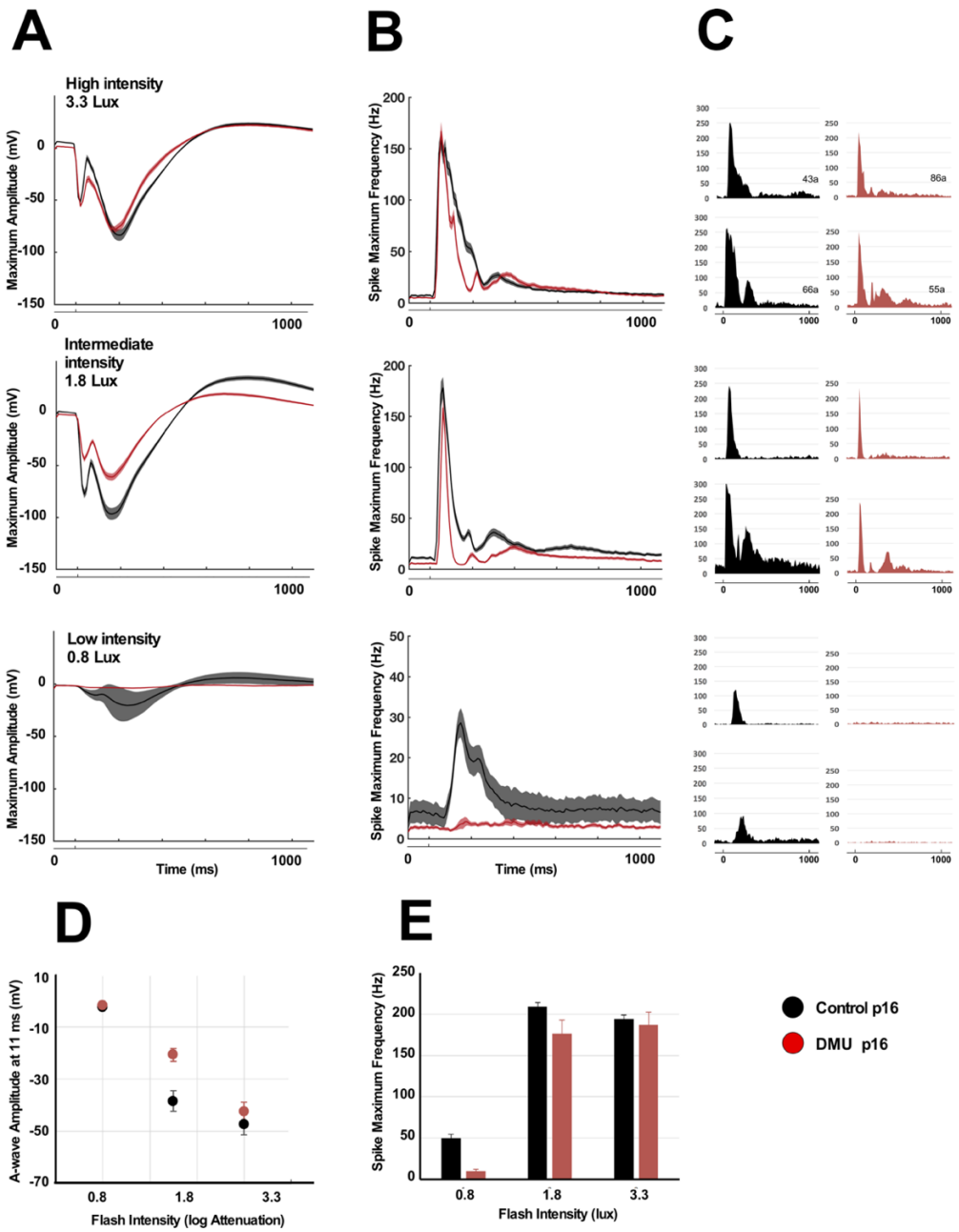

Figure 5.2: ***In vitro*** **visual function is relatively normal in** ***Scn8a*****^{dmu} mice.**
A) Population average Post Stimulus Time Histograms (thick line) and standard error of the mean (SEM: corresponding shaded area) of retinal ganglion cell spiking activity collected on multielectrode array following a 10 ms 530nm-LED flash stimulus to high (3.31lux, top row), intermediate (1.81 lux, middle row) and low intensity (-0.81 lux, bottom graph) stimulus. (B) example single cell responses from P16 control (black) and *Scn8a*^{dmu} (red) mice. C) Population average local field potentials (LFP) with (thick line) SEM (corresponding shaded area) to the same response D) Maximum Spike frequency (Hz). E) Amplitude at 11 ms after stimulus for the negative trough of the LFP, representing photoreceptor function.

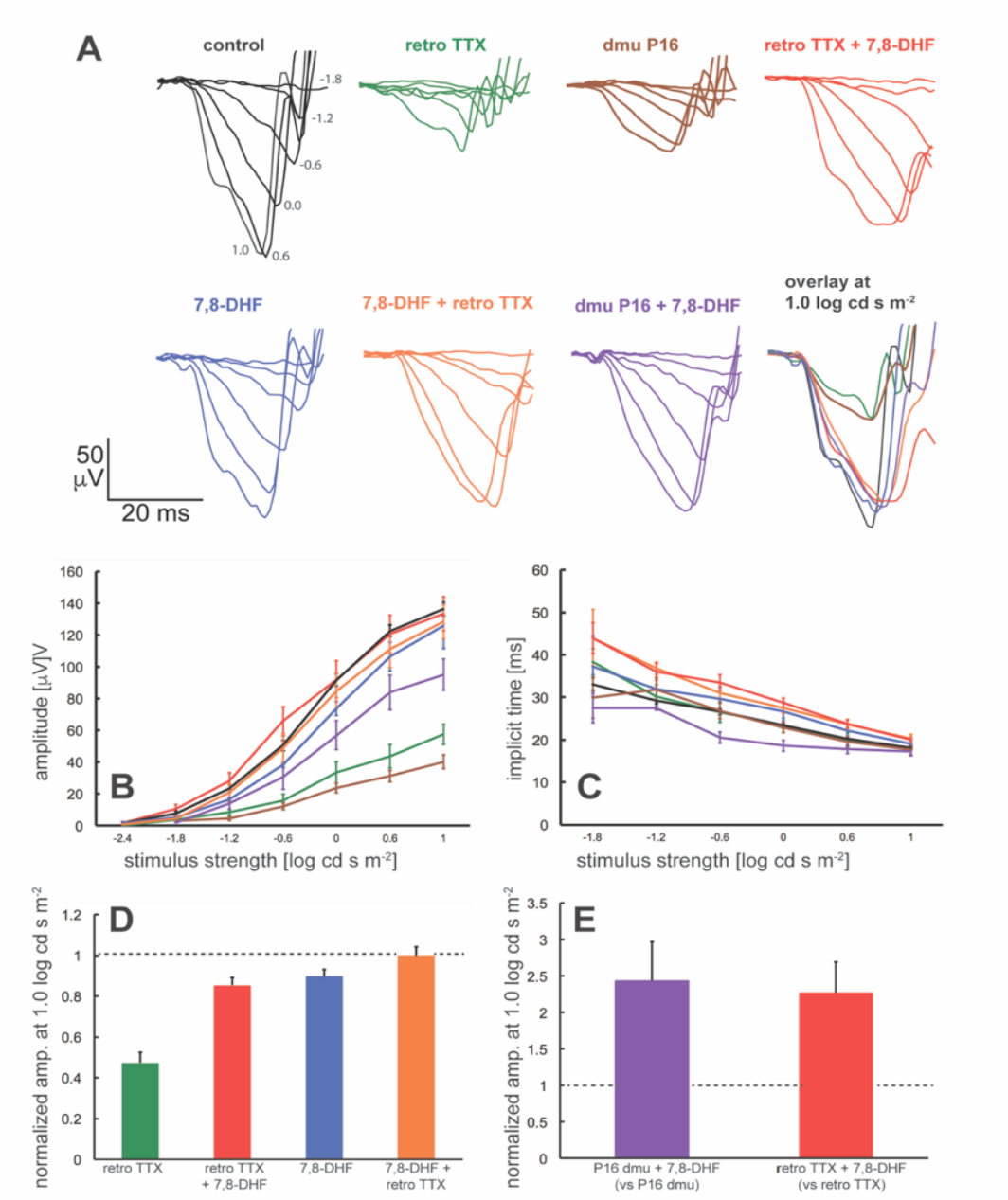

Figure 5.3: Acute block of optic nerve Na_v channels via retrobulbar injection of TTX reduces photoreceptor function.
A) Example waveforms from dark adapted ERG recordings of P16 mice (black), retrobulbar injection of TTX (green), *Scn8a*^{dmu} $Na_v1.6$ knockout mice , acute intravitreal injection of TTX (red), and prolonged (since P8) dark adaptation (blue).
B) averaged a-wave amplitude at P16 from experimental conditions in (A) C) A-wave implicit time D) normalized a-wave amplitude at the brightest stimulus strength used (1.0 log cd s/m^2).

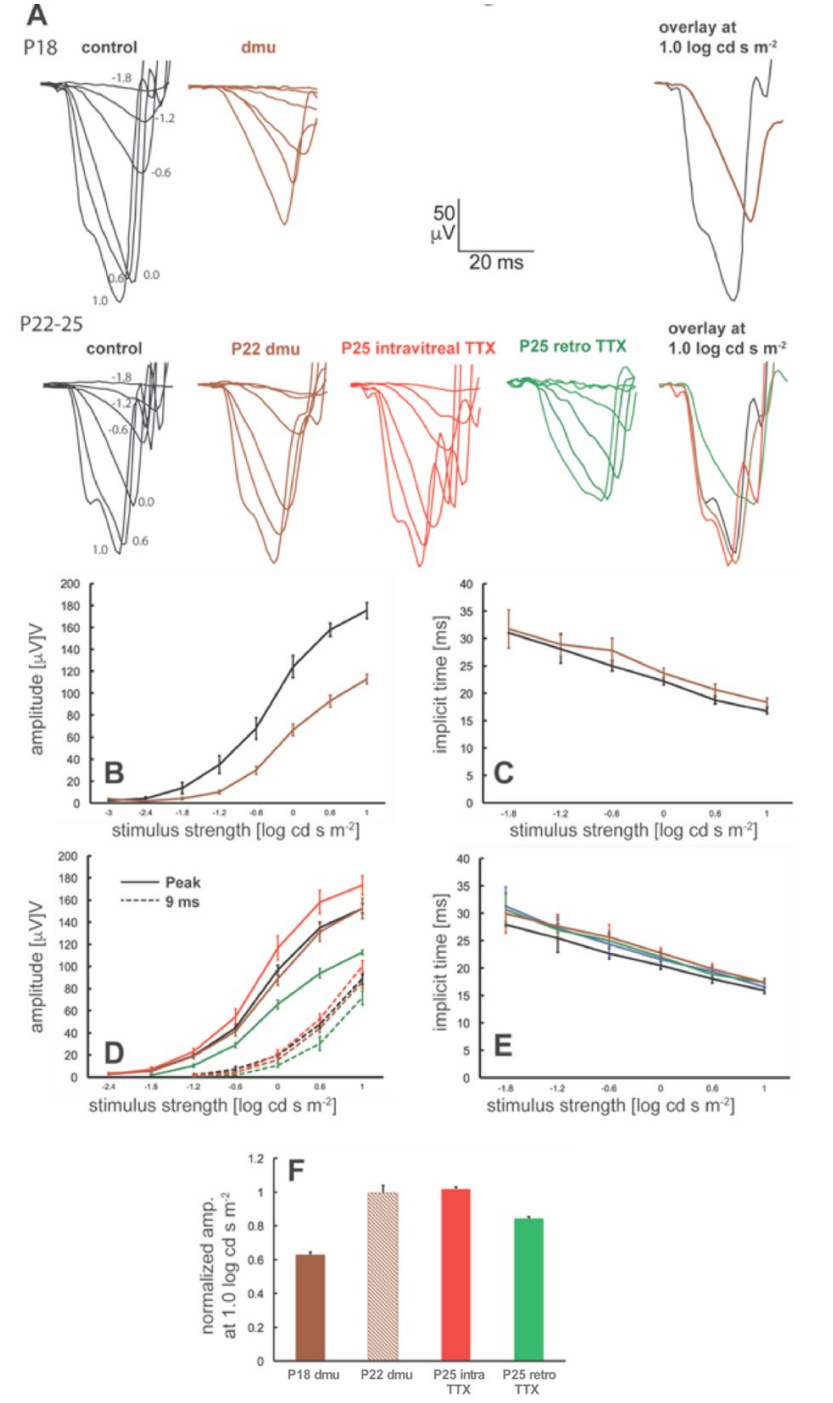

Figure 5.4: Retroaxonal modulation of photoreceptor function lessens with age. A) Example waveforms from dark -adapted ERG recordings of P18 and P22-25 control (black) and *Scn8a*^{dmu} (brown) mice, P20-25 acute intravitreal injection of TTX (red), and P20-25 retrobulbar injection of TTX. B) averaged a-wave amplitude at P18 from control and *Scn8a*^{dmu} C) A-wave implicit time at P18 D) averaged a-wave amplitude at P20-25 from experimental conditions in (A) E) A-wave implicit time at P20-25 F) normalized a-wave amplitude at the brightest stimulus strength used (1.0 log cd s/m^2).

CHAPTER 6: CONTRIBUTION OF $Na_V1.8$ SODIUM CHANNELS TO RETINAL FUNCTION

Publication information

Smith, B. J., Côté, P. D., & Tremblay, F. (2017). Contribution of Nav1.8 sodium channels to retinal function. *Neuroscience*, *340*, 279–290. http://doi.org/10.1016/j.neuroscience.2016.10.054

6.1 Abstract

We examined the contribution of the sodium channel isoform $Na_v1.8$ to retinal function using the specific blocker A803467. We found that A803467 has little influence on the electroretinographic (ERG) a- and b-waves, but significantly reduces the oscillatory potentials to 40-60% of their original amplitude, with significant changes in implicit time in the rod-driven range. To date, only two cell types were found in mouse to express $Na_v1.8$; the starburst amacrine cells (SBAC), and a subtype of retinal ganglion cells (RGC). When we recorded light responses from ganglion cells using a multielectrode array we found significant and opposing changes in two physiological groups of RGCs. ON sustained cells showed significant decreases while transient ON-OFF cells showed significant increases. The effects on ON-OFF transient cells but not ON sustained cells disappeared in the presence of an inhibitory cocktail. We have previously shown that RGCs have only a minor contribution to the oscillatory potentials (Smith et al., 2014), therefore suggesting that starburst amacrine cells might be a significant contributor to this ERG component. Targeting SBACs with the cholinergic neurotoxin ethylcholine mustard aziridinium (AF64A) caused reduction in the amplitude of the OPs similar to A803467. Our results, both using the ERG and MEA recordings from retina ganglion cells, suggest that $Na_v1.8$ plays a role in modulating specific aspects of the retinal physiology and that SBACs are a fundamental cellular contributor to the OPs in mice, a clear demonstration of the dichotomy between ERG b-wave and oscillatory potentials.

6.2 INTRODUCTION

Voltage-gated sodium channels (Na_v) are best known for supporting the electrogenesis of the rising phase of the action potential (Dugandzija-Novaković et al., 1995). Na_v channels are composed of a pore-forming α subunit, sufficient for functional expression and a modulatory β subunit. There are 10 different Na_v channel α subunits and although there appear to be relatively small functional differences between subtypes when studied in isolation (Kohrman et al., 1996; Smith et al., 1998; Chen et al., 2008; Wilson et al., 2011), there is substantial evidence for tissue, cell type or intracellular specificity of expression. For instance, $Na_v1.1$, 1.2, 1.3, 1.6 are expressed in CNS neurons, where $Na_v1.1$, 1.2 and 1.6 are associated with the axon initial segment and nodes of Ranvier (Caldwell et al., 2000; Boiko et al., 2003; Van Wart and Matthews, 2006a; Hu et al., 2009). $Na_v1.4$ has been described in association with skeletal muscles, $Na_v1.5$ with heart cells, while $Na_v1.7$, $Na_v1.8$, and 1.9 are essentially found in the peripheral nervous system (Catterall, 2000; Goldin et al., 2000; Goldin, 2001; Trimmer and Rhodes, 2004).

Mammalian retinas express at least 6 Na_v α subunit isoforms ($Na_v1.1$, 1.2, 1.3, 1.6, 1.8, and 1.9) (Fjell et al., 1997; Mojumder et al., 2007; O'Brien et al., 2008) with what appears to be specific and restricted expression both in terms of cellular types and temporal patterns of expression during development (Boiko et al., 2001; Boiko et al., 2003). For instance, Na_v 1.1 are found associated with mouse AII amacrine cells (Boiko et al., 2003; Wu et al., 2011) and with primate DB3a and DB4 cone bipolar cells (Puthussery et al., 2013), while a developmental switch from $Na_v1.2$ to isoform $Na_v1.6$ at initial segments and nodes of Ranvier in rat retinal ganglion cells has been documented (Van Wart and Matthews, 2006a).

$Na_v1.8$, a TTX-resistant Na_v primarily associated with the peripheral nervous system, is expressed in both starburst amacrine cells (SBACs) and a subset of retinal ganglion cells (O'Brien et al., 2008). $Na_v1.8$ generates a persistent sodium current (Akopian et al., 1996; 1997) and is partially resistant to inactivation caused by high frequency (>20 Hz)

and sustained depolarization (Vijayaragavan et al., 2001). Rabbit SBACs have been shown to have a TTX-resistant and ambroxol-sensitive Na_v current that contributes to the light response to centrifugal motion (Oesch and Taylor, 2010). SBACs generate membrane potential oscillations spontaneously (Petit-Jacques et al., 2005), after electrical stimulation (Tsai et al., 2011) and in response to light (Petit-Jacques and Bloomfield, 2008), suggesting the possibility that SBACs might contribute to the oscillatory behavior of the field potentials elicited by diffuse flashes of light, namely the electroretinographic (ERG) signal.

The ERG is the retinal field potential generated by the summed cellular responses, typically to a brief light stimulus. The largest components of the ERG, the a- and b-waves, have been shown to be generated predominately by the photoreceptors and ON bipolar cells respectively (Dowling, 2012), modulated by inhibitory cells that synapse with the ON bipolar cells and photoreceptors (Lukasiewicz et al., 1994; Dong and Hare, 2000; Kapousta-Bruneau, 2000; Awatramani et al., 2001). In addition to the well-characterized low frequency components of the ERG, a group of high frequency (50-150 Hz) oscillations occur on the rising limb of the ERG b-wave (Cobb and Morton, 1954) which are referred to collectively as the oscillatory potentials (OPs). It is believed that these oscillations arise from light-evoked inner-retinal activity, however, the precise cellular generators are unknown (reviewed in Wachtmeister, 1998). Since OPs can be non-invasively measured in humans, understanding how they are generated in model species should facilitate the diagnostic power and the pathophysiological understandings of major human retinal dysfunctions.

The restricted expression of $Na_v1.8$ to SBACs and some RGCs, the modest RGC contributions to the OPs (Smith et al., 2014), as well as the partial resistance of $Na_v1.8$ channels to high frequency stimulation, make $Na_v1.8$ a good potential target for identifying SBAC contributions to the OPs. In this study we determined the role of $Na_v1.8$ in retinal processing using the ERG field potential signal and the extracellular spiking activity of the RGCs. We found that $Na_v1.8$ predominately affects the OPs with only a minor additional effect on the b-wave. We also found that a subset of ON sustained RGCs had light responses that were augmented by $Na_v1.8$ which was conserved in the presence of inhibitory neurotransmitter antagonists. In addition, ON-OFF transient

RGCs showed a decrease in their peak frequency for both ON and OFF components, decrease that was removed in the presence of inhibitory neurotransmitter antagonists. Our results, in combination with the restricted expression of $Na_v1.8$ (O'Brien et al., 2008) and the limited contribution of RGCs to the OPs (Smith et al., 2014) suggest a role for SBACs in the generation of the OPs. To test this hypothesis, we ablated the SBACs using the cholinergic neurotoxin ethylcholine mustard aziridinium ion (Leventer et al., 1987) as well as blocking glycine receptors as a positive control for the elimination of light evoked SBAC oscillations (see Petit-Jacques and Bloomfield, 2008). We show that SBACs generate a substantial component of the OPs potentially by amplifying oscillations generated by upstream circuitry. In addition, we show that Nav1.8 plays a critical role in the post-synaptic generation of synchronous SBAC oscillations.

6.3 Material and methods

6.3.1 Ethics approval

All animal manipulation and procedures were accomplished in accordance to the animal care guidelines established by the Canadian Council on Animal Care and in agreement with the ARVO statement for the Use of Animals in Ophthalmic and Vision Research. Mice were housed under a 12h light/dark cycle with free access to food and water. Each experiment was terminal and mice were sacrificed by anesthetic overdose followed by cervical dislocation.

6.3.2 Electroretinography

Electroretinographic and intravitreal injection protocols have been described in detail elsewhere (Smith and Côté, 2012; Smith et al., 2013; 2014). Briefly, 8- to 16-week old C57Bl/6 mice (Charles River Laboratories, St. Constant, QC, Canada) were dark-adapted overnight and anesthetized with Avertin (2,2,2 Tribromoethanol, Sigma Aldrich, St-Louis, MO, USA) dissolved in amylene hydrate (tertiary amyl alcohol, 275 mg/kg, Sigma Aldrich). The mydriatic agent cyclopenolate HCl 0.5% (Alcon, Fort-Worth, TX) was

topically applied to dilate the pupils while a 0.5% proparacaine hydrocloride (Alcon) was used to reduce eye movements and irritation. Body temperature was maintained at 37 °C. The active electrode consisted in a silver-coated nylon microfiber (the DTL-plus microconductive fiber ;Diagnosys, Littleton, MA) apposed to the corneal surface and hydrated with a solution of 2.5% hydroxypropyl methylcellulose to maintain conductivity. Platinum sub-dermal electrodes (Grass Instruments, Quincy, Mass) were inserted at the base of the nose (reference) and in the tail (ground). The signal collected from the corneal electrodes was amplified 10,000 fold using a differential amplifier with a 0.3-300 Hz bandwidth (P511, Grass instruments). The analog data was converted to digital one through an A/D board (PCI 6281, National Instruments, Austin, TX, USA) with an acquisition rate of 1 kHz and stored for processing using a dedicated LabVIEW 9.0 interface (National Instruments). Flash stimuli were generated by a Ganzfeld stimulator (LKC Technologies, Gaithersburg, MD, USA) from a white xenon bulb (Grass PS22) that produced a maximum integrated luminance of 10.1 log cd s/m^2 at the corneal surface. Stimulus strengths were attenuated in steps of 0.4 log units by manual interposition of neutral density filters (Kodak Wratten, Rochester, NY, USA), up to 7.0 log attenuation. Inter-stimulus intervals varied from 5 s at the lowest strengths to 30 s at the highest ones with 2 to 10 responses averaged according to the signal to noise ratio.

The OPs were isolated by high-pass filtering of the ERG using an eight-order Butterworth filter centered at 50 Hz (custom ERG analysis toolbox in Matlab, Mathworks, Natick, MA). Such a high-order filter was used following recommendation from Lei et al (2006) who demonstrated the absence of a-wave intrusion in the isolated OPs when using higher order Butterworth filters as well as minimal phase delays in the frequency range (60-200 Hz) occupied by the OPs. Individual OPs amplitude was computed as the differences between the absolute voltage of the trough preceding the OP and its peak, while the summed OPs was calculated by adding the computed amplitudes of OPs identified as post-receptoral; the two first OPs immediately following the stimulus onset were not included as found to be resistant to synaptic block and thus likely to be produced by the photoreceptors (B. Smith; personal observation). For the measurements of the a- and b-wave, the OPs were filtered out by applying a low-pass eight-order Butterworth filter centered at 50 Hz; the resulting signal was then measured

from baseline to trough voltage (a-wave) and from trough to first peak positive voltage (b-wave).

As previously reported (Smith et al., 2013), we divided the range of the scotopic b-wave into four sections in according to the elicited cellular responses. We refer to those stimulus ranges as follows: cone-rod mixed response with substantial cone contribution (Cr_i) corresponding to the highest stimulus strength range (1.0 to −0.6 log cd s/m^2), rod-cone mixed responses with less cone contribution (Rc_i) at intermediate stimulus strengths (−0.6 to −1.5 log cd s/m^2), rod-driven responses (R_i) at lower stimulus strengths (−1.5 to −3.6 log cd s/m^2), and finally responses elicited predominantly by retinal ganglion cell (Rg_i) at the lowest strengths (−3.6 to −6 log cd s/m^2).

6.3.3 Drug injections

The $Na_v1.8$ channel blocker A803467 (Tocris Bioscience, Bristol, UK) was dissolved in saline to a concentration of 250 µM (1 µL injected for a final predicted intravitreal concentration of 50 µM, n=8). The cholinergic neurotoxin ethylcholine mustard aziridinium ion (AF64A) was freshly prepared from AF-64 (Sigma Aldrich) to a concentration of 5 mM as described by Amthor et al., (2002) and 1µL was injected into the vitreous for a final intravitreal concentation of 1µM (n=8). A solution of strychnine (Sigma Aldrich) was prepared in saline to a concentration of 250 µM and 1 µL was injected for a final predicted intravitreal concentration of 50 µM (n =6). Following injection, the mice were either allowed to recover (AF64A) or further dark-adapted for approximately 30 minutes to allow for diffusion of the drug before recording (A803467 and strychnine). For MEA experiments, concentration of A803467 used for the retinal perfusion was 50 µM while the GTS inhibitory cocktail consisted in Gabazine (Sigma-Aldrich: 200 µM), TPMPA (Sigma-Aldrich; 150 µM) and strychnine (50 µM).

6.3.4 Multi-electrode array recording

The retina was dissected free from the eyecup and pigmentary epithelium and positioned with brushes, photoreceptor side down, on a piece of filter membrane

(Millipore, Billerica, MA). The membrane was transferred to the cylindrical chamber of a 60MEA200/30iR-ITO 8 x 8 grid MEA with 30 μm electrodes at 200 μm spacing (Multi Channel System GmbH, Reutlingen, Germany). This preparation was stabilized by the weight of a harp slice grid (SHD-26H/10, Warner Instruments LLC, Hamden, CT, USA). Ames solution bubbled with carbogen (pH □7.4, 35– 36 °C) was continuously superfused (2 mL/min) over the preparation. A full-field flash was presented to the retina (LED 530 nm, 1 s duration) every 10 s. Data were digitized and sampled at 50 kHz, recorded with MC Rack software (Multi Channel Systems) and spikes high-pass filtered at 200 Hz. Baseline recordings were obtained after a 30-min to 2-hour period once the number of cells recorded and responses appeared stable. Spikes recorded on each electrode were sorted into individual cells offline using K-mean algoritm (Offline Sorter, Plexon, Dallas, TX, USA) and then analyzed with Neuroexplorer software (Nex Technologies, Littleton, MA, USA). For each cell, post-stimulus time histograms (PSTHs) were computed over 60 consecutive sweeps over 1800 ms. Cells were classified as ON-, ON-OFF and OFF-dominated when the ratio of ON vs OFF responses over the first 100 ms for each of the two responses was <3, between 3 and 0.6, and >0.6, respectively. Cells were considered to have sustained responses when the spike rate count between 300 and 700 ms after the stimulus onset was larger than 0.2 times the count of the initial 200 ms of the response. The cell type was determined prior to any drug application.

6.3.5 Statistical analysis

Data for the control and treated eyes were collected simultaneously and results compiled with Microsoft Excel for Mac (version 14.2; Microsoft Corporation, Redmond, WA) and analyzed with SPSS software (version 20 for Mac; International Business Machines, Armonk, NY). Stimulus series for individual ERG components were submitted to repeated-measures ANOVA (rmANOVA) analysis with within-subject factor including flash strength matched for treatment effect. Because of the limited sample size, normality was difficult to assess so we confirmed the significance level of the rmANOVA using the non-parametric Wilcoxon Signed Ranked Test.

6.4 Results

Consistent with the retinal expression pattern of $Na_v1.8$ being limited to the inner part of the retina (2008), the amplitude and implicit time of the a-wave was not significantly different from controls after injection of A803467 (Table 1; Fig 1, 2A). The b-wave implicit time (IT) was likewise unaffected however, its amplitude was slightly but significantly reduced ($p<0.05$) at stimulus intensities above -1.2 log cd m s^{-2} by about 10% (Table 1).

We analyzed the amplitude and implicit time of the OPs individually (Fig 1, 2C,D) since it is still unknown whether each OP is independently generated or whether the OPs are a generated by a single oscillatory cell type (Wachtmeister, 1998; Dong et al., 2004). OPs were isolated from the raw ERG waveforms by a high-pass filter at 50 Hz (Lei et al., 2006; Zhang et al., 2007). Only the 4 most prominent OPs were analyzed since we found that the first two small OPs were unchanged even under conditions of general synaptic block (CNQX+L-AP4, B. Smith, data not shown).

A803467 caused a significant reduction of all 4 OPs, particularly obvious in the rod-dominated Rc_i stimulus response range (see Materials and Methods, Table 1; fig 1 and 2 C,D). In detail, A803467 significantly reduced OP1 at stimulus intensities of -1.2 log cd m s^{-2} and above with a larger effect (~60% reduction) in the Rc_i vs. the Cr_i range. The effects on OP2 and OP3 were nearly identical to the effects on OP1 with significant reductions in amplitude at stimulus intensities of -1.8 and above (see Table 1). However, A803467 had less effect on the amplitude of OP4 with significant reduction only in the Rc_i range at stimulus strengths of -1.2 to -0.6 log cd m s^{-2} (~30% of control). A803467 caused a consistent and significant ($p<0.05$) delay in the IT, averaging 6.3±2.1 ms to all OPs at stimulus strengths below -1.2 log cd m s^{-2}; in contrast, little or no change was observed at higher stimulus strengths (fig 2D).

6.4.1 $Na_v1.8$ augments spiking light responses from ON sustained cells and contributes to the inhibition of ON-OFF transient cells.

Previous work (O'Brien et al., 2008) showed $Na_v1.8$ expression in SBACs and a subset of RGCs. In addition to our results with ERGs, we tested the responses of individual RGCs to a 1 second full-field stimuli in an *ex vivo* MEA preparation. We divided the RGC light responses into 6 physiological types; transient and sustained versions of ON, OFF and ON-OFF cells. Obviously, given that the lowest estimates of mouse RGC types are between 12 and 15 (Coombs et al., 2006; Sun et al., 2002), and that the ganglion cell in mice retina can include up to 50% displaced amacrine cell (Jeon et al., 1998), these 6 groups are likely to be heterogenous. Nonetheless we found significant changes in only two groups, consistent with the findings from (O'Brien et al., 2008) suggesting a restricted but physiologically important contribution of $Na_v1.8$ to retinal signaling.

Application of A803467 to the *ex vivo* retinal preparation significantly reduced peak spike frequency in sustained ON cells (Table 1: 83.0±5.5% of control, n=60 cells from 10 preparations, $p<0.001$). We also compared the average spike frequency over the length of the light response, which was also significantly reduced (90.2±8.7% of control, $p<0.01$). When we blocked $GABA_a$, $GABA_c$ and glycine receptors (gabazine, TPMPA, and strychnine; GTS) prior to treatment with A803467, a similar effect was seen (Peak spike frequency: 79.7±4.3% of GTS, n=38 cells in 10 preparations, $p<0.0001$; Average spike frequency: 79.4±6.2% of GTS, $p<0.001$). In transient ON cells, we found essentially no effect on peak spike frequency (106.6±7.9% of control, n=55 cells in 10 preparations). When inhibitory pathways are blocked, we saw a small but significant reduction in peak spike frequency (88.3±3.3% of GTS, n=65 cells, $p<0.005$).

In opposition to the effects of sustained ON cells, ON-OFF transient cells showed a significant increase in peak spike frequency of both the ON and OFF components of the light response after A803467 (ON response: 134.6±13.2% of control, $p<0.05$; OFF response: 124.1±9.4% of control, n=45, $p<0.01$). Blocking inhibition eliminated the effect on both peak spike frequency (ON response: 114.8±6.8% of GTS, n=30; OFF response: 113.9±8.7% of GTS n=47 cells). ON-OFF sustained cells did not show a

significant increase in peak spike frequency following A803467 (ON response peak spike frequency: 95.8±6.8% of control, n=30; OFF response peak spike frequency: 95.5±8.5% of control; Average ON response 93.6±12.0%). Like in control conditions, A803476 caused no significant change in peak spike frequencies in the ON or OFF component of the light response compared to GTS alone (ON response peak frequency: 102.5±7.9% of GTS, n=30; OFF response: 115.8±14.0% of GTS; Average ON response 100.7±12.0%). A803467 did not significantly increased the peak light response of OFF transient cells (138.1±14.4% of control, n=28) and similar results were found after blocking inhibition (136.4±37.5% of GTS, n=19); however the high variability in our control responses may have impeded reaching a significant effect. We did not find that the peak spike frequency of sustained OFF cells was significantly changed by A803467 in normal conditions (107.0±12.8% of control, n=19) or following inhibitory block (125.2±27.7% of GTS, n=22).

6.4.2 SBAC contributions to ERG oscillatory potentials.

We found that $Na_v1.8$ causes a fairly selective reduction in the ERG OPs. We previously have shown that following optic nerve transection to ablate the RGCs the OPs are essentially unchanged (Smith et al., 2014). Given the restricted expression of $Na_v1.8$, in combination with the increase in spiking in ON-OFF transient cells following A803467, it is likely that the reduction in OPs following A803467 is due to an effect on SBACs. To test whether this was the case, we first targeted SBACs with the cholinergic toxin AF64A (Amthor et al., 2002). AF64A did not significantly change the amplitude of the a-wave, however, like A803467 the b-wave showed a small (~10%.) but significant decreased at stimulus strengths above -2.4 log cd m s^{-2}.

The most noticeable effect of AF64A was a substantial reduction in the amplitude of the oscillatory potentials similar to that seen with A803467. Like with A803467, the effects of AF64A were similar between the 4 OPs analyzed, showing reductions of ~40% in the Cr_i range and ~50% in the Rc_i range (Table 1), the difference between the two ranges being significant for all 4 OP. When the OPs were analyzed individually (Fig 4D) we found that AF64A significantly reduced the amplitude of OP1 at stimulus intensities

of -1.2 log cd m s^{-2} and above. AF64A caused a significantly larger reduction in Rc_i (~50% of control) compared to Cr_i (~30% of control). AF64A significantly reduced OP2 and OP3 at stimulus intensities of -2.4 log cd m s^{-2} and above again with a significantly larger effect in the Rc_i range (Table 1). Unlike A803467, AF64A caused a significant reduction in OP4 at all flash intensities higher than -3.0 log cd m s^{-2} (Table 1) with larger effects in the Rc_i range. We also analyzed the effect of AF64A on the IT of the individual OPs; however, we did not find a significant change for any of the OPs.

Petit-Jacques and Bloomfield (2008) have shown that light evoked oscillations in mouse SBACs are strongly reduced by strychnine while the peak light response is unchanged. Although strychnine is likely to have numerous additional effects on other retinal cell types expressing glycine receptors, we used it here as a positive control to strongly reduce light evoked oscillations in SBACs. Regardless of any additional effects of strychnine on the retina, an equal or lesser effect of strychnine on the amplitude of the OPs compared to our previous experiments indicates that AF64A and A803467 were able to strongly reduce or eliminate light evoked oscillations in SBACs.

Like AF64A, we found that strychnine caused no significant change in the amplitude of the a-wave although the a-wave IT was increased slightly and this reached significance in the high Rc_i range (Fig 4C). The b-wave amplitude was reduced by strychnine in the same range as AF64A and A803467, ie. ~15% reduction at stimulus energies above -1.2 log cd m s^{-2}. Strychnine did not have any consistent effect on the b-wave IT but caused a significant ($p<0.05$) increase in the Rc_i range (6.58±1.92 ms delay; Fig 4C).

Injecting strychnine caused a similar reduction in the OP amplitude as AF64A and A803467, differing only in that there was a smaller effect seen on OP4 relative to AF64A (Fig 4D). Like AF64A and A803467 in OPs 1, 2, and 3 the effects of strychnine were always significantly larger in Rc_i (~50%) relative to Cr_i (~25%, see able 1). The stronger effect of AF64A on OP4 is similar to the effect reported by Petit-Jacques and Bloomfield (2008), where strychnine appears to preferentially spare late oscillations (see example trace from their Fig 8). Unlike AF64A, strychnine caused significant delays in IT (Fig 2D, average of 10.4±4.3 ms) for all OPs at stimulus strengths below -1.2 log cd m s^{-2} and sporadically at higher strength stimuli. The similarity between the effects of AF64A and

strychnine on the OPs suggests that SBACs cannot be the only cell types contributing to the OPs. These results suggest however that our concentration of AF64A is sufficient to eliminate SBAC contributions to the OPs and also that $Na_v1.8$ contributes to light evoked SBAC oscillations.

6.5 Discussion

We investigated the contribution of $Na_v1.8$ to retinal function using both the ERG and MEA in combination with a recent $Na_v1.8$ specific blocker, A803467. Although a $Na_v1.8$ knockout mouse is available, we chose to acutely block $Na_v1.8$ channels with A803467 both to avoid developmental effects and because compensation by other channels has been shown to occur in other Na_v channel knockout mice. For example, in $Na_v1.6$-null mice, up-regulation of additional Na_v channel isoforms and other ion channels was shown to compensate for the loss of $Na_v1.6$ (Van Wart and Matthews, 2006b).

We present 2 main findings. First, using the ERG we found that the strongest effect of blocking $Na_v1.8$ was on the OPs. Secondly, we found that, although there was relatively little effect of A803467 overall on RGC light responses, there was a significant increase in light evoked spiking in transient ON-OFF cells after blocking $Na_v1.8$ that was eliminated when inhibition was blocked, suggesting that $Na_v1.8$ augments inhibitory input to at least a subset of the RGCs. Interestingly, we also documented that the light response of sustained ON cells was reduced in the presence of A803467, an effect that was preserved in presence of inhibitory blockers. These results are consistent with the previous results from (O'Brien et al., 2008), which suggested that $Na_v1.8$ play a functional role in supporting oscillations in SBACs' light responses as well as contributing to light responses in a subset of RGCs, probably ON alpha ganglion cells which have sustained light responses. In addition, our results suggest that the OPs are partially amplified by the SBACs. The dichotomy between the strong effects on OPs and relatively small influence on RGCs could suggest that OPs contribute minimally to the temporal envelope of RGC responses to diffuse illumination; although speculative, one may infer that OPs have more to do with spatial information. In that respect, it is

interesting to consider that SBACs are crucial to the detection of stimulus motion (Amthor et al., 2002, Yoshida et al., 2001; Fried et al., 2002; Zhou and Lee, 2008; although see He and Masland, 1997) by at least some directionally selective RGCs, implying that coordinated oscillations may be useful for the prediction of large moving stimuli and removing time lag (Trenholm, 2012; Berry et al., 1999). Oscillations in the retinal response of frog dimming detector are necessary for escape behavior from widening dark stimuli (Ishikane et al., 2005).

6.5.1 $Na_v1.8$ augments light responses in ON sustained cells.

In mouse RGCs, O'Brien et al. (2008) found that two morphological types of neurons in the ganglion cell layer express $Na_v1.8$, one with a small soma that expressed GABA and vesicular acetylcholine transporter, probably ON SBACs, and a set of cells with large somas that also stained for neurofilament 200, which predominately labels α type RGCs. In mice, there are three well-characterized α ganglion cells types: ON sustained, OFF transient, and OFF sustained (e.g. Margolis and Detwiler, 2007; Murphy et al., 2011; Schmidt et al., 2014). Although the ON sustained classification likely included more than ON α cells, A803467 reduced the light responses of enough cells to cause a significant reduction in peak and average spiking response of the entire population. Significant reductions in peak and average spike frequency were also observed when inhibition was blocked. In addition there was no reduction in light responses following A803467 in cells with sustained or transient OFF responses. These results together with the results from O'Brien et al. (2008) suggest that $Na_v1.8$ augments light responses in ON α RGCs.

6.5.2 $Na_v1.8$ is likely to contribute to starburst amacrine cell light responses.

The existence of Na_v channels and spikes in SBACs is controversial. In mice, Ozaita et al. (2004), Kaneda et al. (2007) and Petit-Jacques et al. (2008) did not find a TTX-sensitive inward current recording directly from SBACs *in vitro*. At the same time Ozaita et al., (2004) did report a transient component at the onset of depolarizing steps in

current clamp that was resistant to TTX (their Fig 1a) and is similar in appearance to spikelets recorded from AII amacrine cells (e.g. Tian et al., 2010). In rabbit, Cohen (2001) reports a TTX-sensitive current, while Bloomfield (1992) and Gavrikov et al. (2003) report SBAC spiking, whereas Taylor and Wassle (1995) and Peters and Masland (1996) did not. Interestingly, Zhou and Fain (1996) did find a TTX-sensitive spiking current in SBACs, but only in juvenile retinas. Most relevant to this study Oesch and Taylor (2010) found a TTX-resistant current that contributes to directional responses in SBACs in rabbit retina.

One issue with previous physiological measurement of Na_v current in SBACs is that they relied on patch-clamp recordings. The differences found using that technique, even within species, suggest that *in vitro* preparations may not accurately measure Na_v channel function in SBACs. Due to the long length of SBAC dendritic processes relative to the small soma, adequate space clamp may be an issue especially if $Na_v1.8$ is expressed predominately in dendritic tips (e.g. Bar-Yehuda and Korngreen, 2008; Williams and Mitchell, 2008; Schachter et al., 2010; Poleg-Polsky and Diamond, 2011). In addition, single cell recordings are unable to show whether oscillations are synchronized between cells. Because the ERG is a massed response, a strong contribution to the ERG suggests synchronized oscillatory light responses across a population of cells.

We first showed that blocking $Na_v1.8$ selectively reduced the ERG OPs. $Na_v1.8$ is expressed only in SBACs and a subset of RGCs and eliminating RGCs in mice has no effect on the OPs (Smith et al., 2014). A cholinergic neurotoxin specific to SBACs caused a nearly identical selective reduction in the OPs as blocking $Na_v1.8$. We also found that blocking $Na_v1.8$ increased the light response of transient ON-OFF RGCs. This was due to decreased inhibition in the presence of A83467, because when the experiment was repeated in a cocktail to block inhibition, the effect disappeared. ON-OFF directionally selective cells, which receive GABAergic inhibition from SBACs (e.g. Zhou and Lee, 2008; Briggman et al., 2011**;** Wei et al., 2011), have transient ON-OFF responses to full-field light (e.g. Weng et al., 2005; Rivlin-Etzion et al., 2011; Hoggarth et al., 2015). In combination, these results suggest that $Na_v1.8$ is important for light responsiveness in SBACs, which leads to inhibition of ON-OFF RGCs.

6.5.3 $Na_v1.8$ in SBACs contribute to the OPs.

Whether the OPs represent a composite signal from several cell types or have independent generators is controversial (Wachtmeister, 1998; Bui et al., 2002; Derr et al., 2002; Dong et al., 2004). Our results suggest that SBACs are not a primary generator of the OPs. The application of A803467 does reduce the OPs amplitude but not completely eliminated them. Furthermore, A803467 does not change the number of OPs (unlike TTX application; Smith et al., 2013) nor does it changes significantly the interval between them (FIG 2D). These results are thus more compatible with the idea of the SBACs amplifying and propagating an already existing OPs signal generated upstream, rather than modifying the OPs characteristics. One possibility is that an upstream oscillator drives oscillations in SBACs, agreeing with the results of Petit-Jacques and Bloomfield (2008), which showed reduced light evoked oscillations in SBACs in the presence of strychnine and DL-*threo*- β -Benzyloxyaspartic acid (TBOA), a excitatory amino acid transporter blocker. Blocking $Na_v1.8$ has a similar effect on the OPs as AF64A. Because of the restricted expression of $Na_v1.8$ and because eliminating RGCs does not substantially affect the OPs (Smith et al., 2014), it implies that synchronized oscillations in response to light are dependent on postsynaptic Na_v current in SBACs. $Na_v1.8$ sodium currents inactivate slowly (Akopian et al., 1996; 1997), rapidly recover from inactivation, and are partially (40%) resistant to high frequency (>20 Hz) and sustained depolarization (Vijayaragavan et al., 2001). Thus, the partial resistance of $Na_v1.8$ channels to high frequency stimulation makes them ideal facilitators of the high frequency light evoked oscillations. Further research is needed to determine the fundamental origins of the OPs. However, our results demonstrate for the first time a specific key cellular type that can be directly associated with the final expression of the mouse OPs as recorded from corneal electrodes.

A small reduction in the amplitude of the b-wave was also observed when $Na_v1.8$ channels were pharmacologically silenced; this may represent a contribution from RGCs since a transection of the optic nerve causes a similar reduction in b-wave amplitude (Alarcón-Martínez et al., 2010; Smith et al.,2014). It is also possible that SBACs may

play a minor role in modulating ON bipolar cell function either directly via acetylcholine receptors (Yamada et al., 2003; Dmitrieva et al., 2007) or via GABAergic or cholinergic modulation of amacrine cells that directly inhibit ON bipolar cells; further testing of this possibility is outside the scope of this report.

6.6 Conclusion

In conclusion, this study contains 2 main results. First, we found that blocking $Na_v1.8$ specifically reduces the OPs particularly at stimulus strengths in the rod-driven range. The selective expression of $Na_v1.8$ in SBACs, in combination with our results using the cholinergic neurotoxin AF64A, suggest that the SBACs are a fundamental cellular contributor to the OPs in mice, the first demonstration of a cell subtype contributing to this ERG component. Second, we demonstrate that $Na_v1.8$ contributes directly, albeit in a limited way, to the light response of sustained ON RGCs as well as to the inhibition of transient ON-OFF RGCs. $Na_v1.8$ contributions to inhibition in transient ON-OFF cells is consistent with them playing a role in SBAC inhibition.

TABLE 6.1: Percent changes in ERG amplitude (a- and b-waves and OP1-4) in presence of Nav1.8 channel blocker A803467, cholinergic neurotoxin ethylcholine mustard aziridinium ion (AF64A) and strychnine (Stry), in mesopic conditions Rci and Cri. Significance were provided for the effect of the drugs compared to non-injected fellow eye (CTRL), as well as for the comparison between effects of A803467 with AF64A or Strychnine. ns: $p>0.05$; * $p<0.05$; # $p<0.01$.

ERG component	Drug	Rci				Cri			
		Ratio vs CTRL, AF64A or Stry	p			Ratio vs CTRL, AF64A or Stry	p		
		(Mean ± SE)	CTRL	AF64A	Stry.	(Mean ± SE)	CTRL	AF64A	Stry
a-wave	A803467	101.2 ± 9.2 %	ns	ns	ns	98.4 ± 2.6 %	ns	ns	ns
	AF64A	99. 0 ± 4.2 %	ns			95.3± 1.3 %	ns		
	Stry	112.0 ± 9.2 %	ns			98.4 ± 2.6 %	ns		
b-wave	A803467	90.3 ± 2.1 %	*	ns	ns	93.9 ± 1.4 %	*	ns	ns
	AF64A	85.6 ± 2.9%	#			90.8 ± 1.7 %	*		
	Stry	90.2 ± 4.7%	*			86.9± 2.1%	#		
OP1	A803467	39.4 ± 4.7 %	#	*	*	62.0 ± 2.2%	#	ns	*
	AF64A	54.5 ± 5.5 %	#			69.0 ± 1.7%	#		
	Stry	51.5 ± 7.8 %	#			75.3± 3.7 %	#		
OP2	A803467	43.8 ± 7.1 %	#	ns	ns	64.8 ± 6.7 %	#	ns	ns
	AF64A	50.4 ±3.6%	#			65.8 ± 1.5%	#		
	Stry	53.4 ± 9.3%	#			69.9 ± 3.5%	#		
OP3	A803467	51.1 ± 3.8 %	#	*	ns	76.8 ± 3.1 %	#	*	ns
	AF64A	42.8 ± 4.3%	#			62.5 ± 2.4 %	#		
	Stry	57.3 ± 7.7 %	#			80.2 ± 4.1 %	#		
OP4	A803467	72.9 ± 6.2 %	#	#	*	90.0 ± 4.1 %	*	#	ns
	AF64A	52.3 ± 5.4 %	#			68.8 ± 3.7 %	#		
	Stry	85.7± 6.7 %	#			85.2 ± 6.7 %	#		

TABLE 6.2: Percent change in RGCs response in the presence of $Na_v1.8$ channel blocker A803467, in control conditions and after application of inhibitory cocktail GTS, by cell types. ns: not significant; # $p<0.01$

		A803467			GTS + A803467		
Cell Type	Response measured	N	% change	p	N	% change	p
ON sustained	ON Peak	60	83.0 ± 5.5	#	38	79.7 ± 4.3	#
	ON Average		90.2 ± 8.7	#		79.4 ± 6.2	#
ON transient	ON Peak	55	106.6 ± 7.9	ns	65	88.3 ± 3.3	#
ON-OFF sustained	ON Peak	30	95.8 ± 8.5	ns	30	102.5 ±7.9	ns
	ON Average		93.6 ± 12.0	ns		100.7 ±12.0	ns
	OFF Peak		95.5 ± 8.5	ns		115.2 ± 14.0	ns
	OFF Average		136.7 ± 16.9	ns		135.0 ±29.0	ns
ON-OFF transient	ON Peak	30	134.6 ± 13.2	#	47	114.8 ± 6.8	ns
	OFF Peak		124.1 ± 9.4	#		113.9 ±8.7	ns
OFF sustained	OFF Peak	19	107.0 ± 12.8	ns	22	125.2 ± 27.7	ns
	OFF Average		102.2 ± 9.0	ns		149.4 ± 11.9	ns
OFF transient	OFF Peak	28	138.1 ± 37.5	ns	19	136.4 ± 37.5	ns

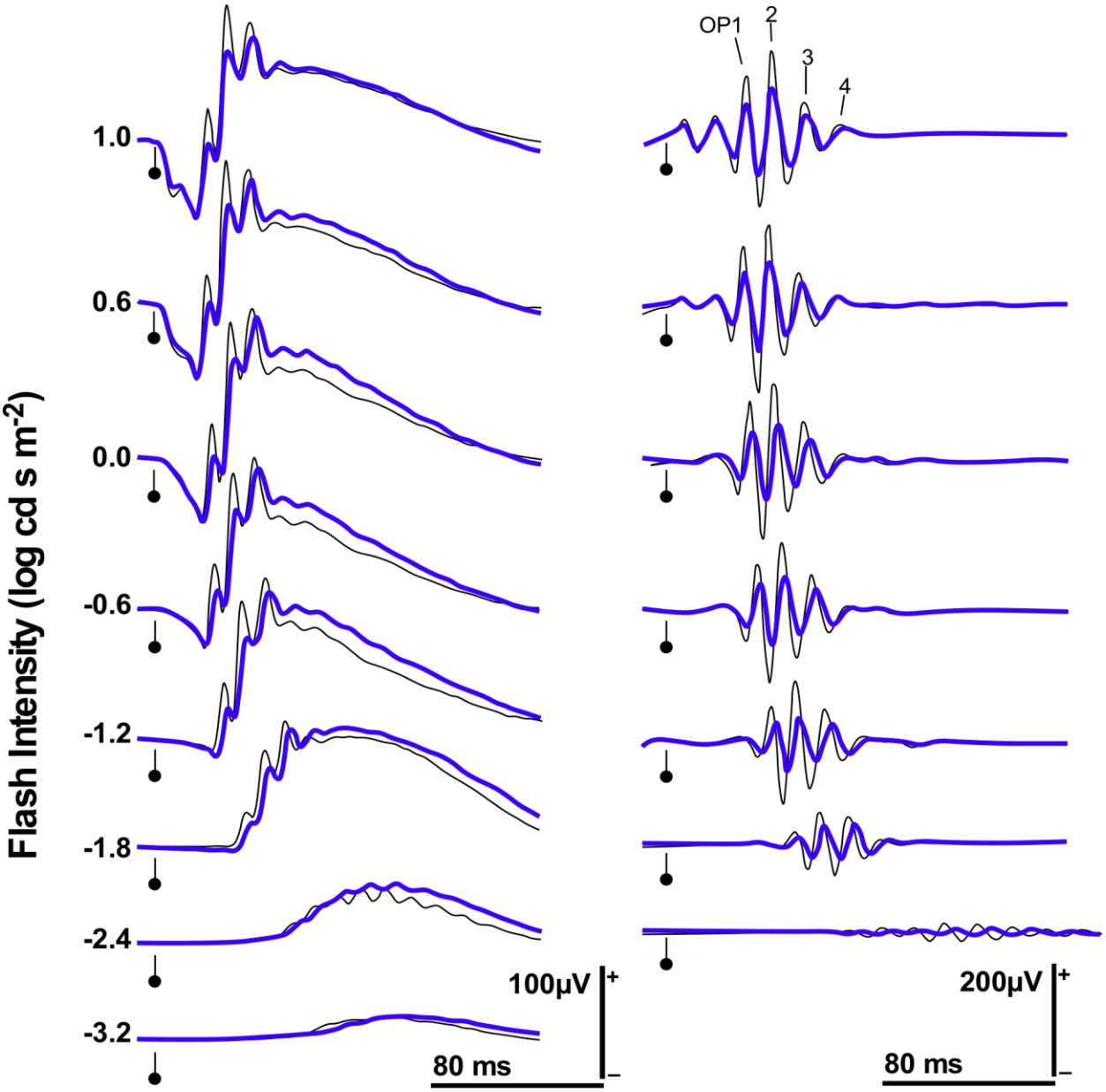

Figure 6.1: A803467 effects on ERG signal. Intensity series of full-bandwidth ERG (left) and isolated OPs (right) recordings of A803467-injected eyes (blue) compared to controls (gray traces). Calibration as indicated. Flash intensities as indicated in log cd s m^{-2}. OP1,2,3,4 refer to OPs analyzed in this study. Markers indicate stimulus onset.

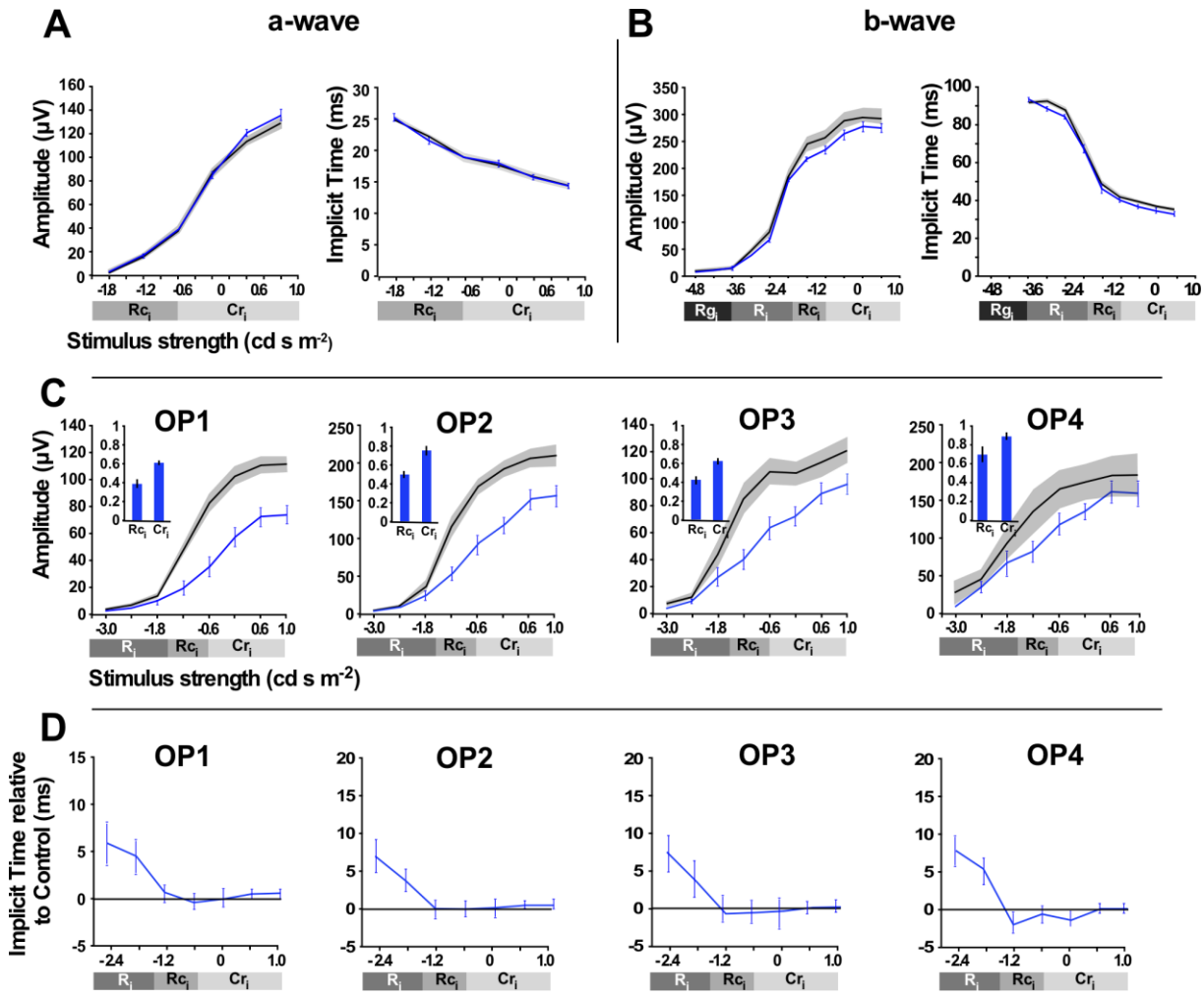

Figure 6.2: Quantitative assessment of A803467 on ERG signal. Intensity-response curves for (A) a-wave and (B) b-wave amplitude (left) and implicit time (right) as well as OP1-4 amplitude (C) and implicit time (D) in control eyes (gray) and A803467-injected eyes (blue). Inserts in (C) document the ratio of A803467 to control amplitude eyes for the averaged cone-dominated (Cr_i) and rod-dominated (Rc_i) response ranges.

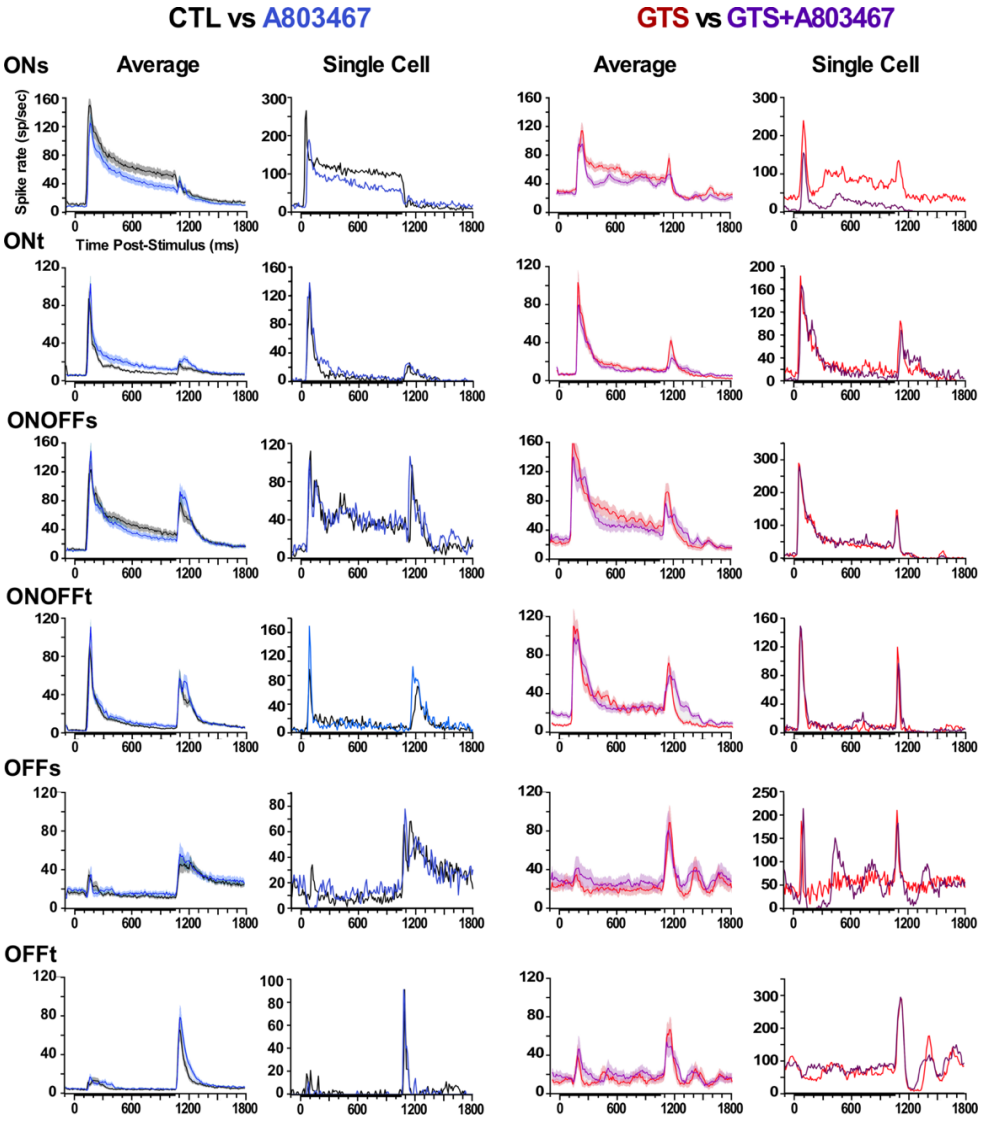

Figure 6.3: Effect of A803467 on RGC activity. Average (thick line) with SE (shadowed area) of PSTH for RGCs classified as sustained (s) and transient (t) versions of ON, ON-OFF and OFF cell types. Population averages are presented in the first and third columns, while single-cell PSTH examples of each of the cell types are provided in the second and fourth columns. Control conditions (black) and after A803467 injection (blue) are presented in the first two columns. The third column depicts the responses obtained after an initial blockade of GABAa, GABAc and glycine receptors by a cocktail of gabazine 200µM, TPMPA 150 µM and strychnine 50µM (GTS; pink) and after A803467 (purple). The cell type was determined prior to the effects of the cocktail as the response profile is modified by the cocktail.

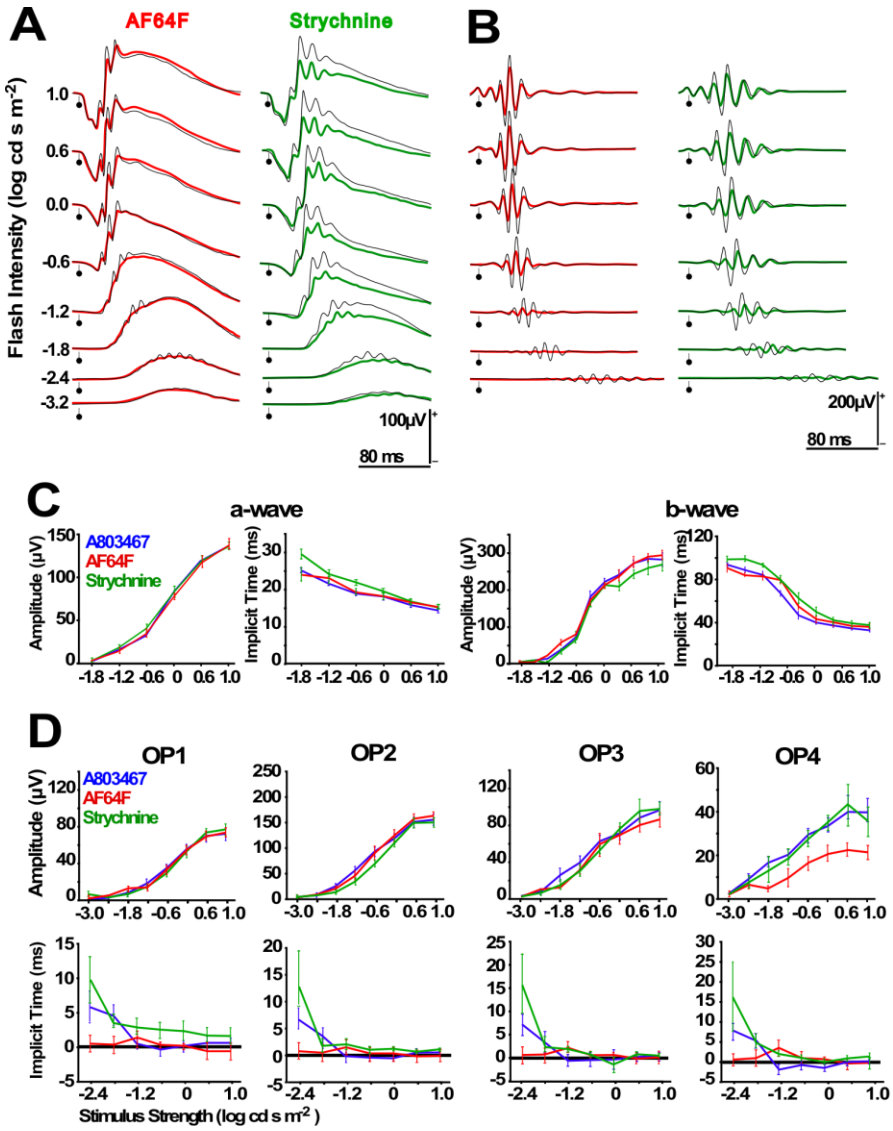

Figure 6.4: Effects of elimination of Starburst Amacrine Cells on ERG signal. Intensity series of (A) full-bandwidth ERG and (B) isolated OPs in control eyes (black) and eyes injected with the cholinergic neurotoxin ethylcholine mustard aziridinium ion (AF64A; red) or with strychnine (green). Calibration as indicated. Flash intensities as indicated in log cd s m^{-2}. In (C), the intensity-response curves for the a-wave and b-wave amplitude are presented for AF64A- (red) and strychnine- (green) injected eyes and compared to the responses obtained for the A803467- (blue) injected eyes. In (D), the implicit time relative to control are presented for the same three drugs. Cr_i correspond to the stimulus intensity range that is cone-dominated, Rc_i when the responses are rod-dominated, and R_i when only rods contribute to the response. Markers indicate stimulus onset.

CHAPTER 7: Na_V CHANNEL ISOFORM CONTRIBUTIONS TO RETINAL LIGHT RESPONSES

Publication information

Smith, B. J., Côté, P. D. and Tremblay, F. Na_v channel isoform contributions to retinal light responses. To be submitted to the journal *Neuroscience*

7.1 ABSTRACT

Voltage-gated sodium channels are key molecular components underlying the propagation of information in the nervous system. The family of Na_v channel α subunits shows precise spatial localization as well as diverse physiological properties, suggesting that individual isoforms may be responsible for shaping electrogenesis in excitable cells. Perinatal lethality of knockout models as well as limited isoform specific pharmacologic blockers has limited research into the role of Na_v channel isoforms in mature neurons.

We compared the effectiveness of membrane-permeablized antibodies against various Na_v channel isoforms to non-selective and selective small molecule blockers, as well as an $Na_v1.6$-null mutant mouse. Membrane-permeablized antibodies against $Na_v1.6$ and $Na_v1.8$ caused similar changes to the ERG as small molecule blockers and in the case of $Na_v1.6$, a knockout mouse. A cocktail of antibodies against $Na_v1.1$, $Na_v1.2$, and $Na_v1.6$ reduced in the dark-adapted b-wave and increased the number of oscillatory potentials, mimicking the effect of TTX. In particular, we found that blocking $Na_v1.6$, but not $Na_v1.1$ or $Na_v1.2$ consistently reduced the amplitude of the light-adapted b-wave. Blocking $Na_v1.1$ selectively increased the number of OPs while blocking $Na_v1.8$ reduced the amplitude of all OPs. Judging by the similarity of the effects on the ERG, mp-antibodies were as effective as both general and subtype specific pharmacologic blockers. In addition, each subtype-specific antibody caused different effects on ERG indicating selectivity.

We extended these results to evaluate the contributions of $Na_v1.6$, $Na_v1.1$ and $Na_v1.2$ to the light responses of retinal ganglion cells as well as to optogenetic stimulation by channelrhodopsin-2. In response to light, we found that mp-anti $Na_v1.6$ and 4,9 ah TTX reduced maximal spike rate by ~60%. In general, the effects of blocking $Na_v1.2$ were small while blocking $Na_v1.1$ caused a reduction in maximal spike rate in response to network derived input. The effects of blocking $Na_v1.1$ and $Na_v1.6$ were reduced when RGCs were stimulated optogenetically suggesting that both isoforms contribute to presynaptic and intrinsic excitability in ganglion cells. We found that, in

ON and ON-OFF cells with sustained light responses blocking $Na_v1.1$ but not $Na_v1.2$ nor $Na_v1.6$ caused a reduction in the sustained component of the light response.

Our results show that currently available anti-Na_v channel monoclonal antibodies are able to block Na_v channels both *in vivo* and *in vitro* matching the effect of commercially available non-selective (TTX, Ambroxel) and selective (A803467, 4,9ahTTX) small molecule blockers and showing effects similar to a KO mouse model. We extend these finding to identify specific contributions of Na_v channel alpha subunit isoforms to retinal function *in vitro* and *in vivo*.

7.2 INTRODUCTION

The wide variety of voltage-gated ion channel isoforms in combination with their specific temporal and spatial expression patterns within electrically active cells indicates that isoform differences play a role in how neurons encode information. Voltage-gated sodium (Na_v) channels generate the rising phase of action potential and have distinctive distribution pattern on multiple spatial scales from the precise distribution in the axon initial segment e.g. (Lorincz & Nusser, 2008) to differences in isoform expression between tissues (Catterall, 2000; Goldin, 2001; Goldin et al., 2000; Trimmer & Rhodes, 2004). The Na_v channel family might therefore be an instructive example on the functional contributions of individual ion channel isoforms to information encoding at the single neuron and circuit levels**.** However, the scarcity of Na_v channel subtype specific blockers, in combination with perinatal mortality in most Na_v channel knockout mouse models ($Na_v1.1$: (Yu et al., 2006); $Na_v1.2$: (Planells-Cases et al., 2000); $Na_v1.6$: (Raman, Sprunger, Meisler, & Bean, 1997)) and compensation by other isoforms and ion channels (e.g. (Swensen & Bean, 2005; Van Wart & Matthews, 2006a; Vega, Henry, & Matthews, 2008; Yu et al., 2006)) has hindered research into isoform function in adult neural circuits.

There are 9 well-characterized mammalian Na_v α -subunit isoforms ($Na_v1.1$-1.9), of which 6 ($Na_v1.1$, 1.2, 1.3, 1.6, 1.8, and 1.9) can be localized to the mammalian retina (Fjell, Dib-Hajj, Fried, Black, & Waxman, 1997; Mojumder, Frishman, Otteson, & Sherry, 2007; O'Brien et al., 2008). Isoforms are localized to specific cell types and intracellular regions and, in addition, isoform expression shifts during development coincident with changes in cellular excitability. Some retinal cell subtypes are known to selectively express Na_v channel isoforms e.g. Na_v 1.1 in mouse AII amacrine cells (Kaneda, Ito, Morishima, Shigematsu, & Shimoda, 2007; Wu, Ivanova, Cui, Lu, & Pan, 2011) and primate DB3a and DB4 cone bipolar cells (Puthussery, Venkataramani, Gayet-Primo, Smith, & Taylor, 2013), $Na_v1.8$ in starburst amacrine cells and select retinal ganglion cells (O'Brien et al., 2008). Cells expressing multiple Na_v channel isoforms, e.g. retinal ganglion cells (RGCs), also show stereotypical intercellular distribution patterns

e.g. $Na_v1.1$, 1.2 and 1.6 in the axon initial segment and nodes of Ranvier (Boiko et al., 2001; 2003; Schaller & Caldwell, 2000; Van Wart & Matthews, 2006b; Van Wart, Trimmer, & Matthews, 2007). Intracellular expression of α-subunit subtypes is also regulated during development in retinal ganglion cells (Boiko et al., 2001; 2003; Van Wart & Matthews, 2006a; 2006b).

When individual α-subunits are expressed in *Xenopus* oocytes, small differences in isoform function and modulation can be appreciated (e.g. (Chen et al., 2008; Patel, Barbosa, Xiao, & Cummins, 2015; Smith, Smith, Plummer, Meisler, & Goldin, 1998). In most cases, peak transient sodium currents are similar between $Na_v1.1$, $Na_v1.2$, and $Na_v1.6$; however, in dorsal root ganglion cells direct comparison of $Na_v1.2$ and 1.6 shows $Na_v1.6$ generates a larger peak Na_v current (Rush et al., 2005). Despite the similarity in their transient sodium currents, $Na_v1.6$ consistently produces larger persistent and/or resurgent currents relative to $Na_v1.2$ (Chen et al., 2008; Rush et al., 2005), $Na_v1.1$ (Patel et al., 2015), or both (Smith et al., 1998). $Na_v1.6$ is better able to sustain repetitive firing (Rush et al., 2005). However, $Na_v1.6$ undergoes more use-dependent reduction relative to $Na_v1.1$ consistent with the hypothesis that $Na_v1.1$ plays a role in maintained fast firing (Patel et al., 2015).

In general, neurons lacking $Na_v1.6$ tend to show only minor reductions in transient current (~40%: (Aman & Raman, 2007; Raman et al., 1997); or no change: (Enomoto, Han, Hsiao, & Chandler, 2007; Levin et al., 2006; Osorio et al., 2010; Royeck et al., 2008)). However, persistent (~40%: (Do & Bean, 2003; Enomoto et al., 2007; Maurice, Tkatch, Meisler, Sprunger, & Surmeier, 2001; Osorio et al., 2010; Royeck et al., 2008) and resurgent (~70%: Levin et al., 2006, Royeck et al., 2008, Mercer, Chan, Tkatch, Held, & Surmeier, 2007; Osorio et al., 2010, Enomoto et al., 2007, Cummins:2005jp, Do & Bean, 2003) sodium currents are substantially reduced in the majority of neuron subtypes studied (but see (Mercer et al., 2007; Osorio et al., 2010)). Reductions in persistent and resurgent currents are correlated with deficits in maximal firing rate and repetitive firing (Aman & Raman, 2007; Enomoto et al., 2007; Grieco & Raman, 2004; Khaliq, Gouwens, & Raman, 2003; Mercer et al., 2007; Raman et al., 1997; Royeck et al., 2008; Van Wart & Matthews, 2006b). It has been suggested that the

well-documented reductions in persistent and resurgent currents in many neuron types in the absence of $Na_v1.6$ directly cause changes in spiking output, in particular reductions in repetitive spiking and gain (Levin et al., 2006; Mercer et al., 2007; Raman et al., 1997). In contrast, some neurons function essentially normally in the absence of $Na_v1.6$. For example, in cerebellar granule cells where only persistent current is reduced in the absence of $Na_v1.6$, maximal spike rate and maintained firing are normal (Osorio et al., 2010) and, in subthalamic nucleus, cells' spontaneous and sustained spiking in response to depolarizing current is unchanged (Do & Bean, 2004).

While a majority of knockout studies have focused on $Na_v1.6$, a few recent studies have looked at effects of knocking out $Na_v1.1$, a common retinal Na_v channel isoform. At P15, in global $Na_v1.1$ KO mice, peak persistent and resurgent Na_v currents were reduced between 58-69% in Purkinje neurons, leading to reduced spontaneous activity and firing in response to injected current (Kalume, Yu, Westenbroek, Scheuer, & Catterall, 2007) while peak transient current were reduced by a similar amount in GABAergic interneurons (Yu et al., 2006). Interneurons from mice with a knock-in loss of function mutation in $Na_v1.1$ showed more transient responses to a depolarizing pulse (Ogiwara et al., 2007; Yu et al., 2006).

In addition to commonly express TTX-sensitive Na_v channel isoforms, there is evidence for the retinal expression of TTX-resistant Na_v channel isoforms ($Na_v1.8$; $Na_v1.9$) that are typically found in the peripheral nervous system (O'Brien et al., 2008; Smith, Côté, & Tremblay, 2017). In heterologous expression systems, the TTX-resistant Na_v channel isoforms have very distinct physiological properties, the most prominent being very slow inactivation kinetics, a persistent sodium current, and a substantially more depolarized voltage dependence of activation (Akopian, Sivilotti, & Wood, 1996; Vijayaragavan, O'Leary, & Chahine, 2001).

There have been some attempts to generate isoform-specific pharmacologic blockers against Na_v channel isoforms, for example against Nav1.6 (Rosker et al., 2007) and Nav1.8 (Jarvis et al., 2007). The most recent method has been to use a panel of μ-conotoxins in combination to differentiate between Nav1.1-1.7 (Wilson et al., 2011). Nevertheless, this panel-based approach has the major disadvantage of requiring a careful

assessment of the drug concentrations to avoid non-specific effects as well as requiring a broad collection of μ-conotoxins. Antibodies targeted to the extracellular E3 region of Na_v channels have been previously used as general (Meiri, Sammar, & Schwartz, 1989), and subtype ($Na_v1.5$) specific blockers {Xu:2005en}. However, a recent report by RazPrag et al., (2010) where retinal potassium channels were selectively blocked by using antibodies coupled to the ampipathic peptide Pep-1 (Gros et al., 2006), which allowed the antibodies to access channel-specific intracellular epitopes, inspired us to use the same strategy against Na_v channels.

Previously we have investigated Na_v channel contributions to the mouse ERG (Smith et al., 2017; Smith & Côté, 2012; Smith, Tremblay, & Côté, 2013). Our results suggested the ERG as a way of measuring whether membrane-permeablized antibodies (mp-anti) are effective in subtype specific block of Na_v channels. Our results show that readily available Na_v channel antibodies are able to block Na_v channels both *in vivo* and *in vitro,* matching the effect of the best commercially available non-selective (TTX, Ambroxol) and selective (A803467, 4,9ahTTX) small-molecule blockers and showing effects similar to KO mouse models. We extend these finding to identify specific contributions of Na_v channel alpha subunit isoforms to retinal function *in vitro* and *in vivo*.

7.3 Material and methods

7.3.1 Animals and ethics considerations

All animal procedures were completed in accordance to animal care guidelines established by the Canadian Council on Animal Care and in accordance to the ARVO Statement for the Use of Animals in Ophthalmic and Vision Research. Protocols were reviewed and approved by the Dalhousie University Committee on Laboratory Animals. Mice were housed under a 12-h light-dark cycle environment with free access to food and water. Luminance inside the room was kept at 180 lux, resulting in 13 lux inside the cages (determined from the average of 5 measurements near the cage rack or from inside five different cages, respectively). At the end of experiments, mice were euthanized by anesthetic overdose followed by cervical dislocation.

For most experiments, C57Bl/6 mice between 8 and 16 weeks of age (Charles River Laboratories, Saint-Constant, QC, Canada) were used. Mice expressing channelrhdopsin2 (ChR2-YFP) under the control of the *Thy1* promoter on the C57Bl/6 background were supplied by Jackson Laboratories (Bar Harbour, ME). We also used *Scn8a*^{dmu} mice and aged-matched C57Bl/6 mice at postnatal day 22-25 at which point the photoreceptor defect reported in Coté et al., (2005) has resolved. *Scn8a*^{dmu} mice harbor a function-blocking mutation in the *Scn8a* gene, and have been described previously (Cote, 2005; De Repentigny et al., 2001; B. J. Smith & Côté, 2012). The mutation was found to consist in a single nucleotide deletion in the sequence coding for the first interdomain loop of $Na_v1.6$ and, as a result, homozygotes are devoid of functional $Na_v1.6$. The resulting frameshift in the open reading frame results in the presence of a stop codon a short distance downstream of the mutation.

7.3.2 Electroretinographic techniques and intravitreal injection

ERGs and intravitreal injections were done as previously described (Smith *et al*., 2013, Smith et al., 2016). Mice were dark adapted for at least 8 hours before being anesthetized under dim red light by intraperitoneal injection of Avertin (2,2,2 Tribromoethanol, Sigma Aldrich, St-Louis, MO) dissolved in amylene hydrate (tertiary amyl alcohol, 275 mg/kg, Sigma Aldrich).

Following application of a topical anesthetic to the cornea, 1 µl of stock concentrations of chemicals were injected into the vitreous via a 30-gauge needle mounted on a Hamilton syringe under dim red illumination. Predicted (see Smith et al., 2013) intravitreal concentrations were: 20 µM tetrodotoxin (TTX, Abcam Biochemicals, Toronto, ON, Canada), 50 µM A803467 (Tocris Bioscience, Bristol, UK), 2 µM 4,9 anhydro tetrodotoxin (Tocris), 1mM Ambroxol hydrochloride (Tocris). Following injection, mice were further dark adapted for approximately 30 minutes to allow for diffusion of the drug before recording.

7.3.3 Membrane-permeable antibodies

The amphipathic peptide carrier Pep-1 (Abbiotech, San Diego, CA) at a concentration of 1 μ g/ μ L was mixed at 1:1 volume with monoclonal antibodies (purified IgG, 1mg/ml) against $Na_v1.1$ (clone K74/71), $Na_v1.2$ (clone K69/3), $Na_v1.6$ (clone K87A/10), and $Na_v1.8$ (clone N134/12) (NeuroMab, Davis, CA). Rat monoclonal antibodies were generated against amino acids 1929-2009 of the cytoplasmic C-terminus of $Na_v1.1$; amino acids 1882-2005 of the cytoplasmic C-terminus of $Na_v1.2$; amino acids 459-476 of the intracellular interdomain loop I-II of $Na_v1.6$; and amino acids 1724-1956 of the cytoplasmic C-terminus of $Na_v1.8$. In addition, a rabbit polyclonal antibody generated against amino acids 1501-1518 of intracellular loop between domains III and IV of rat $Na_v1.1$ (Alomone Laboratories, Jerusalem, Israel) was used. Finally, a mouse gamma globulin (Jackson Immunoresearch Laboratories, West Grove, PA) was used as negative control. One microliter of the resulting mixture was injected intravitreally (Raz-Prag et al., 2010; M. H. Wang, Frishman, & Otteson, 2009).

7.3.4 Multi-electrode array recording

The retina was dissected free from the eyecup and pigmentary epithelium and positioned with brushes, photoreceptor side down, on a piece of filter membrane (Millipore, Billerica, MA). The membrane was transferred to the cylindrical chamber of a MEA electrode (8 x 8 grid of 30 µm electrodes, with 200 µm spacing: 60MEA200/30iR-ITO, Multi Channel System MCS GmbH, Reutlingen, Germany). This preparation was stabilized by the weight of a harp slice grid (SHD-26H/10, Warner Instruments LLC, Hamden, CT, USA). Ames solution (Sigma Aldrich) bubbled with carbogen (pH7.4, 35– 36 °C) was continuously superfused (2 mL/min) over the preparation. A full-field flash was presented to the retina: we used a LED-based light source (530 nm; HPLS-36, Lightspeed Technologies, CA, USA) with 1 ms duration every 10 seconds and, for the optogenetic stimulation, a 447 nm LED (Luxeon Star Lethridge, AB, Canada). Data were digitized and sampled at 50 kHz, recorded with MC_Rack software (Multi Channel Systems) and spikes high-pass filtered at 200 Hz. Baseline recordings were obtained after a 30- to 60-minute period, once the number of

cells recorded and responses appeared stable. Spikes recorded on each electrode were sorted into individual cells offline (Offline Sorter, Plexon, Dallas, TX, USA) and then analyzed with Neuroexplorer software (Nex Technologies, Littleton, MA, USA). For each cell, Post-Stimulus Time Histograms (PSTHs) were computed over 60 consecutive sweeps over 1900 ms post stimulus. Cells were classified as ON-, ON/OFF, and OFF-dominated when the ratio of ON vs OFF responses over the first 100 ms for each of the two responses was <3, between 3 and 0.6, and >0.6, respectively. Cells were considered to have sustained responses when the spike frequency count between 300 and 700 ms after the stimulus change was larger than 0.2 times the frequency of the initial 200 ms of the response.

7.3.5 Data Analysis

Analysis of ERG waveforms was completed using a custom ERG analysis toolbox written for Matlab (Mathworks, Natick, MA). Waveforms were low pass filtered at 50 Hz to remove high frequency oscillatory potentials (Lei, Yao, Zhang, Hofeldt, & Chang, 2006). The a-wave amplitude was measured from the baseline to the maximum negative trough and the b-wave was measured from the a-wave trough to the maximum positive peak. The a-wave amplitudes and implicit times (IT) were examined to ensure that the b-wave amplitude and IT were not influenced by the photoreceptors activity. All drug treatments had no effect on the a-wave nor caused amplitude and IT to increase slightly, consistent with a slowing in b-wave initiation. Comparison of a- and b-wave amplitudes was carried out using Microsoft Excel (Redmond, WA).

Stimulus intensities ranged from –6 to 1 log cd m s^{-2}. To simplify interpretation, we refer to flash intensity ranges as follows: primarily cone–driven responses (Cr_i) corresponding to the highest flash intensity range (1.0 to –0.6 log cd m s^{-2}), rod-cone mixed responses (Rc_i) corresponding to intermediate flash intensities (–0.6 to –1.5 log cd m s^{-2}), rod–driven responses (R_i) at lower flash intensities (–1.5 to –3.6 log cd m s^{-2}), and finally predominantly retinal ganglion cell-elicited responses (RG_i) at the lowest intensities (–3.6 to –6 log cd m s^{-2}).

7.4 Results

7.4.1 Blocking function of $Na_v1.6$ using membrane-permeable antibody, subtype-specific tetrodotoxin derivative, and genetic knockout have similar effects on the ERG.

We first investigated the contribution of $Na_v1.6$ to the ERG using both 4,9 anhydro TTX (Rosker et al., 2007), a $Na_v1.6$ specific sodium channel blocker (fig:1,4 red: n=6), as well as a membrane-permeablized antibody to $Na_v1.6$ (fig:1 blue: n=11). In both cases, the a-wave was unaffected, similar to TTX (B. J. Smith et al., 2013). We found that 4,9 ahTTX significantly reduced the dark-adapted b-wave to ~60% of controls at all stimulus intensities above -4.2 log cd m s^{-2} (fig1D; Table 1). Likewise, mp-anti $Na_v1.6$ caused a nearly identical reduction (~45%) in the dark-adapted b-wave with significant reductions at all stimulus intensities above -4.2 log cd m s^{-2}**.** We additionally tested the effects of genetic knockout of $Na_v1.6$ on the dark-adapted b-wave (fig 2; dashed blue). Although our previous results have shown reductions in photoreceptor function around the time of eye opening (Cote, 2005; Smith & Côté, 2012), by P22-25 photoreceptor function has matured to normal levels (Smith et al., 2017). At this stage, the dark-adapted b-wave in $Na_v1.6$ KO mice is significantly reduced at all stimulus intensities above -3.0 log cd m s^{-2} (table 1). At P22-25 $Na_v1.6$ KO mice had a less reduced b-wave than adult mice injected with 4,9 ahTTX and mp-anti 1.6; however, the contribution of Na_v channels to the b-wave of juvenile mice has not been tested, and could be reduced relative to adult mice. We therefore injected TTX in control C57Bl/6 mice at P22-25, finding that the reduction in the b-wave of P22-25 controls after TTX was similar to the reduction in the b-wave seen in $Na_v1.6$ KO mice (fig 2, dashed red; table 1)**.**

The photopic b-wave is a measure of the response of the cone ON bipolar cells that has been repeatedly shown to contain a Na_v-dependent component. In some cases, it has been demonstrated that the Na_v component of the b-wave is due to Na_v channels intrinsic to ON CBCs (Mojumder et al., 2007; Mojumder, Sherry, & Frishman, 2008; Smith et al., 2013), matching with recent reports of Na_v channels on specific subtypes of both ON and OFF CBCs in mice (Cui & PAN, 2008; Hellmer, Zhou, Fyk-Kolodziej, Hu, & Ichinose, 2016; Ichinose & Hellmer, 2016; Ma, Cui, & Pan, 2005; Vielma & Schmachtenberg,

2016). While in macaques $Na_v1.1$ channels are collected into an axon initial segment like band that can be easily visualized (Puthussery et al., 2013), in mice and rats immunoflorescence has been unsuccessful in definitively localizing a subtype of Na_v channel to the CBCs (Mojumder et al., 2007; Puthussery et al., 2014).

We found that in both dark- and light-adapted conditions, the cone driven b-wave was reduced with an effect similar to TTX itself (Smith et al., 2013; Smith, Wang, Chauhan, Côté, & Tremblay, 2014) by mp-Anti 1.6 and 4,9 ahTTX (fig 1C,E). Paired-flash ERGs (Smith et al., 2014) to isolate the dark-adapted cone pathways showed significant reductions of ~30-35% in both cases (table 1). TTX has a slightly larger effect (~45% see Smith et al., 2014), indicating a small contribution from some other Na_v channel isoforms. In light-adapted conditions, both mp-Anti 1.6 and 4,9 ahTTX reduced the photopic b-wave to the same extent as TTX (~35%) (Smith et al., 2013) with significant reductions at all stimulus strengths**.** We recorded from *Scn8a*^{dmu} mice prior to adopting the paired-flash protocol. In light-adapted conditions at P22-25, the *Scn8a*^{dmu} mice also show significantly reduced b-wave amplitudes at stimulus strengths above -0.2 log cd m s^{-2} of ~30%, similar in extent to intravitreal injection of TTX in age-matched control (fig 2C,E). At this age, unlike P16 (Smith and Côté, 2012), the photopic a-wave is not different between *Scn8a*^{dmu} mice and controls, indicating that an effect on cones is unlikely to contribute to the reduction in the photopic b-wave.

In addition to the low frequency b-wave, the ERG contains a high frequency component (50-150 hz in mice (Lei et al., 2006)) that predominately represents interactions between inhibitory cells and ON bipolar cells (reviewed in (Wachtmeister, 1998)). In all the techniques we used to block $Na_v1.6$ function, we observed significant reductions in the amplitude of the OPs. For simplicity, we summed the amplitudes of the four largest OPs (B. J. Smith et al., 2017). We found that in mp-anti 1.6 (~ 25% reduction significant above -0.6 log cd m s^{-2}), 4,9ahTTX (~ 40% reduction significant above -1.8 log cd m s^{-2}), and $Na_v1.6$ KO mice (~ 45% reduction significant above -1.2 log cd m s^{-2}) the summed amplitude of the first 4 OPs were reduced (Table 1)**.**

We used three methods to block $Na_v1.6$ function with similar results. The previously described Na_v-dependent modulation of the dark-adapted b-wave amplitude

by $GABA_cRs$ (Smith et al., 2013; Smith, Côté, & Tremblay, 2015b) appears to be predominately due to $Na_v1.6$. In addition, blocking or knocking out $Na_v1.6$ reduces the amplitude of the cone driven b-wave suggesting that the Na_v channel isoform augmenting cone ON bipolar cell light responses is $Na_v1.6$. Interestingly, while blocking $Na_v1.6$ largely reproduces the effects of TTX on the amplitude of the b-wave in both light- and dark- adapted conditions, in mice TTX increases the amplitude of the late OPs (e.g. (Smith et al., 2013)) while blocking $Na_v1.6$ reduced the first 4 OPs and had no effect on the late OPs in all models we used. This suggests a role for an additional Na_v channel isoform in GABAR-mediated inhibition. We therefore looked for the Na_v channel isoform or isoforms responsible for the suppression of the late OPs.

7.4.2 A cocktail with a combination of membrane-permeable antibodies against $Na_v1.1$, 1.2, and 1.6 has an identical effect on the ERG as TTX.

TTX, the canonical sodium channel blocker, has two effects on the dark-adapted mouse ERG. First, the amplitude of the b-wave is significantly reduced by about 40% (Smith et al., 2013) and second, although the first two OPs are reduced by about 30% (similar to the effects of blocking $Na_v1.6$ alone), the late OPs (3-5) are significantly increased at stimulus strengths above -1.8 log cd m s^{-2}. Like the effects on the amplitude of the b-wave, the increased amplitude of the late OPs is likely due to effects on GABA release onto $GABA_cRs$ (Smith et al., 2013; J. Wang et al., 2015).

There is evidence in the retina for both $Na_v1.1$ and 1.2 TTX-sensitive Na_v channels (Mojumder et al., 2007). We therefore tested whether blocking both these channels in combination with $Na_v1.6$ might replicate the effects of TTX on the b-wave and OPs. We found that a cocktail of membrane-permeable antibodies for $Na_v1.1$, 1.2, and 1.6 (fig 3; light blue, mp-TTX-S cocktail) and TTX (fig 3; maroon) had nearly identical effects on the dark-adapted b-wave amplitude (cocktail: n=7; significant reduction above -4.2 log cd m s^{-2} of ~45%), which is unsurprising given the effect of $Na_v1.6$ alone. TTX and the mp-TTX-S cocktail also caused significant increases of ~190% and ~160% respectively in the summed late OPs (Fig 3G) at stimulus intensities above -1.8 log cd m s^{-2} (Table 1). In addition to providing further proof of the efficacy of

mp-antibodies in selectively recreating the effects of pharmacologic blockers on the ERG, these results suggest that, although contributions to the amplitude of the dark-adapted b-wave are minor, either $Na_v1.1$ or 1.2 contributes to the suppression of the late OPs by GABA acting at the $GABA_cR$.

7.4.3 Blocking $Na_v1.1$ but not $Na_v1.2$ specifically increases the amplitude of the late OPs.

We next tested separately mp-antibodies against $Na_v1.1$ or 1.2. If these two isoforms contributed similarly to the ERG it would be difficult to know whether the antibodies were specific; however, we show that while both $Na_v1.2$ and 1.1 had little effect on the dark-adapted b-wave (Fig 3E; mp-$Na_v1.2$: n=6, significant reductions between -3 and –0.6 log cd m s^{-2}; mp-$Na_v1.1$: n=9 significantly reductions for stimulus strengths between -2.4 and 0 log cd m s^{-2}), only mp-antibodies against $Na_v1.1$ increased the late OPs**.** mp-antibodies against $Na_v1.1$ significantly increased the late OPs at all stimulus intensities above -0.6 log cd m s^{-2} (fig 3D,F; table 1) by ~130%. Unlike $Na_v1.6$, both $Na_v1.1$ or 1.2 had no significant effect on amplitude of the photopic b-wave (fig 3F).

7.4.4 Membrane-permeable antibodies can reproduce the specific effects of pharmacologic blockers of TTX-resistant Na_v channels.

To further test the effectiveness of mp-antibodies, we compared the effect of two additional pharmacologic blockers of Na_v channel subtypes against mp-antibodies directed towards the same targets. We have previously investigated the effects of blocking the TTX-resistant Na_v channel $Na_v1.8$ using A803467 (B. J. Smith et al., 2017), finding that the summed OPs are significantly reduced by ~40% at all stimulus strengths tested with only minor reductions (~10%) in the b-wave at higher stimulus strengths. MP-anti $Na_v1.8$ had similar, selective effects on the summed OPs, causing ~40% reduction in OP1-4 significant above -1.2 log cd m s^{-2}, with no significant effects on the amplitude of the b-wave (fig 4: A803467, olive; mp-anti Nav1.8, pink; n=5 ~5% increase at higher stimulus strengths). Like A803467, the effect on the OPs was increased at lower stimulus

strengths. We also used a combination of both TTX and ambroxol, a blocker of TTX-resistant Na_v channels, in comparison to the unselective anti-Pan Na_v channel antibody. Both the combination of TTX and ambroxol and mp-anti Pan Na_v (fig 4C, D: TTX + ambroxol; orange n=6), mp-anti NavPan: teal n=6) significantly reduced the dark-adapted b-wave, like TTX alone. TTX and ambroxol reduced it by ~45% at all stimulus strengths tested, while mp-anti Pan Na_v reduced it by 40% at stimulus strengths above -1.8 log cd m s^{-2} (fig 4E). The first 4 OPs were also significantly reduced in similar ways by both treatments (fig 4F; TTX + ambroxol: ~55% reduction at all stimulus strengths; mp-anti Pan Na_v: ~50% reduction at all stimulus strengths).

We thus found that, in every example tested, mp-antibodies against Na_v channel isoforms had similar effects on the ERG compared to pharmacologic blockers, or in the case of $Na_v1.6$, to knockout mice of the same isoform. In addition, each antibody affected differently the components of the ERG. Mp-anti $Na_v1.6$ reduced the b-wave in both light- and dark-adapted conditions, as well as the OPs. Mp-anti $Na_v1.1$ had little effect on the b-wave and, like TTX, increased the amplitude of the late OPs while mp-anti $Na_v1.2$ only affected the dark-adapted b-wave. Mp-anti $Na_v1.8$ reduced only the OPs, while Mp-anti Pan Na_v reduced all components measured.

7.4.5 Membrane-permeable antibodies have selective effects on the light responses of retinal ganglion cells.

Our ERG results suggest that mp-antibodies are efficient selectively block Na_v channel isoforms. We have previously investigated how the Na_v channel isoform $Na_v1.8$ affects the light response of RGCs (Smith et al., 2017). Here we used similar methods to investigate the light responses of RGCs to a 1000 milliseconds duration full-field stimulus after blocking common TTX-S Na_v channel isoforms ($Na_v1.1$, 1.2, and 1.6). We divided the RGC light responses into 3 physiological types (ON, OFF and ON-OFF) according to their physiological responses to full-field light. These experiments had two objectives. First, we wanted to further characterize the mp-antibodies functional discrimination at the level of the RGCs, which responses are not readily embedded in the ERG signal. In addition, we hoped that, although it would be difficult to separate effects

on the presynaptic retinal circuitry from direct effects on the intrinsic properties of RGCs, there might be some correlation between subtype specific block and effects specific to either the ON or OFF pathways.

7.4.6 Blocking $Na_v1.6$ either with 4,9-ahTTX or mp-anti $Na_v1.6$ strongly reduces the amplitude but not the shape of RGC light responses.

We first tested the effects of acutely blocking $Na_v1.6$ with mp-anti $Na_v1.6$ or 4,9-ahTTX (fig 5A; blue and red, respectively). This allowed us to test the effectiveness of mp-Na_v antibodies *in vitro*. In all cell types, we found that the spike peak frequency of RGC light responses was significantly reduced with little variation between cell types or method of $Na_v1.6$ block (~60% across cell types, see Table 2). The difference in the reduction in spike peak frequency in each cell type was similar between treatments, with mp-anti $Na_v1.6$ typically reducing the maximal spike frequency by ~10% more.

Given the previous ERG results, in combination with previous results showing the presence and functional significance of $Na_v1.6$ in RGCs using KO mice, the large reduction in RGC peak spike frequency after blocking $Na_v1.6$ appears to be a combination of presynaptic effects and reduced ability of RGCs to spike. To separate these effects, we stimulated RGCs directly using mice where channelrhodopsin-2 was expressed selectively in RGCs under the control of the *Thy1* promoter, in combination with blocking synaptic input to RGCs with a cocktail of synaptic blockers (CNQX, AP-7, AP-4, TPMPA, gabazine, strychnine)**.** We found that in *Thy1*-ChR2 mice, peak spike frequencies were reduced significantly (~45%) after mp-anti $Na_v1.6$ in all cell types (fig 5B). The effects were smaller than when $Na_v1.6$ was blocked in the whole retina suggesting, in concordance with our ERG results, that $Na_v1.6$ plays a significant role in network input to RGCs.

7.4.7 Blocking $Na_v1.1$ reduces peak spike frequency to a lesser extent than blocking $Na_v1.6$ and changes the shape of the RGC light responses in sustained cells.

Given the similarity between the effects of mp-anti $Na_v1.6$ and 4,9 ahTTX, we conducted *in vitro* experiments with $Na_v1.1$ and 1.2 mp-antibodies (fig 6A). Neither blocking $Na_v1.1$ or $Na_v1.2$ caused as large a reduction in spike peak frequency as $Na_v1.6$; however, both antibodies caused significant reductions in spike peak frequency in all cell types, mp-$Na_v1.1$ more (~35%) than mp-$Na_v1.2$ (~15%). Interestingly, while the effects of blocking $Na_v1.1$ and $Na_v1.6$ were relatively similar between ON and OFF cells and the ON vs. OFF responses in ON-OFF cells, the effects of $Na_v1.2$ were larger on the spike peak frequency of OFF cells (~35% reduction) relative to ON cells (~10% reduction). In addition, the effects on the OFF response of ON-OFF cells were likewise larger, suggesting a presynaptic contribution of $Na_v1.2$ to the OFF pathway.

Given the stronger effects after we blocked $Na_v1.1$ in comparison to $Na_v1.2$, we repeated the ChR2 experiments with mp-anti $Na_v1.1$ (Fig 6B). Like with mp-anti $Na_v1.6$, effects on the spike peak frequency were generally smaller when RGCs were stimulated directly; however, the spike peak frequency of both ON (~20%) and ON-OFF (~10%) cells were still significantly reduced. The reduced effect of mp-anti $Na_v1.1$ on optogenetically stimulated RGCs suggests that $Na_v1.1$ contributes to both presynaptic input and intrinsic excitability of RGCs. In the case of OFF cells, there was no significant change following treatment with mp-anti $Na_v1.1$, indicating that $Na_v1.1$ plays a relatively strong role in the presynaptic input to these cells but little role in the intrinsic excitability of OFF cells.

7.4.8 Blocking $Na_v1.1$ but not $Na_v1.6$ or $Na_v1.2$ makes sustained RGC light responses more transient.

When inspecting the light responses of individual ON and ON-OFF RGCs, we found that many ON and ON-OFF cells with more sustained light responses became transient following treatment of mp-anti $Na_v1.1$. Previous work in $Na_v1.1$-knockout mice has shown that elimination of $Na_v1.1$ caused spiking responses to depolarizing current to become more transient in hippocampal pyramidal cells and GABAergic interneurons (Yu et al., 2006) and neocortical interneurons (Ogiwara et al., 2007). At the same time, in immature retinal ganglion cells, elimination of $Na_v1.6$ reduced but did not eliminate

sustained spiking in response to depolarizing current (Van Wart & Matthews, 2006a). We therefore compared the effects of mp-anti $Na_v1.1$, $Na_v1.2$, and $Na_v1.6$ on sustained spiking in response to light in both ON and ON-OFF cells. We found that in ON sustained cells (fig 7A), spiking peak frequency was significantly reduced in ON sustained cells in response to mp-anti $Na_v1.6$ (~60% reduction) and mp-anti $Na_v1.1$ (~35%) but not mp-anti $Na_v1.2$. In ON-OFF sustained cells, the pattern was similar with significant reductions in peak spike frequency following application of mp anti $Na_v1.6$ (~60%) and mp anti $Na_v1.1$(~25%) but not mp-anti $Na_v1.2$ (fig 7B).

To quantify effects on the sustained component of light responses we subtracted the average normalized transient response from the normalized responses of sustained cells from equivalent cell classes (ON and ON-OFF) and summed the spike count for the last 900 ms of this response (fig 7 C,D). We also calculated a sustained/transient index (STI e.g Zhang et al., 2015) by normalizing the average spike count of the second 200 ms of the light response to the first 200 ms. By both of these metrics, blocking $Na_v1.1$ but not $Na_v1.2$ or $Na_v1.6$ caused a significant reduction in sustained firing in ON sustained cells (sustained component: ~25%; STI: ~35%). Likewise, in ON-OFF cells blocking $Na_v1.1$ but not $Na_v1.2$ or $Na_v1.6$ significantly reduced sustained firing (sustained component: ~100%; STI: ~45%). These results suggest segregation in the roles of the various Na_v channel isoforms in supporting maximal firing ($Na_v1.6$) vs. sustained firing over the length of a prolonged stimulus ($Na_v1.1$).

Peak spike frequency in response to ChR2 stimulation in ON sustained cells (fig 7 E,F) was significantly reduced by blocking either $Na_v1.1$ (~15%) or $Na_v1.6$ (~40%). Similar results were obtained from ON-OFF sustained cells ($Na_v1.1$: 10%; $Na_v1.6$: ~40%). Transient ChR2-driven responses were relatively rare (see e.g. Zhang et al., 2015) so to approximate the sustained component of ChR2 responses from ON and ON-OFF cells with sustained light responses we summed the last 900 ms of the ChOP-2 response as well as calculating the STI. We found that the sustained component of ChR2 derived responses from ON and ON-OFF sustained cells were significantly reduced by ~30% after mp-anti $Na_v1.1$. Mp-anti $Na_v1.1$ also significantly reduced STI in both cell types by ~35% (table 4). In general, despite the large reduction in peak firing frequency, $Na_v1.6$ had variable and mainly non-significant effects on sustained ChR2-driven

responses from ON and ON-OFF sustained cells. Only the STI, but not the sustained component, of ON-OFF sustained cells was significantly reduced by mp-anti $Na_v1.6$.

7.5 Discussion

The precise molecular machinery underlying the neural code is a important ongoing question in neuroscience. Although other families of ion channels play important roles in electrogenesis of excitable cells, Na_v channels are the key players in the rising phase of the action potentials. Thus, a method of blocking individual Na_v channel subtypes could lead to insight into which properties of spike patterns encode information. We combined genetic knockout mice, small molecule blockers, and a membrane-permeablized antibody method principally to identify contributions of $Na_v1.6$ to retinal function, as well as benchmarking the effectiveness of the membrane-permeable antibody method. Finding that all three methods of blocking $Na_v1.6$ caused similar reductions in both ERG parameters and RGC spiking, we used mp-antibodies to explore the contribution of $Na_v1.1$ and $Na_v1.2$ to retinal function.

There are few subtypes of specific blockers of Na_v channel isoforms, most of which target the TTX-r Na_v channel isoforms implicated in chronic pain (e.g. McGaraughty et al., 2008, Zhang et al., 2010). Previously we investigated the retinal function of $Na_v1.8$ using the subtype specific blocker A803467 (B. J. Smith et al., 2017); however, we wanted to find a general approach to blocking Na_v channels that could be applied acutely. There are a number of drawbacks to analyzing Na_v-channel knockout mice, particularly juvenile morbidity that may confound results and early death. Although this can in principal be circumvented by use of tissue-specific knockouts, there is evidence that compensation both by other Na_v channels isoforms and other ion channels in general (e.g. (Swensen & Bean, 2005; Van Wart & Matthews, 2006b; Vega et al., 2008; Yu et al., 2006)). There have been previous efforts to generally (Meiri et al., 1989) and selectively ($Na_v1.5$: (Xu et al., 2005) block Na_v channels using antibodies targeted to extracellular epitopes. Two recent papers in the ERG literature (Raz-Prag et al., 2010; M. H. Wang et al., 2009) suggested the use of antibodies targeted to intracellular epitopes in

combination with an amphipathic peptide (Pep-1) to achieve isoform-specific block of Na_v channel isoforms.

We used the ERG to evaluate the effects of subtype-specific Na_v channel blockers. There are two obvious drawbacks to this methodology. The cellular origins of the ERG have not been completely described, particularly with regards to the OPs, and, although the major cell classes all contribute to the ERG in some measurable way, in some cases, principally the amacrine and ganglion cells, their contribution to the summed ERG signal cannot be reliably distinguished. However, we previously found a substantial contribution of both TTX-s Na_v channels (Smith et al., 2013) and $Na_v1.8$ to retinal function (Smith et al., 2017). There are nevertheless advantages to using the ERG over the analysis of single cells. For instance, because the ERG contains summed contributions from many cells, small contributions that might be overlooked in the response of single cells can be readily observed when responses of many cells are summed. For example, we were able to predict the presence of Na_v channels in mouse cone ON bipolar cells (Smith et al., 2013) that were only recently confirmed using intracellular recording (Hellmer et al., 2016; Ichinose & Hellmer, 2016). In combination with preliminary experiments on $Na_v1.6$ function in *Scn8a*^{dmu} mice (Smith & Côté, 2012) these results suggested to us that the ERG is an efficient method to test the selectivity and effectiveness of membrane permeable antibodies to block Na_v channels.

7.5.1 Roles of $Na_v1.6$ in the retina

Until recently, it was difficult to investigate the retinal function of $Na_v1.6$ due to significant photoreceptor dysfunction of unknown etiology (Cote, 2005; Smith & Côté, 2012) and early mortality in $Na_v1.6$ knockout mice (see Van Wart & Matthews, 2006a). Only recently were we able to show that the photoreceptor dysfunction was a transient developmental phenomenon that resolves by P22 (manuscript in preparation). Although the $Na_v1.6$ selectivity of 4,9 ahTTX was first demonstrated in 2007 (Rosker et al., 2007) and recently confirmed (Hargus, Nigam, Bertram, & Patel, 2013), only recently has it become commercially available. Using a combination of mp-anti $Na_v1.6$, *Scn8a*^{dmu} mice, and 4,9 ahTTX *in vivo* we found that all 3 methods resulted in reductions in the

amplitude of the dark-adapted b-wave and OPs similar in extent to age-matched injections of TTX. In combination with our previous work demonstrating Na_v channel-dependent modulation of the b-wave via $GABA_c$Rs (Smith, Côté, & Tremblay, 2015a) as well as studies suggesting that the OPs are a result of interactions between amacrine cells and bipolar cells in the inner retina (reviewed in Wachtmeister (1998)), these results show that $Na_v1.6$ plays a important role in Na_v-dependent modulation of inhibition in the mouse retina.

Herrmann et al., (2011) suggest that the amplitude of the rod-driven b-wave is increased by GABA acting on $GABA_c$Rs on rod bipolar cells. Expanding on the results from Jones and Palmer, (2011) in goldfish, $GABA_c$Rs is suggested to mediate a tonic hyperpolarization of the rod-bipolar cell and thus increases the dynamic range of rod bipolar cell depolarization. $Na_v1.6$ is known to mediate a persistent Na_v current in other preparations (Osorio et al., 2010; Royeck et al., 2008; Rush et al., 2005; Smith et al., 1998)**.** Our results (Smith, Côté, & Tremblay, 2015a) show that modulation of the dark-adapted b-wave by $GABA_c$Rs is strongly Na_v-channel dependent. The similarity between the effects of $Na_v1.6$ block and TTX in control mice suggests that $Na_v1.6$ controls the majority of Na_v-dependent GABA input to rod bipolar cells. The ability of $Na_v1.6$ to carry a persistent Na_v current may facilitate tonic release of GABA onto rod bipolar cell, $GABA_c$Rs driving tonic inhibition and leading to an increase in rod-driven b-wave amplitude.

We also found that $Na_v1.6$ contributes to the amplitude of the light adapted b-wave. Previously we demonstrated that most of the Na_v channel contribution to the light adapted b-wave persists in the presence of ionotropic glutamate receptor blockers, which isolates the cone to cone ON bipolar cell circuit from a majority of synaptic input including inhibition (Smith et al., 2013; B. J. Smith, Côté, & Tremblay, 2015b)**.** These results suggested a direct contribution of Na_v channels to ON-cone bipolar cell light responses, confirmed by the presence of TTX-s Na_v channels in mouse type 5 ON-bipolar cells (Hellmer et al., 2016). The presence of Na_v channels in mammalian ON-cone bipolar cells is now well established (Mojumder et al., 2007). In monkey, the restriction of $Na_v1.1$ to an axon initial segment-like section of the bipolar cell axon has facilitated identification of the Na_v channel isoform responsible. In rodents however, no similar

section was identified and while there is evidence that in $Na_v1.1$ is not localized to cone bipolar cells (Van Wart, Boiko, Trimmer, & Matthews, 2005; Wu et al., 2011) Puthessary et al., (2013) confirmed the absence of $Na_v1.2$ or $Na_v1.6$ in that region. Although Mojumder et al., (2007) also did not find clear expression of $Na_v1.1$, $Na_v1.2$, or $Na_v1.6$ in mouse bipolar cell bodies, all three isoforms were present in the outer plexiform layer indicating that they might be localized to the bipolar cell dendrites, consistent with the TTX-sensitive Na_v current in mouse { Hellmer:2016b } and rat (Ma et al., 2005; Pan & Hu, 2000; Vielma & Schmachtenberg, 2016) cone bipolar cells.

7.5.2 Membrane permeable Na_v channel antibodies can replicate in vivo and in vitro effects of pharmacological Na_v channel blockers.

We used four pharmacologic blockers as a reference to test the efficacy of membrane permeable antibodies to block Na_v channels. We have previously shown that TTX has two highly reproducible effects on the dark-adapted mouse ERG, reducing the amplitude of the b-wave by ~40% and increasing the amplitude and number of the late OPs (Smith et al., 2013). We were able to replicate both the effects of TTX using a cocktail of membrane permeable antibodies to $Na_v1.1$, 1.2, and 1.6. The TTX resistant Na_v channel isoform $Na_v1.8$ in the mouse retina is localized only to the starburst amacrine cells and a restricted set of RGCs (O'Brien et al., 2008). Using the restricted expression of $Na_v1.8$ we identified a contribution of $Na_v1.8$ channels on starburst amacrine cells to the OPs (Smith et al., 2017). Here we found that the OPs were selectively reduced in a nearly identical manner by mp-anti $Na_v1.8$. Lastly, we used a combination of the TTX-r Na_v channel blocker ambroxel and TTX to block all Na_v channels in the retina. Unsurprisingly this led to large reductions in both the dark-adapted b-wave and OPs, which were entirely replicated by a membrane permeable Pan Na_v antibody.

In sum, we have identified a number of ERG components that are selectively reduced by pharmacological Na_v channel blockers. In every case, we were able to selectively reproduce these effects with membrane permeable Na_v channel antibodies. The selectivity for specific components (e.g. the OPs or the b-wave) by antibodies

targeted against TTX-s vs. TTX-r Na_v channels, and the large and reproducible reductions in components suggest that membrane-permeablized antibodies are efficacious and selective blockers of Na_v channel isoforms.

7.5.3 Membrane permeable Na_v channel antibodies against common TTX sensitive Na_v channel isoforms have selective effects on retinal function in vivo and in vitro.

We hypothesized that if Na_v channel isoforms were selectively expressed in cell types underlying components of the ERG then membrane permeable Na_v antibodies against TTX-s Na_v channel isoforms might selectively mimic the effect of TTX on either the b-wave or the OPs. If this was the case the selectivity of different Na_v antibodies would support our proposal that these antibodies were acting to block the function of the desired isoform as well as supplying information regarding the role of the individual isoforms in retinal function. We found that the effects of TTX on the ERG, e.g. a decrease in the b-wave coupled with an increase in the number of OPs, separated neatly by isoform. Membrane permeable anti-Na_v1.1 had little effect on the amplitude of the b-wave but replicated the effect of TTX or the mp-antibody cocktail on the late OPs. Blocking Na_v1.6, either via mp-antibody or 4,9 ah TTX in adult mice reduced the b-wave amplitude and did not significantly increase the late OPs. Finally, blocking Na_v1.2 had only a minor effect on the dark-adapted b-wave amplitude and OPs. As mentioned above only mp-anti Na_v1.6 reduced the light-adapted b-wave.

7.5.4 Common TTX sensitive Na_v channel isoforms contribute in diverse ways to network derived retinal ganglion cell light responses as well as direct optogenetic stimulation.

Our results *in vivo* indicated that membrane permeable antibodies are effective and selective blockers of Na_v channel isoforms. Our secondary aim was to identify broad patterns in the contribution of Na_v channel isoforms to responses of RGCs to network and optogenetic stimulation. In addition, these experiments were designed to obtain additional evidence of the selectivity of antibodies to individual Na_v channel isoforms. We recorded

from neurons in the mouse retinal ganglion cell layer, presumably retinal ganglion cells, although a contribution from displaced spiking amacrine cells cannot be excluded (e.g. (Pérez De Sevilla Müller, Shelley, & Weiler, 2007)). We first grouped cells physiologically based on responses to a full field light stimulus (ON, ON-OFF, OFF). We found that mp-anti $Na_v1.6$ and 4,9 ah TTX cause similar (~60%) reductions in maximal spike rate in response to light in all three cell types. When we stimulated RGCs directly via expression of channelrhodopsin2 under the control of the *Thy-1* promoter we found that the reduction in peak spike rate was ~20% smaller after application of mp-anti $Na_v1.6$. Combined with the *in vivo* effects of mp-anti $Na_v1.6$, 4,9 ah TTX, or genetic elimination of $Na_v1.6$ on the ON bipolar cell contribution to the ERG this suggests that $Na_v1.6$ contributes to presynaptic input to RGCs in both the ON and OFF pathways. These results show that $Na_v1.6$ is an important contributor to excitability both in the presynaptic input to RGCs and postsynatically. Previous results in mouse RGCs (Boiko et al., 2001; 2003; Van Wart & Matthews, 2006a) show the presence of $Na_v1.6$ in the AIS as well as a reduction in the rate of spiking (~30%) in response to current injection in RGCs from juvenile mice (Van Wart & Matthews, 2006a). Our results using optogenetic stimulation of RGCs are also similar to the findings of Van Wart and Matthews (2006a), i.e. approximatively 35-45% reduction in peak spike rate.

Deficits in repetitive firing correlated with very reduced resurgent current in Purkinje cells have been reported by Raman et al., (1997), Aman and Raman (2007), and Grieco and Raman (2004). One key study by Khaliq et al., (2003) combining modeling and electrophysiology studied the functional effects of loss of resurgent current on maintained firing in Purkinje cells. The absence of $Na_v1.6$ cause irregular and relatively slow spontaneous activity (~30% of control rate), reduced maximal (~50% of controls) and repetitive firing (~14% of controls) in response to depolarizing current, and spiking became noticeably more transient at higher current steps ((Khaliq et al., 2003); Fig. 2). This study suggested that resurgent current supported by $Na_v1.6$ is indispensable in supporting high frequency spiking.

In a detailed study of globus pallidus cells, which exhibit sustained high frequency spiking, Mercer et al., (2007) show that significant reductions in resurgent current cause ~50% reduction in maintained spiking, irregularity in spiking, increased

spiking threshold, and an earlier failure to maintain spiking in response to increasing injected current ramps. However maximal spike rate was only reduced by ~25%. Lack of $Na_v1.6$ also causes significant changes in spiking in pyramidal cells (Royeck et al., 2008) reducing evoked spiking by ~50%, delaying the time to first spike and reducing gain. In mesencephalic trigeminal neurons the absence of $Na_v1.6$ causes profound changes in spiking response to depolarizing current (Enomoto et al., 2007). While normal mice have responses to 1 second current steps that are predominately (~65%) sustained over the length of the stimulus $Na_v1.6$ knockout mice have ~30% of cells which respond with a single spike, and ~55% have transient responses. This dramatic shift towards transient responses is also apparent in the number of spikes elicited by depolarizing current with maximal spike number for knockout mice of ~15% of controls. In contrast in cerebellar granule cells where only persistent current is reduced in the absence of $Na_v1.6$ maximal spike rate and maintained firing are normal, however firing did become more irregular (Osorio et al., 2010). In subthalamic nucleus cells despite significant reductions in transient, resurgent and persistent currents both spontaneous spiking and sustained spiking in response to depolarizing current is unchanged (Do & Bean, 2004).

We found that blocking $Na_v1.1$ and $Na_v1.2$ also cause significant reductions in light evoked spiking in the three cell classes we identified. In general, the effects of blocking $Na_v1.2$ on the peak firing frequency in response to the onset of light were quite small (~10% reduction), similar to the small effects we saw on the ERG in the presence of mp-anti $Na_v1.2$. The effects on OFF cells were larger than the effect on the ON cells (~35%) and interestingly we found that in ON-OFF cells the effects on the ON response were quite small, like the effects on ON cells, while the effect on the OFF response was relatively large similar the effect on OFF cells. A differential effect between the ON and OFF responses in the same ON-OFF cell likely indicates a contribution of $Na_v1.2$ to the OFF presynaptic network rather than a direct contribution to spike production at the AIS. This is somewhat surprising considering that Boiko et al., (2003) find that $Na_v1.2$ is co-expressed with $Na_v1.6$ in the axon initial segment and Fjell et al., (1997) found that $Na_v1.2$ is expressed by RGCs. At the same time, early in development when RGCs express predominately $Na_v1.2$ spike rate is lower and RGCs don't spike repetitively (Boiko et al., 2003; G. Y. Wang, Ratto, Bisti, & Chalupa, 1997), suggesting that while

$Na_v1.2$ can support limited spiking it may make a relatively small contribution to the excitability of mature RGCs. As a result of premature mortality, the $Na_v1.2$ knockout mice has limited research into the role of $Na_v1.2$ in neuronal excitability making it impossible to compare our findings directly to others. Here we show for the first time that in the retina $Na_v1.2$ plays a limited but not insignificant role in RGC spiking in response to light, as well as potentially playing a role in the presynaptic OFF pathway.

Consistent with evidence of $Na_v1.1$ expression both in the mouse presynaptic network (AII cells: Kaneko & Watanabe, 2007; Wu et al., 2011) and in RGC axon initial segments (Van Wart et al., 2007) we found that blocking $Na_v1.1$ caused a reduction in peak firing frequency in response to network derived light responses in all three cell classes of between 25 and 35%. When RGCs are stimulated directly via ChR2 the effect on peak spike frequency was smaller, between 10 and 20% for ON and ON-OFF cells, while OFF cells showed no change following $Na_v1.1$ block. This was surprising given the widespread expression of $Na_v1.1$ in RGCs (~85% of RGC axon initial segments Van Wart et al., (2007)). However, it is possible that we missed a subtle effect of $Na_v1.1$ considering the small number of OFF cells we recorded ChR2 driven responses from. In Purkinje cells and GABAergic interneurons maximal spike rate in response to injected current was reduced to a similar extent (~30%: (Kalume et al., 2007; Yu et al., 2006)).

The reduction in effect of $Na_v1.1$ when RGCs are directly stimulated suggests a role for $Na_v1.1$ in excitatory network input to RGCs. As mentioned above we found that the majority of the effect of TTX on the cone driven ERG b-wave was replicated by blocking $Na_v1.6$ while blocking $Na_v1.1$ had no observable effect. However, given the imprecise nature of ERG recordings we cannot eliminate the possibility of $Na_v1.1$ contributing to ON CBC function. Given that we recorded from dark adapted retinas in combination with the robust evidence for $Na_v1.1$ expression in AII amacrine cells presynaptic effects on AII amacrine cells are likely to contribute to the reduction in peak firing rate in ON RGCs and may have reduced the effects on OFF RGCs by reducing glycinergic inhibition derived from AII cells. However, OFF alpha ganglion cells also receive excitatory input from the vesicular glutamate receptor 3 positive cells (Lee, Zhang, Chen, & Zhou, 2016), which have Na_v channels (Grimes, Seal, Oesch, Edwards, & Diamond, 2011).

7.5.5 $Na_v1.1$ but not $Na_v1.6$ or $Na_v1.2$ plays a role in sustained firing in response to prolonged light.

Both $Na_v1.6$ and $Na_v1.1$ knockout mice show deficits in sustained firing in some neuronal subtypes and under some circumstances ($Na_v1.1$: (Kalume et al., 2007; Ogiwara et al., 2007; Yu et al., 2006); $Na_v1.6$: (Khaliq et al., 2003; Raman et al., 1997; Van Wart & Matthews, 2006b)). In retinal ganglion cells although sustained firing in response to moderate depolarizing current steps is supported in the absence of $Na_v1.6$ at maximum instantaneous spike frequency $Na_v1.6$ deficient RGCs failed to spike over the length of the stimulus more often than controls (Van Wart & Matthews, 2006b). In $Na_v1.1$ knockout mice recordings from other neuronal subtypes (Kalume et al., 2007; Ogiwara et al., 2007; Yu et al., 2006) show both reduced peak spike frequency in combination with sustained spiking in response to intermediate depolarizing current and transient spiking in response to increased depolarizing current (Yu et al., 2006). The spiking response to depolarizing current in Purkinje cells of $Na_v1.1$ knockout mice is reduced by ~30% relative to controls (Kalume et al., 2007), however the effect of eliminating $Na_v1.1$ on repetitive spiking was not tested. In neocortical interneurons spiking responses from heterozygous mice show deficits in repetitive firing in response to depolarizing current (Ogiwara et al., 2007). However, the role of $Na_v1.1$ in RGC spiking, and the response of neurons to natural, as opposed to electrical, stimuli in the absence of $Na_v1.1$ has not been tested.

We found that in ON and ON-OFF cells with sustained light responses blocking $Na_v1.1$ but not $Na_v1.2$ or $Na_v1.6$ caused a reduction in sustained spiking, particularly in response to network input. Direct stimulation of RGCs with sustained light responses with ChR2 caused smaller reductions in sustained spiking with $Na_v1.1$ relative to $Na_v1.6$, however in some cases cells with sustained light responses had transient channelrhodopsin responses (e.g. (Thyagarajan et al., 2010)), reducing the overall sustained nature of the channelrhodopsin driven responses. These results suggest segregated roles of $Na_v1.6$ and $Na_v1.1$ to overall spike rate and sustained spiking

respectively in retinal ganglion cells and a more detailed investigation into this is currently under way.

7.6 Conclusion

Expression of Na_v channel isoforms may create intrinsic differences between cells' subtypes leading to varying properties in the parallel pathways through the retina. Differences in intrinsic properties between cell subtypes driven by the expression of a single Na_v channel isoform can be seen in monkey cone bipolar cells bipolar cells (Puthussery et al., 2014). On the other hand, cells might have an essential complement of Na_v channel isoforms with differences in relative expression levels or overall expression, meaning that the ratio of Na_v channel isoforms would remain the same but the overall Na_v current would increase in cells with higher spike rates.

We found that different cell types (ON bipolar vs RGCs) employ each of these strategies. We found that the amplitude of the light adapted b-wave was decreased after blocking $Na_v1.6$ but not $Na_v1.1$ or 1.2 suggesting that in mice ON cone bipolar cells augment light responses with a single Na_v channel isoform, albeit $Na_v1.6$ rather than $Na_v1.1$. In RGCs however we found similar effects in our broadly defined RGC cell types following block with mp- anti $Na_v1.6$, $Na_v1.2$, and $Na_v1.1$ showing that three broadly defined classes of RGCs express Na_v channel isoforms in generally similar ratios. These results show that on average most RGCs have both $Na_v1.1$ and 1.6 channels with $Na_v1.6$ playing a stronger role in maximal firing rate and less in repetitive firing leading to sustained responses. $Na_v1.1$ plays a stronger role in repetitive firing in sustained type cells and has less effect on the maximal firing rate. However, these broad conclusions clearly require further work into the precise function of individual Na_v channel isoform in more rigorously defined RGC types.

Table 7.1. Percent change in b-wave and oscillatory potential amplitude under various conditions targeting individual Na_v channel isoforms. Data from normalized dark-adapted b-waves, cone dark-adapted (second response of paired flash) and light-

adapted cone responses are presented. The summed oscillatory potentials were extracted from the dark-adapted b-waves. Mean (μV) ± SEM.

Treatment		Normalized b-wave amp			Paired flash	Photopic (1.0)	Summed OPs			
		R	Rci	Cri			(1-4)		(3-5)	
							Rci	Cri	Rci	Cri
mp-anti $Na_v1.6$		62.1 ±4.2	72.3 ±2.1	69.5 ±1.8	65.7 ±5.2	65.7 ±3.0	92.8 ±4.2	74.0 ±4.2	1.14 ±11.2	88.6 ±5.2
4,9 ahTTX		47.3 ±5.1	70.3 ±3.3	70.9 ±2.2	70.4 ±3.4	64.8 ±4.5	63.1 ±6.5	61.8 ±5.9	125.2 ±28.0	122.8 ±20.3
$Scn8a^{dmu}$		65.9 ±1.2	67.6 ±2.6	83.0 ±2.4	---	68.4 ±6.6	62.8 ±6.3	55.2 ±3.0	79.9 ±10.3	68.8 ±4.0
Normalized to TTX	4,9 ahTTX	72.9 ±10.0	104.9 ±6.2	109.9 ±4.5	128.9 ±9.2	98.3 ±8.4	---	---	---	---
	mp-anti $Na_v1.6$	66.1 ±5.5	108 ±5.4	104.8 ±3.2	129.0 ±5.6	109.6 ±6.2	---	---	---	---
	$Scn8a^{dmu}$	86.9 ±4.8	105.0 ±5.1	119.5 ±4.2	---	108.9 ±10.5	---	---	---	---
Cocktail		57.3 ±2.9	52.8 ±1.7	59.0 ±1.3	---	---	---	---	170.1 ±17.3	160.3 ±6.9
TTX							102.9 ±9.4	97.3 ±3.1	214.5 ±29.6	176.6 ±12.0
mp-anti $Na_v1.1$		94.9 ±12.7	86.4 ±2.8	90.3 ±2.4	1.17 ±9.2	1.05 ±6.1			136.3 ±24.4	130.4 ±3.6
mp-anti $Na_v1.2$		79.5 ±2.8	87.7 ±3.2	91.4 ±4.0	---	1.07 ±10.2	117.0 ±37.3	116.9 ±24.6	86.7 ±33.6	90.7 ±18.6
Anti-pan		80.0 ±15.1	58.5 ±2.1	64.6 ±1.6	---	---	39.4 ±7.9	43.0 ±5.6	44.8 ±12.3	48.6 ±6.7
Ambroxol+TTX		48.7 ±3.3	58.5 ±3.1	66.9 ±2.3	---	---	45.5 ±2.4	42.6 ±2.1	76.3 ±8.1	75.2 ±7.9
$Na_v1.8$		90.4 ±7.9	103.2 ±4.2	103.0 ±3.9	---	---	50.0 ±8.0	66.8 ±5.9	60.5 ±7.5	79.5 ±4.6
A803467					---	---	49.2 ±3.8	69.5 ±2.7		

Table 7.2. Percent change in retinal ganglion cell maximal spike rate (Hz) following $Na_v1.6$ block. Retinal ganglion cells are segregated into ON, ON-OFF, and OFF types driven by network light responses and optogenetic stimulation. Mean ± SEM.

Cell Type	Response measured	N	mp-anti $Na_v1.6$	*p*	N	ChR2 mp-anti $Na_v1.6$	*p*	N	4,9-ahTTX	*p*
ON	ON Peak	68	35.4 ± 3.7	<0.001	38	56.4 ± 1.2	<0.001	94	38.2 ± 3.8	<0.001
ON-OFF	ON Peak	61	34.8 ± 3.5	<0.001	44	57.7 ± 5.9	<0.01	84	44.1± 5.1	<0.001
	OFF Peak		29.6 ± 3.1	<0.001		--------	--------		44.0 ± 5.2	<0.001
OFF	OFF Peak	18	28.2 ± 7.3	<0.001	13	63.3 ± 9.0	<0.01	37	41.6 ± 6.5	<0.001

Table 7.3. Percent change in retinal ganglion cell maximal and sustained spike rate (Hz) following mp-anti Na_v 1.1, Na_v 1.2 and Na_v1.6 treatment in sustained cells driven by network light responses and optogenetic stimulation. Sustained responses are the summed over the last 900 ms of this response (Fig 7 C,D). The sustained/transient index (STI e.g Zhang et al., 2015) by normalizing the average spike count of the second 200 ms of the light response to the first 200 ms.

Cell Type		mp-anti Na_v1.1			mp-anti Na_v1.2			mp-anti Na_v1.6		
		N	Average	*p*	N	Average	*p*	N	Average	*p*
ON	Peak	28	63.0 ±5.9	<0.001	7	97.2 ±15.1	n.s	20	39.2 ± 7.6	<0.001
	Sustained		61.4 ±65.8	<0.001		81.4 ±17.2	n.s		71.1 ±33.2	n.s.
	STI		52.2 ±10.9	<0.001		108.4 ±31.9	n.s		106.8 ±19.1	n.s.
ON ChR2	Peak	50	84.8 ± 7.4	<0.001	--	---------	-----	12	58.5 ± 8.9	<0.001
	Sustained		74.1 ±12.1	<0.001					74.1 ±18.3	n.s.
	STI		66.7 ±4.9	<0.001		---------	-----		73.1 ±9.2	n.s.
ON-OFF	ON-Peak	12	74.6 ±9.0	<0.001	5	78.8 ±29.7	n.s	29	40.5 ± 5.9	<0.001
	ON-Sustained		1.4 ±52.2	<0.001		121.6 ±84.1	n.s		162.9 ±44.4	<0.005
	STI		54.2 ±6.4	<0.001		120.8 ±28.4	n.s		120.3 ±14.2	n.s.
ON-OFF ChR2	Peak	21	91.9 ±7.7	n.s.	--	---------	-----	13	62.5 ± 12.1	<0.05
	Sustained		72.3 ±8.1	<0.001					85.1 ± 13.2	n.s.
	STI		63.8 ±4.9	<0.001		---------	-----		71. 0 ± 9.5	<0.001

Table 7.4. Percent change in retinal ganglion cell maximal spike rate (Hz) following mp-anti $Na_v1.1$ and mp-anti $Na_v1.2$ block. Responses were driven by network light responses and optogenetic stimulation.

		mp-anti $Na_v1.1$			ChR2 mp-anti $Na_v1.1$			mp-anti $Na_v1.2$		
Cell Type	Response measured	N	average	p	N	average	p	N	average	p
ON	Peak	91	66.0±4.4	<0.001	76	82. 0± 6.1	<0.01	57	88.4±6.2	<0.05
ON-OFF	ON Peak	24	76.0±6.4	<0.001	39	90.3±7.0	<0.05	41	89.2±6.3	<0.05
	OFF Peak		58.9±10.2	<0.001					72.9±6.4	<0.05
OFF	OFF Peak	12	67.1 ± 16.2	<0.01	7	107.6 ±17.0	n.s.	14	65.1 ± 15.2	<0.005

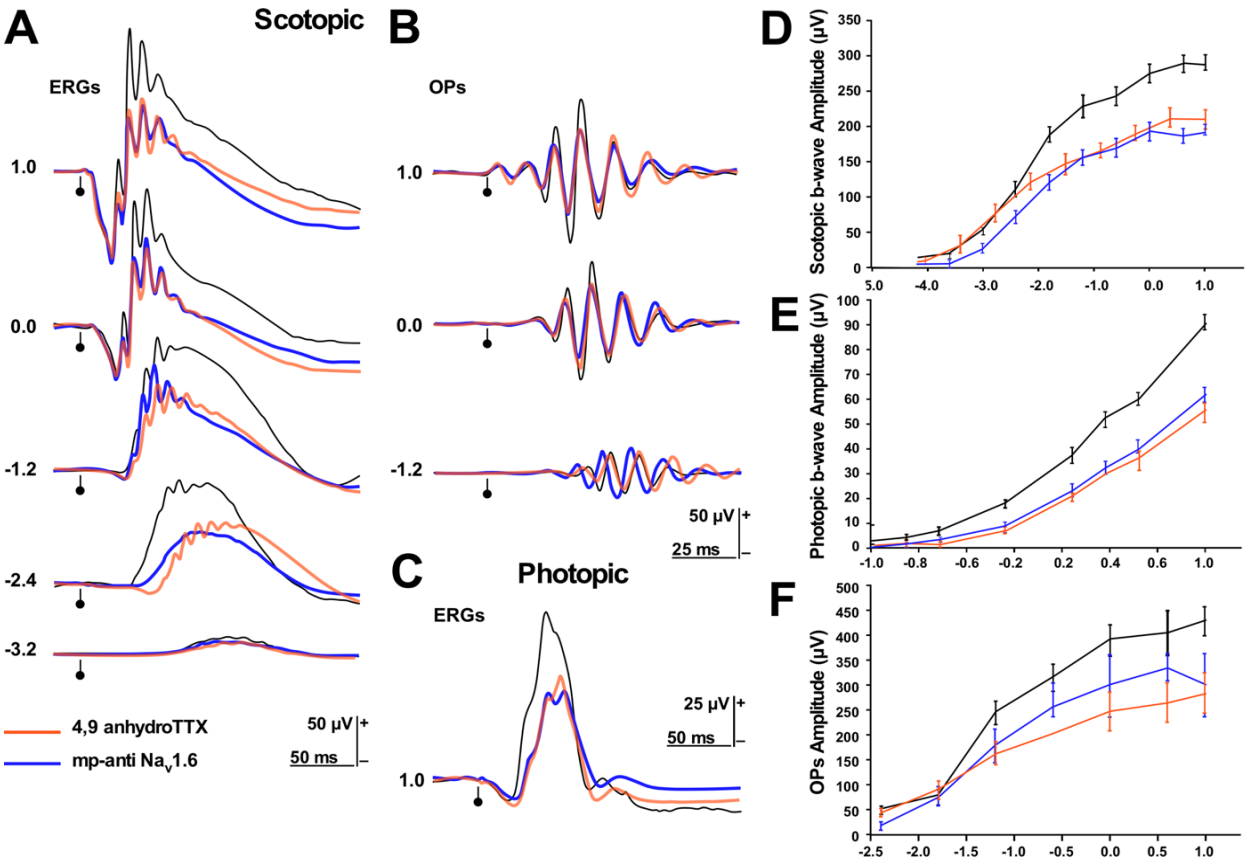

Figure 7.1: Comparing effects of a small molecule blocker and membrane-permeable antibody targeted to Na$_V$1.6 using the ERG. A) Intensity series of full-bandwidth ERG, isolated OPs (B), and photopic ERGs (C) from recordings of 4,9 anhydro TTX (orange) and mp-anti Na$_V$1.6 injected eyes (blue) compared to controls (black). D) b-wave amplitude in dark and (E) photopic conditions. (E) Summed OPs amplitude.in dark adapted conditions Calibration as indicated. Flash intensities as indicated in log cd s m^{-2}. Markers indicate stimulus onset.

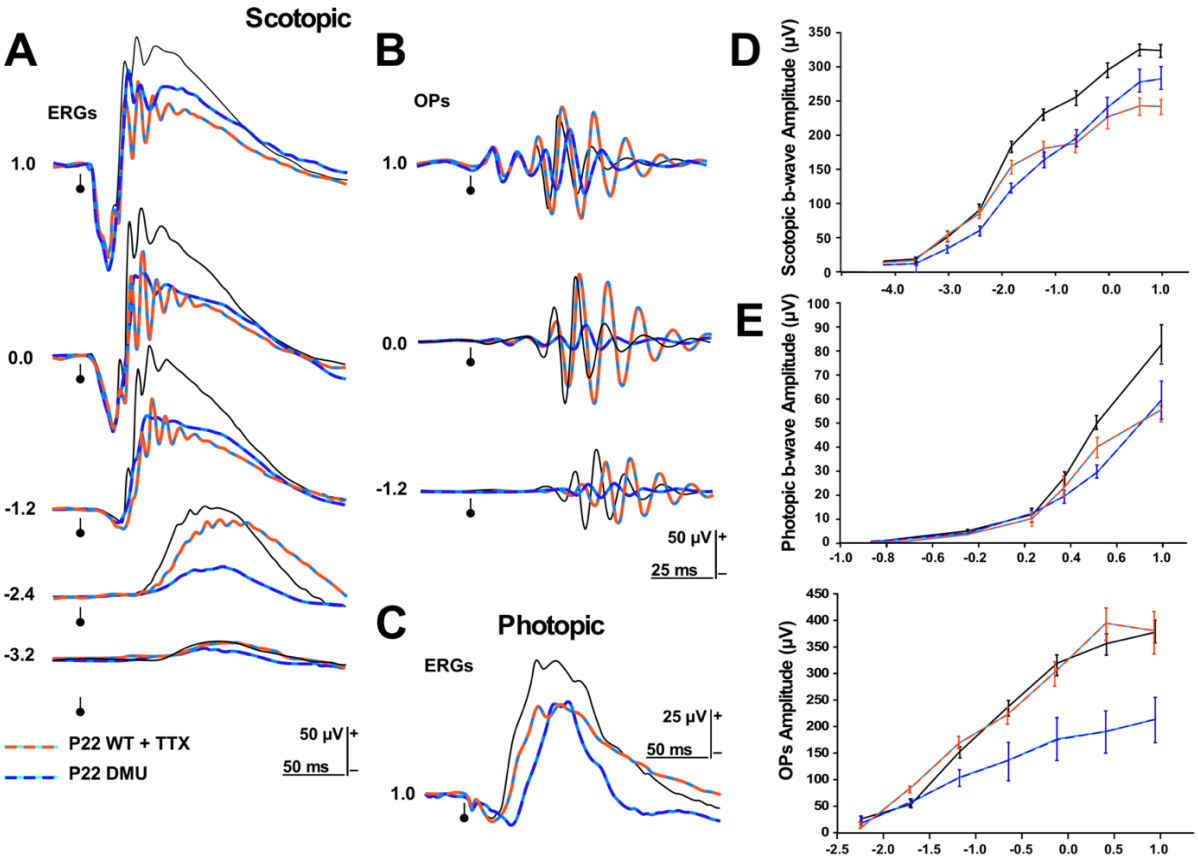

Figure 7.2: $Na_v1.6$ contributions to the ERG assessed using genetic knockout at P22-25. A) Intensity series of full-bandwidth ERG, isolated OPs (B), and photopic ERGs (C) from recordings in *Scn8a*^{dmu} mice at P22-25 (blue) and age matched TTX (orange/blue) injected eyes compared to controls (black). D) b-wave amplitude in dark and (E) photopic conditions. Calibration as indicated. Flash intensities as indicated in log cd s m^{-2}. Markers indicate stimulus onset.

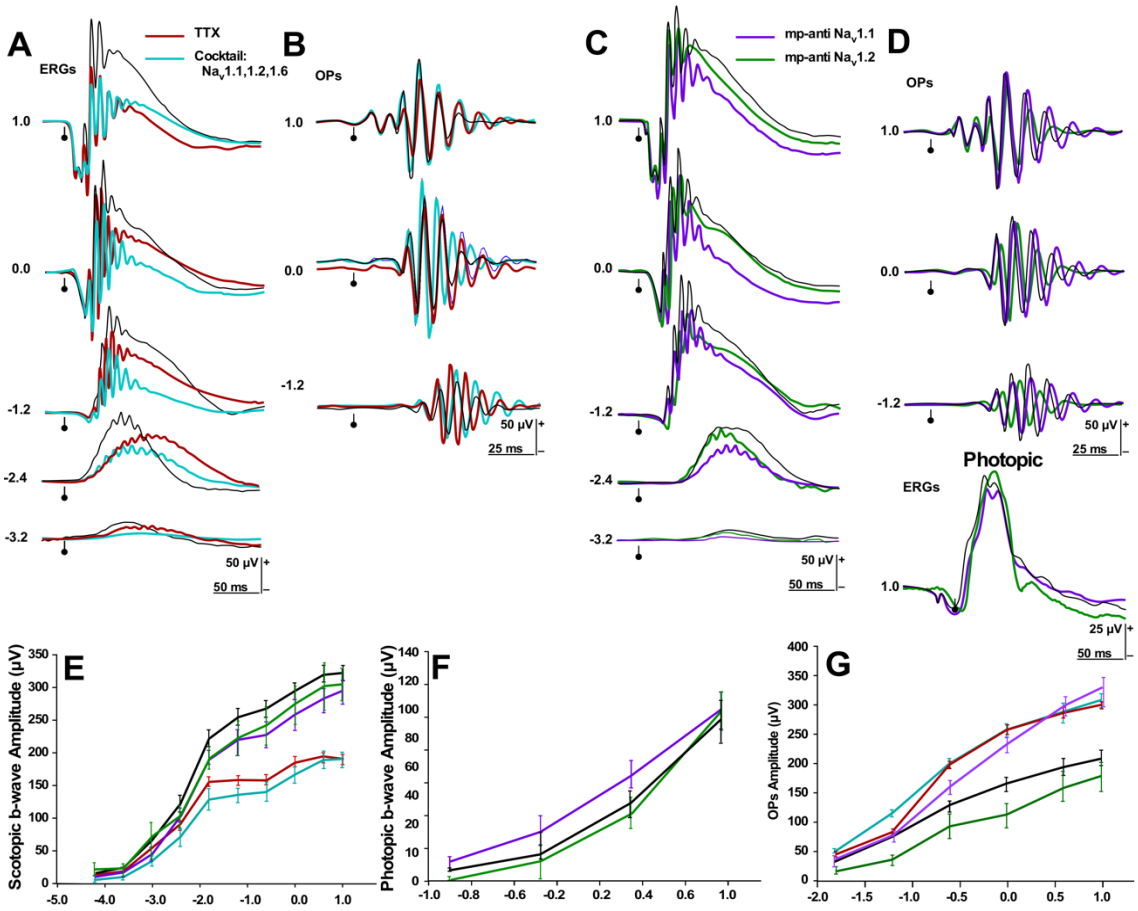

Figure 7.3: TTX-sensitive Na_v channel isoform ($Na_v1.1$, $Na_v1.2$, and $Na_v1.6$) contributions to the ERG assessed using membrane-permeable antibodies. A) A) Intensity series of full-bandwidth ERG, and isolated OPs (B), from recordings of eyes injected with TTX (red) or a cocktail of mp-antibodies to $Na_v1.1$, $Na_v1.2$, and $Na_v1.6$ injected eyes (light blue) compared to controls (black). C) Intensity series of full-bandwidth ERG, isolated OPs (D), and photopic ERGs from recordings of mp-anti $Na_v1.1$ (purple), and mp-anti $Na_v1.2$ (green) injected eyes compared to controls (black). E) b-wave amplitude in dark and (F) photopic conditions. F) summed OP amplitudes in dark adapted conditions. Calibration as indicated. Flash intensities as indicated in log cd s m^{-2}. Markers indicate stimulus onset.

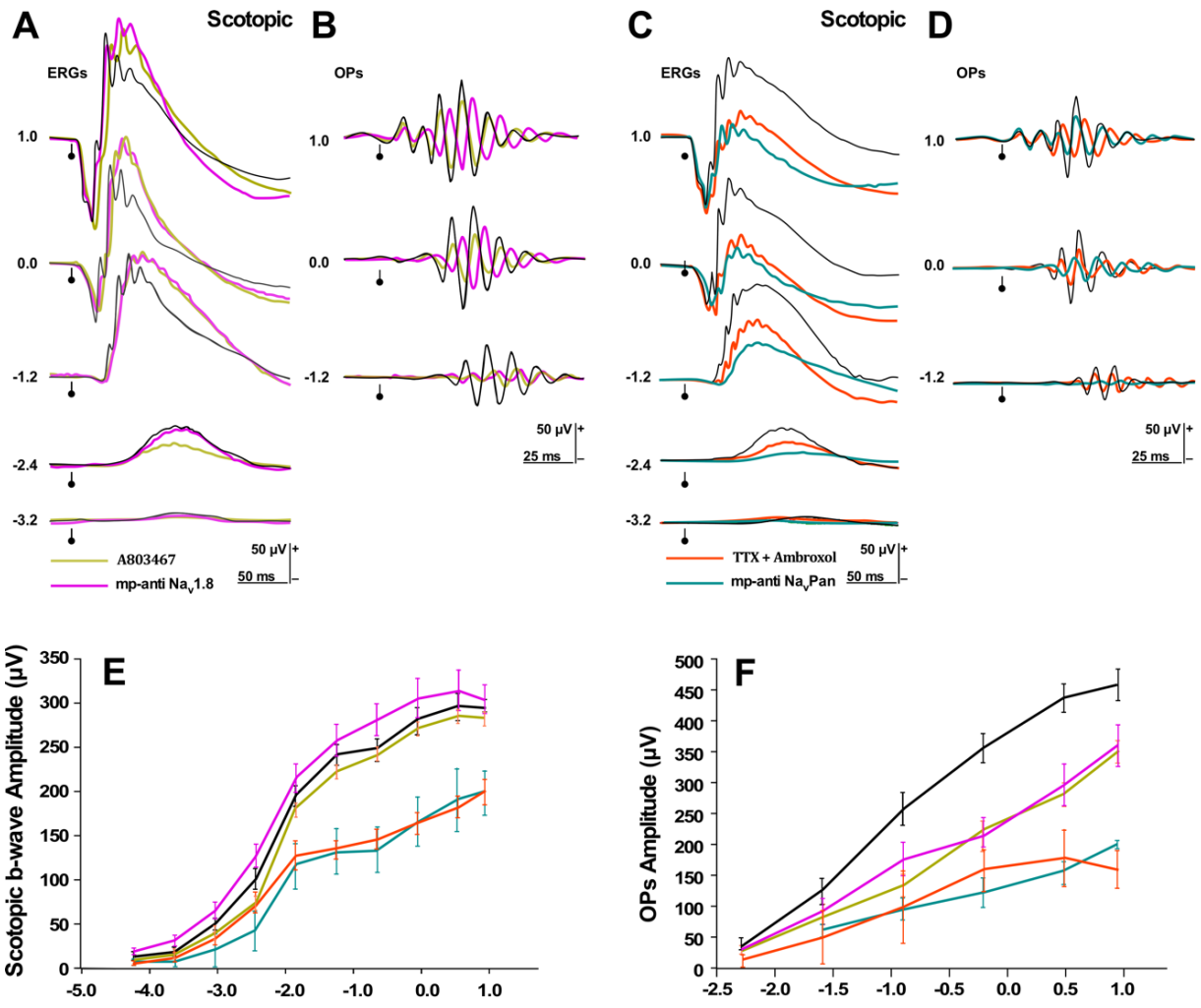

Figure 7.4: **TTX-resistant Na$_v$ channel isoform (Na$_v$1.8) contributions to the ERG assessed using membrane-permeable antibody and specific channel blocker A803467, and comparison of the mp-anti Pan Na$_v$ with a combination of TTX and Ambroxol.** A) Intensity series of full-bandwidth ERG, isolated OPs (B), from recordings of A803467 (pink) and mp-anti Na$_v$1.8 injected eyes (olive) compared to controls (black). C) Intensity series of full-bandwidth ERG, isolated OPs (D), from recordings of TTX + Ambroxol (orange) and mp-anti Pan Na$_v$ injected eyes (teal) compared to controls (black). E) B-wave amplitude in dark and F) summed OP amplitudes in dark adapted conditions. Calibration as indicated. Flash intensities as indicated in log cd s m^{-2}. Markers indicate stimulus onset.

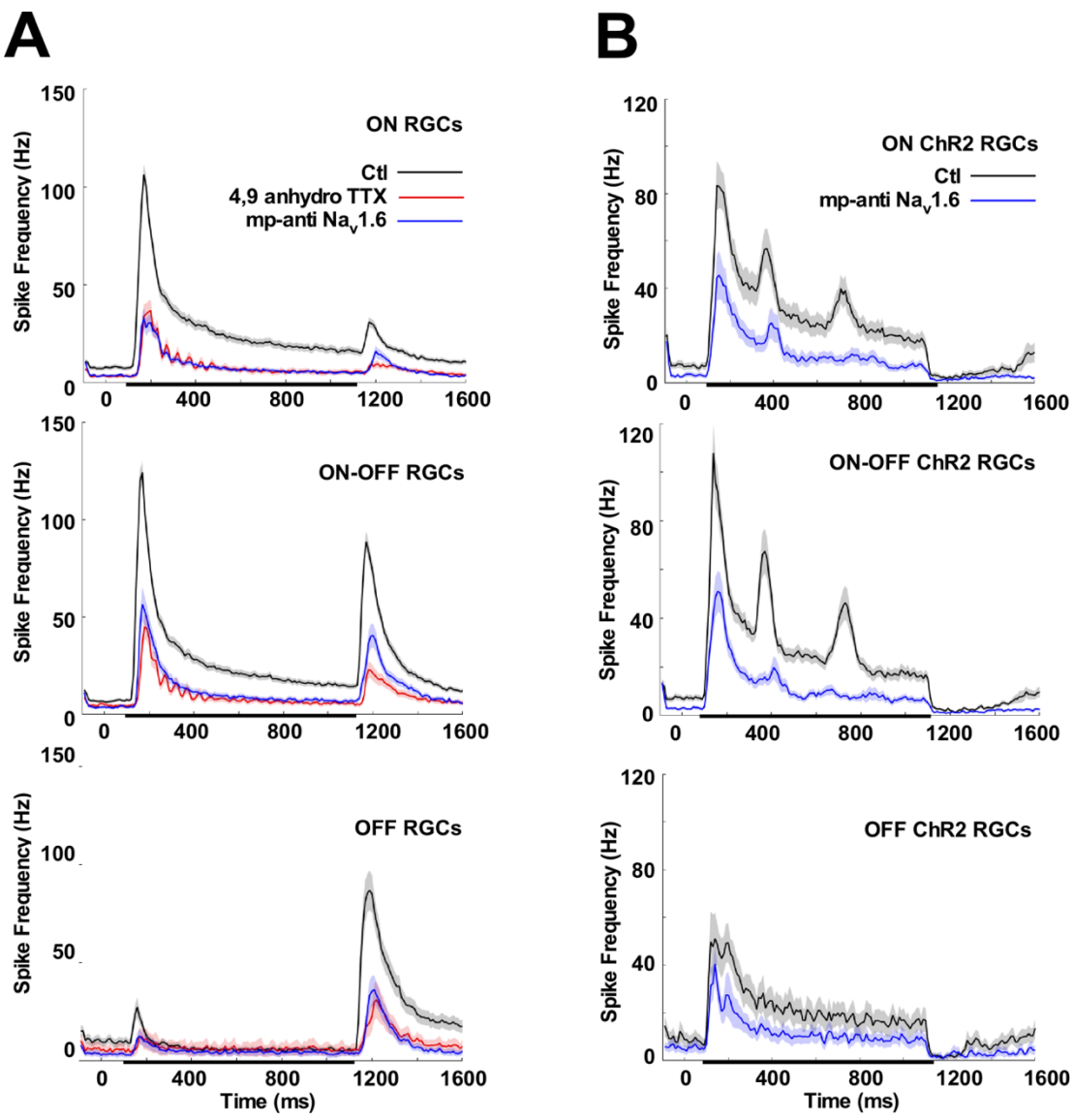

Figure 7.5: **Comparison of the effect of 4,9 anhydro TTX and mp-anti $Na_v1.6$ on ganglion cell spiking in response to network vs. optogenetically driven light responses.**

A) Effects of 4,9 anhydro TTX (orange) and mp-anti $Na_v1.6$ (blue) contrasted with control (black) light responses in normal and (B) Optogentically driven responses from *Thy1*-ChR2 mouse retinal ganglion cells treated with a cocktail of synaptic blockers (CNQX 50 µM , 200µM AP-7, 500 µM AP-4, TPMPA 150 µM, Gabazine 200µM, strychnine 50µM). Post Stimulus Time Histograms are single cell averages (thick line) and SEM (corresponding shaded area) regrouped according to their full-field flash (thick black line on x axis; 1000 ms, 830nm LED) responses. Optogenetic responses were grouped according to their response to network derived light responses.

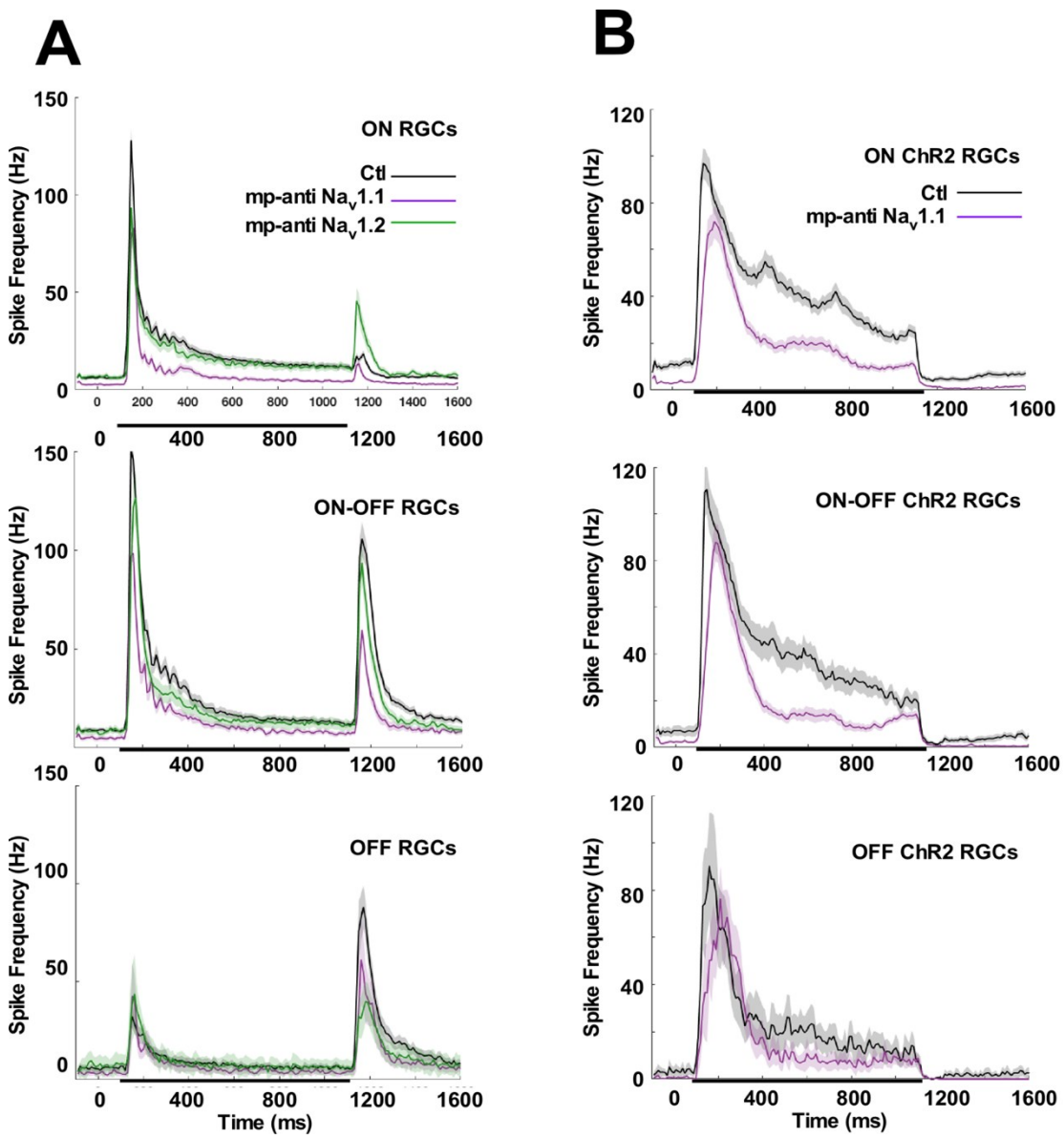

Figure 7.6: Comparison of the effect of mp-anti $Na_v1.1$ and Na_v 1.2 on retinal ganglion cells responses, regrouped according to their full-flash responses into predominantly ON, ON-OFF and predominantly OFF cells.
A) Effects mp-anti $Na_v1.1$ (purple) and mp-anti $Na_v1.2$ (green) contrasted with control (black) light responses in normal and (B) Optogentically driven responses from *Thy1*-ChR2 mouse retinal ganglion cells treated with a cocktail of synaptic blockers (CNQX 50 µM, 200µM AP-7, 500 µM AP-4, TPMPA 150 µM, Gabazine 200µM, strychnine 50µM). Post Stimulus Time Histograms are single cell averages (thick line) and SEM (corresponding shaded area) regrouped according to their full-field flash (thick black line on x axis; 1000 ms, 830nm LED) responses. Optogenetic responses were grouped according to their response to network derived light responses.

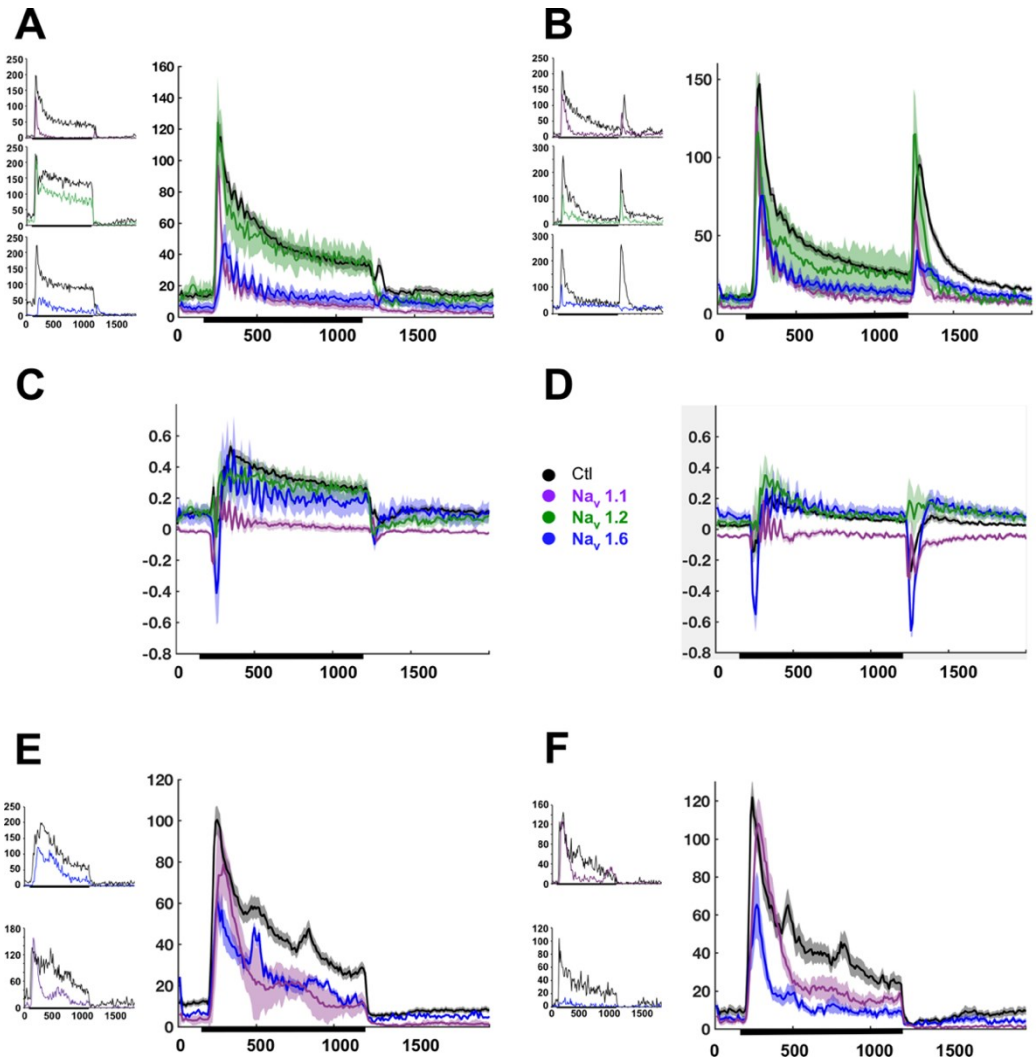

Figure 7.7: Blocking $Na_v1.1$ but not $Na_v1.6$ or $Na_v1.2$ makes sustained RGC light responses more transient.

Cells with high STI index were selected and the effect of mp-anti $Na_v1.1$ (purple), mp-anti $Na_v1.2$ (green) mp-anti $Na_v1.6$ (blue) contrasted with control (black) for ON (A) and ON-OFF (B) cells. Post Stimulus Time Histograms are MEA single cell averages (thick line) and SEM (corresponding shaded area). with inset examples from single cells. C) The isolated normalized sustained component of light responses from (A) derived by subtracting the average light response of ON transient cells from each ON sustained cell D) Sustained component of ON-OFF cells from (B). E) Optogentically driven responses from retinal ganglion cells with network derived sustained ON light responses from *Thy1*-ChR2 mouse in treated with a cocktail of synaptic blockers (CNQX 50 µM , 200µM AP-7, 500 µM AP-4, TPMPA 150 µM, Gabazine 200µM, strychnine 50µM) before and after treatment with mp-anti $Na_v1.1$ (purple) or mp-anti $Na_v1.2$ (green). D) Optogenetically driven responses from ON-OFF sustained cells.

CHAPTER 8: DISCUSSION

8.1 What can studying Na_v channel isoforms reveal about retinal development and function?

The underlying questions propelling the work presented in this thesis are threefold, originating with an ongoing problem studied in Dr. Coté's laboratory where it was found that mice lacking $Na_v1.6$ had profound deficits in photoreceptor function (Cote et al., 2005). While this was my primary project, the selective expression of Na_v channels in retinal neurons suggested that Na_v channels might be a key in understanding the neural circuitry underlying the ERG, in particular, the poorly understood oscillatory potentials. In addition, the precise spatial and temporal localization of Na_v channel isoforms, including $Na_v1.6$, in the nervous systems suggested that Na_v channels might play an important role in the intrinsic neuronal properties that translate an analog input to the retinal ganglion cells into a binary neural code for transmission along the optic nerve.

8.1.1 What might the link between $Na_v1.6$ and photoreceptor function be?

TTX administered intravitreally in adult rats (Bui and Fortune 2004; Mojumder et al., 2007; 2008), rabbits (Dong and Hare 2000), and both adult and juvenile mice (P.D. Côté unpublished observations; Smith and Côté 2012; Smith et al., 2013), thereby blocking Na_v channel function acutely, including Na_v 1.6 did not affect photoreceptor function. Although there is some evidence for Na_v channels in the distal retina (e.g. Mojumder et al., 2007), clearly an unusual mechanism or more prosaically some global health defect was responsible for the strong reduction in photoreceptor function in these mice.

8.1.2 What neural circuitry drives the generation of the OPs?

While the principle generators of the low frequency a- and b-waves have been known for some time (Frishman and Wang, 2011) beyond some very general predictions involving inhibition between the amacrine cells and bipolar or retinal ganglion cells the neural circuits underlying the OPs were completely unknown (e.g. Wachtmeister, 1998).

While studying $Na_v1.6$ knockout mice and the effects of TTX on the mouse electroretinogram I noticed specific changes in the OPs, which suggested the possibility that targeting specific Na_v channel isoforms could reveal the circuitry underlying the OPs. Because of the limited expression of some Na_v channel isoforms blocking these could suggest the underlying circuitry involved in the OPs.

8.1.3 Are Na_v channel subtypes a key component of intrinsic differences in how neurons translate input into a spike based code?

When studied in single cell preparations, the various Na_v channel isoforms control relatively small differences in physiological membrane potential dynamics. Yet the precise localization of individual Na_v channel isoforms on multiple spatial scales, from a polarized gradient in the axon initial segment to isoform differences between the peripheral and central nervous systems, led us to consider the proposition that individual isoforms play a critical role in determining electrogenesis and transmission of encoded information in the nervous system. This isoform specific localization could be a key to beginning to understand the molecular basis of the neural code. We thus started to study how the various Na_v isoform would influence the neural code, in the form of spiking activity, in the retinal ganglion cells. The RGCs, being the most downstream cells of the retina, are responsible for integrating the retinal processing of visual stimuli and encoding that information for transmission to central integration.

This thesis contains at least a partial answer to each of these three questions. Ongoing work described below, in combination with the results contained herein will demonstrate that the first two questions are close to a solution. Although the third question, which refers to the molecular basis of neural encoding and the role of Na_v channel isoforms in electrogenesis, is far from being conclusively answered, the topic is addressed in an innovative manner. With respect to Na_v channels in the retina, I have proposed a practical method for the acute block of common CNS Na_v channel isoforms and used this antibody-based methodology to begin to isolate contributions of four Na_v channel isoforms to full field light responses.

8.2 TTX sensitive Na_v channels contribute to both dark- and light-adapted ERGs in mice and rats.

I started by identifying the contribution of Na_v channels to the mouse and rat ERGs (Smith et al., 2013, CHAPTER 2). This work laid the groundwork for all additional work on Na_v channel function in the mouse retina. Surprisingly, we obtained results differing from previous work in rat (Mojumder et al., 2007, 2008, Bui and Fortune 2004) and were able to explain this divergence by demonstrating that TTX concentrations that were sufficient to eliminate retinal output caused a reduction in the dark-adapted b-wave that could be attributed principally to GABA release onto $GABA_cRs$. Na_v channel dependent GABA release onto rod bipolar cell axon terminals has been demonstrated *in vivo* by Chavez et al., (2010) and blocking $GABA_cRs$ has been conclusively demonstrated to reduce the dark adapted b-wave (e.g. Herrmann et al., 2011; Smith et al., 2015) so these results were consistent with known retinal circuitry. In addition, I confirmed previous findings indicating that Na_v channels reduce the cone driven b-wave in both dark and light adapted conditions. Essentially isolating the cone to ON cone bipolar circuit by blocking ionotropic glutamate receptors suggested that in the cone pathway Na_v channels are located on ON cone bipolar cells rather than modulating GABAergic inhibition.

8.3 Roles of Na_v channels in daily variation in ON cone bipolar cell light responses.

While pursuing this project I found serendipitously that when ERGs were recorded from the cone pathway in the middle of the night TTX had little effect on the amplitude of the b-wave (CHAPTER 3). At the same time, I noticed a pattern in ERG recordings in rats and mice showing that Na_v channels contribute to the amplitude of the cone driven b-wave even when the retina is fully light adapted (e.g. Smith et al., 2013; Mojumder et al., 2007, 2008, Bui and Fortune 2004). This pattern was, in contrast to the work of Ichinose and Lukasiewicz (2007), showing that dopamine released in response to light adaptation suppresses Na_v currents on ON cone bipolar cells via D1Rs in the salamander. These results from the Lukasiewicz lab described an interesting form of gain control in which Na_v channels in the cone pathway essentially acted like amplifiers under

the control of ambient light. Using this paper as a guide I repeated similar experiments showing that while D1Rs indeed controlled Na_v channels on ON cone bipolar cells, light adaptation unexpectedly did not reduce the contribution of Na_v channels. In combination with the initial findings that TTX has little effect at midnight these results suggested that daily rhythms in dopamine control Na_v currents to reduce gain in response to light adaptation at midnight but not midday. This was counterintuitive given the accepted pattern of circadian release of dopamine release is higher at midday. However, a recent report in mice found that dopamine release driven by 90 minutes of light adaptation is significantly higher at CT18 (circadian night) than CT6 (circadian day) in mice (Cameron et al., 2009). Although speculative, this work as well as an additional project investigating the different roles of A17 cells in mice and rabbits, was pursued based on the hypothesis that existing retinal circuitry evolves to support the needs of species adapted to ecological niches with different constraints (e.g. Ding et al., 2016).

8.4 Na_v-dependent photoreceptor modulation by retroaxonal feedback

Next, I continued the investigation of retinal function in the $Na_v1.6$-null *Scn8a*^{dmu} mutant mice initiated by Côté et al., (2005) and continued in Smith and Côté (2012). Surprisingly I found that as the global health of the mice deteriorated, close to their typical early mortality around P25, the ERG a-wave and thus photoreceptor function could be seen to progressively improve (CHAPTER 4). This finding suggested that a global health defect could not be responsible for the reduced photoreceptor function at P16, an important consideration given the substantial reduction in photoreceptor function in global TrkB knockout mice relative to the smaller but still significant reduction seen in these mice.

Long-range spread of retrograde signals from postsynaptic neurons leading to changes in excitability of presynaptic cells has been demonstrated in culture cells (Ganguly et al., 2001; Li et al., 2004). Studies on developing retinotectal circuit have shown that there is long-range rapid retrograde feedback from the output synapses of the retinal ganglion cells (RGC) in the optic tectum to their input synapses from the bipolar cells (Du and Poo, 2004; Du et al., 2009). This feedback requires axonal transport in the

optic nerve and both retinal and tectal neurotrophin receptor TrkB expression (Du et al., 2009). This work suggests an even stronger effect in developing mouse retina reaching to the photoreceptors. In addition TrkB feedback to the photoreceptors may explain via a completely different mechanism the increase in RGC EPSCs in reported in Du and Poo (2004) and Du et al., (2009).

My work here showed that the effects of retroaxonal feedback on photoreceptor function are much stronger at P16 then at P22, however there is still about a 20% reduction at P22-25. Interestingly two side projects also showed a transient reduction in photoreceptor function in adult mice correlated with optic nerve damage. While photoreceptor function is normal 8-12 weeks after optic nerve transection (Smith et al., 2014a) at short periods after transection (12 hours-3 days) there is a transient reduction in the a-wave. The EAE mouse model of multiple sclerosis, that has significant optic neuritis, also has a reduced a-wave. Consistent with these results, work in rat (Gargini et al. 2004) has shown a short term (1-3 week) suppression of the a-wave post transection associated with upregulation of CNTF, which is known to suppress photoreceptor function (e.g. Liang et al., 2001; Zein et al., 2014). Preliminary results showed that in adults retrobulbar injection of TTX, EAE, and short term optic nerve transection had a similar effect to at P22-25 (~20% reduction in a-wave amplitude).

The ERG is arguably the best method for investigating changes in photoreceptor function in the presence of the intact retinogeniculate circuit despite the fact that the ERG is a composite waveform. Manipulations of the adult retina are easier that those of juvenile mice, thus the existence of a retroaxonal feedback mechanism in the adult retina, albeit with a substantially smaller effect, will provide a more tractable model for elucidating this circuitry. Already these results, both in juveniles and adults, show a surprisingly extensive feedback mechanism from the brain to the first steps of visual transduction in retina. Furthermore, the reduction in the a-wave following optic nerve transection or sodium channel blockade may be an early but transient indicator of degeneration in the retinal ganglion cells and optic nerve.

8.5 Specific roles of Na_v isoforms in signal processing

The third question guiding my thesis work, understanding the molecular underpinnings of the neural code and the roles of individual Na_v channel isoforms in the electrogenisis of excitable cells (CHAPTERS 5 and 6), ended up being a formidable challenge. Initially I proposed to study the effects of $Na_v1.6$ deletion in *Scn8a*^{dmu} mutant mice specifically on the light responses both of bipolar cells using the ERG, and RGCs using the MEA. In the *Scn8a*^{dmu} line the effects on photoreceptors in combination with early mortality made sorting out effects on downstream neurons from the effects of reduced light sensitivity of photoreceptors nearly impossible in theory (in fact as reported in chapter 4 the reduced photoreceptor function in P16 mice nearly disappears *in vitro* a fact learned long after alternative approaches were successful), so we created a retinal specific knockout of $Na_v1.6$. This project eventually ended when it became obvious that the slow production of the knockout mice precluded enough physiological recordings to reach a meaningful conclusion. The possibility of using intracellularly delivered antibodies in the retina was raised by an interesting paper from Raz-Prag et al., (2011) where potassium channels are targeted with antibodies against their intracellular epitopes. and the literature showed examples of subtype specific Na_v channel block using antibodies directed to extracellular epitopes (e.g Meiri et al., 1987). By using antibodies obtained from the NeuroMab repository, I attempted to use the method from Raz-Prag et al. (2011) to specifically target Na_v isoforms. Early results using mixed cocktails of antibodies against retinal TTX sensitive Na_v channel isoforms were promising, showing effects on the b-wave of the ERG that approached those of TTX.

Novel subtype specific blockers of some Na_v channels, particularly $Na_v1.8$, became commercially available around this time and so an early effort was made using A803467 to block $Na_v1.8$ and lay out the methodological ground work for the ongoing antibody based project. This project also provided a pharmacologic benchmark to test the membrane permeable antibody method. Surprisingly these experiments also provided a key to partially solving the second question guiding my thesis work. I found that A803467 selectively suppressed the amplitude of the OPs. In combination with previous work, that showed little contribution of the RGCs to the OPs in mice (Smith et al., 2014b) and the restricted expression of $Na_v1.8$ in the mouse retina to the starburst amacrine cells

and RGCs (O'Brien et al., 2008), this led to the identification of one cell type (SBACs) that contributes to the generation of the OPs. Whether the OPs represent a composite signal from several cell types or have independent, or partially independent generators is unknown (Wachtmeister, 1998; Bui et al., 2002; Derr et al., 2002; Dong et al., 2004) and apart from some generalities involving feedback inhibition in the IPL, the cellular generators of the OPs were previously unknown. Our results suggest that SBACs are not the primary generator of the OPs. The application of A803467 as well as a SBAC specific neurotoxin (AF64A) did reduce the OPs amplitude but did not completely eliminate them nor change their temporal properties. These results are thus more compatible with the idea of the SBACs amplifying and propagating oscillations generated upstream. One possibility is that an upstream oscillator drives oscillations in SBACs, agreeing with the results of Petit-Jacques and Bloomfield (2008) that showed reduced light evoked oscillations in SBACs in the presence of strychnine and DL-*threo*- β -Benzyloxyaspartic acid (TBOA), a excitatory amino acid transporter blocker.

Continuing this project I identified another contributor to the OPs (A17 cells), which in combination with SBACs, generates more than half of the OP signal. Further work shows that the combination of a specific cellular neurotoxin against A17 cells (DHT**)** with strychnine completely eliminates the OPs in mice with only a minor effect on the b-wave. Thus we are able to narrow down the source of the OPs to A17 cells and a glycinergic amacrine cell upstream of the SBACs that drives SBAC oscillations (Petit-Jacques and Bloomfield, 2008). Other studies show that eliminating Cx45, one of the heteromeric partners in the gap junctions connecting AII amacrine cells and ON cone bipolar cells, also reduces the OPs (Maxeiner et al., 2005). The extent of the reduction in OPs is similar to that seen in the absence of SBAC function and rod bipolar cells have not been shown to synapse directly with SBACs in mice to my knowledge (Ding et al., 2016; Park et al., 2015; Greene et al., 2016; Kim et al., 2014). In any case SBACs have been suggested to express the GlyR subunit α4 (Majumdar et al., 2009; Wassle et al., 2009). Limited possibilities for the unidentified glycinergic source of the OPs can therefore be predicted to act either on the ON bipolar cells (presumably the rod bipolar cells given the small size of cone driven OPs in our ERG preparations) or the AII amacrine cells, both of which receive glycinergic inhibition. Because different GlyR subunits are expressed in

rod bipolar cells (GlyRα1) and AII amacrine cells (GlyRα3) and knockout mice for both subunits are available, in theory it should be relatively straightforward to identify the remaining circuit elements underlying the OPs.

Returning to the fundamental goal of these experiments, I also found that selectively blocking $Na_v1.8$ caused a reduction in the spiking light response of sustained ON RGCs. ON alpha cells in mice are well known to produce sustained responses to the onset of light (e.g. Margolis and Detwiler, 2007; Murphy et al., 2011; Schmidt et al., 2014). Although the ON sustained classification likely included more than ON α cells, A803467 reduced the light responses of enough cells to cause a significant reduction in peak and average spiking response of the entire population. In addition, responses from OFF transient and sustained cells showed no significant change consistent with the report of O'Brien et al., (2008) that $Na_v1.8$ is expressed in at least one type of alpha RGCs in mice.

These results together showed that isoform selective Na_v channel block can selectively reduce specific components of the ERG as well as demonstrating a selective contribution to a physiological defined subgroup of RGCs. I compared the membrane permeable antibody method against pharmacological broad spectrum and where possible isoform specific blockers as well as to $Na_v1.6$ mutant mice using the ERG and MEA. I found that that the membrane permeable antibody method was able to replicate the isoform specific effects of all pharmacologic blockers tested as well as replicating the ERG effects seen in the $Na_v1.6$ knockout mouse. Firstly, these results demonstrate for the first time an affordable method for blocking individual sodium channel isoforms acutely in mature tissues avoiding the known issues of developmental compensation in Na_v channel knockout mice. Given the proposed involvement of Na_v channel isoforms in human channelopathies (Waxman 2013; Waxman 2007; Meisler et al., 2010; Waxman 2010; Dib-Hajj et al., 2010), as well as the obvious difficulties involved in dosing broad spectrum sodium channel blockers (e.g. Lago et al., 2015), subtype specific block of Na_v channels (e.g. Alexandrou et al., 2016; Shields et al., 2015; Waxman and Zamponi 2014) has been a goal for treatment of chronic pain among other aliments (e.g. Dib-Hajj et al.,

2017; Han et al., 2017; Tanaka et al., 2016; Yang et al., 2016; Han et al., 2016; Dib-Hajj et al., 2015) and our monoclonal antibody-based strategy offers hope in this regard.

8.6 Contribution of Nav1.6 to ON bipolar cell light responses

Of particular interest with respect to broader retinal physiology, I found that $Na_v1.6$ is the Na_v channel isoform contributing to cone ON bipolar cell light responses. This is interesting because I have also shown that Na_v channels in ON cone bipolar cells are sensitive to dopamine modulation via D1Rs. It is interesting to note that relative to $Na_v1.1$ and 1.2 channels ($Na_v1.2$: Gershon et al., 1992; Li et al., 1992; $Na_v1.1$: Smith and Goldin 1998) $Na_v1.6$ is relatively insensitive to modulation by PKA and PKC (Chen et al., 2008), which mediate dopaminergic modulation of Na_v channels (e.g. Cantrell and Catterall 2001, Scheuer 2011). Although it is counterintuitive, given a recent report that dopamine release driven by 90 minutes of light adaptation is significantly higher at midnight than midday in mice, it is possible that the expression of $Na_v1.6$ in murine ON bipolar cells makes them relatively resistant to modulation by dopamine under light adaptation during midday (e.g. CHAPTER 2).

I have previously shown that blocking $GABA_cRs$ or Na_v channels has two distinct effects on the dark-adapted ERG. With $GABA_cR$ blockade the b-wave is significantly reduced and with Na_v channel blockade the number and amplitude of the late OPs is increased (Smith et al., 2013). As demonstrated by the pronounced reduction in the dark-adapted b-wave in young $Na_v1.6$-null mutant mice, 4,9 ah-TTX, and mp-anti $Na_v1.6$, Na_v-1.6 also played the dominant role in the Na_v channel-dependent GABAergic input to rod-driven ON bipolar cell $GABA_cRs$. $GABA_cRs$ are well known to support sustained or tonic GABA currents (Lukasiewicz and Shields 1998; Eggers and Lukasiewicz 2006ab; Lukasiewicz et al., 2004; Jones and Palmer 2009). Herrmann et al., (2011) suggest that $GABA_cRs$ mediate a tonic hyperpolarization of the rod bipolar cell and thus increases the dynamic range of rod bipolar cell depolarization. $Na_v1.6$ is known to mediate a persistent Na_v current in other preparations (Rush et al., 2005; Smith et al., 1998; Osario et al., 2010; Royeck et al., 2008), suggesting the possibility that persistent Na_v current supports tonic release of GABA onto rod bipolar cell $GABA_cRs$.

$GABA_cRs$ are typically considered to be expressed predominately at ON bipolar cell axon terminals (but see Herrmann et al., 2011 for evidence of dendritic expression). These results are not absolutely conclusive but if $GABA_cR$ expression is limited to ON bipolar cells and eliminating GABA release from horizontal cells has little effect on the OPs (B. Smith unpublished observations) then the increase in OPs seen in the absence of $GABA_cR$ function at primarily rod driven light intensities is likely to be localized to the rod bipolar cell axon terminal. Although the full generators of the OPs are not yet known at this point, eliminating A17 derived fast feedback in combination with glycine receptor block can effectively eliminate the OPs in dark adapted mice.

The OPs are reduced in amplitude in all three models of $Na_v1.6$ block, while blocking $Na_v1.1$ completely reproduces the increase in the late OPs seen with TTX or the mp-antibody cocktail (anti-$Na_v1.1$ + anti-$Na_v1.2$ + anti-$Na_v1.6$). In combination with evidence that suggests a single source for Na_v dependent GABA input to rod bipolar cell $GABA_cRs$ (Chavez et al., 2010), the separation of Na_v dependent input to $GABA_cRs$ by isoform suggests an intriguing possibility for future work. $Na_v1.1$ and $Na_v1.6$ may be serving different purposes, with $Na_v1.6$ mediating tonic GABA release and $Na_v1.1$ acute release to limit ongoing oscillations. Many other explanations are possible such as, for example, multiple amacrine cell types that inhibit rod bipolar cells and express either $Na_v1.6$ or $Na_v1.1$, or a different circuitry underlying the OPs that is more complex than we envision but still consistent with our experimental results. However, evaluating the individual Na_v channel isoform contributions to inhibitory feedback at the rod bipolar cell axon terminal would be an interesting future project.

8.7 Na_vs and the neural code

At this point we still don't understand the mechanism used by neurons to encode information and deliver it to their postsynaptic partners. At least three patterns in spiking are proposed to contribute to information encoding in neurons. Spike rate within some defined temporal window (aka rate coding), the precise timing of the first spike in response to some reference event (e.g. Van Rullen et al., 2005; Gollisch and Meister 2008; Gutig et al., 2013) or synchrony between cells (e.g. Singer, 1999; Shlens et al.,

2008). Although information is contained in each of these patterns, the relative importance of each factor is unknown (reviewed in Van Rullen and 2001; Brette 2015). I had hoped that blocking selected Na_v channel isoforms would alter each of the proposed patterns in a defined way (e.g. reducing the overall spike rate while leaving the temporal precision of spikes intact) while allowing the RGCs free to encode information via the alternative properties of spike trains. Ideally recording from the post-synaptic partners of RGCs in combination with identifying consequent behavioral changes could identify the important components of the RGC neural code. Even if a single isoform contributed to rate, timing, and synchrony, it would suggest that these factors may not be separable (e.g. de la Rocha et al., 2007).

Thus far, I've managed to derive the contributions of four Na_v channel isoforms to post synaptic processing of full field light in three physiologically defined groups of cells from the ganglion cell layer, presumably RGCs, although a contribution from amacrine cells cannot be excluded (e.g. De Sevilla Muller et al., 2007). Some patterns have emerged that suggest how these isoforms contribute to spiking patterns and provide the foundation for future work progressing towards my initial goal of comprehensively defining the encoding mechanism. While, limits in both time and infrastructure have prevented me from ultimately testing this proposal, these preliminary results point the way towards future projects that might resolve this question.

$Na_v1.2$ typically played only a minor role in regulating the maximal firing rate in response to the onset of light. The effects on OFF cells were larger than the effect on the ON cells and in ON-OFF cells the effects on the ON response were similar to the effects on ON cells, while the effect on the OFF response were similar to the effect on OFF cells. A differential effect between the ON and OFF responses in the same ON-OFF cell suggests a contribution of $Na_v1.2$ to the OFF presynaptic network rather than a direct contribution to spike production at the AIS. This is surprising considering that Boiko et al., (2003) found that $Na_v1.2$ is co-expressed with $Na_v1.6$ in the axon initial segment and Fjell et al., (1997) found that $Na_v1.2$ is expressed by RGCs. As mentioned previously $Na_v1.8$ also contributes directly, albeit to a relatively small extent, to the light response of sustained spiking ON cells from the ganglion cell layer, suggesting a role for this channel

in electrogenesis for ON alpha RGCs, but with little contribution to the direct encoding of light in other broadly defined cell types.

At this point it is obvious that the dominating Na_v channel driving the overall spike rate in all groups of RGCs is $Na_v1.6$. mp-anti-$Na_v1.6$ and 4,9 ah TTX cause similar (~60%) reductions in maximal spike rate in response to light in all three cell types. Previous results in mouse RGCs (Van Wart and Matthews, 2006) show a reduction in firing rate (~30%) in response to current injection in RGCs from juvenile mice (Van Wart and Matthews 2006). Our results, using optogenetic stimulation of RGCs, are similar to the findings of Van Wart and Matthews (2006) with a ~35-45% reduction in peak spike rate. Previous results in other types of neurons lacking $Na_v1.6$ show similar results with only minor reductions in transient current (~40%: Raman et al., 1997; Aman and Raman 2007; no change: Levin et al., 2006; Osorio et al., 2010; Enomoto et al., 2007; Royeck et al., 2008). However persistent (~40%: Osorio et al., 2010; Royeck et al., 2008; Do and Bean 2003; Enomoto et al., 2007; Maurice et al., 2001) and resurgent sodium currents (~70%: Levin et al., 2006; Royeck et al., 2008; Mercer et al., 2007; Do and Bean, 2003; Enomoto et al., 2007; Cummins et al., 2005) are substantially reduced in the majority of neuron subtypes. Reductions in persistent and resurgent currents are correlated with deficits in maximal firing rate and repetitive firing (Raman et al., 1997; Aman and Raman, 2007; Grieco and Raman, 2004; Khaliq et al., 2003; Van Wart and Matthews 2006; Mercer et al., 2007, Royeck et al., 2008; Enomoto et al., 2007). It has been suggested that the well documented reductions in persistent and resurgent current in many neuron types in the absence of $Na_v1.6$ directly cause changes in spiking output, in particular reductions in repetitive spiking and gain (Levin et al. 2006; Mercer et al. 2007; Raman et al. 1997).

Here I show for the first time that blocking $Na_v1.6$ in mature neurons from the mouse ganglion cell layer causes pronounced deficits in the maximal firing rate in response both to light and following direct optogenetic stimulation. Interestingly while other types of neurons show disproportionate deficits in repetitive firing in the absence of $Na_v1.6$, I found that both network and optogenetic stimulation drove sustained responses that were reduced only in proportion to the reduction in maximal firing rate. Essentially

$Na_v1.6$ sets the maximal firing rate of RGCs but does not control the shape of the response.

Consistent with evidence of $Na_v1.1$ expression both in the mouse presynaptic network (Kaneko and Wantanabe 2007; Wu et al., 2011) and in RGC axon initial segments (Van Wart et al., 2007), I found that blocking $Na_v1.1$ using mp-anti-$Na_v1.1$ reduced the maximal firing rate in response to network derived light responses in all three cell classes by ~30%. When RGCs are stimulated directly via ChR2, the effect on maximal firing rate was smaller for ON and ON-OFF cells (~15%), while OFF cells showed no change. This was surprising given the widespread expression of $Na_v1.1$ in RGCs (~85% of RGC axon initial segments, Van Wart et al., 2007). In $Na_v1.1$ knockout mice, recordings from other neuronal subtypes (Kalume et al., 2007; Yu et al., 2006; Ogiwara et al., 2007) show both reduced peak spike frequency in combination with sustained spiking in response to intermediate depolarizing current and transient spiking in response to increased depolarizing current (Yu et al., 2006). In neocortical interneurons spiking responses from heterozygous mice show deficits in repetitive firing in response to depolarizing current (Ogiwara et al., 2007). These results in combination with my findings in cells from the ganglion cell layer in the mouse retina suggest a general role for $Na_v1.1$ in repetitive firing that may exceed that of $Na_v1.6$.

I found that in ON and ON-OFF cells with sustained light responses blocking $Na_v1.1$ but not $Na_v1.2$ or $Na_v1.6$ caused a reduction in repetitive firing that exceeded the effect on maximal firing rate, particularly in response to network input. Direct stimulation of RGCs with sustained light responses with channelrhodopsin-2 caused smaller reductions in sustained spiking in the absence of $Na_v1.1$, possibly due to the fact that some cells with sustained light responses had transient responses to optogenetic stimulation (e.g. Thyagarajan et al., 2010), reducing their overall sustained nature. These results suggest preferred roles of $Na_v1.6$ and $Na_v1.1$ to overall spike rate and sustained spiking respectively.

I am continuing to elaborate on the findings presented in chapter 6 by using retrobulbar injection of membrane permeable antibodies against $Na_v1.1$ and 1.6 to target the contributions of RGC Na_v channel isoforms in the otherwise functionally intact retina.

In addition, I am matching the network derived input to the optogenetic response of RGCs, looking specifically at cases where cells with sustained responses to network input also had sustained responses when stimulated optogenetically. Thus far, I have determined that while $Na_v1.6$ amplifies the post synaptic responses of RGCs it is $Na_v1.1$ that gives a majority of sustained RGCs the appropriate intrinsic properties to encode sustained responses. My preliminary results show that while the input of RGCs is subject to multifaceted modulation shaping the tonicity of the input (e.g. Awatramani and Slaughter 2000; Dong and Hare 2003), in some cases the appropriate postsynaptic properties are also required to appropriately encode input.

8.9 Conclusions

This work in aggregate demonstrates new roles for Na_v channels in the retina. These roles range from adaptation to shifting background luminance, achieved via GABAergic signaling, and daily rhythms in ambient light, achieved via Na_v channels intrinsic to the ON cone bipolar cells, to an unusual retroaxonal feedback circuit operating in the optic nerve during development. In addition, by blocking Na_v channel isoforms directly, using a range of techniques from genetic inactivation to membrane permeable antibodies, I have elaborated on the role of each common retinal Na_v channel in the light response of retinal ganglion cells, albeit to a very simple stimulus. In addition, using Na_v channels, as well as confirming with cellular toxins, the circuitry underlying the macroscopic ERG signal can be understood more accurately.

APPENDIX I : NOVEL ROLES OF VOLTAGE-GATED SODIUM CHANNELS IN THE RETINA; EVALUATING THE EVIDENCE FOR DIGITAL SIGNALING IN TYPICALLY ANALOG RETINA CELL TYPES.

Animals must react to continuously changing environmental stimuli in order to survive. Commonly, as discussed in Copenhagen (2001) and Baden et al., (2013) sensory systems typically first encode information in a continuously varying amplitude modulated signal, also known as an analog or graded response. Stimuli are sampled continuously at early stages and later converted to a binary code based on temporal patterns of action potentials ("spikes"). In a majority of neurons voltage gated sodium (Na_v) channels are critical for the production of a spike based neural code because of the role that transient sodium influx plays in the rising phase of the action potential. The stage that neurons shift from graded potentials to spikes carries important implications for signal processing. While the relative advantages of graded vs. digital communications have both been completely described saltatory conduction, dependent on spiking, is necessary for rapid long distance communication without degradation. Conversely analog signaling can encode both increments and decrements in signaling and carry substantially more information (Juusola and French 1997) for less metabolic expense (Balasubramanian and Berry 2002; Balasubramian et al., 2001, Laughlin et al., 2001).

In the vertebrate retina, the majority of cell types have been classically thought to communicate via graded potentials. Across model species only neurons with receptive fields that spread across substantial segments of the visual field (widefield amacrine cells) and neurons with myelinated axons (retinal ganglion cells; RGCs) had been thought to use spikes to communicate (e.g Bloomfield 1992). This division into mainly high bandwidth graded neurons preserving information and communicating over short distances, with a few spiking cells communicating over long distances appeared to be a general pattern common across many species. However, within the last 15 years research has revealed that Na_v channels, and potentially digital signaling, are more widely distributed in the distal retina than initially thought; Na_v channels have been found in cell

types previously thought to communicate predominately via graded signals in at least one species. Because Na_v channels are typically associated with spiking neurons, expression of these proteins in typically graded retinal cell classes suggests that conversion from analog to digital signaling may occur earlier than generally thought.

A detailed survey of the structure to function relationship and the pharmacology of Na_v ion channels can be found elsewhere (e.g. Ahern et al., 2016). Briefly however, Na_v channels are a family of proteins composed of a pore forming α subunit, sufficient for functional expression in heterologous expression systems (e.g. Smith et al., 1998), and a modulatory β subunit. Na_v channel α subunits open upon depolarization from negative membrane potentials and inactivate within a few milliseconds, creating a large but transient depolarizing current that contributes to the initiation of action potentials. In addition to the transient Na_v current underlying the rising phase of action potentials, some Na_v channel isoforms support a steady-state, non-inactivating, or persistent current (French et al., 1990; Cepeda et al., 1995; Smith et al., 1998; Rush et al., 2005; Osorio et al., 2010).

Persistent Na_v current is known to play a role in amplifying EPSCs (Deisz et al., 1991; Stuart and Sakmann, 1995; Schwindt and Crill 1995; Carter et al., 2012; Gonzalez-Burgos and Barrioneuvo 2001) and IPSCs (Stuart, 1999; Hardie and Pearce 2006) in CNS neurons. In the retina neurons expressing Na_v channels may also use them to increase gain of graded signals by amplifying synaptic input. In fact in salamander ON cone bipolar cells this has been show to be the case with Na_v channels modulated by the release of dopamine to tune the gain of the bipolar cell to ambient light levels (Ichinose and Lukasiewicz, 2007). Expression of Na_v channels in classically non-spiking cells may indicate that these cells communicate information via spiking in response to specific, rare stimuli that were missed due to experimental limitations, or alternatively that in addition to their role in spike generation Na_v channels could increase gain of graded signals by modulating synaptic input.

There are 10 different Na_v channel α subunits and while there appear to be relatively small functional differences between subtypes studied in isolation (Chen et al., 2008; Rush et al., 2005; Smith et al., 1998) both temporal expression patterns and

selective expression on multiple scales (e.g. Van Wart and Matthews 2006a,b; Boiko et al,. 2001, 2003) suggest that isoforms are functionally unique. Mammalian retinas express at least 6 Na_v channel α subunit isoforms (Na_v1.1, 1.2, 1.3, 1.6, 1.8, and 1.9) (Mojumder, et al., 2007; O'Brien, et al., 2008; Fjell et al., 1997) with what appears to be specific and restricted expression of Na_v isoforms. Such restricted expression occurs both in terms of cell types expressing specific Na_v channel isoforms, and in temporal patterns of Na_v channel isoform expression during development (e.g. shifts from Na_v1.2 to 1.6 in RGC axon initial segment (Boiko et al., 2001; 2003). Examples of retinal cell type-specific expression include AII amacrine cells (Kaneko et al., 2007; Wu et al., 2011) and primate DB3a and DB4 cone bipolar cells (Puthussery et al., 2013), which express Na_v 1.1, while Na_v1.8 is expressed in starburst amacrine cells and a subset of RGCs (O'Brien et al., 2008). Again, the precise expression patterns of individual Na_v channel subtypes suggests the possibility that Na_v channel expression is a factor in differentiating parallel pathways through the retina.

In the last 15 years, a number of papers have suggested that Na_v-based spiking may encode information earlier in the retinal circuitry than previously thought. For instance, Na_v channel dependent spiking responses to light have recently been recorded in cone bipolar cells (e.g. Puthussery et al., 2013, Saszik and DeVries 2012). These findings, in combination with the sparse distribution of Na_v channels in the distal retina, suggest that the division of retinal processing into parallel pathways may be accomplished in part by the expression of Na_v channels in selected cell subtypes. To evaluate the evidence for this hypothesis, the first half of this review will be a general introduction to the roles Na_v channels play in retinal circuitry, excluding the retinal ganglion cells because of their obligatory Na_v channel expression and the relatively well understood mechanism of spike generation in the axon initial segment. In the photoreceptors and horizontal cells, although the presence of Na_v channels and spikes is controversial and probably species-dependent, some findings indicate a very early shift to partially encoding information using spikes. The second half of the review will be an in-depth review of recent evidence for Na_v channel function in excitatory pathways in the inner retina, focusing on a subset of cone bipolar cells and two types of amacrine cell that convey excitatory signaling in addition to performing the usual amacrine cell role of

inhibition. The AII amacrine cell acts as a bridge linking the rod and ON cone excitatory pathways via gap junctions, and vesicular glutamate transporter 3-expressing (VGLUT3+) amacrine cells, have recently been demonstrated to provide direct excitatory input to four types of RGC.

GENERAL ROLES OF NAv CHANNELS IN INNER RETINAL CIRCUITRY

Anatomically the neural retina is divided into three cellular layers connected by two synaptic layers. The distal outer nuclear layer contains the photoreceptor cell bodies, the inner nuclear layer contains bipolar and amacrine cells, while the most proximal ganglion cell layer contains retinal ganglion cells and displaced amacrine cells. Functionally the retina can be divided into parallel vertical excitatory pathways and horizontally ramifying inhibitory circuit elements. The vertical pathways can be divided into rod circuit, highly sensitive due to its convergent nature, and the parallel cone-driven pathways, less light sensitive but able to sort the visual signal by colour and spatiotemporal frequency. The rod pathway, active in low light conditions, consists of a highly convergent rod to rod bipolar cell circuit which is piggybacked onto the cone driven pathways primarily via the AII amacrine cell. In contrast to the single photoreceptor and bipolar cell in the rod pathway, the cone pathways are diverse, starting from 2-3 types of spectrally selective photoreceptors that diverge into approximately 12 types (9 anatomically defined, vs. 12 physiologically defined) of cone bipolar cells (Helmstadtler et al., 2013; Wassel et al., 2009; Breuninger et al., 2011; Ichinose et al., 2014), feeding forward to at least 12 types of retinal ganglion cells (Field and Chinchilnisky 2007; Masland et al., 2012; Sanes and Masland 2015 but see Baden et al., 2016). Within the horizonal ramifying inhibitory interneurons one can find 1-3 types of horizontal cells depending on species and approximately 30 types of amacrine cells including a subset of interplexiform cells with dendrites ramifying in both inner and outer plexiform layers (reviewed in Sanes and Masland 2015).

Bipolar cells

The segregation of signals resulting from the onset of a light stimulus (ON cells) vs. the offset of a light stimulus (OFF cells) first occurs in the dendrites of the bipolar cells, the second order retinal neurons. Expression of mGluR6, a metabotropic glutamate

receptor (Masu et al., 1995) coupled to transient receptor potential cation channel subfamily M member 1 (TrpM1) channels (Morgans et al., 2009; Koike et al., 2010) in ON cells and ionotropic α-amino-3-hydroxy-5-methyl-4-isoxazolepropionic acid (AMPA) or kainite-sensitive glutamate receptors in OFF cells (DeVries 2000; Li and DeVries 2006; Borghuis et al., 2014; Puthessary et al. 2014) differentiates the ON and OFF pathways. The bipolar cells maintain the segregation between primary rod and cone pathways with a single type of ON rod bipolar cell (RBCs) collecting responses from many rods, increasing the sensitivity of the low light pathway (Dunn et al., 2006), while an array of approximately 12 cone bipolar cell types (CBCs), of both the ON and OFF variety, pool responses from a smaller number of cones (Helmstadtler et al., 2013; Wassel et al., 2009; Breuninger et al., 2011; Ichinose et al., 2014).

It is now established that light responses within a type (ON vs. OFF) of cone bipolar cell exist on a spectrum from tonic (sustained for the duration of the stimulus) to phasic (a transient response near the onset of the stimulus). In the ON pathway, sustained and transient subtypes have different responses to the mGluR antagonist (RS)-a-cyclopropyl-4-phosphonophenylyglycine ((RS)-CPPG; Awatramani and Slaughter 2000) and agonist L-(+)-2-Amino-4-phosphonobutyric acid (L-AP4; Ichinose et al., 2014). However, a molecular mechanism underlying this difference has not been described. In the OFF pathway, it was initially suggested that differences in sustained vs. transient cells may be due to expression of AMPA receptors in transient cells and kainate receptors in sustained cells, primarily based on results from ground squirrel retina (DeVries 2000; Li and DeVries 2006). In the mouse retina, Borghuis et al. (2014) showed that kainate receptors drive both sustained and transient bipolar cell responses, similar to results from the primate retina (Puthessery et al., 2014). However, Ichinose and Hellmer (2016) found that while all OFF CBCs have at least a small kainate receptor component type 1, 3b, and 4 cells have a significant AMPA contribution (~50%) as well. Multiple other contributing factors have been suggested to contribute to cone bipolar cell tonicity. For instance modifiers of glutamate receptor dynamics (Cao et al., 2012), differences in axonal calcium dynamics (Baden et al., 2013), and amacrine cell input (Eggers and Lukasiewicz 2011; Nirenberg and Meister 1997; Dong and Hare 2003) have all been suggested as contributing to tonicity. With regard to the hypothesis that Na_V channel expression

contributes to the formation of distinct parallel processing pathways in the inner heterogenous expression of ion channels, including Na_v channels, in CBCs has been suggested to be correlated with the tonicity of cone bipolar cells (Burrone & Lagnado, 1997; Mao et al., 1998; Zenisek & Matthews, 1998; Protti et al., 2000; Pan 2000; Hu & Pan, 2002; Ma and Pan 2003; Ma et al., 2005; Müller et al., 2003; Cui and Pan, 2008; Hu et al. 2009; Puthussery et al., 2013). Anatomically, there is evidence that more transient CBC types, including those that spike and/or express Na_v channels, ramify in the middle of the IPL (Awatramani and Slaughter 2000; Baden et al., 2013). A more detailed examination of Na_v channel contribution to CBC signal processing follows below. Classically, both RBCs and CBCs were considered to carry analog signals only, however in the last 15 years evidence from a range of experimental techniques and in a number of model species (fish, amphibians, rodents and primates) has demonstrated the presence both of Na_v channels and in some cases temporally-precise spiking in a subset of CBCs, as reviewed in detail below.

Amacrine cells

As a population, amacrine cells provide inhibition in the inner plexiform layer, shaping the outputs of the bipolar cells and playing an important role in the microcircuits that generate feature selectivity in RGCs. Amacrine cells are commonly categorized based on the spread of their dendritic arbors (e.g. Werblin et al., 2010). The ability to generate action potentials has long been considered to link form and function in amacrine cells. In general, wide field amacrine (WFA) cells are much more likely to generate action potentials, controlling neurotransmitter release over large patches of retina. For instance, Bloomfield (1992) demonstrated a correlation between spiking amacrine cells and their dendritic field size: amacrine cells with a dendritic field size > 436 μm exhibit spike activity. However, although the trend for WFA cells to spike was conserved in other studies some medium and narrow field amacrine cells also spiked. In tiger salamander for instance Heflin and Cook (2007) found that more narrow field than wide field cells fired single action potentials while wide field cells were more likely to show sustained spiking. Wide field amacrine cells are capable of generating TTX-sensitive action potentials, allowing robust signaling over long distances. Na_v channels in WFA, in particular the polyaxonal WFA cell (Greshner et al., 2014; Völgyi et al., 2001; Olveczky

et al., 2003; Davenport et al., 2007; Cook and Werblin 1994; Murphy-Baum and Taylor 2015; Manookin et al., 2015) have been implicated in mediating lateral inhibition, in some cases generating spatial tuning in RGCs (Cook and McReynolds, 1998; Hoggarth et al., 2015; Protti et al., 2014; Shields and Lukasiewicz, 2003). Na_v channel-based spike trains also drive release of dopamine from wide field dopaminergic amacrine cells (Hirasawa et al., 2009; Zhang et al., 2007; Feiganspan et al., 1998; Gustincich et al., 1997).

Although small and medium field amacrines can produce trains of action potentials in some cases (Heflin and Cook 2007), there is accumulating evidence that they may use Na_v channels in unconventional ways, particularly AII and vesicular glutamate transporter type 3 positive (VGLUT3+) cells, two atypical amacrine cells that act as intermediates in the excitatory pathway (reviewed in detail below). In addition to producing single spikes, Na_v channels have also been implicated in boosting the graded responses of amacrine cells in a range of species (Fish: Wantanabe et al. 2000, rabbit: Bloomfield 1996; rat: Koizumi et al., 2001). Some cells (most notably AIIs; see below but see also Miller et al., 2006) produce spikelets, which have strong similarities to dendritic spiking in RGCs, (Trenholm et al., 2014, Sivyer and Williams 2013; Oesch et al., 2005; Velte and Masland 1999).

Given the diversity of the amacrine cells (~40 subtypes), drawing many general conclusions about the function of Na_v channels and spiking in these cells is difficult. However, despite this diversity and the resulting difficulty in repeatedly and unambiguously recording from a given cell type, some general trends in the literature do exist. Amacrine cells with extensive dendritic arbors typically use spikes to convey information rapidly across broad sections of retina while small and medium field amacrine cells use Na_v channels to amplify graded responses, occasionally producing full spikes or spikelets. It is not yet conclusively known whether spikelets generate a binary code or are an epiphenomenon due to the expression of Na_v channels (reviewed in detail in section II e, AII amacrine cell Na_v channels). The increasing number mouse models with fluorescently labeled amacrine cell populations in combination with optogenetic targeting particular amacrine cell classes should help clarify this point.

CLASSICAL ROLES OF NA_V CHANNELS IN WIDEFIELD AMACRINE CELLS

Polyaxonal amacrine cells

Polyaxonal cells (PACs) are a heterogenous group of widefield amacrine cells with a unique morphology defined by multiple millimeter long axonal processes extending past their relatively small (~600 μm) dendritic arbor (Rodieck, 1988; Dacey, 1989, 1990; Famiglietti, 1992a,b,c). Stratification of these axons in the IPL enables PACs to modulate other amacrine cells as well as RGCs. In the rabbit retina there have been 4 types described morphologically (Famiglietti 1992a,b,c) and six types based on a combination of morphology, coupling patterns and physiological light responses (Volgyi et al., 2001). All recorded polyaxonal cells have either ON or ON-OFF light responses and have inhibitory surrounds that are largely inherited from their presynaptic bipolar cells that synapse with their dendrites (Volgyi et al., 2001; Davenport et al. 2007; Stafford and Dacey 1997). Typically the receptive field center is similar to the extent of the dendritic field and is much smaller than the axonal arbor (Volgyi et al., 2001). Both the dendritic and axonal processes of PACs ramify in the middle of the IPL on the border of the ON and OFF sublamina (Volgyi et al., 2001). Despite the distinct morphology of PACs the synaptic inputs and outputs of a majority of these cells are unknown both because of the heterogeneaity of the population, the sparseness of the PAC mosaic, and, except for the dopaminergic subtype of PAC, the absence of genetically encoded labels. Morphologically undefined polyaxonal cells in the rabbit and salamander retina are important in saccadic suppression, suppressing visual processing in object motion sensitive types of RGCs (ON brisk transient and ON-OFF direction selective cells in rabbit and fast OFF cells in salamander) during rapid eye movements (Roska and Werblin, 2003) and identifying differential motion of object and background (Olveczky et al. 2003, 2007; Baccus et al. 2008).

While there are numerous reports on the function of polyaxonal amacrine cells as a class only a few individual types of polyaxonal cells have been studied in detail. These include the PA1 (Famiglietti 1992a,b), also known as A1 (Stafford and Dacey, 1997) or type I (Volgyi et al., 2001) subtype (Davenport et al., 2007), the $PA_{1/3}$ cells (Murphy-Baum and Taylor 2015) similar to the PA3 cells of Famiglietti (1992c) and type V cells

(Volgyi et al., 2001), and the PA4 (Famiglietti 1992c) probably the dopaminergic amacrine cells.

A1 cells are transient ON-OFF cells (Volgyi et al., 2001; Davenport et al., 2007). The inhibitory surround of OFF cells is partially but not totally driven by inhibition derived from the ON pathway, consistent with a role of glycinergic crossover inhibition in creating the inhibitory surround of both ON and OFF responses blocking GABA receptors increased the amplitude of light responses but did not change the inhibitory surround (Davenport et al., 2007). Na_v channels controlled calcium influx in response to light in some, but not all dendrites, but completely eliminated axonal calcium influx. This shows that while action potentials are necessary for long range signaling in the dendrites they play only a small role in dendritic integration of synaptic input (Davenport et al., 2007).

In the primate retina ON-OFF PACs (possibly the A1 subtype studied in detail by Dacey, 1989; Stafford and Dacey, 1997; Davenport et al., 2007) comprise a highly coupled population of cells which suppress visual responses in RGCs in response to sharp transitions in visual input rather than slow global movement (Greshner et al., 2014). Additionally in the primate retina Greshner et al., (2016) another type of PAC is coupled via gap junctions to ON parasol cells (observed anatomically in Dacey and Brace 1992) and mediates recurrent inhibitory feedback derived from the electrical input from one ON parasol cell to its neighbors that receive inhibitory synaptic input from the PAC. Because spike propagation in the PAC axons is relatively slow each ON parasol cells is inhibited over long periods by the aggregate activity of its nearest neighbors (Greshner et al., 2016).

Dopaminergic amacrine cells

Dopaminergic amacrine cells are a subset of polyaxonal cells that have a relatively small dendritic field (~600 μM) and stratify in the distal (OFF) layers of the IPL as well as extending processes to the OPL, categorizing them as interplexiform cells (Dacey 1990; Gustincich et al. 1997; Kolb et al. 1991; Versaux-Botteri et al. 1984). DACs have axons extending across the retina for millimeters (Contini and Raviola, 2003). These extended processes facilitate widespread release of dopamine, which has

been suggested to modulate retinal circuitry in a paracrine fashion (reviewed in Witkovsky 2004). In isolated DACs dopamine release is controlled predominately by Na_v channel dependent action potentials (Feigenspan et al., 1998; Gonon, 1988; Puopolo et al., 2001; Floresco et al., 2003). In the intact retina in addition to Na_v channels inhibitory but not excitatory synaptic input controls the pattern but not the overall rate of spontaneous activity in the dark (Zhang et al., 2007).

Isolated DACs typically have identical physiological characteristics, and DACs in the intact retina are morphologically homogenous (e.g. Zhang et al., 2007; Qiao et al., 2016), spiking at a uniform rate (~ 6 Hz) without bursting (Feigenspan et al. 1998; Gustincich et al. 1997; Steffen et al. 2003; Xiao et al. 2004). DACs, while morphologically homogenous show varying physiological properties (Newkirk et al., 2013; Zhang et al., 2007) both in response to light, in spontaneous activity, and in the absence of synaptic input (Newkirk et al., Zhang et al., 2007). Newkirk et al., (2013) report that spontaneous activity of DACs in dark adapted retina have 4 distinct patterns, a minority of cells (~5%) are nearly silent with only a few spikes (<0.1 Hz), ~25% of cells spike regularly at ~5 Hz or burst (~60%) at similar frequencies, finally ~5% of cells show high frequency intermittent bursts of activity. These patterns of spontaneous activity were maintained in the absence of synaptic input suggesting intrinsic variations in the overall population of DACs

The synaptic input to DACs has been extensively investigated with similar conclusions (Newkirk et al., 2013; Qiao et al., 2016) The rod pathway drives a hyperpolarizing current in response to dim light via a glycinergic amacrine cell (Newkirk et al., 2013; Qiao et al., 2016). As stimulus intensity increases ON cone bipolar cells drive DACs directly via *en passant* synapses between ON cone bipolar cell axons and DAC dendrites ramifying in the OFF sublamina of the IPL (Dumitrescu et al., 2009; Contini et al., 2010; Hoshi et al., 2009). Slower ON excitation is derived from M1 ipRGCs (Newkirk et al., 2013; Prigge et al., 2016). DACs receive GABAergic inhibition from cone OFF bipolar cells, surprisingly given the dendritic arbor ramifying in the OFF sublamina of the IPL there is no excitatory input at light offset (Newkirk et al., 2013; Qiao et al., 2016).

Transient light responses appear to be derived predominately from cone ON bipolar cells (Zhang et al., 2007) while sustained responses are not blocked by the metabotropic glutamate receptor L-AP4, or in mouse models of retinal degeneration (Prigge et al., 2016 but are eliminated by ionotropic glutamate receptor blockers (Prigge et al., 2016; Newkirk et al., 2013; Qiao et al., 2016). Intrinsically photosensitive RGCs, expressing melanopsin mediate a retrograde signaling pathway feeding back to drive delayed and sustained light responses in DACs (Zhang et al., 2012; Zhang et al., 2008; Prigge et al., 2016). Zhang et al. (2007) report three types of DACs based on light response, those with transient and sustained responses to light onset, and light independent cells. They suggest that these represent cells tuned to steady light, flickering light and light independent cells controlled predominately by circadian rhythms in the retina. However Newkirk et al., (2013) found no evidence of DACs without light responses.

Dopamine released from DACs plays multiple roles in modulating retinal function (reviewed in Witkovsky 2004) but the underlying theme in the neural retina seems to be a role in the adaptation to longer term changes in background light levels, both on the short term during light adaption (Jackson et al., 2012), and at longer intervals .by playing a key role in maintenence of both daily and circadian rhythms in retinal function (Iuvone 1978, Doyle et al., 2002, Li et al., 2013 Nir et al., 2000; Doyle et al., 2002; Cameron et al., 2008; Jackson et al., 2012; Storch et al., 2007; Barnard et al., 2006; Smith et al., 2014).

Dopamine secretion is modulated by background light and prolonged darkness (Bauer et al., 1980; Mangel and Dowling, 1985; Umino et al., 1991; Weiler et al., 1997) and circadian rhythms (Nir et al., 2000; Doyle et al., 2002a,b; Ribelayga et al., 2004; Iuvone et al., 1978; Li et al., 2013). Cameron et al., (2009) report that circadian rhythm acts on the release of dopamine in response to light adaptation, surprisingly dopamine release is higher at night following light adaptation in mice.

Dopamine acting through 5 types of metabotropic dopamine receptor D1-5 plays multiple roles in modulating neuronal responses in the retina. In the salamander retina dopamine acting via D1 receptors reduces ON cone bipolar cell Na_v current and thus light responses to prevent the cone ON system from saturating as ambient light levels increase

(Ichinose and Lukasiewicz, 2007). The results of Ichinose and Lukasiewicz (2007) are consistent with ERG results from Awatramani et al. (2001), also in salamander, and in primates (Rangaswarmy et al., 2004; Ueno et al., 2004; Hare and Ton 2002; Rangaswarmy et al., 2007), which either show no effect or increase in the amplitude of the cone driven b-wave following TTX in light adapted conditions. Interestingly, in a number of species (mice, rats, rabbits, and frogs), Na_v channels contribute to the ON CBC-derived ERG b-wave even when the retina is fully light adapted (Rats: Bui and Fortune, 2004, 2006; Mojumder et al., 2007; 2008 mice: Miura et al., 2009; Smith et al., 2013; rabbits: Becker et al., 2015; frogs: Kupenova and Popova 2010). When studied in detail, we found in mice (Smith et al., 2015) that light adaptation during midday is unable to cause sufficient dopamine release to strongly suppress Na_v channels as seen in salamander (Ichinose and Lukasiewicz, 2007).

NOVEL ROLES PLAYED BY NA_V CHANNELS IN EXCITATORY PATHWAYS IN THE INNER RETINA.

Cone bipolar cells: Na_v channel dependent spiking in subsets of a largely graded type of neuron.

Na_v channels were first found in rat (Pan and Hu 2000) and fish (Zenisek et al. 2001) bipolar cells, around the same time that it was demonstrated that fish bipolar cells can generate calcium spikes (e.g. Burrone and Lagnado 1997). These results implied for the first time that at least some CBC types use a combination of graded and binary signaling. Further work (Ma and Pan 2005) in isolated bipolar cells identified TTX-sensitive spikes in a subset of CBCs. Later work in rats (Cui and Pan 2008) identified two types of Na_v containing bipolar cells that spiked following current injection ramifying in the middle of the IPL. First, it has been reported that rat ON type CBCs with axons ramifying in IPL layer 3 (their type 3a and 3b cells) can be split into two groups on the basis of Na_v-channels expression and depolarization-induced spiking. These cells appeared to be identical morphologically to type 5 CBCs in rat (Euler & Wässle, 1995) and mice (Ghosh et al., 2004; Ivanova & Müller, 2006). Second, OFF CBCs with axons terminating in sublamina 2 proximal to the OFF cholinergic band also expressed Na_v channels (CB2, equivalent to type 3 CBCs in rats: Euler & Wässle, 1995 and mice:

Ghosh et al., 2004; Pignatelli & Strettoi, 2004; Ivanova & Müller, 2006). Unlike CB3a cells, which consistently spiked, CB2 cells rarely spiked. Further work in ground squirrel (Sazsik and Devries 2012) and primates (Puthessery et al., 2014) generally confirmed and extended these initial findings.

Until recently, there was no direct *in vitro* evidence for Na_v channels or TTX-sensitive spikes on mouse CBCs. In fact, Trenholm et al. (2012) and Ichinose et al. (2014) did not record spiking activity in mouse ON CBCs, in contrast to AII amacrine cells (Trenholm et al., 2012). This may be accounted for by the fact that in both cases, recording pipettes did not contain creatine phosphate, which prevents rapid rundown of spikes during whole cell recording (Baden et al., 2011). Supporting a role for Na_v channels in mouse CBCs, Baden et al. (2013) recorded fast calcium transients similar to spikes found in fish and mouse BCs cells; however, it was not reported whether these spikes were Na_v channel dependent. Other evidence for the presence of Na_v channels in ON CBCs includes the fact that the ERG b-wave, which is derived from the light evoked activity produced by these cells, is reduced following treatment with TTX even when the cone to ON CBC circuit is essentially isolated by ionotropic glutamate receptor blockers (Rats: Bui & Fortune, 2004, 2006; Mojumder et al., 2007; 2008 mice: Miura et al., 2009; Smith and Côté, 2012; Smith et al., 2013). Very recently, two types of type 5 (ON) and one type of type 3 (OFF) CBCs in mice have been shown to consistently express Na_v channels (Hellmer et al., 2016; Ichinose and Hellmer, 2016), along with sporadic expression in type 2 and type 7 CBCs. These results are similar to the CBC subtypes expressing Na_v channels in rat CBCs (Cui and Pan, 2008) denoted earlier. It been shown that type 5 CBCs can be divided into three types 5-1, 5-2 and XBC (Ichinose et al., 2014, Helmstaedter et al., 2013) and type 3 can be divided in to type 3A and 3B, of these types 5-2, XBCs, and 3A consistently express Na_v channels in mice (Hellmer et al., 2016; Ichinose and Hellmer, 2016). In contrast to the growing evidence for Na_v channel expression in CBCs Na_v channels have never been shown to contribute to rod bipolar cell signaling (Pan and Hu, 2000; Gillette and Dacheux 1995; Karschin and Wässle 1990).

Across species, Na_v channel expressing CBCs have axon terminals that tend to stratify towards the border of the ON and OFF sublamina (Stratum 2 for OFF cells, Stratum 3 for ON cells) where there is some evidence that transient signals are processed (Awatramani

& Slaughter, 2000; Baden et al., 2013). CBCs expressing Na_v channels tend to drive transient RGCs in both the ON and OFF pathways**;** at this point, there is evidence from 3 species that CBCs expressing Na_v channels contribute to transient as opposed to sustained pathways (Salamander: Ichinose and Lucasiewicz 2005; Primate: Puthussery et al., 2013; Ground Squirrel: Saszik and DeVries 2012), with additional evidence for spiking and transient light responses from bipolar cells with axon terminals in the middle of the IPL (mice: Baden et al., 2013). In addition, the ON CBCs that express Na_v channels (5-2) are the same as those type 5f cells described in Ichinose et al (2014) that process high frequency stimuli.

Roles of CBC Na_v channels

The roles of CBC Na_v channels and spiking studied *in vitro* appear to be related to gain control during light adaptation (e.g. Ichinose and Lukasiewicz, 2007) and temporal precision in transient high temporal frequency pathways processed in the middle of the IPL (Ichnose and Lukasiewicz 2005; Baden et al., 2011; Sazsik and De Vries 2012; Puthessery et al., 2013; Ichinose and Hellmar 2016; Hellmar et al., 2016**)**. There are distinct patterns in the projections of CBCs that express Na_v channels in mice (Ichinose and Hellmar 2016; Hellmar et al., 2016**)**. Although each cell type projects to multiple other cell types that are unidentified, Type 3A, 5-2, and XBC cells contribute to W3 cells , a cell type that detects motion of small spots on static background (Zhang et al., 2012, Kim et al., 2015**),** while Type 3A, 5-2 project to ON-OFF directionally selective cells (reviewed in Dunn and Wong, 2014**)**. Spikes can phase-lock to variations in visual stimuli with millisecond precision (Baden et al., 2011; Sazsik and De Vries 2012), suggesting that spiking may improve temporal fidelity in high temporal frequency low acuity pathways. Within primate retina, where this has recently been studied in depth, an AIS-like band drives Na_v channel-based spiking in diffuse bipolar cells projecting to the magnocellular pathway that processes transient low acuity vision but not in midget bipolar cells projecting to the parvocellular pathway and processing high acuity low temporal frequency vision (Puthessery et al., 2013). Supporting a role for spiking in bipolar cell light responses calcium spikes in the goldfish retina generate calcium based spikes (Dreosti et al., 2011; Baden et al., 2011**)** in a surprisingly high percentage of bipolar cells (~40). Calcium spikes in goldfish bipolar cell axon terminals have been

shown to trigger inward calcium current and more efficiently drive glutamate release as lower stimulus intensities (Lipin and Vigh, 2015).

Does Dopamine modulate cone bipolar cell Na_v channels?

The retina must compensate for significant variations in ambient light, with the primary signal being the global release of dopamine from dopaminergic amacrine cells (reviewed in Witkowski 2004). Activation of dopamine receptors phosphorylates Na_v channels via protein kinase A and C (PKA, PKC) and thus can alter peak sodium current (reviewed in Cantrell and Catterall, 2001). In the salamander retina dopamine acting via D1 receptors reduces ON cone bipolar cell Na_v current and thus light reponses to prevent the cone ON system from saturating as ambient light levels increase (Ichinose and Lukasiewicz, 2007). The results of Ichinose and Lukasiewicz (2007) are consistent with ERG results from Awatramani et al. (2001), also in salamander, and in primates (Rangaswarmy et al., 2004; Ueno et al., 2004; Hare and Ton 2002; Rangaswarmy et al., 2007), which either show no effect or increase in the amplitude of the cone driven b-wave following TTX in plight adapted conditions. Interestingly, in a number of species (mice, rats, rabbits, and frogs), Na_v channels contribute to the ON CBC-derived ERG b-wave even when the retina is fully light adapted (Rats: Bui and Fortune, 2004, 2006; Mojumder et al., 2007; 2008 mice: Miura et al., 2009; Smith et al., 2013; rabbits: Becker et al., 2015; frogs: Kupenova and Popova 2010). When studied in detail, we found in mice (Smith et al., 2015) that light adaptation during midday is unable to cause sufficient dopamine release to strongly suppress Na_v channels as seen in salamander (Ichinose and Lukasiewicz, 2007). At night, dopamine released during light adaptation is able to strongly suppress Na_v channels via D1R, leading to the robust daily rhythm that reduces ON-CBC function at midnight relative to midday as previously shown by others (Barnard et al., 2006; Cameron et al., 2008; Jackson et al., 2012; Storch et al., 2007). Consistent with this hypothesis, dopamine release driven by 90 min of light adaptation is significantly higher at circadian time (CT) 18 (equivalent to midnight) than CT6 (midday) in mice (Cameron et al., 2009). It is interesting to consider why mice avoid suppressing ON-CBC cell Na_v currents during light adaptation during the day in contrast to salamander. In ground squirrel, Na_v channels generate action potentials that are strongest during a flicker stimulus that should light adapt the retinas (Saszik & DeVries,

2012) and increase dopamine release (Dong and McReynolds, 1992). Suppressing light adaptation-dependent dopamine release onto ON-CBC D1Rs may maintain the ability for mice to encode stimuli with high temporal fidelity even in fully light-adapted conditions during the day.

Anatomically, there is evidence for dopamine type 1 receptors (D1Rs) on CBCs (Veruki and Wassle, 1996; Nguyen-Legros et al., 1997; Mora-Ferrer et al., 1999). ON CBCs that express Na_v channels can be immunolabeled with Protein Kinase C alpha (PKCα) antibody and in some cases PKCα staining intensity corresponds with size of Na_v currents (ground squirrel: Fig. 3 of Saszik and Devries 2012; also compare type 5 cells in table 1 in Light et al., 2012, Puller et al., 2011 to results from Saszik and DeVries, 2012; Primate DB4 cells: Haverkamp et al., 2003b; Lee and Grünert, 2007; compare to Puthussery et al., 2013). Recent evidence using D1R promoter-driven expression of fluorescent protein in mice supports the modulation of Na_v channels by D1 receptors in ON CBCs that express Na_v channels (5-2 and XBC, Farshi et al., 2016). At the same time OFF cells with Na_v channels (3A) are not fluorescent (Farshi et al., 2016) and, interestingly, ON cells without Na_v channels (5-1) and OFF cells with Na_v channels (3B) are not fluorescent. This is important given the extensive evidence of modulation of Na_v channels by PKC and PKA in response to dopamine (e.g. Cantrell and Catterall 2001, Scheuer 2011).

Na_v contributions to AII and vesicular glutamate transporter (VGLUT3+) glycinergic amacrine cells that contribute to excitatory pathways in the inner retina

AII amacrine cells are narrow field glycinergic interneurons that both electrically couple the output of the primary (rod to rod bipolar cell) rod-driven pathway to cone ON bipolar cells and provide inhibition to OFF cone bipolar cells and ganglion cells (Bloomfield and Dacheux, 2001; Tsukamoto et al., 2001; Manookin et al., 2008; Murphy and Rieke 2008; Münch et al., 2009). Although AIIs are generally considered to be a single subtype of glycinergic amacrine cell, there is evidence in mice that they are comprised of 3 identifiable physiological subtypes (Pang et al., 2012) and using dopamine D1 receptor promoter driven reporter gene expression found fluorescent

protein expression in only a subset (~25%) of mouse AII cells (Farshi et al., 2016) suggesting a heterogenous population.

In the primary rod pathway, AIIs increase the sensitivity (via convergence; Dunn et al., 2006) and redundancy (via divergence; Tsukamoto et al., 2001) of the primary rod pathway (reviewed in Demb and Singer 2012). In addition to convergence at the RBC to AII synapse, electrical synapses coupling AII cells are suggested to increase AII cell sensitivity in mesopic conditions. AII cells are coupled to other AII cells via homologous gap junctions formed by Connexin36 (Feigenspan et al., 2001; Mills et al., 2001) and to ON CBCs by heterologous gap junctions formed by Cx36 and Cx45 (Maxeiner et al., 2005). Coupling of AII cells varies as a U-shaped function of light adaptation (Bloomfield et al., 1997). Uncoupling in total darkness may reduce the dissipation of low intensity stimuli driving only a few rods with coupling in mesopic conditions improving signal to noise ratio by allowing synchronous responses in neighbouring AIIs to sum (suggested theoretically by Smith and Vardi, 1995). In addition to an excitatory role in the primary rod pathway (Famiglietti and Kolb 1975; reviewed in Bloomfield and Dacheux 2001), AII cells generate so-called crossover inhibition, ON pathway-derived feed-forward inhibition of the OFF pathway (Xin and Bloomfield 1999). Tonic glycine release by AIIs modulates OFF CBC and OFF RGC resting potentials, with disinhibition combined with excitation to increase the dynamic range of OFF RGCs (Manookin et al., 2008; Murphy and Rieke, 2006; Manookin et al., 2010). In light-adapted retina, AII-mediated crossover inhibition has been suggested to control the response of PV-5 RGCs (equivalent to transient OFF alpha cells: Sanes and Masland 2015) to approaching dark objects (Munch et al., 2009).

The main component of the AII light response is graded (e.g Xin and Bloomfield 1999) and AIIs seem to convey information predominately via graded potentials (e.g. Tian et al., 2010). However early results demonstrated that AII cells contain Na_v channels and generate Na_v channel-driven spikelets (Boos et al., 1993) and a number of recent papers have attempted to determine the anatomical distribution, identity, and functional roles of AII Na_v channels (Veruki and Hartveit, 2002a; Veruki and Hartveit, 2002b; Kaneko and Wantanabe 2007; Tamalu and Watanabe, 2007; Tian et al., 2010; Cembrowski et al., 2012; Trenholm et al., 2012; Choi et al., 2014; Wu et al., 2011). AII

cells don't spike in the conventional sense, i.e. like retinal ganglion cells with spikes showing a distinct refractory period initiated at the AIS, even though it has become apparent that AIIs have an AIS-like process that drives spiking (Wu et al., 2011; Cembrowski et al., 2012; Tsukamoto and Omi 2013). AII spikelets have smaller amplitudes, lower activation thresholds and little sign of after-hyperpolarization (Tamalu and Wantanabe 2007; Boos et al., 1993; Veruki & Hartveit, 2002a; Cembrowski et al., 2012; Wu et al., 2011). The spikelets observed in AII amacrine cells share many characteristics with dendritic spikelets observed in RGCs (Hidaka et al., 2004; Velte and Masland, 1999; Tayor et al, 2000; Sivyer and Williams 2013; Trenholm et al., 2014; Oesch et al., 2005) suggesting that they may play similar functional roles.

Whether AII spikelets encode information remains unresolved. Tamalu and Wantanabe (2007) found that AII spike frequency was determined both by membrane potential and by glutamatergic input. This seems to suggest that spikelets carry information and may be important, potentially in combination with gap junctional coupling, in improving the signal to noise ratio in the primary rod pathway. In light-adapted retina Na_v channels boosted rod bipolar cell-derived threshold stimulus derived EPSCs in AII cells but in scotopic conditions, when threshold EPSCs might reasonable be expected, TTX did not substantially affect light evoked currents in OFF or ON RGCs (Tian et al., 2010) driven by AII cells. Light evoked spikelets have been recorded in dark-adapted rabbit AIIs (Bloomfield and Xin, 2000) arguing that the lack of affect of TTX on light evoked EPSCs in RGCs is not because spikelets are absent in dark-adapted retina. AII Na_v channels did however slightly increase the speed of the correlated AII input to ON and OFF transient RGCs (Tian et al., 2010). One possibility suggested by Tian et al. (2010) is that the AII cell is too depolarized in dark-adapted conditions to generate spikelets.

Cembrowski et al., (2012; see also Choi et al., 2014) suggest an interesting hypothesis based on their findings that the pattern of AII spikelets changes from bursting to tonic spiking depending on the level of membrane depolarization. Results from Cembrowski et al. (2012), Choi et al. (2014) and Trenholm et al. (2012) suggest that membrane hyperpolarization in AIIs can be driven by coupled ON CBCs, moving the AII spikelet pattern in the bursting direction. Notably at the same time AIIs are highly

coupled in mesopic conditions ON CBCs would be hyperpolarized by tonic glutamate release from cones because ambient light levels are below the cone threshold (Cembrowski et al., 2012; Choi et al., 2014). Na_v channel dependent spikelets might therefore contribute to AII cell signaling in specific ambient lighting conditions missed by the experiments of Tian et al. (2010). Recordings from coupled pairs of AII cells (Veruki & Hartveit, 2002a) and coupled AII to ON CBCs (Veruki & Hartveit, 2002b) show that spikes in one cell can drive slow membrane depolarizations in the coupled cell, synchronizing subthreshold membrane potential oscillations. Bursting may generate lower temporal resolution events to reduce the low pass filtering effects of gap junctions (Veruki and Hartviet 2002a,b). Coupling in combination with bursting may synchronize and amplify threshold events across coupled AIIs (e.g. Tian et al., 2010; Cembroski et al., 2012) as a way to increase signal to noise ratio in the highly coupled AII network in mesopic conditions.

Interactions between highly coupled neurons with spikelets produced by dendritic Na_v channels have been relatively well studied in directionally selective RGCs. In both ON- (Sivyer and Williams 2013) and ON-OFF- directionally selective (DS: Oesch et al., 2005; Trenholm et al., 2014) RGCs, Na_v channels support active dendritic conductances that enhance information processing. In the HB9+ subtype of ON-OFF DS cells, Na_v dendritic channels facilitate synchronous responses in neighbouring cells by enabling back-propagation of somatic action potentials and allowing current to pass through electrical synapses to neighbouring cells (Trenholm et al., 2014). The combination of back-propagating dendritic spikelets and temporally coincident synaptic input triggers somatic action potentials in neighbouring cells with high synchrony (Trenholm et al., 2014). AII cells are not directionally selective however a similar combination of gap-junctional coupling and dendritic spikelets may enhance synchrony between AII light responses during mesopic conditions when AII cells are highly coupled. It is also possible that spikelets in AII cells that are coupled to Na_v channel-expressing ON bipolar cells may drive spiking in these cells. Spikelets produced in active dendrites could prevent dissipation of electrical signals across the highly coupled AII network and facilitate synchronous signaling in neighbouring AII cells increasing signal to noise ratio (Smith and Vardi, 1995) .

Could bursting in AII cells drive highly correlated firing in retinal ganglion cells under some circumstances? In the *rd1* model of retinal degeneration in mice this seems to be the case (Choi et al., 2014). It is well known that in this model, both ON and OFF, α-RGCs show synchronized 10 hz oscillations in spike rate following loss of photoreceptor function (Margolis et al., 2008; Borowska et al., 2011; Menzler and Zeck 2011; Trenholm et al., 2012) that is anti-correlated between ON and OFF cells (Margolis et al., 2014) suggesting that oscillations in a single source drives both ON and OFF α-RGC oscillatory spiking. Synchronized spiking in the ON pathway disappears following the application of gap junction blockers (Menzler and Zeck 2011; Borowska et al., 2011; Trenholm et al., 2012) or genetic ablation of Cx36 (Ivanova et al., 2015), as well as following the application of TTX (Trenholm et al., 2012; Choi et al., 2013; Margolis et al., 2014). Choi et al. (2014) suggest that *rd1* oscillations are directly due to hyperpolarization in ON CBCs coupled to AIIs paired with Na_v channels and a slow, M-type K^+ conductance (similar to the wild type AIIs in Cembrowski al., 2012). If this is the case, hyperpolarization of ON CBCs in response to release of glutamate below the cone threshold may have a functional role in normal retina. If, however, the oscillations in *rd1* mice are an emergent property of the coupled ON CBC AII network in degenerated retina (Trenholm et al., 2012; Borowska et al., 2011; reviewed in Trenholm and Awatramani 2015) they may be due to degeneration-induced remodeling following retinal degeneration. Supporting the former hypothesis, hyperpolarizing ON CBCs pharmacologically with L-AP4 in combination with CNQX (reducing inhibition and AII input from RBCs) causes oscillations in wildtype retina (Trenholm et al., 2012). In addition the results of Choi et al. (2014) support a model in which hyperpolarization of either wildtype or *rd1* AII amacrine cells can drive network oscillations.

Together the results in *rd1* mice show that Na_v-dependent oscillations can drive anti-correlated release in ON and OFF RGCs via glycinergic inhibtion (OFF cells) and electrical synaptic input to ON CBCs then ON RGCs. Although recent research both in normal and *rd1* mice has expanded knowledge regarding potential functional roles of AII spikelets and isolated the anatomical structure driving spike generation, the precise function of AII spikelets remains a puzzle. However, recent research expressing channelrhodopsin-2 targeted to the AIS-like lobe of AII cells (Wu et al., 2011) combined

with multielectrode array recording could be a plausible method of resolving this question by directly showing the effects of lobe driven spikelets on RGC firing under various light conditions.

Functional consequences of AII cell modulation by dopamine

There is no direct evidence for dopaminergic modulation of Na_v channels on AII cells. At the same time, there is indirect evidence that dopamine acting through D1Rs is involved in the modulation of gap junctional coupling of AII cells via phosphorylation (Hampson et al., 1992; Kothmann et al., 2009). If dopamine modulates gap junctional coupling of AII cells, its D1R-coupled second messengers, such as cAMP, may also modulate Na_v channels. Anatomically, dopaminergic amacrine cells form ring-like structures surrounding AII cells (Debertin et al., 2015; Volygi et al., 2014). Kothmann et al. (2009) show that a D1R agonist modulates phosphorylation of Cx36 via a pathway that involves PKA modulation of protein phosphatase 2a. A number of other studies have shown similarities between D1R agonist and membrane-permeable cAMP analog modulation of AII cell coupling (Mills & Massey, 1995; Xia & Mills, 2004; Urschel et al., 2006; Kothmann et al., 2009). DARPP-32, a dopamine and cAMP-regulated phosphoprotein is expressed by AII cells (Partida et al., 2004; Witkovsky et al., 2007; Kothman et al., 2009) supporting the possibility that dopamine modulates AII cell function.

However, while there is evidence that D1Rs and PKA modulate AII cell coupling, it is controversial whether AII cells express D1Rs. Using immunohistochemistry in rat Veruki et al. (1996) did not find them while Nguyen-Legros et al. (1997) did. In addition, Singer did not find that GFP-driven by the D1R promoter shows up in AII cells in mice (unpublished but referred to in Demb and Singer, 2012). These unpublished experiments in combination with results from single examples of recordings from coupled pairs of AII cells (Hartveit and Veruki, 2012) suggest that junctional conductance between coupled AII cells are not changed by D1R agonists and antagonists. In contrast a similar experiment using D1R driven reporter gene expression found that the D1R promoter drives fluorescent protein expression in a subset (~25%) of AII cells (Farshi et al., 2016).

As mentioned above, shifts in light adaptation may play a role in the shift from bursting to tonic spiking in AIIs. Given that this might involve changes in gap junctional coupling between AIIs, removal of ON CBC hyperpolarization and potentially dopaminergic modulation of AII and ON CBC Na_v channels, it is difficult to predict how this might change AII input to RGCs. Given that AIIs are known to feed forward to the largest, well-characterized and easily identifiable RGC class in mice the ON, OFF transient and OFF sustained alpha cells (e.g. Tian et al., 2010), in theory it should be possible to determine functional roles of AII spiking during light adaptation and whether dopamine acts as a gain control by modulating Na_v channels, similar to salamander ON CBCs (Ichinose and Lukasiewicz, 2007).

VGLUT3+ Amacrine cells

VGLUT3+ amacrine cells are medium field ON-OFF glycinergic cells first described by Fremeau et al. (2002) Haverkamp and Wassle (2003) and Johnson et al., (2004). Interestingly, for the normally inhibitory amacrine cells VGLUT3+ cells release glutamate (Lee et al., 2014) as well as glycine. Recently it has been shown that VGLUT3+ cells provide excitatory glutamatergic input to W7 (transient OFF alpha cells, Kim et al., 2010), ON-OFF directionally selective cells, ON DS and the small W3 ganglion cell (Zhang et al., 2012; Kim et al., 2015; Krishnaswarmy et al., 2015; Lee et al. 2014, 2016). Krishnaswarmy et al. (2015) found that the input from VGLUT3+ cells was much stronger to W3B cells relative to the other synaptic partners, consistent with the findings of Kim et al. (2015) suggesting that VGLUT3+ cells play a robust role in the circuit controlling feature selectivity of W3B cells (Krishnaswarmy et al., 2015; Kim et al., 2015). W3 cells signal differential motion of an object on a stationary background at high resolution (Zhang et al., 2012; Baccus et al., 2008; Krishnaswarmy et al., 2015; Kim et al., 2015). VGLUT3+ cells also inhibit the asymmetric ON-OFF DS cells described in Trenholm et al. (2011; 2013) and transient OFF alpha cells (Lee et al., 2016). In addition to excitatory signaling, VGLUT3+ cells inhibit type-2 tyrosine hydroxylase expressing wide field amacrine cells (Knop et al., 2011) as well as suppressed by contrast (aka uniformity detector) retinal ganglion cells (Lee et al., 2016).

VGLUT3+ cells contain TTX sensitive Na_v channels (Grimes et al., 2011; Johnson et al., 2004) but generate only a single spike in response to light. Grimes et al., (2011), found that blocking Na_v channels reduced the post-synaptic response to excitatory input from bipolar cells. In addition, although preliminary, an abstract from Lee et al., (2015) reported that TTX suppresses the fast transient response in post-synaptic partners of VGLUT3+ cells. What functional role might Na_v channels in VGLUT3+ amacrine cells play in object motion sensitivity? W3B cells fire when motion in the center and surround of the receptive field occurs asynchronously (Kim et al., 2010; Baccus et al., 2008; Olveczky et al., 2003; Krishnaswarmy et al., 2015). Spiking in the intermediary VGLUT3+ cells may contribute to temporal precision between excitation and inhibition derived from wide field spiking amacrine cells in object-motion sensitive (OMS) circuitry (Kim et al., 2010; Baccus et al., 2008; Kim et al., 2015). However arguing against a critical role for Na_v channels in the post synaptic response of VGLUT3+ cells, central responses to object motion were not affected following the application of TTX (Kim et al., 2015). It is possible that the amplifying effect of Na_v channels is specific to full-field stimulation (Grimes et al., 2011) or that because TTX reduced inhibition of VGLUT3+ cells derived from wide field amacrine cells it may have obscured effects on excitatory input from bipolar cells. Because optogenetic and reporter gene expression tools targeting this amacrine cell subtype have only recently been generated the role of Na_v channels in VGUT3+ cells is largely a mystery. However both Lee et al., (2015) and Lee et al., (2016) contain speculative comments regarding the dendritic mechanisms that might play a role in glutamate vs. glycine release from VGUT3+ cells indicating that this is an ongoing project in the Zhou lab.

Starburst amacrine cells

Starburst amacrine cells are radially symmetrical interneurons that play important roles in computing directional selectivity and in retinal waves that direct early retinal development. Ablation of SBACs suppresses directionally selective signaling (Yoshida et al., 2001; Amthor et al., 2002). SBACs respond more strongly to centrifugal rather than centripetal motion, with conclusive recent evidence showing that the computation of direction selectivity occurs in the distal dendrites of SBACs (Fried et al., 2002, 2005; Lee & Zhou, 2006; Zhou & Lee, 2008; Wei et al., 2011; Yonehara et al., 2011; Briggman et

al., 2011; Yonehara et al., 2013). Starburst amacrine cells (SBAC) generate membrane potential oscillations spontaneously {PetitJacques:2005dm}, after electrical stimulation {Tsai:2011hm}, and following light stimulation {PetitJacques:2008gs}. In the retina $Na_v1.8$, a TTX-resistant voltage-gated sodium channel (Na_v) which generates a persistent sodium current {Akopian:1996hw, Akopian:1997wm} and is partially (40%) resistant to inactivation caused by high frequency (>20 Hz) depolarization {Vijayaragavan:2001wl}, is expressed in SBACs {OBrien:2008ki} and a subset of RGCs. Rabbit SBACs have been shown to have a TTX-resistant and ambroxol-sensitive Na_v current that contributes to the light response to centrifugal motion {Oesch:2010hl}.

The existence of Na_v channels and spikes in SBACs is controversial. In mice, Ozaita et al. (2004), Kaneda et al. (2007) and Petit-Jacques et al. (2008) did not find a TTX-sensitive inward current recording directly from SBACs *in vitro*. At the same time Ozaita et al., (2004) did report a transient component at the onset of depolarizing steps in current clamp that was resistant to TTX (their Fig 1a) and is similar in appearance to spikelets recorded from AII amacrine cells (e.g. Tian et al., 2010). In rabbit, Cohen (2001) reports a TTX-sensitive current, while Bloomfield (1992) and Gavrikov et al. (2003) report SBAC spiking, whereas Taylor and Wassle (1995) and Peters and Masland (1996) did not. Interestingly, Zhou and Fain (1996) did find a TTX-sensitive spiking current in SBACs, but only in juvenile retinas. Oesch and Taylor (2010) found a TTX-resistant current that contributes to directional responses in SBACs in rabbit retina.

One issue with previous physiological measurement of Na_v current in SBACs is that they relied on patch-clamp recordings. The differences found using that technique, even within species, suggest that *in vitro* preparations may not accurately measure Na_v channel function in SBACs. Due to the long length of SBAC dendritic processes relative to the small soma, adequate space clamp may be an issue especially if $Na_v1.8$ is expressed predominately in dendritic tips (e.g. Bar-Yehuda and Korngreen, 2008; Williams and Mitchell, 2008; Schachter et al., 2010; Poleg-Polsky and Diamond, 2011). Recent models of SBACs include $Na_v1.8$ specifically in medial and distal dendritic segments (Ding et al., 2016).

Connectivity of Na_v-expressing elements in the inner retina

Recent research has defined new roles for Na_v channels in excitatory pathways in the inner retina. The rarity of Na_v channels within these cell types (bipolar cells and small and medium field amacrine cells) has led to the generalization that these cell types signal only via graded potentials and lack Na_v channels. Might the sparsity of Na_v channels in these cells define processing properties of individual parallel pathways within the retina? I looked for evidence for synaptic links between Na_v expressing CBC subtypes and the AII, SBAC, and VGLUT3+ amacrine cells. There is no evidence for increased coupling between between AII amacrine cells and Na_v channel expressing ON CBC subtypes, (e.g. Helmstaedtler et al., 2013). However, there is some evidence suggesting that VGLUT3+ amacrine cells interact with Na_v channel-expressing bipolar cells and share a common projection to the W3B RGC cell subtype.

Local edge detectors (LEDs), first described in the rabbit (Levick 1967, Cleland & Levick 1974b; Van Wyk et al. 2006, Baccus et al. 2008, Russell and Werblin 2010) are homologous to the mouse W3B RGC type (Kim et al., 2010; Zhang et al., 2012; Krishnaswamy et al., 2015 Kim et al., 2015). W3B cells have small dendritic fields with dendritic arbors that cover multiple layers in the middle of the IPL (Zhang et al., 2012). W3B cells are transient ON-OFF cells and are tuned both for high spatial frequency vision and objects that move independent of the background of the visual mileau (Zhang et al., 2012), so called object motion sensitive cells (Olveczky et al. 2003, 2007; Baccus et al. 2008). Under normal circumstances with extensive global motion (images projected on a mouse retina from a camera mounted on a rats head) W3B cells are silent (Zhang et al., 2012) however as hypothesized by Levick (1967) who suggested that rabbit LEDs are optimized to see aerial predators W3B mice will response strongly to the movement of a moving owl siloutte at the right height to cover only the small receptive field centers (Zhang et al., 2012).

In mice, rats and primates, calcium-binding protein CaB5+ bipolar cells ramify close to the center of the IPL and appear to be morphologically similar between species (see Fig. 8 Ghosh et al., 2004 also Havekamp et al., 2003). In rats, mice and primates, subtypes of these cells (DB3 and DB4 and type 3 and 5 cells respectively) are know to express Na_v channels (Puthussery et al., 2013; Cui and Pan 2008; Hellmar et al., 2016). In

mice, rats and primates VGLUT3+ processes ramify in layers 2 and 3 in the middle of the IPL with CaB5+ bipolar cells (Havercamp and Wassle 2004). VGLUT3+ cells project to W3B RGCs (Krishnaswamy et al., 2015 Kim et al., 2015) that also receive input from Na_v channel expressing 3a, 5a, and XBC types of cone bipolar cells (Helmstaedter et al., 2013). On the other hand, excitatory input to VGLUT3+ cells from bipolar cells does not appear to be enhanced by presynaptic Na_v channels in mice (Grimes et al., 2011) arguing against a comprehensive role of Na_v channels in this pathway.

Inhibition in response to global motion depends on Na_v channels and the extent of the inhibitory surround is large suggesting that it is mediated by polyaxonal cells as mentioned in Olveczky et al. (2003, 2007) and Baccus et al. (2008). W3B cells receive excitatory glutamatergic input from VGlut3+ cells (Krishnaswamy et al., 2015 Kim et al., 2015; Lee et al., 2016) driving some but not all of their spiking response to differential motion in the receptive field center (~50% reduction Kim et al., 2015) and eliminating the OFF component of the transient ON-OFF response to a light step (Krishnaswamy et al., 2015).

Although the roles of Na_v channels in excitatory pathways require further clarification, one common functional role of Na_v channels in VGLUT3+ amacrine cells and CBCs appears to be the amplification of graded potentials, possibly with spikes generated in response to select stimuli or as an epiphenomenon. On the other hand, TTX has only a small effect on the graded response of AII amacrine cells (Tian et al., 2010) indicating that Na_v channels may play a different role in these cells. At the same time both cone bipolar cells and VGLUT3+ cells seem to produce single action potentials in response to light while AII cells produce trains of small spikelets without discernable refractory periods. If the hypothesis proposed by Cembrowski et al. (2012) is correct, AIIs, like directionally selective RGCs, may be an example of Na_v channels in active dendrites working to drive synchronous responses in gap junctionally coupled cells. In both cases whether spikelets and spikes are an epiphenomenon due to the presence of Na_v channels rather than directly encoding information remains to be resolved. In addition to direct roles in information processing, Na_v channels may provide a means to modulate gain in excitatory pathways in response to slower changes in ambient illumination

signaled by shifts in retinal dopamine levels (Ichinose and Lukasiewicz, 2007; Smith et al., 2014; Hellmar et al., 2016; Farshi et al., 2016).

CONCLUSION

Faced with the daunting task of understanding the retina it is not surprising that most early research was focused on discovering generalities common within morphologically distinct cell classes in the retina. However recent improvements allowing *in vivo* visualization and directed recordings from amacrine and bipolar cell subtypes have revealed exceptions to many of these generalizations. Here I focused on new results highlighting Na_v channel function and spiking in classically graded or analog cell types. Although much of the function of Na_v channels expressed in predominately graded cell types remains a mystery some similarities have emerged between reports. Evidence for Na_v channels in photoreceptor function exists only in photoreceptors harvested from human retina and only from one research group suggesting that Na_v channels do not commonly contribute to photoreceptor function. In horizontal cells both morphological and physiological results from a range of model species suggests that Na_v channel expression may be a common feature of horizontal cells. However the role of Na_v channels in mammalian horizontal cells and whether these cells ever spike in response to light remains unknown.

Unlike the outer retina there is considerable recent evidence supporting novel Na_v channel contributions to specific excitatory pathways in the inner retina. While the precise function of Na_v channels is not completely understood Na_v channels in both transient cone bipolar cells and VGLUT3+ cells appear to both produce single spikes as well as acting to amplify graded potentials in response to light and electrical stimulation (Bipolar cells: Cui and Pan 2008; Ichinose and Lukasiewicz 2007; Saszik and Devries 2012; Puthussery et al., 2013; VGLUT3+: Grimes et al., 2011). In contrast Na_v channels in AII amacrine cells may fulfill a different role. Although threshold level EPSCs are amplified by Na_v channels the graded component of AII cell voltage responses to depolarizing current is similar in magnitude after TTX (Cembrowski et al., 2012; Tian et al., 2010), and light responses in rabbit AIIs are increased in response to TTX (Bloomfield and Xin, 2000). Although speculative Cembrowski et al. (2012) suggest that

bursts of Na_v channel dependent spikelets could synchronize responses in the highly coupled AII network in mesopic conditions, increasing signal to noise ratio and reducing signal dissipation.

APPENDIX II: Copyrights

License Number 4130871286575
License date Jun 16, 2017
Licensed Content Publisher Elsevier
Licensed Content Publication Experimental Eye Research
Licensed Content Title Voltage-gated sodium channels contribute to the b-wave of the rodent electroretinogram by mediating input to rod bipolar cell GABAc receptors
Licensed Content Author Benjamin J. Smith,François Tremblay,Patrice D. Côté
Licensed Content Date Nov 1, 2013
Licensed Content Volume 116
Licensed Content Issue n/a
Licensed Content Pages 12
Start Page 279
End Page 290
Type of Use reuse in a thesis/dissertation
Portion full article
Format both print and electronic
Are you the author of this Elsevier article? Yes
Will you be translating? No
Order reference number
Title of your thesis/dissertation Contribution of individual Nav channel isoforms to the development and function of the retina.
Expected completion date Aug 2017
Estimated size (number of pages) 200
Elsevier VAT number GB 494 6272 12
Requestor Location Mr. Benjamin Smith
15 Mahar Dr.
Shad Bay, NS B3T 2B6
Canada
Attn: Mr. Benjamin Smith
Total 0.00 USD

License Number 4134360872458
License date Jun 22, 2017
Licensed Content Publisher Elsevier
Licensed Content Publication Neuroscience
Licensed Content Title Contribution of Nav1.8 sodium channels to retinal function
Licensed Content Author Benjamin J. Smith,Patrice D. Côté,François Tremblay
Licensed Content Date Jan 6, 2017
Licensed Content Volume 340
Licensed Content Issue n/a
Licensed Content Pages 12
Start Page 279
End Page 290
Type of Use reuse in a thesis/dissertation
Portion full article
Format both print and electronic
Are you the author of this Elsevier article? Yes
Will you be translating? No
Order reference number
Title of your thesis/dissertation Contribution of individual Nav channel isoforms to the development and function of the retina.
Expected completion date Aug 2017
Estimated size (number of pages) 200
Elsevier VAT number GB 494 6272 12
Requestor Location Mr. Benjamin Smith
15 Mahar Dr.
Shad Bay, NS B3T 2B6
Canada
Attn: Mr. Benjamin Smith
Total 0.00 USD

BIBLIOGRAPHY

Abd-El-Barr MM, Pennesi ME, Saszik SM, Barrow AJ, Lem J., Bramblett DE, Paul DL, Frishman LJ, Wu SM. Genetic dissection of rod and cone pathways in the dark-adapted mouse retina. J. Neurophysiol. 2009; 102, 1945-1955.

Ahern CA, Payandeh J, Bosmans F, Chanda B. The hitchhiker's guide to the voltage-gated sodium channel galaxy. J Gen Physiol 2016; 147(1), 1-24.

Akimov NP and Renteria RC. Dark rearing alters the normal development of spatiotemporal response properties but not of contrast detection threshold in mouse retinal ganglion cells. Dev Neurobiol. 2014; 74(7), 692-706.

Akopian AN, Sivilotti L, Wood JN. A tetrodotoxin-resistant voltage-gated sodium channel expressed by sensory neurons. Nature 1996 379:257–262.

Akopian AN, Souslova V, England S, Okuse K, Ogata N, Ure J, Smith A, Kerr BJ, McMahon SB, Boyce S, Hill R, Stanfa LC, Dickenson AH, Wood JN. The tetrodotoxin-resistant sodium channel SNS has a specialized function in pain pathways. Nat Neurosci. 1999; 2(6), 541-8.

Akrouh A and Kerschensteiner D. Morphology and function of three VIP-expressing amacrine cell types in the mouse retina. J Neurophysiol. 2015 Oct;114(4):2431-8.

Alarcón-Martínez L, Avilés-Trigueros M, Galindo-Romero C, Valiente-Soriano J, Agudo-Barriuso M, Villa P de L, Villegas-Pérez MP, Vidal-Sanz M. ERG changes in albino and pigmented mice after optic nerve transection. Vision Res 2010; 50, 2176–2187.

Alexandrou AJ, Brown AR, Chapman ML, Estacion M, Turner J, Mis MA, Wilbrey A, Payne EC, Gutteridge A, Cox PJ, Doyle R, Printzenhoff D, Lin Z, Marron BE, West C, Swain NA, Storer RI, Stupple PA, Castle NA, Hounshell JA, Rivara M, Randall A, Dib-Hajj SD, Krafte D, Waxman SG, Patel MK, Butt RP, Stevens EB. Subtype-Selective Small Molecule Inhibitors Reveal a Fundamental Role for Nav1.7 in Nociceptor Electrogenesis, Axonal Conduction and Presynaptic Release. PLoS One. 2016 Apr 6;11(4):e0152405.

Aman TK, Raman IM. Subunit dependence of Na channel slow inactivation and open channel block in cerebellar neurons. Biophys J 2007; 92(6), 1938-51

Aman TK and Raman IM. Inwardly permeating Na ions generate the voltage dependence of resurgent Na current in cerebellar Purkinje neurons. J Neurosci 2010; 30(16), 5629-34.

Amthor FR, Keyser KT, Dmitrieva NA. Effects of the destruction of starburst-cholinergic amacrine cells by the toxin AF64A on rabbit retinal directional selectivity. Vis Neurosci 2002; 19, 495–509.

Armstrong F and Bezanilla CM Inactivation of the sodium channel. I. Sodium current experiments. OR Inactivation of the sodium channel. II. Gating current experiments. J Gen Physiol 1977; 70(5), 549-66.

Awatramani G, Wang J, Slaughter MM. Amacrine and ganglion cell contributions to the electroretinogram in amphibian retina. Vis Neurosci 2001; 18(1), 147-56.

Awatramani GB, Slaughter MM. Origin of transient and sustained responses in ganglion cells of the retina. J Neurosci 2000; 20(18), 7087-95.

Baccus SA, Olveczky BP, Manu M, Meister M. A retinal circuit that computes object motion. J Neurosci 2008; 28(27), 6807-17.

Baden T, Esposti F, Nikolaev A, Lagnado L. Spikes in retinal bipolar cells phase-lock to visual stimuli with millisecond precision. Curr Biol 2011; 21(22), 1859-69.

Baden T, Berens P, Bethge M, Euler T. Spikes in mammalian bipolar cells support temporal layering of the inner retina. Curr Biol 2013; 23(1), 48-52.

Baden T, Berens P, Franke K, Román Rosón M, Bethge M, Euler T. The functional diversity of retinal ganglion cells in the mouse. Nature 2016; 529(7586), 345-50.

Balasubramanian V, Berry MJ 2nd. A test of metabolically efficient coding in the retina. Network. 2002 Nov;13(4):531-52.

Balasubramanian V, Kimber D, Berry MJ 2nd. Metabolically efficient information processing. Neural Comput 2001;13(4):799-815.

Balkowiec A, Katz DM. Activity-dependent release of endogenous brain-derived neurotrophic factor from primary sensory neurons detected by ELISA in situ. J Neurosci 2000; 20(19), 7417-23.

Balkowiec A, Katz DM. Cellular mechanisms regulating activity-dependent release of native brain-derived neurotrophic factor from hippocampal neurons. J Neurosci 2002; 22(23), 10399-407.

Bar-Yehuda D, Korngreen A. Space-clamp problems when voltage clamping neurons expressing voltage-gated conductances. J Neurophysiol 2008; 99, 1127–36.

Barnard AR, Hattar S, Hankins MW, Lucas RJ. Melanopsin regulates visual processing in the mouse retina. Curr Biol 2006; 16: 389–95.

Barnes S, Deschênes MC. Contribution of Ca and Ca-activated Cl channels to regenerative depolarization and membrane bistability of cone photoreceptors. J Neurophysiol 1992; 68(3), 745-55.

Barnes S, Hille B. Ionic channels of the inner segment of tiger salamander cone photoreceptors. J Gen Physiol 1989; 94(4), 719-43.

Baro JA, Lehmkuhle S, Kratz KE. Electroretinograms and visual evoked potentials in long-term monocularly deprived cats. Invest Ophthalmol Vis Sci 1990; 31(7), 1405-9.

Baylor DA, Fettiplace R. Synaptic drive and impulse generation in ganglion cells of turtle retina. J Physiol 1979; 288, 107-27.

Becker S, Jayaram H, Holder GE, Limb GA. Contribution of Voltage-Gated Sodium Channels to the Rabbit Cone Electroretinograms. Curr Eye Res 2016; 41(4), 569-73.

Berry MJ, Brivanlou IH, Jordan TA, Meister M. Anticipation of moving stimuli by the retina. Nature 1999; 398, 334–8.

Berson DM. Strange vision: ganglion cells as circadian photoreceptors. Trends Neurosci 2003; 26: 314–20.

Berson DM, Dunn FA, Takao M. Phototransduction by retinal ganglion cells that set the circadian clock. Science 2002;295(5557), 1070-3.

Blanco R, de la Villa P. Ionotropic glutamate receptors in isolated horizontal cells of the rabbit retina. Eur J Neurosci 1999;11(3), 867-73.

Bloomfield SA. Relationship between receptive and dendritic field size of amacrine cells in the rabbit retina. J Neurophysiol 1992 68:711–25.

Bloomfield SA. Effect of spike blockade on the receptive-field size of amacrine and ganglion cells in the rabbit retina. J Neurophysiol 1996; 75(5), 1878-93.

Bloomfield SA, Dacheux RF. Rod vision: pathways and processing in the mammalian retina. Prog Retin Eye Res 2001; 20(3), 351-84.

Bloomfield SA, Xin D, Osborne T. Light-induced modulation of coupling between AII amacrine cells in the rabbit retina. Vis Neurosci 1997;14(3), 565-76.

Boiko T, Rasband MN, Levinson SR, Caldwell JH, Mandel G, Trimmer JS, Matthews G. Compact myelin dictates the differential targeting of two sodium channel isoforms in the same axon. Neuron 2001; 30, 91–104.

Boiko T, Van Wart A, Caldwell JH, Levinson SR, Trimmer JS, Matthews G. Functional specialization of the axon initial segment by isoform-specific sodium channel targeting. J Neurosci 2003; 23(6), 2306-13.

Boos R, Schneider H, Wässle H. Voltage- and transmitter-gated currents of all-amacrine cells in a slice preparation of the rat retina. J Neurosci 1993; 13(7): 2874-88.

Borghuis BG, Looger LL, Tomita S, Demb JB. Kainate receptors mediate signaling in both transient and sustained OFF bipolar cell pathways in mouse retina. J Neurosci 2014; 34(18), 6128-39.

Borowska J, Trenholm S, Awatramani GB. An intrinsic neural oscillator in the degenerating mouse retina. J Neurosci 2011; 31, 5000-12.

Brecha N. Peptide and Peptide Receptor Expression and Function in the Vertebrate Retina. The Visual Neurosciences. Ed. Chalupa LM, Ed. Werner JS. MIT Press, 2004 334-54.

Brette R: Philosophy of the Spike: Rate-Based vs. Spike-Based Theories of the Brain. Front Syst Neurosci 2015; 9, 151-64.

Breuninger T, Puller C, Haverkamp S, Euler T. Chromatic bipolar cell pathways in the mouse retina. J Neurosci 2011; 31(17), 6504-17.

Briggman KL, Helmstaedter M, Denk W. Wiring specificity in the direction-selectivity circuit of the retina. Nature 2011 471:183–188.

Burrone J, Lagnado L. Electrical resonance and Ca2+ influx in the synaptic terminal of depolarizing bipolar cells from the goldfish retina. J Physiol 1997; 505, 571-84.

Bui BV, Armitage JA, Vingrys AJ. Extraction and modelling of oscillatory potentials. Doc ophthalmol 2002 104:17–36.

Bui B., Fortune B. Ganglion cell contributions to the rat full-field electroretinogram. J. Physiol 2004; 555, 153-73.

Bui BV, Fortune B. Origin of electroretinogram amplitude growth during light adaptation in pigmented rats. Vis. Neurosci 2006; 23, 155-67.

Burbidge SA1, Dale TJ, Powell AJ, Whitaker WR, Xie XM, Romanos MA, Clare JJ. Molecular cloning, distribution and functional analysis of the $Na_v1.6$. Voltage-gated sodium channel from human brain. Brain Res Mol Brain Res 2002; 103(1-2), 80-90.

Caldwell JH, Schaller KL, Lasher RS, Peles E, Levinson SR. Sodium channel Na(v)1.6 is localized at nodes of ranvier, dendrites, and synapses. Proc Natl Acad Sci USA 2000; 97, 5616–20.

Cameron MA, Barnard AR, Hut RA, et al. Electroretinography of wild-type and Cry mutant mice reveals circadian tuning of photopic and mesopic retinal responses. J Biol Rhythms 2008a; 23: 489–501.

Cameron MA, Barnard AR, Lucas RJ. The electroretinogram as a method for studying circadian rhythms in the mammalian retina. J Genet 2008b; 87: 459–66.

Cameron MA, Pozdeyev N, Vugler AA, Cooper H, Iuvone PM, Lucas RJ. Light regulation of retinal dopamine that is independent of melanopsin phototransduction. Eur J Neurosci 2009; 29(4), 761-7.

Cantrell AR, Catterall WA. Neuromodulation of Na+ channels: an unexpected form of cellular plasticity. Nat Rev Neurosci 2001; 2(6), 397-407.

Catterall WA. Voltage-gated sodium channels at 60: structure, function and pathophysiology. J Physiol 2012; 590, 2577–89.

Catterall WA. From ionic currents to molecular mechanisms: the structure and function of voltage-gated sodium channels. Neuron 2000; 26, 13–25.

Cao Y, Pahlberg J, Sarria I, Kamasawa N, Sampath AP, Martemyanov KA. Regulators of G protein signaling RGS7 and RGS11 determine the onset of the light response in ON bipolar neurons. Proc Natl Acad Sci USA 2012; 109(20), 7905-10.

Carras PL, Coleman PA, Miller RF. Site of action potential initiation in amphibian retinal ganglion cells. J Neurophysiol 1992; 67(2), 292-304.

Carter BC, Giessel AJ, Sabatini BL, Bean BP. Transient sodium current at subthreshold voltages: activation by EPSP waveforms. Neuron 2012; 75(6), 1081-93.

Castilho A, Ambrosio AF, Harveit, E, Veruki, ML. Disruption of a neural microcircuit in the rod pathway of the mammalian retina by diabetes mellitus. J Neurosci 2015: 35(13), 5422–33.

Catterall WA (2000) From ionic currents to molecular mechanisms: the structure and function of voltage-gated sodium channels. Neuron 26:13–25.

Cellerino A, Kohler K. Brain-derived neurotrophic factor/neurotrophin-4 receptor TrkB is localized on ganglion cells and dopaminergic amacrine cells in the vertebrate retina. J Comp Neurol 1997; 386, 149–60.

Cembrowski MS, Logan SM, Tian M, Jia L, Li W, Kath WL, Riecke H, Singer JH. The mechanisms of repetitive spike generation in an axonless retinal interneuron. Cell Rep 2012;1(2), 155-66.

Cepeda C, Chandler SH, Shumate LW, Levine MS. Persistent Na+ conductance in medium-sized neostriatal neurons: characterization using infrared videomicroscopy and whole cell patch-clamp recordings. J Neurophysiol 1995; 74(3), 1343-8.

Chan YC, Chiao CC. Effect of visual experience on the maturation of ON-OFF direction selective ganglion cells in the rabbit retina. Vision Res 2008; 48(23-24), 2466-75.

Chang B1, Heckenlively JR, Bayley PR, Brecha NC, Davisson MT, Hawes NL, Hirano AA, Hurd RE, Ikeda A, Johnson BA, McCall MA, Morgans CW, Nusinowitz S, Peachey NS, Rice DS, Vessey KA, Gregg RG. The nob2 mouse, a null mutation in Cacna1f: anatomical and functional abnormalities in the outer retina and their consequences on ganglion cell visual responses. Vis Neurosci 2006; 23(1), 11-24.

Chaplin C, Borchert MS, Fink C, Garcia-Filion P, McCulloch DL. Light-adapted electroretinograms in optic nerve hypoplasia. Doc Ophthalmol 2009; 119, 123–32.

Chávez AE, Singer JH, Diamond JS. Fast neurotransmitter release triggered by Ca influx through AMPA-type glutamate receptors. Nature 2006; 443(7112), 705-8.

Chávez AE, Grimes WN, Diamond JS Mechanisms underlying lateral GABAergic feedback onto rod bipolar cells in rat retina. J Neurosci 2010; 30(6), 2330-9.

Chen X, Hsueh HA, Greenberg K, Werblin FS. Three forms of spatial temporal feedforward inhibition are common to different ganglion cell types in rabbit retina. J Neurophysiol. 2010 May;103(5):2618-32.

Chen Y, Yu FH, Sharp EM, Beacham D, Scheuer T, Catterall WA. Functional properties and differential neuromodulation of $Na_v1.6$ channels. Mol Cell Neurosci. 2008; 38(4), 607-15.

Choi H, Zhang L, Cembrowski MS, Sabottke CF, Markowitz AL, Butts DA, Kath WL, Singer JH, Riecke H.Intrinsic bursting of AII amacrine cells underlies oscillations in the rd1 mouse retina. J Neurophysiol 2014; 112(6), 1491-504.

Chou TH, Park KK, Luo X, Porciatti V. Retrograde Signaling in the Optic Nerve Is Necessary for Electrical Responsiveness of Retinal Ganglion Cells. Invest Ophthalmol Vis Sci 2013; 54, 1236–43.

Chytrova G, Johnson JE. Spontaneous retinal activity modulates BDNF trafficking in the developing chick visual system. Mol Cell Neurosci 2004; 25(4), 549-57.

Cia D, Bordais A, Varela C, Forster V, Sahel JA, Rendon A, Picaud S. Voltage-gated channels and calcium homeostasis in mammalian rod photoreceptors. J Neurophysiol 2005; 93(3), 1468-75.

Cibis GW, Fitzgerald KM. Optic nerve hypoplasia in association with brain anomalies and an abnormal electroretinogram. Doc ophthalmol 1994; 86, 11–22.

Cobb W, Morton HB. The human retinogram in response to high-intensity flashes. EEG Clinical Neurophysiol 2954; 4, 547–56.

Cohen ED. Voltage-gated calcium and sodium currents of starburst amacrine cells in the rabbit retina. Vis Neurosci 2001;18(5), 799-809.

Cook PB, McReynolds JS. Lateral inhibition in the inner retina is important for spatial tuning of ganglion cells. Nat Neurosci 1998; 1, 714-9.

Cook PB, Werblin FS. Spike initiation and propagation in wide field transient amacrine cells of the salamander retina. J Neurosci 1994; 14(6), 3852-61.

Coombs J, van der List D, Wang GY, Chalupa LM. Morphological properties of mouse retinal ganglion cells. Neuroscience 2006; 140, 123–36.

Copenhagen D. Is the retina going digital? Neuron 2001; 30(2), 303-5.

Côté PD, De Repentigny Y, Coupland SG, Schwab Y, Roux MJ, Levinson SR, Kothary R. Physiological maturation of photoreceptors depends on the voltage-gated sodium channel NaV1.6 (Scn8a). J Neurosci 2005; 25(20), 5046-50.

Crill WE, Persistent sodium current in mammalian central neurons. Annu Rev Physiol 1996; 58, 349-62

Cui J, Pan ZH. Two types of cone bipolar cells express voltage-gated Na+ channels in the rat retina. Vis Neurosci 2008; 25(5-6), 635-45.

Cummins TR, Dib-Hajj SD, Herzog RI, Waxman SG. $Na_v1.6$ channels generate resurgent sodium currents in spinal sensory neurons. FEBS Lett 2005; 579(10), 2166-70.

Dacey DM. The mosaic of midget ganglion cells in the human retina. J Neurosci. 1993; 13(12), 5334-55.

Dang TM, Tsai TI, Vingrys AJ, Bui BV. Post-receptoral contributions to the rat scotopic electroretinogram a-wave. Doc Ophthalmol 2011; 122, 149-56.

Davenport CM, Detwiler PB, Dacey DM. Functional polarity of dendrites and axons of primate A1 amacrine cells. Vis Neurosci 2007; 24(4), 449-57.

Davis SF, and Linn CL. Activation of NMDA receptors linked to modulation of voltage-gated ion channels and functional implications. Am J Physiol Cell Physiol 2003; 284(3), C757-68.

Davis SF, and Linn CL. Mechanism linking NMDA receptor activation to modulation of voltage-gated sodium current in distal retina. Am J Physiol Cell Physiol 2003; 284(5), C1193-204.

de la Rocha J, Doiron B, Shea-Brown E, Josić K, Reyes A. Correlation between neural spike trains increases with firing rate. Nature 2007; 448(7155), 802-6.

De Repentigny Y, Coté PD, Pool M, Bernier G, Girard S, Vidal SM, Kothary R. Pathological and genetic analysis of the degenerating muscle (dmu) mouse: a new allele of Scn8a. Hum Mol Genet 2001; 10, 1819–27.

De Sevilla Müller Perez L, Shelley J, Weiler R..: Displaced amacrine cells of the mouse retina. J Comp Neurol. 2007; 505(2), 177-89.

Debertin G, Kántor O, Kovács-Öller T, Balogh L, Szabó-Meleg E, Orbán J, Nyitrai M, Völgyi B. Tyrosine hydroxylase positive perisomatic rings are formed around various amacrine cell types in the mammalian retina. J Neurochem 2015; 134(3): 416-28.

Deisz RA, Fortin G, Zieglgänsberger W. Voltage dependence of excitatory postsynaptic potentials of rat neocortical neurons. J Neurophysiol 1991;65(2), 371-82.

Demb JB, Singer JH. Intrinsic properties and functional circuitry of the AII amacrine cell. Vis Neurosci 2012; 29(1), 51-60.

Deplano S1, Gargini C, Maccarone R, Chalupa LM, Bisti S. Long-term treatment of the developing retina with the metabotropic glutamate agonist APB induces long-term changes in the stratification of retinal ganglion cell dendrites. Dev Neurosci 2004; 26(5-6), 396-405.

Derr PH, Meyer AU, Haupt EJ, Brigell MG. Extraction and modeling of the Oscillatory Potential: signal conditioning to obtain minimally corrupted Oscillatory Potentials. Doc Ophthalmol 2002; 104, 37–55.

DeVries SH. Bipolar cells use kainate and AMPA receptors to filter visual information into separate channels. Neuron 2000; 28(3), 847-56.

DeVries SH, Li W, Saszik S. Parallel processing in two transmitter microenvironments at the cone photoreceptor synapse. Neuron 2006; 50(5), 735-48.

Dib-Hajj SD, Waxman SG. Isoform-specific and pan-channel partners regulate trafficking and plasma membrane stability; and alter sodium channel gating properties. Neurosci Lett 2010; 486(2), 84-91.

Dib-Hajj SD, Black JA, Waxman SG. $Na_v1.9$: a sodium channel linked to human pain. Nat Rev Neurosci 2015; 16(9), 511-9.

Dib-Hajj SD, Geha P, Waxman SG. Sodium channels in pain disorders: pathophysiology and prospects for treatment. Pain. 2017;158 Suppl 1, S97-S107.

Di Marco S, Nguyen VA, Bisti S, Protti DA. Permanent functional reorganization of retinal circuits induced by early long-term visual deprivation. J Neurosci 2009; 29(43), 13691-701.

Diamond JS, Copenhagen DR. The relationship between light-evoked synaptic excitation and spiking behaviour of salamander retinal ganglion cells. J Physiol 1995; 487, 711-25.

Dietrich PS, McGivern JG, Delgado SG, Koch BD, Eglen RM, Hunter JC, Sangameswaran L. Functional analysis of a voltage-gated sodium channel and its splice variant from rat dorsal root ganglia. J Neurochem 1998; 70(6), 2262-72.

Ding H, Smith RG, Poleg-Polsky A, Diamond JS, Briggman KL. Species-specific wiring for direction selectivity in the mammalian retina. Nature 2016; 535, 105-10.

Dkhissi-Benyahya O, Coutanson C, Knoblauch K, et al. The absence of melanopsin alters retinal clock function and dopamine regulation by light. Cell. Mol Life Sci 2013; 70, 3435–47.

Dmitrieva NA, Dmitrieva NA, Strang CE, Strang CE, Keyser KT, Keyser KT. Expression of alpha 7 nicotinic acetylcholine receptors by bipolar, amacrine, and ganglion cells of the rabbit retina. J Histochem Cytochem 2007; 55, 461–476

Do MTH, Bean BP. Subthreshold sodium currents and pacemaking of subthalamic neurons: modulation by slow inactivation. Neuron 2003;39(1), 109-20.

Do MTH, Bean BP. Sodium currents in subthalamic nucleus neurons from Nav1.6-null mice. J Neurophysiol 2004; 92(2), 726-33.

Dong CJ, Hare WA. Contribution to the kinetics and amplitude of the electroretinogram b-wave by third-order retinal neurons in the rabbit retina. Vision Res 2000; 40(6), 579-89.

Dong CJ, Hare WA. GABAc feedback pathway modulates the amplitude and kinetics of ERG b-wave in a mammalian retina in vivo. Vision Res 2002; 42, 1081-7.

Dong CJ, Hare WA. Temporal modulation of scotopic visual signals by A17 amacrine cells in mammalian retina in vivo. J Neurophysiol 2003; 89, 2159-66.

Dong CJ, Agey P, and Hare WA. Origins of the electroretinogram oscillatory potentials in the rabbit retina. Vis Neurosci 2004; 21, 533–43.

Dong CJ, McReynolds JS. Comparison of the effects of flickering and steady light on dopamine release and horizontal cell coupling in the mudpuppy retina. J Neurophys 1992; 67:364–72

Dong CJ and Werblin FS. Temporal contrast enhancement via GABAC feedback at bipolar terminals in the tiger salamander retina. J Neurophysiol 1998;79(4), 2171-80.

Dorenbos R, Contini M, Hirasawa H, Gustincich S, Raviola E. Expression of circadian clock genes in retinal dopaminergic cells. Vis Neurosci 2007; 24, 573–80.

Dowling JE. The Retina: An Approachable Part of the Brain. Cambridge: Harvard University Belknap Press, 2nd ed., 2012.

Doyle SE, Grace MS, McIvor W, Menaker M. Circadian rhythms of dopamine in mouse retina: the role of melatonin. Vis Neurosci 2002a; 19, 593–601.

Doyle SE, McIvor WE, Menaker M. Circadian rhythmicity in dopamine content of mammalian retina: role of the photoreceptors. J Neurochem 2002b; 83, 211–9.

Du J, Feng L, Yang F, Lu B. Activity- and Ca(2+)-dependent modulation of surface expression of brain-derived neurotrophic factor receptors in hippocampal neurons. J Cell Biol 2000; 150(6), 1423-34.

Du JL, Poo MM. Rapid BDNF-induced retrograde synaptic modification in a developing retinotectal system. Nature 2004; 429(6994), 878-83.

Du JL, Wei HP, Wang ZR, Wong ST, Poo MM. Long-range retrograde spread of LTP and LTD from optic tectum to retina. Proc Natl Acad Sci USA 2009; 106(45), 18890-6.

Du JL, Yang XL. Subcellular localization and complements of GABA(A) and GABA(C) receptors on bullfrog retinal bipolar cells. J Neurophysiol 2000; 84, 666–76.

Duan X, Krishnaswamy A, De la Huerta I, Sanes JR. Type II cadherins guide assembly of a direction-selective retinal circuit. Cell 2014; 158(4), 793-807.

Duflocq A, Le Bras B, Bullier E, Couraud F, Davenne M. Nav1.1 is predominantly expressed in nodes of Ranvier and axon initial segments. Mol Cell Neurosci 2008; 39(2): 180-92.

Dunn FA, Doan T, Sampath AP, Rieke F. Controlling the gain of rod-mediated signals in the Mammalian retina. J Neurosci 2006; 26(15), 3959-70.

Dunn FA, Santina Della L, Parker ED, Wong RO. Sensory experience shapes the development of the visual system's first synapse. Neuron 2013; 80, 1159–66.

Dugandzija-Novaković S, Koszowski AG, Levinson SR, Shrager P. Clustering of Na+ channels and node of Ranvier formation in remyelinating axons. J Neurosci 1995; 15, 492–503.

Eggers ED, McCall MA, Lukasiewicz PD.. Presynaptic inhibition differentially shapes transmission in distinct circuits in the mouse retina. J Physiol 2007; 582: 569-82.

Eggers ED, Lukasiewicz PD. GABA(A), GABA(C) and glycine receptor-mediated inhibition differentially affects light-evoked signalling from mouse retinal rod bipolar cells. J Physiol 2006; 572, 215-25.

Eggers ED, Lukasiewicz PD. Receptor and transmitter release properties set the time course of retinal inhibition. J Neurosci, 2006; 26(37), 9413-25.

Eggers ED, Lukasiewicz PD. Interneuron circuits tune inhibition in retinal bipolar cells. J Neurophysiol 2010; 103(1), 25-37.

Eggers ED, Lukasiewicz PD. Multiple pathways of inhibition shape bipolar cell responses in the retina. Vis Neurosci 2011; 28(1), 95-108.

Eickenscheidt M, Zeck G. Action potentials in retinal ganglion cells are initiated at the site of maximal curvature of the extracellular potential. J Neural Eng. 2014; 11(3), 036006.

Enomoto A, Han JM, Hsiao CF, Chandler SH. Sodium current in mesencephalic trigeminal neurons from Nav1.6 null mice. J Neurophysiol 2007; 98(2), 710-9.

Euler T, Wässle H. Immunocytochemical identification of cone bipolar cells in the rat retina. J Comp Neurol 1995; 361(3), 461-78.

Euler T, Wässle H. Different contributions of GABAA and GABAC receptors to rod and cone bipolar cells in a rat retinal slice preparation. J Neurophysiol 1998; 79, 1384-95.

Fain GL, Gerschenfeld HM, Quandt FN. Calcium spikes in toad rods. J Physiol 1980; 303, 495-513.

Famiglietti EV Jr, Kolb H. A bistratified amacrine cell and synaptic cirucitry in the inner plexiform layer of the retina. Brain Res 1975; 84(2), 293-300.

Farrow K, Teixeira M, Szikra T, Viney TJ, Balint K, Yonehara K, Roska B. Ambient illumination toggles a neuronal circuit switch in the retina and visual perception at cone threshold. Neuron 2013; 78(2), 325-38.

Farshi P, Fyk-Kolodziej B, Krolewski DM, Walker PD, Ichinose T. Dopamine D1 receptor expression is bipolar cell type-specific in the mouse retina. J Comp Neurol 2016; 524(10), 2059-79.

Feigenspan A, Gustincich S, Bean BP, Raviola E. Spontaneous activity of solitary dopaminergic cells of the retina. J Neurosci 1998; 18, 6776-89.

Feigenspan A, Teubner B, Willecke K, Weiler R. Expression of neuronal connexin36 in AII amacrine cells of the mammalian retina. J Neurosci. 2001; 1;21(1), 230-9.

Feigenspan A, Weiler R. Electrophysiological properties of mouse horizontal cell GABAA receptors. J Neurophysiol 2004; 92, 2789-801.

Field GD, Chichilnisky EJ. Information processing in the primate retina: circuitry and coding. Annu Rev Neurosci 2007; 30, 1-30.

Fjell J, Dib-Hajj S, Fried K, Black JA, Waxman SG. Differential expression of sodium channel genes in retinal ganglion cells. Brain Res Mol Brain Res 1997 ; 50, 197–204.

Fohlmeister JF, Coleman PA, Miller RF. Modeling the repetitive firing of retinal ganglion cells. Brain Res 1990;510(2), 343-5

Fohlmeister JF, Miller RF. Impulse encoding mechanisms of ganglion cells in the tiger salamander retina. J Neurophysiol 1997; 78(4), 1935-47.

Forte JD, Bui BV, Vingrys AJ. Wavelet analysis reveals dynamics of rat oscillatory potentials. J Neurosci Methods 2008; 169(1), 191-200.

Freed MA. Rate of quantal excitation to a retinal ganglion cell evoked by sensory input. J Neurophys 2000; 83, 2956–66.

Fremeau RT Jr, Burman J, Qureshi T, Tran CH, Proctor J, Johnson J, Zhang H, Sulzer D, Copenhagen DR, Storm-Mathisen J, Reimer RJ, Chaudhry FA, Edwards RH. The identification of vesicular glutamate transporter 3 suggests novel modes of signaling by glutamate. Proc Natl Acad Sci USA 2002; 99(22), 14488-93.

French CR, Sah P, Buckett KJ, Gage PW. A voltage-dependent persistent sodium current in mammalian hippocampal neurons. J Gen Physiol 1990; 95(6), 1139-57.

Fried SI, Lasker AC, Desai NJ, Eddington DK, Rizzo JF 3rd. Axonal sodium-channel bands shape the response to electric stimulation in retinal ganglion cells. J Neurophysiol 2009; 101(4), 1972-87.

Fried SI, Münch TA, Werblin FS. Mechanisms and circuitry underlying directional selectivity in the retina. Nature 2002; 420, 411–4.

Friedburg C, Allen CP, Mason PJ, Lamb TD. Contribution of cone photoreceptors and post-receptoral mechanisms to the human photopic electroretinogram. J Physiol. 2004; 556: 819-34.

Frishman LJ. Origins of the Electroretinogram. In: Heckenlively JR, Arden GB, editors. Principles and Practice of Clinical Electrophysiology of Vision. 2nd ed. Cambridge, MA: The MIT Press. 2006; 139–83.

Frishman LJ, Yamamoto F, Bogucka J, Steinberg RH. Light-evoked changes in [K+]o in proximal portion of light-adapted cat retina. Neurophysiol 1992; 67(5), 1201-12.

Frishman LJ, and Steinberg RH. Light-evoked increases in [K+]o in proximal portion of the dark-adapted cat retina. J Neurophysiol 1989; 61(6), 1233-43.

Frishman LJ, and Wang MH. Electroretinogram of human, monkey and mouse. Adlers Physiology of the Eye. Ed. Levin LA, Ed. Nilsson SFE, Ed. Ver Hoeve J, Ed. Wu SM. Saunders Elsevier, 2011, 480-501.

Fujii M, Sunagawa GA, Kondo M, Takahashi M & Mandai M. Evaluation of micro electroretinograms recorded with multiple electrode array to assess focal retinal function. Scientific Reports 2016; 6, 30719–30.

Fulton AB, Rushton WA. The human rod ERG: correlation with psychophysical responses in light and dark adaptation. Vision Res 1978; 18(7), 793-800.

Ganguly K, Schinder AF, Wong ST, Poo M. GABA itself promotes the developmental switch of neuronal GABAergic responses from excitation to inhibition. Cell 2001; 105(4), 521-32.

Gargini C1, Bisti S, Demontis GC, Valter K, Stone J, Cervetto L. Electroretinogram changes associated with retinal upregulation of trophic factors: observations following optic nerve section. Neuroscience 2004; 126(3), 775-83.

Gärtner A, Staiger V. Neurotrophin secretion from hippocampal neurons evoked by long-term-potentiation-inducing electrical stimulation patterns. Proc Natl Acad Sci USA 2002; 99(9), 6386-91.

Gavrikov KE, Dmitriev AV, Keyser KT, Mangel SC. Cation--chloride cotransporters mediate neural computation in the retina. Proc Natl Acad Sci USA 2003; 100, 16047–52.

Gershon E, Weigl L, Lotan I, Schreibmayer W, Dascal N. Protein kinase A reduces voltage-dependent Na+ current in Xenopus oocytes. J Neurosci 1992;12(10), 3743-52.

Gibson R, Fletcher EL, Vingrys AJ, Zhu Y, Vessey KA, Kalloniatis M. Functional and neurochemical development in the normal and degenerating mouse retina. J Comp Neurol 2013; 521(6), 1251-67.

Giovannelli A1, Di Marco S, Maccarone R, Bisti S. Long-term dark rearing induces permanent reorganization in retinal circuitry. Biochem Biophys Res Commun 2008; 365(2), 349-54.

Ghosh KK, Bujan S, Haverkamp S, Feigenspan A, Wässle H. Types of bipolar cells in the mouse retina. J Comp Neurol 2004; 469(1), 70-82.

González-Burgos G, Barrionuevo G. Voltage-gated sodium channels shape subthreshold EPSPs in layer 5 pyramidal neurons from rat prefrontal cortex. J Neurophysiol 2001; 86(4), 1671-84.

Goldin AL, Barchi RL, Caldwell JH, Hofmann F, Howe JR, Hunter JC, Kallen RG, Mandel G, Meisler MH, Netter YB, Noda M, Tamkun MM, Waxman SG, Wood JN, Catterall WA. Nomenclature of voltage-gated sodium channels. Neuron 2000 28:365–8.

Goldin AL. Resurgence of sodium channel research. Annu Rev Physiol 2001 63:871–94.

Goldin AL, Barchi RL, Caldwell JH, Hofmann F, Howe JR, Hunter JC, Kallen RG, Mandel G, Meisler MH, Netter YB, Noda M, Tamkun MM, Waxman SG, Wood JN, Catterall WA. Nomenclature of voltage-gated sodium channels. Neuron 2000; 28, 365–8.

Gollisch and Meister. Rapid neural coding in the retina with relative spike latencies. Science 2008;319(5866), 1108-11.

Gordon D1, Merrick D, Auld V, Dunn R, Goldin AL, Davidson N, Catterall WA. Tissue-specific expression of the RI and RII sodium channel subtypes. Proc Natl Acad Sci USA 1987;84(23):8682-6.

Greene MJ, Kim JS2, Seung HS3; EyeWirers. Analogous Convergence of Sustained and Transient Inputs in Parallel On and Off Pathways for Retinal Motion Computation. Cell Rep 2016; 14(8), 1892-900.

Greschner M, Field GD, Li PH, Schiff ML, Gauthier JL, Ahn D, Sher A, Litke AM, Chichilnisky EJ. A polyaxonal amacrine cell population in the primate retina. J Neurosci 2014; 34(10), 3597-606.

Grieco TM, Raman IM. Production of resurgent current in NaV1.6-null Purkinje neurons by slowing sodium channel inactivation with beta-pompilidotoxin. J Neurosci 2004; 24(1), 35-42.

Grimes WN, Seal RP, Oesch N, Edwards RH, Diamond JS. Genetic targeting and physiological features of VGLUT3+ amacrine cells. Visual Neuroscience 2011; *28*(5), 381–92

Grimes WN, Zhang J, Graydon CW, Kachar B, Diamond JS. Retinal parallel processors: more than 100 independent microcircuits operate within a single interneuron. Neuron 2010; 65(6), 873-85.

Grishanin RN1, Yang H, Liu X, Donohue-Rolfe K, Nune GC, Zang K, Xu B, Duncan JL, Lavail MM, Copenhagen DR, Reichardt LF. Retinal TrkB receptors regulate neural development in the inner, but not outer, retina. Mol Cell Neurosci 2008; 38(3), 431-43.

Gros E, Deshayes S, Morris MC, Aldrian-Herrada G, Depollier J, Heitz F, Divita G. A non-covalent peptide-based strategy for protein and peptide nucleic acid transduction. Biochimica Biophysica Acta, 2006; 1758(3), 384–93.

Gurevich L, Slaughter MM. Comparison of the waveforms of the ON bipolar neuron and the b-wave of the electroretinogram. Vision Res 1993; 33(17), 2431-5.

Gustincich S, Contini M, Gariboldi M. Gene discovery in genetically labeled single dopaminergic neurons of the retina. Proc Natl Acad Sci USA 2004; 101, 5069–74.

Gustincich S, Feigenspan A, Wu DK, Koopman LJ, Raviola E. Control of dopamine release in the retina: a transgenic approach to neural networks. Neuron 1997;18, 723-36.

Gütig R, Gollisch T, Sompolinsky H, Meister M. Computing complex visual features with retinal spike times. PLoS One 2013; 8(1),e53063.

Hack I, Frech M, Dick O, Peichl L, Brandstätter JH. Heterogeneous distribution of AMPA glutamate receptor subunits at the photoreceptor synapses of rodent retina. Eur J Neurosci 2001; 13(1), 15-24.

Hampson EC, Vaney DI, Weiler R. Dopaminergic modulation of gap junction permeability between amacrine cells in mammalian retina. J Neurosci 1992; 12(12): 4911-22.

Han C, Yang Y, de Greef BT, Hoeijmakers JG, Gerrits MM, Verhamme C, Qu J, Lauria G, Merkies IS, Faber CG, Dib-Hajj SD, Waxman SG. The Domain II S4-S5 Linker in Nav1.9: A Missense Mutation Enhances Activation, Impairs Fast Inactivation, and Produces Human Painful Neuropathy. Neuromolecular Med 2015; 17(2), 158-69.

Han C, Yang Y, Te Morsche RH, Drenth JP, Politei JM, Waxman SG, Dib-Hajj SD. Familial gain-of-function Nav1.9 mutation in a painful channelopathy. J Neurol Neurosurg Psychiatry 2017; 88(3), 233-40.

Hardie JB, Pearce RA. Active and passive membrane properties and intrinsic kinetics shape synaptic inhibition in hippocampal CA1 pyramidal neurons. J Neurosci 2006; 26(33), 8559-69.

Hare WA, Ton H. Effects of APB, PDA, and TTX on ERG responses recorded using both multifocal and conventional methods in monkey. Doc Ophthalmol 2002;105, 189-222.

Hargus NJ, Nigam A, Bertram EH, Patel MK. Evidence for a role of Nav1.6 in facilitating increases in neuronal hyperexcitability during epileptogenesis. J Neurophysiol, 2013; 110(5), 1144–57.

Harris KD. Cellular determination in the Xenopus retina is independent of lineage and birth date. Neuron 2008; 60(3), 395-6.

Harris KD. Stability of the fittest: organizing learning through retroaxonal signals. Trends Neurosci 2008: 31, 130–6.

Hartveit E. Reciprocal synaptic interactions between rod bipolar cells and amacrine cells in the rat retina. J Neurophysiol 1999;81, 2923-36.

Hartveit E1, Veruki ML. Electrical synapses between AII amacrine cells in the retina: Function and modulation. Brain Res 2012; 1487, 160-72.

Haverkamp S, Haeseleer F, Hendrickson A. A comparison of immunocytochemical markers to identify bipolar cell types in human and monkey retina. Vis Neurosci 2003; 20(6), 589-600.

Haverkamp S, Wässle H. Characterization of an amacrine cell type of the mammalian retina immunoreactive for vesicular glutamate transporter 3. J Comp Neurol 2004; 468(2), 251-63.

He S, Masland RH. Retinal direction selectivity after targeted laser ablation of starburst amacrine cells. Nature 1997; 389, 378–82.

Heflin SJ, Cook PB. Narrow and wide field amacrine cells fire action potentials in response to depolarization and light stimulation. Vis Neurosci 2007; 24(2), 197-206.

Hellmer CB, Zhou Y, Fyk-Kolodziej B, Hu Z, Ichinose T. Morphological and physiological analysis of type-5 and other bipolar cells in the Mouse Retina. Neuroscience, 2016; 315, 246–58.

Helmstaedter M, Briggman KL, Turaga SC, Jain V, Seung HS, Denk W. Connectomic reconstruction of the inner plexiform layer in the mouse retina. Nature 2013; 500(7461), 168-74.

Hendrickson A, Boothe R. Morphology of the retina and dorsal lateral geniculate nucleus in dark-reared monkeys (Macaca nemestrina). Vision Res 1976; 16(5), 517-21.

Herrmann R, Heflin SJ, Hammond T, Lee B, Wang J, Gainetdinov RR, Caron MG, Eggers ED, Frishman LJ, McCall MA, Arshavsky VY.Rod vision is controlled by dopamine-dependent sensitization of rod bipolar cells by GABA. Neuron 2011; 72(1), 101-10.

Hetling JR, Pepperberg DR. Sensitivity and kinetics of mouse rod flash responses determined in vivo from paired-flash electroretinograms. J Physiol (Lond) 1999; 516, 593–609.

Hidaka S, Akahori Y, Kurosawa Y. Dendrodendritic electrical synapses between mammalian retinal ganglion cells. J Neurosci 2004; 24(46), 10553-67.

Hidaka S, Ishida AT.: Voltage-gated Na+ current availability after step- and spike-shaped conditioning depolarizations of retinal ganglion cells. Pflugers Arch 1998; 436(4), 497-508.

Hidaka S, Akahori Y, Kurosawa Y. Dendrodendritic electrical synapses between mammalian retinal ganglion cells. J Neurosci 2004; 24(46), 10553-67.

Hoggarth A, McLaughlin AJ, Ronellenfitch K, Trenholm S, Vasandani R, Sethuramanujam S, Schwab D, Briggman KL, Awatramani GB. Specific wiring of distinct amacrine cells in the directionally selective retinal circuit permits independent coding of direction and size. Neuron 2015; 86, 276–91.

Hood DC, and Birch DG. A computational model of the amplitude and implicit time of the b-wave of the human ERG. Vis Neurosci 1992; 8(2), 107-26.

Hooks BM, Chen C. Distinct roles for spontaneous and visual activity in remodeling of the retinogeniculate synapse. Neuron 2006; 52, 281–91.

Hsueh HA, Molnar A, Werblin FS. Amacrine-to-amacrine cell inhibition in the rabbit retina. J Neurophysiol 2008; 100(4), 2077-88.

Hu C, Bi A, Pan ZH. Differential expression of three T-type calcium channels in retinal bipolar cells in rats. Vis Neurosci 2009; 26(2), 177-87.

Hu C, Hill DD, Wong KY. Intrinsic physiological properties of the five types of mouse ganglion-cell photoreceptors. J Neurophysiol 2013; 09(7), 1876-89.

Hu W, Tian C, Li T, Yang M, Hou H, Shu Y. Distinct contributions of Na(v)1.6 and Na(v)1.2 in action potential initiation and backpropagation. Nat Neurosci 2009; 12, 996–1002.

Huberman AD, Wei W, Elstrott J, Stafford BK, Feller MB, Barres BA. Genetic identification of an On-Off direction-selective retinal ganglion cell subtype reveals a layer-specific subcortical map of posterior motion. Neuron 2009; 62(3), 327-34.

Hughes A. The artefact of retinoscopy in the rat and rabbit eye has its origin at the retina/vitreous interface rather than in longitudinal chromatic aberration. Vision Res 1979;19, 1293-4.

Huppé-Gourgues F, Coudé G, Lachapelle P, Casanova C. Effects of the intravitreal administration of dopaminergic ligands on the b-wave amplitude of the rabbit electroretinogram. Vis Res 2005; 45, 137–45.

Ichinose T, Fyk-Kolodziej B, Cohn J. Roles of ON cone bipolar cell subtypes in temporal coding in the mouse retina. J Neurosci 2014; 34(26), 8761-71.

Ichinose T, Hellmer CB. Differential signalling and glutamate receptor compositions in the OFF bipolar cell types in the mouse retina. J Physiol 2016; 594(4), 883-94.

Ichinose T, Lukasiewicz PD. Inner and outer retinal pathways both contribute to surround inhibition of salamander ganglion cells. J Physiol 2005; 565, 517-35.

Ichinose T, Lukasiewicz PD. Ambient light regulates sodium channel activity to dynamically control retinal signaling. J Neurosci 2007; 27(17), 4756-64.

Ichinose T, Shields CR, Lukasiewicz PD. Sodium channels in transient retinal bipolar cells enhance visual responses in ganglion cells. J Neurosci 2005; 25, 1856-65.

Ishida AT. Retinal Ganglion cell excitability. The Visual Neurosciences. Ed. Chalupa LM, Ed. Werner JS. MIT Press, 2004 422-50.

Ishikane H, Gangi M, Honda S, Tachibana M. Synchronized retinal oscillations encode essential information for escape behavior in frogs. Nat Neurosci 2005; 8,1087–95.

Iuvone PM, Galli CL, Garrison-Gund CK, Neff NH. Light stimulates tyrosine hydroxylase activity and dopamine synthesis in retinal amacrine neurons. Science 1978; 202, 901–2.

Ivanova E, and Müller F. Retinal bipolar cell types differ in their inventory of ion channels. Vis Neurosci. 2006; 23(2),143-54.

Ivanova E, Yee CW, Baldoni R Jr, Sagdullaev BT. Aberrant activity in retinal degeneration impairs central visual processing and relies on Cx36-containing gap junctions. Exp Eye Res 2015; S0014-4835(15)00166-9.

Jackson CR, Ruan GX, Aseem F, Abey J, Gamble K, Stanwood G, Palmiter RD, Iuvone PM, McMahon DG. Retinal dopamine mediates multiple dimensions of light-adapted vision. J Neurosci 2012; 32(27):9359-68.

Jaissle GB, May CA, Reinhard J, Kohler K, Fauser S, Lutjen-Drecoll E, Zrenner E, Seeliger MW. Evaluation of the rhodopsin knockout mouse as a model of pure cone function. Invest Ophthalmol Vis Sci 2001; 42, 506-13.

Jarvis MF, Honore P, Shieh C-C, Chapman M, Joshi S, Zhang X-F, et al. A-803467, a potent and selective Nav1.8 sodium channel blocker, attenuates neuropathic and inflammatory pain in the rat. Proc Nat Acad Sci 2007; 104(20), 8520–5.

Jensen RJ, Rizzo JF Thresholds for activation of rabbit retinal ganglion cells with a subretinal electrode. Exp Eye Res 2006; 83(2), 367-73.

Jensen RJ, Rizzo JF. Activation of ganglion cells in wild-type and rd1 mouse retinas with monophasic and biphasic current pulses. J Neural Eng 2009; 6(3), 035004.

Jeon CJ, Strettoi E, Masland RH. The major cell populations of the mouse retina. J Neurosci 1998;18, 8936-46.

Jepson LH, Hottowy P, Mathieson K, Gunning DE, Dabrowski W, Litke AM, Chichilnisky EJ. Focal electrical stimulation of major ganglion cell types in the primate retina for the design of visual prostheses. J Neurosci 2013; 33(17), 7194-205.

Johnson J, Sherry DM, Liu X, Fremeau RT Jr, Seal RP, Edwards RH, Copenhagen DR. Vesicular glutamate transporter 3 expression identifies glutamatergic amacrine cells in the rodent retina. J Comp Neurol 2004; 477(4), 386-98.

Jones SM, Palmer MJ. Pharmacological analysis of the activation and receptor properties of the tonic GABA(C)R current in retinal bipolar cell terminals. PLoS ONE 2011; 6(9), e24892.

Jones SM, Palmer MJ. Activation of the tonic GABAC receptor current in retinal bipolar cell terminals by nonvesicular GABA release. J Neurophysiol 2009; 102(2), 691-9.

Juusola M, French AS. The efficiency of sensory information coding by mechanoreceptor neurons. Neuron 1997; 18(6), 959-68.

Kalume F, Yu FH, Westenbroek RE, Scheuer T, Catterall WA. Reduced sodium current in Purkinje neurons from Nav1.1 mutant mice: implications for ataxia in severe myoclonic epilepsy in infancy. J Neurosci 2007;27(41), 11065-74.

Kaneda M, Ito K, Morishima Y, Shigematsu Y, Shimoda Y. Characterization of voltage-gated ionic channels in cholinergic amacrine cells in the mouse retina. J Neurophysiol 2007; 97, 4225–34.

Kaneko Y, Watanabe S. Expression of $Na_v1.1$ in rat retinal AII amacrine cells. Neurosci Lett 2007; 424(2), 83-8.

Kaplan HJ, Chiang C, Chen J, Song S. Vitreous Volume of the Mouse Measured by Quantitative High-Resolution MRI. ARVO Meeting Abstracts 2010; 51, 4414.

Kapousta-Bruneau N. Opposite effects of GABA(A) and GABA(C) receptor antagonists on the b-wave of ERG recorded from the isolated rat retina. Vision Res 2000; 40, 1653-65.

Karwoski CJ, Newman EA, Shimazaki H, Proenza LM. Light-evoked increases in extracellular K+ in the plexiform layers of amphibian retinas. J Gen Physiol 1985; 86(2):189-213.

Karwoski CJ and Xu X. Current source-density analysis of light-evoked field potentials in rabbit retina. Vis Neurosci 1999; 16(2), 369-77.

Kawai F, Horiguchi M, Suzuki H, Miyachi E. Na(+) action potentials in human photoreceptors. Neuron 2001; 30(2), 451-8.

Kawai F, Horiguchi M, Ichinose H, Ohkuma M, Isobe R, Miyachi E. Suppression by an h current of spontaneous Na+ action potentials in human cone and rod photoreceptors. Invest Ophthalmol Vis Sci 2005; 46(1), 390-7.

Kemmler R, Schultz K, Dedek K, Euler T, Schubert T. Differential regulation of cone calcium signals by different horizontal cell feedback mechanisms in the mouse retina. J Neurosci 2014; 34(35), 11826-43.

Khaliq ZM, Gouwens NW, Raman IM. The contribution of resurgent sodium current to high-frequency firing in Purkinje neurons: an experimental and modeling study. J Neurosci 2003; 23(12), 4899-912.

Kim IJ, Zhang Y, Yamagata M, Meister M, Sanes JR. Molecular identification of a retinal cell type that responds to upward motion. Nature 2008; 452(7186), 478-82.

Kim IJ, Zhang Y, Meister M, Sanes JR. Laminar restriction of retinal ganglion cell dendrites and axons: subtype-specific developmental patterns revealed with transgenic markers. J Neurosci 2010;30(4), 1452-62.

Kim T, Soto F, Kerschensteiner D. An excitatory amacrine cell detects object motion and provides feature-selective input to ganglion cells in the mouse retina. Elife 2015;4.

Knop GC, Feigenspan A, Weiler R, Dedek K. Inputs underlying the ON-OFF light responses of type 2 wide-field amacrine cells in TH:GFP mice. J Neurosci 2011; 31(13), 4780-91.

Kofuji P, Ceelen P, Zahs KR, Surbeck LW, Lester HA, Newman EA. Genetic inactivation of an inwardly rectifying potassium channel (Kir4.1 subunit) in mice: phenotypic impact in retina. J Neurosci 2000; 20(15), 5733-40.

Kohara K, Kitamura A, Morishima M, Tsumoto T. Activity-dependent transfer of brain-derived neurotrophic factor to postsynaptic neurons. Science 2001; 291(5512), 2419-23.

Kohrman DC, Smith MR, Goldin AL, Harris J, Meisler MH. A missense mutation in the sodium channel Scn8a is responsible for cerebellar ataxia in the mouse mutant jolting. J Neurosci 1996; 16, 5993–5999.

Koike C, Obara T, Uriu Y, Numata T, Sanuki R, Miyata K, Koyasu T, Ueno S, Funabiki K, Tani A, Ueda H, Kondo M, Mori Y, Tachibana M, Furukawa T.. TRPM1 is a component of the retinal ON bipolar cell transduction channel in the mGluR6 cascade. Proc Natl Acad Sci USA 2010; 107(1), 332-7.

Koizumi A, Watanabe S, Kaneko A. Persistent Na+ current and Ca2+ current boost graded depolarization of rat retinal amacrine cells in culture. J Neurophysiol 2001; 86(2), 1006-16.

Kojima M1, Takei N, Numakawa T, Ishikawa Y, Suzuki S, Matsumoto T, Katoh-Semba R, Nawa H, Hatanaka H. Biological characterization and optical imaging of brain-derived neurotrophic factor-green fluorescent protein suggest an activity-dependent local release of brain-derived neurotrophic factor in neurites of cultured hippocampal neurons. J Neurosci Res 2001; 64(1), 1-10.

Kole MH and Stuart GJ. Signal processing in the axon initial segment. Neuron 2012; 73(2), 235-47.

Kothmann WW, Massey SC, O'Brien J. Dopamine-stimulated dephosphorylation of connexin 36 mediates AII amacrine cell uncoupling. J Neurosci 2009; 29(47), 14903-11.

Krishnaswamy A, Yamagata M, Duan X, Hong YK, Sanes JR. Sidekick 2 directs formation of a retinal circuit that detects differential motion. Nature 2015; 524(7566), 466-70.

Krzemien DM, Schaller KL, Levinson SR, Caldwell JH. Immunolocalization of sodium channel isoform NaCh6 in the nervous system. J Comp Neurol 2000; 420(1), 70-83.

Lachapelle P, Little JM, Polomeno RC. The photopic electroretinogram in congenital stationary night blindness with myopia. Invest Ophthalmol Vis Sci 1983; 24(4), 442-50.

Lago J, Rodríguez LP, Blanco L, Vieites JM, Cabado AG. Tetrodotoxin, an Extremely Potent Marine Neurotoxin: Distribution, Toxicity, Origin and Therapeutical Uses. Mar Drugs 2015; 13(10), 6384-406.

Landi S, Cenni MC, Maffei L, Berardi N. Environmental enrichment effects on development of retinal ganglion cell dendritic stratification require retinal BDNF. PLoS ONE 2007; 2, e346.

Landi S, Sale A, Berardi N, Viegi A, Maffei L, Cenni MC. Retinal functional development is sensitive to environmental enrichment: a role for BDNF. FASEB J 2007; 21(1), 130-9.

Lasater EM. Ionic currents of cultured horizontal cells isolated from white perch retina. J Neurophysiol 1986; 55(3), 499-513.

Laughlin SB. Energy as a constraint on the coding and processing of sensory information. Curr Opin Neurobiol 2001; 11(4), 475-80.

Lavoie J, Hébert M, Beaulieu J-M. Glycogen synthase kinase-3 β haploinsufficiency lengthens the circadian locomotor activity period in mice. Behav Brain Res 2013; 253, 262–65.

Lavoie J, Illiano P, Sotnikova TD, et al. The Electroretinogram as a Biomarker of Central Dopamine and Serotonin: Potential Relevance to Psychiatric Disorders. Biol Psychiatry 2014; 75, 479–86.

Leach MJ, Marden CM, Canning HM. (±)-cis-2,3-piperidine dicarboxylic acid is a partial n-methy-d-aspartate agonist in the in vitro rat cerebellar cGMP model. Eur J Pharmacol 1986; 121, 173-179.

Lee EJ, Gibo TL, Grzywacz NM. Dark rearing induced reduction of GABA and GAD and prevention of the effect by BDNF in the mouse retina. Eur J Neurosci 2006; 24, 2118–2134.

Lee S, Chen L, Chen M, Ye M, Seal RP, Zhou ZJ. An unconventional glutamatergic circuit in the retina formed by vGluT3 amacrine cells. Neuron 2014; 84(4), 708-15.

Lee S, Chen M, Zhang Y, Chen L, Zhou ZJ. Synaptic properties of vGluT3 amacrine cells in the mouse retina. Invest Ophthalmol Vis Sci 2015; 56, 4377-84.

Lee S, Grünert U. Connections of diffuse bipolar cells in primate retina are biased against S-cones. J Comp Neurol 2007; 502(1), 126-40.

Lee S, Zhang Y, Chen M, Zhou ZJ. Segregated Glycine-Glutamate Co-transmission from vGluT3 Amacrine Cells to Contrast-Suppressed and Contrast-Enhanced Retinal Circuits. Neuron, 2016: 90(1), 27–34.

Lei B, Yao G, Zhang K, Hofeldt KJ, Chang B. Study of rod- and cone-driven oscillatory potentials in mice. Invest Ophthalmol Vis Sci, 2006: 47(6), 2732–8.

Lei B and Perlman I. The contributions of voltage- and time-dependent potassium conductances to the electroretinogram in rabbits. Vis Neurosci 1999;16(4), 743-54.

Leventer SM, Wulfert E, Hanin I. Time course of ethylcholine aziridinium ion (AF64A)-induced cholinotoxicity in vivo. Neuropharmacol 1987; 26, 361–5.

Levin SI, Khaliq ZM, Aman TK, Grieco TM, Kearney JA, Raman IM, Meisler MH. Impaired motor function in mice with cell-specific knockout of sodium channel Scn8a (NaV1.6) in cerebellar purkinje neurons and granule cells. J Neurophysiol 2006; 96(2), 785-93.

Lewis AH and Raman IM. Resurgent current of voltage-gated Na(+) channels. J Physiol 2014; 592(22), 4825-38.

Li B, Barnes GE, Holt WF. The decline of the photopic negative response (PhNR) in the rat after optic nerve transection. Doc Ophthalmol 2005;111, 23-31.

Li C-Y, Lu J-T, Wu C-P, Duan S-M, Poo M-M. Bidirectional modification of presynaptic neuronal excitability accompanying spike timing-dependent synaptic plasticity. Neuron 2004; 41, 257–68.

Li H, Zhang Z, Blackburn MR, et al. Adenosine and dopamine receptors coregulate photoreceptor coupling via gap junction phosphorylation in mouse retina. J Neurosci 2013; 33, 3135–50.

Li M, West JW, Lai Y, Scheuer T, Catterall WA. Functional modulation of brain sodium channels by cAMP-dependent phosphorylation. Neuron 1992;8(6), 1151-9.

Li W and DeVries SH. Bipolar cell pathways for color and luminance vision in a dichromatic mammalian retina. Nat Neurosci 2006; 9(5), 669-75.

Light AC, Zhu Y, Shi J, Saszik S, Lindstrom S, Davidson L, Li X, Chiodo VA, Hauswirth WW, Li W, DeVries SH. Organizational motifs for ground squirrel cone bipolar cells. J Comp Neurol 2012; 520(13), 2864-87.

Lin B and Masland RH. Populations of wide-field amacrine cells in the mouse retina. J Comp Neurol. 2006; 499(5), 797-809.

Lipin MY, Vigh J. Calcium spike-mediated digital signaling increases glutamate output at the visual threshold of retinal bipolar cells. J Neurophysiol 2015; 113(2), 550-66.

Lipton SA, Tauck DL. Voltage-dependent conductances of solitary ganglion cells dissociated from the rat retina. J Physiol 1987; 385, 361-91.

Liu X, Grishanin RN, Tolwani RJ, Rentería RC, Xu B, Reichardt LF, Copenhagen DR. Brain-derived neurotrophic factor and TrkB modulate visual experience-dependent refinement of neuronal pathways in retina. J Neurosci 2007; 27, 7256–67.

Liu X, Grove JC, Hirano AA, Brecha NC, Barnes S. Dopamine D1 receptor modulation of calcium channel currents in horizontal cells of mouse retina. J Neurophysiol 2016; 116(2), 686-97.

Liu X, Hirano AA, Sun X, Brecha NC, Barnes S. Calcium channels in rat horizontal cells regulate feedback inhibition of photoreceptors through an unconventional GABA- and pH-sensitive mechanism. J Physiol. 2013; 591(13), 3309-24.

Liu X, Zhang Z, Ribelayga CP. Heterogeneous expression of the core circadian clock proteins among neuronal cell types in mouse retina. PLoS ONE 2012; 7, e50602.

Löhrke S, Hofmann HD. Voltage-gated currents of rabbit A- and B-type horizontal cells in retinal monolayer cultures. Vis Neurosci 1994;11(2), 369-78.

Lom B, Cogen J, Sanchez AL, Vu T, Cohen-Cory S. Local and target-derived brain-derived neurotrophic factor exert opposing effects on the dendritic arborization of retinal ganglion cells in vivo. J Neurosci 2002; 22(17), 7639-49.

Lorincz A and Nusser Z. Cell-type-dependent molecular composition of the axon initial segment. J Neurosci 2008; 28(53), 14329-40.

Lorincz A and Nusser Z 2010: Molecular identity of dendritic voltage-gated sodium channels. Science 2010; 328(5980), 906-9.

Lukasiewicz PD, Eggers ED, Sagdullaev BT, McCall MA. GABAC receptor-mediated inhibition in the retina. Vision Res 2004; 44(28), 3289-96.

Lukasiewicz PD, Maple BR, Werblin FS. A novel GABA receptor on bipolar cell terminals in the tiger salamander retina. J Neurosci 1994; 14, 1202–12.

Lukasiewicz PD, Shields CR. Different combinations of GABAA and GABAC receptors confer distinct temporal properties to retinal synaptic responses. J Neurophysiol 1998; 79(6), 3157-67.

Lukasiewicz PD, Werblin FS. The spatial distribution of excitatory and inhibitory inputs to ganglion cell dendrites in the tiger salamander retina. J Neurosci 1990; 10(1), 210-21.

Ma YP, Cui J, Pan ZH. Heterogeneous expression of voltage-dependent Na+ and K+ channels in mammalian retinal bipolar cells. Vis Neurosci 2005; 22, 119-33.

Ma YP, Pan ZH. Spontaneous regenerative activity in mammalian retinal bipolar cells: roles of multiple subtypes of voltage-dependent Ca2+ channels. Vis Neurosci 2003; 20(2), 131-9.

Ma YT, Hsieh T, Forbes ME, Johnson JE, Frost DO. BDNF injected into the superior colliculus reduces developmental retinal ganglion cell death. J Neurosci 1998; 18(6), 2097-107.

Majumdar S, Weiss J, Wässle H. Glycinergic input of widefield, displaced amacrine cells of the mouse retina. J Physiol 2009;587, 3831-49.

Mandolesi G, Menna E, Harauzov A, von Bartheld CS, Caleo M, Maffei L. A role for retinal brain-derived neurotrophic factor in ocular dominance plasticity. Curr Biol. 2005; 15(23), 2119-24.

Manglapus MK, Uchiyama H, Buelow NF, Barlow RB. Circadian rhythms of rod-cone dominance in the Japanese quail retina. J Neurosci 1998;18, 4775–84.

Manookin MB, Beaudoin DL, Ernst ZR, Flagel LJ, Demb JB. Disinhibition combines with excitation to extend the operating range of the OFF visual pathway in daylight. J Neurosci 2008; 28(16), 4136-50.

Manookin MB, Puller C, Rieke F, Neitz J, Neitz M. Distinctive receptive field and physiological properties of a wide-field amacrine cell in the macaque monkey retina. J Neurophysiol 2015; 114(3), 1606-16.

Manookin MB, Weick M, Stafford BK, Demb JB. NMDA receptor contributions to visual contrast coding. Neuron 2010; 67(2), 280-93.

Mao BQ, MacLeish PR, Victor JD. The intrinsic dynamics of retinal bipolar cells isolated from tiger salamander. Vis Neurosci 1998; 15(3), 425-38.

Margolis DJ, Detwiler PB. Different mechanisms generate maintained activity in ON and OFF retinal ganglion cells. J Neurosci 2007; 27, 5994-6005.

Margolis DJ, Newkirk G, Euler T, Detwiler PB. Functional stability of retinal ganglion cells after degeneration-induced changes in synaptic input. J Neurosci 2008; 28(25), 6526-36

Maricq AV, Korenbrot J. Calcium and calcium-dependent chloride currents generate action potentials in solitary cone photoreceptors. Neuron 1988;1(6), 503-15.

Martin DK, Anderton PJ, Bursill JA, Le Dain AC, Millar TJ. Kainic acid blocks a TTX-sensitive sodium channel in retinal horizontal cells of the turtle (Pseudemys scripta elegans). Neuroreport 1996;7(15-17), 2429-33.

Masland RH. The neuronal organization of the retina. Neuron 2012; 76(2), 266-80.

Massey SC, Miller RF. Excitatory amino acid receptors of rod- and cone-driven horizontal cells in the rabbit retina. J Neurophysiol 1987;57, 645-59.

Masu M, Iwakabe H, Tagawa Y, Miyoshi T, Yamashita M, Fukuda Y, Sasaki H, Hiroi K, Nakamura Y, Shigemoto R, Masahiko T, Kenji N, Kazuki N, Motoya K, Shigetada N. Specific deficit of the ON response in visual transmission by targeted disruption of the mGluR6 gene. Cell 1995; 80(5), 757-65.

Maurice N, Tkatch T, Meisler M, Sprunger LK, Surmeier DJ. D1/D5 dopamine receptor activation differentially modulates rapidly inactivating and persistent sodium currents in prefrontal cortex pyramidal neurons. J Neurosci 2001;21(7), 2268-77.

Maxeiner S, Dedek K, Janssen-Bienhold U, Ammermüller J, Brune H, Kirsch T, Pieper M, Degen J, Krüger O, Willecke K, Weiler R. Deletion of connexin45 in mouse retinal neurons disrupts the rod/cone signaling pathway between AII amacrine and ON cone bipolar cells and leads to impaired visual transmission. J Neurosci 2005; 25(3), 566-76.

McCulloch DL, Garcia-Filion P, Garcia-Fillion P, van Boemel GB, Borchert MS. Retinal function in infants with optic nerve hypoplasia: electroretinograms to large patterns and photopic flash. Eye (Lond) 2007; 21, 712–20.

Meiri H, Goren E, Bergmann H, Zeitoun I, Rosenthal Y, Palti Y. Specific modulation of sodium channels in mammalian nerve by monoclonal antibodies. Proc Natl Acad Sci USA 1986; 83(21), 8385-9.

Meiri H, Spira G, Sammar M, Namir M, Schwartz A, Komoriya A, Kosower EM, Palti Y. Mapping a region associated with Na channel inactivation using antibodies to a synthetic peptide corresponding to a part of the channel. Proc Natl Acad Sci USA 1987; 84, 5058-62.

Meiri H, Sammar M, Schwartz A. Production and use of synthetic peptide antibodies to map region associated with sodium channel inactivation. Methods Enzymol 1989; 178, 714-39.

Meiri H, Zeitoun I, Grunhagen HH, Lev-Ram V, Eshhar Z, Schlessinger J. Monoclonal antibodies associated with sodium channel block nerve impulse and stain nodes of Ranvier. Brain Res 1984; 310(1), 168-73.

Meisler MH, O'Brien JE, Sharkey LM. Sodium channel gene family: epilepsy mutations, gene interactions and modifier effects. J Physiol 2010; 588, 1841-8.

Menzler J, Zeck G. Network oscillations in rod-degenerated mouse retinas. J Neurosci 2011; 31(6), 2280-91.

Mercer JN, Chan CS, Tkatch T, Held J, Surmeier DJ. Nav1.6 sodium channels are critical to pacemaking and fast spiking in globus pallidus neurons. J Neurosci 2007; 27(49), 13552-66.

Miguel-Hidalgo JJ, Snider CJ, Angelides KJ, Chalupa LM. Voltage-dependent sodium channel alpha subunit immunoreactivity is expressed by distinct cell types of the cat and monkey retina. Vis Neurosci 1994; 11(2), 219-28.

Miller RF, Dowling JE. Intracellular responses of the Müller (glial) cells of mudpuppy retina: their relation to b-wave of the electroretinogram. J Neurophysiol 1970; 33(3), 323-41.

Miller RF, Staff NP, Velte TJ. Form and function of ON-OFF amacrine cells in the amphibian retina. J Neurophysiol 2006;95(5), 3171-90.

Mills SL, Massey SC. Differential properties of two gap junctional pathways made by AII amacrine cells. Nature 1995;377(6551), 734-7.

Mills SL, Xia X-B, et al. Dopaminergic modulation of tracer coupling in a ganglion-amacrine cell network. Vis Neurosci 2007; 24, 593–608.

Miura G, Wang MH, Ivers KM, Frishman LJ. Retinal pathway origins of the pattern ERG of the mouse. Exp Eye Res 2009; 89, 49–62.

Mojumder DK, Frishman LJ, Otteson DC, Sherry DM. Voltage-gated sodium channel alpha-subunits Na(v)1.1, Na(v)1.2, and Na(v)1.6 in the distal mammalian retina. Mol Vis 2007; 13, 2163–82.

Mojumder DK, Sherry DM, Frishman LJ. Contribution of voltage-gated sodium channels to the b-wave of the mammalian flash electroretinogram. J Physiol 2008; 586, 2551-80.

Möller A, Eysteinsson T. Modulation of the components of the rat dark-adapted electroretinogram by the three subtypes of GABA receptors. Vis Neurosci 2003; 20, 535-42.

Molnar A, Werblin FS. Inhibitory feedback shapes bipolar cell responses in the rabbit retina. J Neurophysiol 2007; 98(6), 3423-35.

Molnar A, Hsueh HA, Roska B, Werblin FS. Crossover inhibition in the retina: circuitry that compensates for nonlinear rectifying synaptic transmission. J Comput Neurosci 2009; 27(3), 569-90.

Moore-Dotson JM, Klein JS, Mazade RE, Eggers ED. Different types of retinal inhibition have distinct neurotransmitter release properties. J Neurophysiol 2015; 113(7), 2078-90.

Mora-Ferrer C, Yazulla S, Studholme KM, Haak-Frendscho M. Dopamine D1-receptor immunolocalization in goldfish retina. J Comp Neurol 1999;411(4), 705-14.

Morgans CW, Zhang J, Jeffrey BG, Nelson SM, Burke NS, Duvoisin RM, Brown RL. TRPM1 is required for the depolarizing light response in retinal ON-bipolar cells. Proc Natl Acad Sci USA 2009; 106(45), 19174-8.

Müller F, Scholten A, Ivanova E, Haverkamp S, Kremmer E, Kaupp UB. HCN channels are expressed differentially in retinal bipolar cells and concentrated at synaptic terminals. Eur J Neurosci 2003; 17(10), 2084-96.

Münch TA, da Silveira RA, Siegert S, Viney TJ, Awatramani GB, Roska B. Approach sensitivity in the retina processed by a multifunctional neural circuit. Nat Neurosci 2009; 12(10), 1308-16.

Murphy GJ, Rieke F. Network variability limits stimulus-evoked spike timing precision in retinal ganglion cells. Neuron. 2006; 52(3), 511-24.

Murphy GJ, Rieke F. Electrical synaptic input to ganglion cells underlies differences in the output and absolute sensitivity of parallel retinal circuits. J Neurosci 2011; 31, 12218–28.

Murphy-Baum B and Taylor WR. The Synaptic and Morphological Basis of Orientation Selectivity in a Polyaxonal Amacrine Cell of the Rabbit Retina. J Neurosci 2015; 35(39), 13336-50.

Naka KI, Rushton WA. S-potentials from colour units in the retina of fish (Cyprinidae). J Physiol 1966; 185(3), 536-55.

Naka KI, Rushton WA. S-potentials from luminosity units in the retina of fish (Cyprinidae). J Physiol 1966; 185(3), 587-99.

Newman EA. Membrane physiology of retinal glial (Müller) cells. J Neurosci 1985; 5(8), 2225-39.

Nguyen-Legros J, Simon A, Caillé I, Bloch B. Immunocytochemical localization of dopamine D1 receptors in the retina of mammals. Vis Neurosci 1997; 14(3), 545-51

Nir I, Haque R, Iuvone PM. Diurnal metabolism of dopamine in the mouse retina. Brain Res 2000; 870, 118–25.

Nirenberg S, Meister M. The light response of retinal ganglion cells is truncated by a displaced amacrine circuit. Neuron 1997; 18(4), 637-50.

O'Brien BJ, Isayama T, Richardson R, Berson DM. Intrinsic physiological properties of cat retinal ganglion cells. J Physiol 2002; 538, 787-802.

O'Brien BJ, Caldwell JH, Ehring GR, Bumsted O'Brien KM, Luo S, Levinson SR. Tetrodotoxin-resistant voltage-gated sodium channels Na(v)1.8 and Na(v)1.9 are expressed in the retina. J Comp Neurol 2008; 508(6), 940-51.

Oesch N, Euler T, Taylor WR. Direction-selective dendritic action potentials in rabbit retina. Neuron. 2005; 47(5), 739-50.

Oesch NW, Taylor WR. Tetrodotoxin-resistant sodium channels contribute to directional responses in starburst amacrine cells. PLoS One 2010; 5(8), e12447.

Ogiwara I, Miyamoto H, Morita N, Atapour N, Mazaki E, Inoue I, Takeuchi T, Itohara S, Yanagawa Y, Obata K, Furuichi T, Hensch TK, Yamakawa K. Nav1.1 localizes to axons of parvalbumin-positive inhibitory interneurons: a circuit basis for epileptic seizures in mice carrying an Scn1a gene mutation. J Neurosci 2007; 27(22), 5903-14.

Ohkuma M, Kawai F, Horiguchi M, Miyachi E. Patch-clamp recording of human retinal photoreceptors and bipolar cells. Photochem Photobiol 2007; 83(2), 317-22.

Olveczky BP, Baccus SA, Meister M. Segregation of object and background motion in the retina. Nature 2003; 423(6938), 401-8.

Osorio N, Cathala L, Meisler MH, Crest M, Magistretti J, Delmas P. Persistent Nav1.6 current at axon initial segments tunes spike timing of cerebellar granule cells. J Physiol 2010; 588(Pt 4), 651-70.

Ozaita A, Petit-Jacques J, Völgyi B, Ho CS, Joho RH, Bloomfield SA, Rudy B. A unique role for Kv3 voltage-gated potassium channels in starburst amacrine cell signaling in mouse retina. J Neurosci 2004; 24, 7335–43.

Pan ZH, Hu HJ. Voltage-dependent Na(+) currents in mammalian retinal cone bipolar cells. J Neurophysiol 2000; 84, 2564-71.

Pan ZH, Ganjawala TH, Lu Q, Ivanova E, Zhang Z. ChR2 mutants at L132 and T159 with improved operational light sensitivity for vision restoration. PLoS One 2014; 9(6), e98924.

Pan ZH. Differential expression of high- and two types of low-voltage-activated calcium currents in rod and cone bipolar cells of the rat retina. J Neurophysiol 2000; 83(1), 513-27

Park SJ, Borghuis BG, Rahmani P, Zeng Q, Kim IJ, Demb JB. Function and Circuitry of VIP+ Interneurons in the Mouse Retina. J Neurosci 2015; 35(30), 10685-700.

Partida GJ, Lee SC, Haft-Candell L, Nichols GS, Ishida AT. DARPP-32-like immunoreactivity in AII amacrine cells of rat retina. J Comp Neurol 2004; 480(3), 251-63.

Patel RR, Barbosa C, Xiao Y, Cummins TR. Human Nav1.6 Channels Generate Larger Resurgent Currents than Human Nav1.1 Channels, but the Nav β 4 Peptide Does Not Protect Either Isoform from Use-Dependent Reduction. PLoS One 2015; 10(7), e0133485.

Peachey NS, Goto Y, al-Ubaidi MR, Naash MI. Properties of the mouse cone-mediated electroretinogram during light adaptation. Neurosci Lett 1993; 162, 9–11.

Pepperberg DR, Birch DG, Hood DC. Photoresponses of human rods in vivo derived from paired-flash electroretinograms. Vis Neurosci 1997; 14(1), 73-82.

Peters BN, Masland RH. Responses to light of starburst amacrine cells. J Neurophysiol 1996; 75, 469–80.

Petit-Jacques J, Bloomfield SA. Synaptic regulation of the light-dependent oscillatory currents in starburst amacrine cells of the mouse retina. J Neurophysiol 2008; 100, 993–1006.

Petit-Jacques J, Völgyi B, Rudy B, Bloomfield S. Spontaneous oscillatory activity of starburst amacrine cells in the mouse retina. J Neurophysiol 2005; 94, 1770–80.

Piccolino M, Gerschenfeld HM. Characteristics and ionic processes involved in feedback spikes of turtle cones. Proc R Soc Lond B Biol Sci 1980; 206(1165), 439-63.

Pignatelli V, Strettoi E. Bipolar cells of the mouse retina: a gene gun, morphological study. J Comp Neurol 2004; 476(3), 254-66.

Planells-Cases R, Caprini M, Zhang J, Rockenstein EM, Rivera RR, Murre C, Masliah E, Montal M. Neuronal death and perinatal lethality in voltage-gated sodium channel alpha(II)-deficient mice. Biophys J 2000; 78(6), 2878-91.

Poleg-Polsky A, Diamond JS. Imperfect space clamp permits electrotonic interactions between inhibitory and excitatory synaptic conductances, distorting voltage clamp recordings. PLoS ONE 2011; 6, e19463.

Pollock GS, Vernon E, Forbes ME, Yan Q, Ma YT, Hsieh T, Robichon R, Frost DO, Johnson JE. Effects of early visual experience and diurnal rhythms on BDNF mRNA and protein levels in the visual system, hippocampus, and cerebellum. J Neurosci 2001; 21(11), 3923-31.

Popova E, Kupenova P. Contribution of voltage-gated sodium channels to b- and d-waves of frog electroretinogram under different conditions of light adaptation. Vision Res 2010; 50, 88-98.

Porciatti V. The mouse pattern electroretinogram. Doc Ophthalmol. 2007;115(3), 145-53.

Porciatti V.2015: Electrophysiological assessment of retinal ganglion cell function. Exp Eye Res 2015; 141, 164-70.

Portaluppi F, Smolensky MH, Touitou Y. Ethics and methods for biological rhythm research on animals and human beings. Chronobiol Int 2010; 27, 1911–29.

Pozdeyev N, Tosini G, Li L, et al. Dopamine modulates diurnal and circadian rhythms of protein phosphorylation in photoreceptor cells of mouse retina. Eur J Neurosci 2008; 27, 2691–700.

Protti DA, Di Marco S, Huang JY, Vonhoff CR, Nguyen V, Solomon SG. Inner retinal inhibition shapes the receptive field of retinal ganglion cells in primate. J Physiol 2014; 592(1), 49-65.

Protti DA, Flores-Herr N, von Gersdorff H. Light evokes Ca2+ spikes in the axon terminal of a retinal bipolar cell. Neuron 2000; 25(1), 215-27.

Puller C, Ondreka K, Haverkamp S. Bipolar cells of the ground squirrel retina. J Comp Neurol 2011; 519(4), 759-74.

Puthussery T, Percival KA, Venkataramani S, Gayet-Primo J, Grünert U, Taylor WR. Kainate receptors mediate synaptic input to transient and sustained OFF visual pathways in primate retina. J Neurosci 2014;34(22), 7611-21.

Puthussery T, Venkataramani S, Gayet-Primo J, Smith RG, Taylor WR. NaV1.1 channels in axon initial segments of bipolar cells augment input to magnocellular visual pathways in the primate retina. J Neurosci 2013; 33, 16045–59.

Qu J, Myhr KL. The development of intrinsic excitability in mouse retinal ganglion cells. Dev Neurobiol 2008; 68(9), 1196-212.

Qu J, Myhr KL. The morphology and intrinsic excitability of developing mouse retinal ganglion cells. PLoS One 2011; 6(7): e21777.

Quigley HA, McKinnon SJ, Zack DJ, Pease ME, Kerrigan-Baumrind LA, Kerrigan DF, Mitchell RS. Retrograde axonal transport of BDNF in retinal ganglion cells is blocked by acute IOP elevation in rats. Invest Ophthalmol Vis Sci 2000;41(11), 3460-6.

Raman IM, Bean BP. Resurgent sodium current and action potential formation in dissociated cerebellar Purkinje neurons. J Neurosci 1997; 17(12), 4517-26.

Raman IM, Bean BP. Inactivation and recovery of sodium currents in cerebellar Purkinje neurons: evidence for two mechanisms. Biophys J 2001; 80(2), 729-37.

Raman IM, Sprunger LK, Meisler MH, Bean BP. Altered subthreshold sodium currents and disrupted firing patterns in Purkinje neurons of Scn8a mutant mice. Neuron 1997;19(4), 881-91.

Rangaswamy NV, Frishman LJ, Dorotheo EU, Schiffman JS, Bahrani HM, Tang RA. Photopic ERGs in patients with optic neuropathies: comparison with primate ERGs after pharmacologic blockade of inner retina. Invest Ophthalmol Vis Sci 2004; 45(10), 3827-37.

Rangaswamy NV, Shirato S, Kaneko M, Digby BI, Robson JG, Frishman LJ. Effects of Spectral Characteristics of Ganzfeld Stimuli on the Photopic Negative Response (PhNR) of the ERG. Invest Ophthalmol Vis Sci 2007; 48(10), 4818-28.

Rasband MN. The axon initial segment and the maintenance of neuronal polarity. Nat Rev Neurosci 2010;11(8), 552-62.

Raz-Prag D, Grimes WN, Fariss RN, Vijayasarathy C, Campos MM, Bush RA, Diamond JS, Sieving PA. Probing potassium channel function in vivo by intracellular delivery of antibodies in a rat model of retinal neurodegeneration. Proc Natl Acad Sci USA 2010; 107(28), 12710-5.

Renganathan M, Cummins TR, Waxman SG. Contribution of Na(v)1.8 sodium channels to action potential electrogenesis in DRG neurons. J Neurophysiol 2001;86(2), 629-40.

Reuter JH. The development of the electroretinogram in normal and light-deprived rabbits. Pflugers Arch. 1976; 363(1), 7-13.

Ribelayga C, Mangel SC. Absence of circadian clock regulation of horizontal cell gap junctional coupling reveals two dopamine systems in the goldfish retina. J Comp Neurol 2003; 467, 243–53.

Rivlin-Etzion M, Zhou K, Wei W, Elstrott J, Nguyen PL, Barres BA, Huberman AD, Feller MB. Transgenic mice reveal unexpected diversity of on-off direction-selective retinal ganglion cell subtypes and brain structures involved in motion processing. J Neurosci 2011 31:8760–69.

Robson JG, Frishman LJ. Response linearity and kinetics of the cat retina: the bipolar cell component of the dark-adapted electroretinogram. Vis Neurosci 1995; 12(5), 837-50.

Robson JG, Frishman LJ. Dissecting the dark-adapted electroretinogram. Doc Ophthalmol 1998; 95, 187-215.

Robson JG, Maeda H, Saszik SM. Frishman LJ. In vivo studies of signaling in rod pathways of the mouse using the electroretinogram. Vision Res 2004; 44, 3253-68.

Rohrer B. Gene dosage effect of the TrkB receptor on rod physiology and biochemistry in juvenile mouse retina. Mol Vis 2001; 7, 288–96.

Rohrer B, Blanco R, Marc RE, Lloyd MB, Bok D, Schneeweis DM, Reichardt LF. Functionally intact glutamate-mediated signaling in bipolar cells of the TRKB knockout mouse retina. Vis Neurosci 2004; 21(5), 703-13.

Rohrer B, Korenbrot JI, LaVail MM, Reichardt LF, Xu B. Role of neurotrophin receptor TrkB in the maturation of rod photoreceptors and establishment of synaptic transmission to the inner retina. J Neurosci 1999; 19(20), 8919-30.

Rohrer B, LaVail MM, Jones KR, Reichardt LF. Neurotrophin receptor TrkB activation is not required for the postnatal survival of retinal ganglion cells in vivo. Exp Neurol 2001: 172, 91-91

Rohrer B, Ogilvie JM. Retarded outer segment development in TrkB knockout mouse retina organ culture. Mol Vis 2003; 9, 18-23.

Roseboom PH, Namboodiri MA, Zimonjic DB, et al. Natural melatonin "knockdown" in C57BL/6J mice: rare mechanism truncates serotonin N-acetyltransferase. Mol Brain Res 1998; 63, 189–97.

Roska B and Werblin FS. Vertical interactions across ten parallel, stacked representations in the mammalian retina. Nature 2001; 410(6828), 583-7.

Rosker C, Lohberger B, Hofer D, Steinecker B, Quasthoff S, Schreibmayer W. The TTX metabolite 4,9-anhydro-TTX is a highly specific blocker of the Nav1.6 voltage-dependent sodium channel. Am J Physiol Cell Physiol 2007;293, C783–C789.

Royeck M, Horstmann MT, Remy S, Reitze M, Yaari Y, Beck H. Role of axonal NaV1.6 sodium channels in action potential initiation of CA1 pyramidal neurons. J Neurophysiol 2008; 100(4), 2361-80.

Ruan G-X, Allen GC, Yamazaki S, McMahon DG. An autonomous circadian clock in the inner mouse retina regulated by dopamine and GABA. Plos Biol 2008; 6, e249.

Ruan G-X, Zhang D-Q, Zhou T, Yamazaki S, McMahon DG. Circadian organization of the mammalian retina. Proc Natl Acad Sci USA 2006; 103, 9703–8.

Rush AM, Dib-Hajj SD, Waxman SG. Electrophysiological properties of two axonal sodium channels, Nav1.2 and Nav1.6, expressed in mouse spinal sensory neurones. J Physiol. 2005; 564, 803-15.

Russell TL, Werblin FS. Retinal synaptic pathways underlying the response of the rabbit local edge detector. J Neurophysiol 2010; 103(5), 2757-69.

Sanes JR, Masland RH. The types of retinal ganglion cells: current status and implications for neuronal classification. Annu Rev Neurosci 2015; 38, 221-46.

Santi S, Cappello S, Riccio M, Bergami M, Aicardi G, Schenk U, Matteoli M, Canossa M. Hippocampal neurons recycle BDNF for activity-dependent secretion and LTP maintenance. EMBO J 2006; 25(18), 4372-80

Saszik S, DeVries SH. A mammalian retinal bipolar cell uses both graded changes in membrane voltage and all-or-nothing Na+ spikes to encode light. J Neurosci 2012; 32(1), 297-307.

Saszik SM, Robson JG, Frishman LJ. The scotopic threshold response of the dark-adapted electroretinogram of the mouse. J Physiol 2002; 543, 899-916.

Schaller KL and Caldwell JH. Developmental and regional expression of sodium channel isoform NaCh6 in the rat central nervous system. J Comp Neurol 2000; 420(1), 84-97.

Schachter MJ, Oesch N, Smith RG, Taylor WR. Dendritic spikes amplify the synaptic signal to enhance detection of motion in a simulation of the direction-selective ganglion cell. PLoS Comput Biol 2010; 6(8), e1000899

Scheuer T. Regulation of sodium channel activity by phosphorylation. Semin Cell Dev Biol 2011; 22(2), 160-5.

Schmidt TM, Alam NM, Chen S, Kofuji P, Li W, Prusky GT, Hattar S. A role for melanopsin in alpha retinal ganglion cells and contrast detection. Neuron 2014; 82(4), 781-8.

Schoups AA, Elliott RC, Friedman WJ, Black IB. NGF and BDNF are differentially modulated by visual experience in the developing geniculocortical pathway. Brain Res Dev Brain Res 1995; 86, 326–34.

Schubert T, Weiler R, Feigenspan A. Intracellular calcium is regulated by different pathways in horizontal cells of the mouse retina. J Neurophysiol 2006; 96(3), 1278-92.

Schwindt PC, Crill WE. Amplification of synaptic current by persistent sodium conductance in apical dendrite of neocortical neurons. J Neurophysiol 1995; 74(5), 2220-4.

Seki M, Nawa H, Fukuchi T, Abe H, Takei N. BDNF is upregulated by postnatal development and visual experience: quantitative and immunohistochemical analyses of BDNF in the rat retina. Invest Ophthalmol Vis Sci 2003; 44(7), 3211-8.

Sekirnjak C, Hottowy P, Sher A, Dabrowski W, Litke AM, Chichilnisky EJ. High-resolution electrical stimulation of primate retina for epiretinal implant design. J Neurosci 2008;28(17), 4446-56.

Sengupta A, Baba K, Mazzoni F, et al. Localization of melatonin receptor 1 in mouse retina and its role in the circadian regulation of the electroretinogram and dopamine levels. PLoS ONE 2011; 6, e24483.

Sheasby BW and Fohlmeister JF. Impulse encoding across the dendritic morphologies of retinal ganglion cells. J Neurophysiol 1999; 81(4), 1685-98.

Sherman SM, Stone J. Physiological normality of the retinal in visually deprived cats. Brain Res 1973; 60(1), 224-30.

Shields CR, Lukasiewicz PD. Spike-dependent GABA inputs to bipolar cell axon terminals contribute to lateral inhibition of retinal ganglion cells. J Neurophysiol 2003 89, 2449-58.

Shields SD, Butt RP, Dib-Hajj SD, Waxman SG. Oral administration of PF-01247324, a subtype-selective Nav1.8 blocker, reverses cerebellar deficits in a mouse model of multiple sclerosis. PLoS One. 2015; 10(3), e0119067.

Shingai R, Christensen BN. Sodium and calcium currents measured in isolated catfish horizontal cells under voltage clamp. Neuroscience 1983; 10(3), 893-7.

Shingai R, Christensen BN. Excitable properties and voltage-sensitive ion conductances of horizontal cells isolated from catfish (Ictalurus punctatus) retina. J Neurophysiol 1986; 56(1), 32-49.

Shirato S, Maeda H, Miura G, Frishman L. Postreceptoral contributions to the light-adapted ERG of mice lacking b-waves. Exp Eye Res 2008; 86, 914-28.

Shlens J, Rieke F, Chichilnisky E. Synchronized firing in the retina. Curr Opin Neurobiol 2008; 18(4), 396-402.

Siegert S, Scherf BG, Del Punta K, Didkovsky N, Heintz N, Roska B. Genetic address book for retinal cell types. Nat Neurosci 2009; 12(9), 1197-204.

Singer W. Neuronal synchrony: a versatile code for the definition of relations? Neuron 1999; 24(1), 49-65.

Sivyer B and Williams SR. Direction selectivity is computed by active dendritic integration in retinal ganglion cells. Nat Neurosci 2013; 16(12), 1848-56.

Skaliora I, Scobey RP, Chalupa LM. Prenatal development of excitability in cat retinal ganglion cells: action potentials and sodium currents. J Neurosci 1993; 13, 313-23.

Slaughter MM, Miller RF. 2-amino-4-phosphonobutyric acid: a new pharmacological tool for retina research. Science 198; 211(4478), 182-5

Smith BJ, Côté PD. Reduced Retinal Function in the Absence of Na(v)1.6. PLoS ONE 2012; 7, e31476.

Smith BJ, Tremblay F, Côté PD. Voltage-gated sodium channels contribute to the b-wave of the rodent electroretinogram by mediating input to rod bipolar cell GABAc receptors. Exp Eye Res 2013; 116: 279–90.

Smith BJ, Wang X, Chauhan BC, Côté PD, Tremblay F. Contribution of retinal ganglion cells to the mouse electroretinogram. Doc Ophthalmol 2014 128:155–168.

Smith BJ, Côté PD, Tremblay F. Dopamine modulation of rod pathway signaling by suppression of GABAC feedback to rod-driven depolarizing bipolar cells. Eur J Neurosci 2015; 42(6), 2258-70.

Smith BJ, Côté PD, Tremblay F. D1 dopamine receptors modulate cone ON bipolar cell Nav channels to control daily rhythms in photopic vision. Chronobiol Int 2015; 32(1), 48-58.

Smith BJ, Tremblay F, Côté PD. Voltage-gated sodium channels contribute to the b-wave of the rodent electroretinogram by mediating input to rod bipolar cell GABAc receptors. Exp Eye Res 2013; 116, 279–90.

Smith MR, Smith RD, Plummer NW, Meisler MH, Goldin AL. Functional analysis of the mouse Scn8a sodium channel. J Neurosci 1998; 18(16), 6093-102.

Smith RD, Goldin AL. Functional analysis of the rat I sodium channel in xenopus oocytes. J Neurosci 1998; 18(3), 811-20.

Spalding KL, Rush RA, Harvey AR. Target-derived and locally derived neurotrophins support retinal ganglion cell survival in the neonatal rat retina. J Neurobiol 2004; 60(3), 319-27.

Spalding KL, Dharmarajan AM, Harvey AR.: Caspase-independent retinal ganglion cell death after target ablation in the neonatal rat. Eur J Neurosci 2005; 21(1), 33-45.

Ströh S, Sonntag S, Janssen-Bienhold U, Schultz K, Cimiotti K, Weiler R, Willecke K, Dedek K. Cell-specific cre recombinase expression allows selective ablation of glutamate receptors from mouse horizontal cells. PLoS One 2013; 8(12), e83076.

Storch K-F, Paz C, Signorovitch J, et al. Intrinsic circadian clock of the mammalian retina: importance for retinal processing of visual information. Cell 2007; 130, 730–41.

Stuart G. Voltage-activated sodium channels amplify inhibition in neocortical pyramidal neurons. Nat Neurosci 1999; 2(2), 144-50.

Stuart G, Sakmann B. Amplification of EPSPs by axosomatic sodium channels in neocortical pyramidal neurons. Neuron 1995; 15(5), 1065-76.

Stys PK, Sontheimer H, Ransom BR, Waxman SG. Noninactivating, tetrodotoxin-sensitive Na+ conductance in rat optic nerve axons. Proc Natl Acad Sci USA 1993; 90(15), 6976-80.

Sun LO, Jiang Z, Rivlin-Etzion M, Hand R, Brady CM, Matsuoka RL, Yau KW, Feller MB, Kolodkin AL. On and off retinal circuit assembly by divergent molecular mechanisms. Science 2013; 342(6158), 1974.

Sun W, Li N, He S. Large-scale morphological survey of mouse retinal ganglion cells. J Comp Neurol 2002; 451, 115–126.

Swensen AM and Bean BP. Robustness of burst firing in dissociated purkinje neurons with acute or long-term reductions in sodium conductance. J Neurosci 2005; 25(14), 3509-20.

Tabata T and Kano M. Heterogeneous intrinsic firing properties of vertebrate retinal ganglion cells. J Neurophysiol 2002; 87(1), 30-41.

Tamalu F, Watanabe S. Glutamatergic input is coded by spike frequency at the soma and proximal dendrite of AII amacrine cells in the mouse retina. Eur J Neurosci 2007; 25(11), 3243-52.

Tanaka BS, Zhao P, Dib-Haji FB, Morisset V, Tata S, Waxman SG, Dib-Haji SD. A gain-of-function mutation in Nav1.6 in a case of trigeminal neuralgia. Mol Medicine 2016; 22, 338-48.

Tanimoto N., Muehlfriedel R.L., Fischer M.D., Fahl E., Humphries P., Biel M., Seeliger M.W.,. Vision tests in the mouse: Functional phenotyping with electroretinography. Front Biosci 2009 14, 2730-7.

Tanimoto N., Sothilingam V., Euler T., Ruth P., Seeliger M.W., Schubert T. BK channels mediate pathway-specific modulation of visual signals in the in vivo mouse retina. J Neurosci 2012 32, 4861-6.

Tassi P, Pins D. Diurnal rhythmicity for visual sensitivity in humans? Chronobiol Int 1997; 14, 35–48.

Taylor WR, He S, Levick WR, Vaney DI. Dendritic computation of directional selectivity by retinal ganglion cells. Science 2000; 289(5488), 2347-50.

Taylor WR, Wässle H. Receptive field properties of starburst cholinergic amacrine cells in the rabbit retina. Eur J Neurosci 1995; 7, 2308–21.

Thoreson WB, Mangel SC. Lateral interactions in the outer retina. Prog Retin Eye Res 2012; 31(5), 407-41.

Tian N, Copenhagen DR. Visual deprivation alters development of synaptic function in inner retina after eye opening. Neuron 2001; 32(3), 439-49.

Tian N, Copenhagen DR. Visual stimulation is required for refinement of ON and OFF pathways in postnatal retina. Neuron 2003; 39(1), 85-96.

Tian M, Jarsky T, Murphy GJ, Rieke F, Singer JH. Voltage-gated Na channels in AII amacrine cells accelerate scotopic light responses mediated by the rod bipolar cell pathway. J Neurosci 2010; 30, 4650–4659.

Tian C, Li T, Yang M, Hou H, Shu Y Distinct contributions of Na(v)1.6 and Na(v)1.2 in action potential initiation and backpropagation. Nat Neurosci 2009 12:996–1002.

Thoreson WB, Mangel SC. Lateral interactions in the outer retina. Prog Retin Eye Res 2012; 31(5), 407-41.

Thyagarajan S, van Wyk M, Lehmann K, Löwel S, Feng G, Wässle H. Visual function in mice with photoreceptor degeneration and transgenic expression of channelrhodopsin 2 in ganglion cells. J Neurosci 2010; 30(26), 8745-58.

Tian M, Jarsky T, Murphy GJ, Rieke F, Singer JH. Voltage-gated Na channels in AII amacrine cells accelerate scotopic light responses mediated by the rod bipolar cell pathway. J Neurosci 2010; 30, 4650-9.

Tosini G, Menaker M. Circadian rhythms in cultured mammalian retina. Science 1996; 272, 419–21.

Trenholm S, Johnson K, Li X, Smith RG, Awatramani GB. Parallel mechanisms encode direction in the retina. Neuron 2011;71(4), 683-94.

Trenholm S, Borowska J, Zhang J, Hoggarth A, Johnson K, Barnes S, Lewis TJ, Awatramani GB. Intrinsic oscillatory activity arising within the electrically coupled AII amacrine-ON cone bipolar cell network is driven by voltage-gated Na+ channels. J Physiol (Lond) 2012; 590, 2501–17.

Trenholm S, McLaughlin AJ, Schwab DJ, Awatramani GB. Dynamic tuning of electrical and chemical synaptic transmission in a network of motion coding retinal neurons. J Neurosci 2013; 33(37), 14927-38.

Trenholm S, McLaughlin AJ, Schwab DJ, Turner MH, Smith RG, Rieke F, Awatramani GB. Nonlinear dendritic integration of electrical and chemical synaptic inputs drives fine-scale correlations. Nat Neurosci 2014;17(12), 1759-66.

Trimmer JS, Rhodes KJ. Localization of Voltage-Gated Ion Channels in Mammalian Brain. Annu Rev Physiol 2004; 66, 477–519.

Tsai D, Morley JW, Suaning GJ, Lovell NH. Frequency-dependent reduction of voltage-gated sodium current modulates retinal ganglion cell response rate to electrical stimulation. J Neural Eng 2011 8, 066007.

Tsukamoto Y, Morigiwa K, Ueda M, Sterling P. Microcircuits for night vision in mouse retina. J Neurosci 2001; 21(21), 8616-23.

Tsukamoto Y, Omi N. Functional allocation of synaptic contacts in microcircuits from rods via rod bipolar to AII amacrine cells in the mouse retina. J Comp Neurol 2013; 521(15):3541-55.

Ueda Y, Kaneko A, Kaneda M. Voltage-dependent ionic currents in solitary horizontal cells isolated from cat retina. J Neurophysiol 1992; 68(4), 1143-50.

Ueno S, Kondo M, Niwa Y, Terasaki H, Miyake Y. Luminance dependence of neural components that underlies the primate photopic electroretinogram. Invest Ophthalmol Vis Sci 2004; 45(3), 1033-40.

Urschel S, Höher T, Schubert T, Alev C, Söhl G, Wörsdörfer P, Asahara T, Dermietzel R, Weiler R, Willecke K. Protein kinase A-mediated phosphorylation of connexin36 in mouse retina results in decreased gap junctional communication between AII amacrine cells. J Biol Chem 2006; 281(44), 33163-71.

Vaney DI, Sivyer B, Taylor WR. Direction selectivity in the retina: symmetry and asymmetry in structure and function. Nat Rev Neurosci 2012; 13(3), 194-208.

Van Rullen R, Thorpe SJ. Rate coding versus temporal order coding: what the retinal ganglion cells tell the visual cortex. Neural Comp 2001; 13(6), 1255-1283.

VanRullen R, Guyonneau R, Thorpe SJ. Spike times make sense. Trends Neurosci 2005; 28(1), 1-4.

Van Wart A, Trimmer JS, Matthews G. Polarized distribution of ion channels within microdomains of the axon initial segment. J Comp Neurol 2007; 500(2), 339-52.

Van Wart A, Matthews G. Expression of sodium channels Nav1.2 and Nav1.6 during postnatal development of the retina. Neurosci Lett 2006a; 403, 315–7.

Van Wart A, Matthews G. Impaired firing and cell-specific compensation in neurons lacking nav1.6 sodium channels. J Neurosci 2006b 26:7172–80.

Van Wart A, Boiko T, Trimmer JS, Matthews G. Novel clustering of sodium channel Na(v)1.1 with ankyrin-G and neurofascin at discrete sites in the inner plexiform layer of the retina. Mol Cell Neurosci 2005; 28(4), 661-73.

Vaquero CF, Pignatelli A, Partida GJ, Ishida AT. A dopamine- and protein kinase A-dependent mechanism for network adaptation in retinal ganglion cells. J Neurosci 2001; 21(21), 8624-35.

Vaquero CF, Villa PDL. Localisation of the GABACreceptors at the axon terminal of the rod bipolar cells of the mouse retina. Neurosci Res 1999; 35, 1-7.

Varela C, Blanco R, Villa PDl,. Depolarizing effect of GABA in rod bipolar cells of the mouse retina. Vision Res. 2005; 45, 2659-67.

Vassilev PM, Scheuer T, Catterall WA. Identification of an intracellular peptide segment involved in sodium channel inactivation. Science 1988; 241(4873), 1658-61.

Vega AV, Henry DL, Matthews G. Reduced expression of Na(v)1.6 sodium channels and compensation by Na(v)1.2 channels in mice heterozygous for a null mutation in Scn8a. Neurosci Lett 2008; 442(1), 69-73.

Velte TJ and Masland RH. Action potentials in the dendrites of retinal ganglion cells. J Neurophysiol. 1999 Mar;81(3):1412-7.

Veruki ML, Hartveit E. Electrical synapses mediate signal transmission in the rod pathway of the mammalian retina. J Neurosci 2002; 22(24), 10558-66.

Veruki ML, Hartveit E.AII (Rod) amacrine cells form a network of electrically coupled interneurons in the mammalian retina. Neuron 2002; 33(6), 935-46.

Veruki ML, Wässle H. Immunohistochemical localization of dopamine D1 receptors in rat retina. Eur J Neurosci 1996; 8(11), 2286-97.

Vielma AH, Schmachtenberg O. Electrophysiological fingerprints of OFF bipolar cells in rat retina. Scientific Reports 2016; 6(1), 30259.

Vigh J. Light-evoked lateral GABAergic inhibition at single bipolar cell synaptic terminals is driven by distinct retinal microcircuits. J Neurosci 2011; 31, 15884.

Vijayaragavan K, O'Leary ME, Chahine M. Gating properties of Na(v)1.7 and Na(v)1.8 peripheral nerve sodium channels. J Neurosci 2001; 21, 7909–7918.

Vistamehr S, Tian N. Light deprivation suppresses the light response of inner retina in both young and adult mouse. Vis Neurosci 2004; 21(1), 23-37.

Viswanathan S, VanDerPloeg BJ, Srinivas SP,. Action potential contributions to the scotopic oscillatory potentials of rat electroretinogram. ARVO Meeting Abstracts 2004; 45, 813.

Völgyi B, Xin D, Amarillo Y, Bloomfield SA. Morphology and physiology of the polyaxonal amacrine cells in the rabbit retina. J Comp Neurol 2001; 440(1), 109-25.

Vroman R, Klaassen LJ, Howlett MH, Cenedese V, Klooster J, Sjoerdsma T, Kamermans M. Extracellular ATP hydrolysis inhibits synaptic transmission by increasing ph buffering in the synaptic cleft. PLoS Biol 2014; 12(5), e1001864.

Vugler AA, Redgrave P, Hewson-Stoate NJ, Greenwood J, Coffey PJ. Constant illumination causes spatially discrete dopamine depletion in the normal and degenerate retina. J Chem Neuroanat 2007; 33, 9–22.

Wachtmeister L. Oscillatory potentials in the retina: what do they reveal. Prog Retin Eye Res 1998; 17, 485–521.

Wachtmeister L, Dowling JE. The oscillatory potentials of the mudpuppy retina. Invest Ophthalmol Vis Sci 1978; 17(12), 1176-88.

Wang GY, Ratto G, Bisti S, Chalupa LM. Functional development of intrinsic properties in ganglion cells of the mammalian retina. J Neurophysiol 1997; 78(6), 2895-903.

Wang J, Mojumder DK, Yan J, Xie A, Standaert RF, Qian H, Pepperberg DR, Frishman, LJ. In vivo electroretinographic studies of the role of GABAC receptors in retinal signal processing. Exp Eye Res 2015; 139, 46-63.

Wang M H, Frishman L J, Otteson D C. Intracellular delivery of proteins into mouse Müller glia cells in vitro and in vivo using Pep-1 transfection reagent. J Neurosci Methods 2009; 177(2), 403–19.

Wang TM, Holzhausen LC, Kramer RH. Imaging an optogenetic pH sensor reveals that protons mediate lateral inhibition in the retina. Nat Neurosci 2014; 17(2), 262-8.

Watanabe S, Satoh H, Koizumi A, Takayanagi T, Kaneko A. Tetrodotoxin-sensitive persistent current boosts the depolarization of retinal amacrine cells in goldfish. Neurosci Lett 2000; 278(1-2), 97-100.

Wässle H, Heinze L, Ivanova E, Majumdar S, Weiss J, Harvey RJ, Haverkamp S. Glycinergic transmission in the Mammalian retina. Front Mol Neurosci 2009; 2, 6.

Wässle H, Puller C, Müller F, Haverkamp S. Cone contacts, mosaics, and territories of bipolar cells in the mouse retina. J Neurosci 2009; 29(1), 106-17.

Watanabe S, Satoh H, Koizumi A, Takayanagi T, Kaneko A. Tetrodotoxin-sensitive persistent current boosts the depolarization of retinal amacrine cells in goldfish. Neurosci Lett 2000; 278(1-2), 97-100.

Waxman SG. Channel, neuronal and clinical function in sodium channelopathies: from genotype to phenotype. Nat Neurosci 2007; 10(4), 405-9.

Waxman SG. Channelopathic pain: a growing but still small list of model disorders. Neuron 2010; 66(5), 622-4.

Waxman SG. Painful Na-channelopathies: an expanding universe. Trends Mol Med 2013; 19(7), 406-9.

Waxman SG, GW Zamponi. Regulating excitability of peripheral afferents: emerging ion channel targets. Nat Neurosci 2014; 17(2), 153-63.

Wei W, Hamby AM, Zhou K, Feller MB. Development of asymmetric inhibition underlying direction selectivity in the retina. Nature 2011;469, 402–6.

Weick M, Demb JB. Delayed-Rectifier K Channels Contribute to Contrast Adaptation in Mammalian Retinal Ganglion Cells. Neuron 2011;71, 166-79.

Weng S, Sun W, He S. Identification of ON-OFF direction-selective ganglion cells in the mouse retina. J Physiol (Lond) 2005; 562, 915–23.

Werblin FS. The retinal hypercircuit: a repeating synaptic interactive motif underlying visual function. J Physiol 2011; 589, 3691-702.

Westenbroek RE, Merrick DK, Catterall WA. Differential subcellular localization of the RI and RII Na+ channel subtypes in central neurons. Neuron 1989; 3(6), 695-704.

Wiesel TN and Hubel DH. Effects of visual deprivation on morphology and physiology of cells in the cats lateral geniculate body. J Neurophysiol 1963a; 26, 978-93.

Wiesel TN and Hubel DH. Single-cell responses in striate cortex of kittens deprived of vision in one eye. J Neurophysiol 1963b; 26, 1003-17.

Williams SR, Mitchell SJ. Direct measurement of somatic voltage clamp errors in central neurons. Nat Neurosci 2008; 11, 790–98.

Wilson MJ, Yoshikami D, Azam L, Gajewiak J, Olivera BM, Bulaj G, Zhang M-M. μ-Conotoxins that differentially block sodium channels NaV1.1 through 1.8 identify those responsible for action potentials in sciatic nerve. Proc Natl Acad Sci USA 2011; 108, 10302–07.

Witkovsky P, Svenningsson P, Yan L, Bateup H, Silver R. Cellular localization and function of DARPP-32 in the rodent retina. Eur J Neurosci 2007; 25(11), 3233-42.

Witkovsky P, Veisenberger E, LeSauter J, et al. Cellular location and circadian rhythm of expression of the biological clock gene Period 1 in the mouse retina. J Neurosci 2003; 23, 7670–6.

Wollner DA and Catterall WA. Localization of sodium channels in axon hillocks and initial segments of retinal ganglion cells. Proc Natl Acad Sci U S A. 1986; 83(21), 8424-8.

Wong RC, Cloherty SL, Ibbotson MR, O'Brien BJ. Intrinsic physiological properties of rat retinal ganglion cells with a comparative analysis. J Neurophysiol 2012; 108(7), 2008-23.

Wu C, Ivanova E, Cui J, Lu Q, Pan ZH. Action potential generation at an axon initial segment-like process in the axonless retinal AII amacrine cell. J Neurosci 2011; 31(41), 14654-9.

Xia XB, Mills SL. Gap junctional regulatory mechanisms in the AII amacrine cell of the rabbit retina. Vis Neurosci 2004; 21(5), 791-805.

Xin D, Bloomfield SA. Comparison of the responses of AII amacrine cells in the dark- and light-adapted rabbit retina. Vis Neurosci 1999; 16(4), 653-65.

Xin D, Bloomfield SA. Dark- and light-induced changes in coupling between horizontal cells in mammalian retina. J Comp Neurol 1999; 405(1), 75-87.

Xu JW, Hou M, Slaughter MM. Photoreceptor encoding of supersaturating light stimuli in salamander retina. J Physiol 2005; 569, 575-85.

Xu X, Karwoski CJ. Current source density analysis of retinal field potentials. II. Pharmacological analysis of the b-wave and M-wave. J. Neurophysiol 1994;72, 96-105.

Yamada ES, Yamada ES, Dmitrieva N, Dmitrieva N, Keyser KT, Keyser KT, Lindstrom JM, Lindstrom JM, Hersh LB, Hersh LB, Marshak DW, Marshak DW. Synaptic connections of starburst amacrine cells and localization of acetylcholine receptors in primate retinas. J Comp Neurol 2003; 461, 76–90.

Yang J, Nemargut JP, Wang GY. The roles of ionotropic glutamate receptors along the On and Off signaling pathways in the light-adapted mouse retina. Brain Res 2011;1390, 70-9.

Yang XL and Wu SM. Feedforward lateral inhibition in retinal bipolar cells: input-output relation of the horizontal cell-depolarizing bipolar cell synapse. Proc Natl Acad Sci USA 1991; 88(8), 3310-3.

Yang Y, Huang J, Mis MA, Estacion M, Macala L, Shah P, Schulman BR, Horton DB, Dib-Hajj SD, Waxman SG. Nav1.7-A1632G Mutation from a Family with Inherited Erythromelalgia: Enhanced Firing of Dorsal Root Ganglia Neurons Evoked by Thermal Stimuli. J Neurosci 2016; 36(28), 7511-22.

Yonehara K, Balint K, Noda M, Nagel G, Bamberg E, Roska B. Spatially asymmetric reorganization of inhibition establishes a motion-sensitive circuit. Nature 2011; 469(7330), 407-10.

Yoshida, K., Watanabe, D., Ishikane, H., Tachibana, M., Pastan, I., and Nakanishi, S. A key role of starburst amacrine cells in originating retinal directional selectivity and optokinetic eye movement. Neuron 2001; 30, 771–80.

Yu FH, Mantegazza M, Westenbroek RE, Robbins CA, Kalume F, Burton KA, Spain WJ, McKnight GS, Scheuer T, Catterall WA.Reduced sodium current in GABAergic interneurons in a mouse model of severe myoclonic epilepsy in infancy. Nat Neurosci 2006; 9(9), 1142-9.

Zaghloul KA, Manookin MB, Borghuis BG, Boahen K, Demb JB. Functional circuitry for peripheral suppression in Mammalian Y-type retinal ganglion cells. J Neurophysiol 2007; 97(6), 4327-40.

Zenisek D, Henry D, Studholme K, Yazulla S, Matthews G. Voltage-dependent sodium channels are expressed in nonspiking retinal bipolar neurons. J Neurosci 2001; 21, 4543–50.

Zenisek D, Matthews G. Calcium action potentials in retinal bipolar neurons. Vis Neurosci 1998; 15(1), 69-75.

Zhang D-Q, Belenky MA, Sollars PJ, Pickard GE, McMahon DG. Melanopsin mediates retrograde visual signaling in the retina. PLoS ONE 2012; 7, e42647.

Zhang DQ, Zhou TR, McMahon DG. Functional heterogeneity of retinal dopaminergic neurons underlying their multiple roles in vision. J Neurosci 2007; 27(3), 692-9.

Zhang K, Yao G, Gao Y, Hofeldt KJ, Lei B. Frequency spectrum and amplitude analysis of dark- and light-adapted oscillatory potentials in albino mouse, rat and rabbit. Doc Ophthalmol 2007; 115, 85–93.

Zhang Y, Kim IJ, Sanes JR, Meister M. The most numerous ganglion cell type of the mouse retina is a selective feature detector. Proc Natl Acad Sci USA 2012; 109(36), E2391-8.

Zhang Z, Feng J, Wu C, Lu Q, Pan ZH.Targeted Expression of Channelrhodopsin-2 to the Axon Initial Segment Alters the Temporal Firing Properties of Retinal Ganglion Cells. PLoS One 2015;10(11), e0142052.

Zhou D, Lambert S, Malen PL, Carpenter S, Boland LM, Bennett V. AnkyrinG is required for clustering of voltage-gated Na channels at axon initial segments and for normal action potential firing. J Cell Biol 1998; 143(5), 1295-304.

Zhou ZJ, Fain GL. Starburst amacrine cells change from spiking to nonspiking neurons during retinal development. Proc Natl Acad Sci USA 1996; 93, 8057–62.

Zhou ZJ, Lee S. Synaptic physiology of direction selectivity in the retina. J Physiol (Lond) 2008; 586, 4371–6.

Zweifel LS, Kuruvilla R, Ginty DD. Functions and mechanisms of retrograde neurotrophin signalling. Nat Rev Neurosci 2005; 6(8), 615-25.